
Theses and Dissertations

2013

In vitro pseudomonas aeruginosa biofilms : improved confocal imaging and co-treatment with dispersion agents and antibiotics

Stacy Sommerfeld Ross
University of Iowa

Copyright 2013 Stacy Sommerfeld Ross

This dissertation is available at Iowa Research Online: <http://ir.uiowa.edu/etd/4738>

Recommended Citation

Ross, Stacy Sommerfeld. "In vitro pseudomonas aeruginosa biofilms : improved confocal imaging and co-treatment with dispersion agents and antibiotics." PhD (Doctor of Philosophy) thesis, University of Iowa, 2013.
<http://ir.uiowa.edu/etd/4738>.

Follow this and additional works at: <http://ir.uiowa.edu/etd>



Part of the [Pharmacy and Pharmaceutical Sciences Commons](#)

IN VITRO PSEUDOMONAS AERUGINOSA BIOFILMS: IMPROVED CONFOCAL
IMAGING AND CO-TREATMENT WITH DISPERSION AGENTS AND
ANTIBIOTICS

by

Stacy Sommerfeld Ross

An Abstract

Of a thesis submitted in partial fulfillment
of the requirements for the Doctor of
Philosophy degree in Pharmacy
in the Graduate College of
The University of Iowa

May 2013

Thesis Supervisor: Assistant Professor Jennifer Fiegel

ABSTRACT

Pseudomonas aeruginosa bacterial biofilms are the leading cause of mortality among cystic fibrosis (CF) patients. Biofilms contain bacteria attached to a surface and encased in a protective matrix. Since bacteria within a biofilm are less susceptible to antibiotics, a new approach is to use dispersion compounds that cause the biofilms to release free-swimming bacteria. Our approach has focused on combining nutrient dispersion compounds with antibiotics to increase eradication of bacteria within biofilms. This approach takes advantage of the enhanced susceptibility of free-swimming bacteria to antibiotics, compared to bacteria within biofilms. Ultimately, this research will guide the development of an aerosol therapy containing both antibiotic and dispersion compounds to treat bacterial biofilm infections.

To study the effect of antibiotic and dispersion compound treatments on biofilm eradication, a high-throughput screening assay was used to assess the effect on young *Pseudomonas aeruginosa* biofilms. In addition, a Lab-Tek chambered coverglass system imaged via confocal microscopy was used to assess the effect on mature *Pseudomonas aeruginosa* biofilms. Seven antibiotics (amikacin disulfate, tobramycin sulfate, colistin sulfate, colistin methanesulfonate (CMS), polymyxinB sulfate, erythromycin, and ciprofloxacin hydrochloride) were tested alone or in combination with four nutrient dispersion compounds (sodium citrate, succinic acid, xylitol, and glutamic acid) to assess the level of eradication of bacteria within biofilms. For young biofilms, 15 of 24 combinations significantly eliminated more live bacteria within the biofilms (measured in colony forming units per milliliter) compared to antibiotics alone. In the more mature biofilm system, only 3 out of 26 combinations resulted in a higher percentage of live biofilm bacteria being eliminated compared to antibiotics alone, showing the importance of biofilm age in the effectiveness of these potential combination therapies.

To aid in confocal microscopic analysis of biofilms, an automated quantification program called STAINIFICATION was developed. This new program can be used to

simultaneously investigate connected-biofilm bacteria, unconnected bacteria (dispersed bacteria), the biofilm protective matrix, and a growth surface upon which bacteria are grown in confocal images. The program contains novel algorithms for the assessment of bacterial viability and for the quantification of bacteria grown on uneven surfaces, such as tissue. The utility of the viability assessments were demonstrated with confocal images of *Pseudomonas aeruginosa* biofilms. The utility of the uneven surface algorithms were demonstrated with confocal images of *Staphylococcus aureus* biofilms grown on cultured human airway epithelial cells and *Neisseria gonorrhoeae* biofilms grown on transformed cervical epithelial cells.

Finally, a proof-of-concept study demonstrated that dry powder aerosols containing both antibiotic and nutrient dispersion compounds could be developed with properties optimized for efficient deposition in the lungs. A design of experiments study showed that solution concentration was the most significant parameter affecting aerosol yield, particle size, and *in vitro* deposition profiles.

Collectively this work demonstrated that bacterial dispersion from biofilms can enhance antibiotic susceptibility and can be better quantified using the new STAINIFICATION software. Formulation of dispersion compounds and antibiotics into a dry powder aerosol could enable more effective treatment of biofilm infections in the lungs.

Abstract Approved: _____
Thesis Supervisor

Title and Department

Date

IN VITRO PSEUDOMONAS AERUGINOSA BIOFILMS: IMPROVED CONFOCAL
IMAGING AND CO-TREATMENT WITH DISPERSION AGENTS AND
ANTIBIOTICS

by

Stacy Sommerfeld Ross

A thesis submitted in partial fulfillment
of the requirements for the Doctor of
Philosophy degree in Pharmacy
in the Graduate College of
The University of Iowa

May 2013

Thesis Supervisor: Assistant Professor Jennifer Fiegel

Graduate College
The University of Iowa
Iowa City, Iowa

CERTIFICATE OF APPROVAL

PH.D. THESIS

This is to certify that the Ph.D. thesis of

Stacy Sommerfeld Ross

has been approved by the Examining Committee
for the thesis requirement for the Doctor of Philosophy
degree in Pharmacy at the May 2013 graduation.

Thesis Committee: _____
Jennifer Fiegel, Thesis Supervisor

Maureen Donovan

Douglas Flanagan

Gary Milavetz

Joseph Reinhardt

To Nathan and Wyatt.

ACKNOWLEDGMENTS

I would like to thank my advisor Dr. Jennifer Fiegel for her guidance and support. I would also like to thank my committee members: Dr. Maureen Donovan, Dr. Douglas Flanagan, Dr. Gary Milavetz, and Dr. Joseph Reinhardt. I would also like to thank Dr. Lee Kirsch and Dr. Aliasger Salem for their feedback on my research throughout the years. I am grateful to my lab mates Dr. Tim Brenza, Dr. Rania Hamed, Emily Thomas, Amir Farnoud, Mai Tu, Dan Schenck, Sachin Gharse, Bharath Kumar, Annie Kock, Lucy Sanchez, and Buffy Stohs. Special recognition is given to Annie Kock and Lucy Sanchez who completed undergraduate research on the dry powder aerosol project. Special recognition is also given to Dr. Stanier for use of his computer program for fitting the aerosol size distributions. I would like to acknowledge Dr. Alex Horswill, Dr. Megan Kiedrowski, Dr. Michael Apicella, Dr. Megan Falsetta Wood, and Meg Ketterer for microbiology discussions and access to confocal images. Special thanks are given to the Central Microscopy Facility and the aid of Tom Moninger, Jean Ross, and Kathy Walters. Last, but not least, I would like to thank my family for their support and encouragement.

ABSTRACT

Pseudomonas aeruginosa bacterial biofilms are the leading cause of mortality among cystic fibrosis (CF) patients. Biofilms contain bacteria attached to a surface and encased in a protective matrix. Since bacteria within a biofilm are less susceptible to antibiotics, a new approach is to use dispersion compounds that cause the biofilms to release free-swimming bacteria. Our approach has focused on combining nutrient dispersion compounds with antibiotics to increase eradication of bacteria within biofilms. This approach takes advantage of the enhanced susceptibility of free-swimming bacteria to antibiotics, compared to bacteria within biofilms. Ultimately, this research will guide the development of an aerosol therapy containing both antibiotic and dispersion compounds to treat bacterial biofilm infections.

To study the effect of antibiotic and dispersion compound treatments on biofilm eradication, a high-throughput screening assay was used to assess the effect on young *Pseudomonas aeruginosa* biofilms. In addition, a Lab-Tek chambered coverglass system imaged via confocal microscopy was used to assess the effect on mature *Pseudomonas aeruginosa* biofilms. Seven antibiotics (amikacin disulfate, tobramycin sulfate, colistin sulfate, colistin methanesulfonate (CMS), polymyxinB sulfate, erythromycin, and ciprofloxacin hydrochloride) were tested alone or in combination with four nutrient dispersion compounds (sodium citrate, succinic acid, xylitol, and glutamic acid) to assess the level of eradication of bacteria within biofilms. For young biofilms, 15 of 24 combinations significantly eliminated more live bacteria within the biofilms (measured in colony forming units per milliliter) compared to antibiotics alone. In the more mature biofilm system, only 3 out of 26 combinations resulted in a higher percentage of live biofilm bacteria being eliminated compared to antibiotics alone, showing the importance of biofilm age in the effectiveness of these potential combination therapies.

To aid in confocal microscopic analysis of biofilms, an automated quantification program called STAINIFICATION was developed. This new program can be used to

simultaneously investigate connected-biofilm bacteria, unconnected bacteria (dispersed bacteria), the biofilm protective matrix, and a growth surface upon which bacteria are grown in confocal images. The program contains novel algorithms for the assessment of bacterial viability and for the quantification of bacteria grown on uneven surfaces, such as tissue. The utility of the viability assessments were demonstrated with confocal images of *Pseudomonas aeruginosa* biofilms. The utility of the uneven surface algorithms were demonstrated with confocal images of *Staphylococcus aureus* biofilms grown on cultured human airway epithelial cells and *Neisseria gonorrhoeae* biofilms grown on transformed cervical epithelial cells.

Finally, a proof-of-concept study demonstrated that dry powder aerosols containing both antibiotic and nutrient dispersion compounds could be developed with properties optimized for efficient deposition in the lungs. A design of experiments study showed that solution concentration was the most significant parameter affecting aerosol yield, particle size, and *in vitro* deposition profiles.

Collectively this work demonstrated that bacterial dispersion from biofilms can enhance antibiotic susceptibility and can be better quantified using the new STAINIFICATION software. Formulation of dispersion compounds and antibiotics into a dry powder aerosol could enable more effective treatment of biofilm infections in the lungs.

TABLE OF CONTENTS

LIST OF TABLES	ix
LIST OF FIGURES	xii
CHAPTER 1 INTRODUCTION	1
1.1 <i>Pseudomonas aeruginosa</i> in Cystic Fibrosis Patients	1
1.2 Antibiotic Treatments	2
1.3 Antibiotic Resistance Mechanisms	4
1.4 Alternative Approaches	8
1.4.1 Compounds that Cue Bacterial Dispersion.....	10
1.4.2 Combining Antibiotics with Compounds that Cue Dispersion	12
1.4.3 Nutrient Dispersion	13
1.5 In Vitro Systems to Study Biofilms.....	14
1.6 Quantification of Biofilms.....	16
1.7 Objectives	18
CHAPTER 2 HIGH-THROUGHPUT SCREENING OF DISPERSION COMPOUNDS AND ANTIBIOTICS AGAINST YOUNG <i>PSEUDOMONAS AERUGINOSA</i> BIOFILMS	24
2.1 Introduction.....	24
2.2 Materials and Methods	26
2.2.1 Materials	26
2.2.2 Bacterial Strain and Culture Conditions.....	27
2.2.3 Biofilm Growth Controls.....	28
2.2.4 Biofilm Treatments.....	30
2.3 Results.....	32
2.3.1 Peg Biofilm Growth Controls.....	32
2.3.2 Dispersion Screening.....	33
2.3.3 Minimum Biofilm Eradication Concentration (MBEC) Assay Screening	35
2.3.3.1 Treatment Effects on Free-swimming Bacteria	35
2.3.3.2 Treatment Effects on Biofilm Bacteria	35
2.3.3.3 Co-treatment with Fluoroquinolone Against Biofilms.....	35
2.3.3.4 Co-treatment with Aminoglycosides Against Biofilms	36
2.3.3.5 Co-treatment with Cyclic Polypeptides Against Biofilms.....	37
2.3.3.6 Further Investigation of Colistin Methanesulfonate with Sodium Citrate and Xylitol	38
2.4 Discussion.....	40
2.4.1 Peg Biofilm Growth Controls.....	40
2.4.2 Dispersion Screening.....	40
2.4.3 MBEC Screening.....	42
2.4.4 Further Studying Colistin Methanesulfonate with Sodium Citrate or Xylitol.....	47
2.5. Conclusions.....	48

CHAPTER 3 DISPERSION ENHANCES CONVENTIONAL ANTIBIOTIC ACTIVITY AGAINST MATURE <i>PSEUDOMONAS AERUGINOSA</i> BIOFILMS.....	76
3.1 Introduction.....	76
3.2 Materials and Methods	78
3.2.1 Materials	78
3.2.2 Bacterial Strain and Culture Conditions.....	78
3.2.3 Biofilm Treatments.....	79
3.2.4 Live/Dead Staining and Confocal Imaging.....	80
3.2.5 Image Quantification and Statistical Analysis	81
3.3 Results.....	81
3.3.1 Growth Controls	81
3.3.2 Investigating Combination Treatments	82
3.3.2.1 Controls	82
3.3.2.2 Co-treatment with Aminoglycosides.....	84
3.3.2.3 Co-treatment with Cyclic Polypeptides.....	85
3.3.2.4 Co-treatment with a Macrolide.....	86
3.4 Discussion.....	86
3.4.1 Growth Controls	86
3.4.2 Investigating Combination Treatments	87
3.5 Conclusions.....	92
 CHAPTER 4 INTRODUCING A NOVEL QUANTIFICATION PROGRAM STAINIFICATION FOR BIOFILM CONFOCAL IMAGE ANALYSIS.....	 109
4.1 Introduction.....	109
4.2 Materials and Methods	113
4.2.1 Development of STAINIFICATION	113
4.2.1.1 Thresholding.....	114
4.2.1.2 Colocalization Adjustment Algorithm for Bacteria	114
4.2.1.3 Applying Connected Volume Filtration to Multiple Channels	115
4.2.1.4 Maintaining the Connected and Unconnected Bacterial Populations	116
4.2.1.5 Quantifying Bacterial Viability.....	117
4.2.1.6 Saving “.tif” Image Sequences.....	117
4.2.1.7 Quantifying Bacteria on an Uneven Surface.....	118
4.2.1.7.1 Surface Quantification Parameters.....	118
4.2.1.7.2 Surface Code	119
4.2.2 <i>Pseudomonas Aeruginosa</i> Biofilm Growth.....	122
4.2.3 <i>Staphylococcus Aureus</i> Bacteria Grown on Cultured Human Airway Epithelial Cells	123
4.2.4 <i>Neisseria Gonorrhoeae</i> Bacteria Grown on Cervical Tissue	124
4.3 Results and Discussion	124
4.3.1 STAINIFICATION User Friendly Interface	125
4.3.2 Confocal Image Thresholding.....	126
4.3.3 Colocalization Adjustment	128
4.3.4 Connected-Biofilm Bacteria and Unconnected Bacteria.....	129
4.3.5 Quantifying Connected-Biofilm Bacteria, Unconnected Bacteria, and a Matrix Component.....	130
4.3.6 Quantifying Connected-Biofilm Bacteria, Unconnected Bacteria, and Surface.....	131

4.3.6.1 MCVF is Needed to Quantify Bacteria Grown on an Uneven Surface	131
4.3.6.2 Two Novel Parameters: Modified Substratum Coverage and Surface Association.....	134
4.3.7 Quantifying 4 Components Simultaneously: Connected-Biofilm Bacteria, Unconnected Bacteria, a Matrix Component, and Surface Material	137
4.4 Conclusions.....	138
CHAPTER 5 INVESTIGATING FORMULATION AND PROCESSING PARAMETERS FOR SPRAY DRIED AEROSOLS	173
5.1 Introduction.....	173
5.2 Materials and Methods	175
5.2.1 Materials	175
5.2.2 Central Composite Design.....	175
5.2.3 Particle Deposition	178
5.2.4 Scanning Electron Microscopy.....	181
5.2.5 Statistical Analysis	181
5.3 Results and Discussion	181
5.3.1 Yield	182
5.3.2 Mass Median Aerodynamic Diameter, MMAD	184
5.3.3 Fine Particle Fraction, FPF.....	188
5.3.4 Fine Particle Dose, FPD	189
5.3.5 Optimization	190
5.4 Conclusions.....	190
CHAPTER 6 CONCLUSIONS AND FUTURE PERSPECTIVES.....	224
6.1 Conclusions.....	224
6.2 Future Perspectives	226
APPENDIX SUPPLEMENTAL CODE.....	228
A.1 Colocalization Adjustment	228
A.2 Connected Volume Filtration (CVF) on Multiple Channels	229
A.3 Maintaining Connected-Biofilm and Unconnected Bacteria Separately	231
A.4 Viability Quantification Parameters	232
A.5 Saving “.tif” Processed Images.....	233
A.6 Uneven Surface Scripts.....	234
REFERENCES	244

LIST OF TABLES

Table 1-1:	Relevant mode of action and limitations for antibiotics of interest.	20
Table 2-1:	Concentrations of antibiotics used spanned the minimum inhibitory concentration (MIC) reported to inhibit free-swimming bacteria and the minimum biofilm eradication concentration (MBEC) reported to inhibit biofilm bacteria growth.	50
Table 2-2:	Absorbance readings by column of bacteria suspended in Hinton Mueller broth after 24 hours of growth in the MBEC assay.....	51
Table 2-3:	Absorbance readings by row of bacteria suspended in Hinton Mueller broth after 24 hours of growth in the MBEC assay.	52
Table 2-4:	Biofilm growth controls (log(CFU/mL)) for the dispersion screening assay plates at each time point tested.....	53
Table 2-5:	Biofilm bacteria growth (log(CFU/mL)) for dispersion screening study.....	54
Table 2-6:	Free-swimming bacteria growth (log(CFU/mL)) for dispersion screening study.....	55
Table 2-7:	Incidence of free-swimming bacteria and biofilm bacteria growth for untreated control, sterility control, and dispersion compound treatments alone in Minimum Biofilm Eradication Concentration (MBEC) assay screening study.....	56
Table 2-8:	Incidence of free-swimming bacteria and biofilm bacteria growth for Minimum Biofilm Eradication Concentration (MBEC) assay screening study with ciprofloxacin hydrochloride alone or in combination with dispersion compounds.....	57
Table 2-9:	Incidence of free-swimming bacteria and biofilm bacteria growth for Minimum Biofilm Eradication Concentration (MBEC) assay screening study with amikacin disulfate treatment alone or in combination with dispersion compounds.....	58
Table 2-10:	Incidence of free-swimming bacteria and biofilm bacteria growth for Minimum Biofilm Eradication Concentration (MBEC) assay screening study with tobramycin sulfate treatment alone or in combination with dispersion compounds.....	59
Table 2-11:	Incidence of free-swimming and biofilm bacteria growth for Minimum Biofilm Eradication Concentration (MBEC) assay screening study with polymyxin B sulfate treatment alone or in combination with dispersion compounds.....	60

Table 2-12: Incidence of free-swimming bacteria and biofilm bacteria growth for Minimum Biofilm Eradication Concentration (MBEC) assay screening study with colistin sulfate treatment alone or in combination with dispersion compounds.....	61
Table 2-13: Incidence of free-swimming bacteria and biofilm bacteria growth for Minimum Biofilm Eradication Concentration (MBEC) assay screening study with colistin methanesulfonate treatment alone or in combination with dispersion compounds.....	62
Table 2-14: Bacteria growth (log(CFU/mL)) of biofilm bacteria and free-swimming bacteria after treatment with colistin methanesulfonate (CM) alone or in combination with sodium citrate or xylitol determined using the plate counting method.	63
Table 3-1: Concentrations of antibiotic and dispersion compounds tested.	93
Table 3-2: Percent live biofilm bacteria and percent live free-swimming bacteria of untreated growth controls.	94
Table 3-3: Percent live biofilm bacteria quantified with STAINIFICATION after 1 day of treatment with antibiotics alone or in combination with dispersion compounds.....	95
Table 4-1: Comparison of COMSTAT, PHLIP, COMSTAT2-Beta, and STAINIFICATION.....	139
Table 4-2: Comparison of Otsu threshold values between STAINIFICATION local, COMSTAT global (substratum-based), and STAINIFICATION global (median-based).....	140
Table 4-3: STAINIFICATION quantification of dead and live connected-biofilm bacteria and unconnected bacteria with or without colocalization adjustment (CA).....	141
Table 4-4: Quantification of surface, connected-biofilm bacteria, and modified substratum coverage for Test Image 1.	142
Table 4-5: Comparison of original connected volume filtration (CVF) and modified connected volume filtration (MCVF) for quantifying connected-biofilm bacteria.....	143
Table 4-6: Quantified data for <i>Staphylococcus aureus</i> biofilms grown on cultured human airway epithelial cells (Calu-3).	144
Table 4-7: Quantification for modified substratum coverage and the bacteria associated with the surface for Test Image 2.	145
Table 4-8: Quantified data for <i>Neisseria gonorrhoeae</i> biofilms grown on transformed cervical epithelial cells.	146
Table 5-1: Central composite design of experiment solution parameters (pH and solution concentration) and processing parameters (inlet temperature atomizer air or spraying air flow rate, and solution flow rate).	192

Table 5-2:	Factor values for 32 runs in the central composite design.	193
Table 5-3:	Next Generation Impactor (MSP, Shoreview, MN) cutoff diameters for 60 L/min inhalation flow rate.....	195
Table 5-4:	Responses (mean \pm standard deviation) of percent yield, outlet temperature, average fine particle fraction in percent (FPF) $<$ 4.46, FPF $<$ 2.82, and fine particle dose (FPD) by run with n=3, except Run 31 with n=1.	196
Table 5-5:	Dry powder aerosol central composite design of experiment responses (mean \pm standard deviation) of mass median aerodynamic diameter (MMAD), bimodal responses (MMAD1, GSD1, MMAD2, and GSD2) by run with n=3, except Run 31 was n=1 due to low yield.	198
Table 5-6:	Optimal factor settings for future aerosol development by maximizing the yield, FPFs, and FPD, minimizing GSD1 and GSD2, and setting a target of MMAD1 and MMAD2 being between 1 and 8 μ m.	200

LIST OF FIGURES

Figure 1-1: Cystic fibrosis patients have a variety of respiratory infections throughout their lives	21
Figure 1-2: Three stages of biofilm evolution	22
Figure 1-3: Structure of alginate, which consists of repeating connections of mannuronic acid and guluronic acid	23
Figure 2-1: Minimum Biofilm Eradication Concentration assay consists of a 96-well plate with a lid that contains 96 plastic pegs protruding from the lid and into the wells	64
Figure 2-2: Structures of fluoroquinolones and aminoglycosides antibiotics	65
Figure 2-3: Structures of cyclic polypeptide antibiotics	66
Figure 2-4: Structures of dispersion compounds	67
Figure 2-5: Image of a streaked lawn of <i>Pseudomonas aeruginosa</i> bacteria.	68
Figure 2-6: Absorbance readings of <i>Pseudomonas aeruginosa</i> biofilm bacteria grown 24 hours in Hinton Mueller broth by MBEC assay column, which were the columns of the 96-well plate.	69
Figure 2-7: Absorbance readings of <i>Pseudomonas aeruginosa</i> biofilm bacteria grown 24 hours in Hinton Mueller broth by MBEC assay row, which were the rows of the 96-well plate.	70
Figure 2-8: Bacteria growth (log(CFU/mL)) of <i>P. aeruginosa</i> bacteria versus time	71
Figure 2-9: Incidence of biofilm growth versus antibiotic concentration for MBEC screening study.....	72
Figure 2-10: Incidence of biofilm growth versus antibiotic concentration for MBEC screening study.....	73
Figure 2-11: Incidence of biofilm growth versus antibiotic concentration for MBEC screening study.....	74
Figure 2-12: Bacteria growth (log(CFU/mL)) of biofilm bacteria and free-swimming bacteria versus antibiotic concentration	75
Figure 3-1: Confocal microscopy images of <i>Pseudomonas aeruginosa</i> biofilms	97
Figure 3-2: Three representative untreated controls for <i>Pseudomonas aeruginosa</i> biofilm growth.	98
Figure 3-3: Confocal microscopy images of the untreated control and dispersion compound treated <i>Pseudomonas aeruginosa</i> bacteria.....	99

Figure 3-4: Confocal images of biofilms after treatment antibiotics alone	100
Figure 3-5: Confocal microscopy images of <i>Pseudomonas aeruginosa</i> bacteria after treatment with amikacin disulfate alone or in combination with dispersion compounds.....	101
Figure 3-6: Confocal microscopy images of <i>Pseudomonas aeruginosa</i> bacteria after treatment with 1.8 mg/mL tobramycin sulfate alone or in combination with dispersion compounds.....	102
Figure 3-7: Confocal microscopy images of <i>Pseudomonas aeruginosa</i> bacteria after treatment with 6.3 mg/mL tobramycin sulfate alone or in combination with dispersion compounds.....	103
Figure 3-8: Confocal microscopy images of <i>Pseudomonas aeruginosa</i> bacteria after treatment with polymyxin B sulfate alone or in combination with dispersion compounds.....	104
Figure 3-9: Confocal microscopy images of <i>Pseudomonas aeruginosa</i> bacteria after treatment with colistin sulfate alone or in combination with dispersion compounds.....	105
Figure 3-10: Confocal microscopy images of <i>Pseudomonas aeruginosa</i> bacteria after treatment with colistin methanesulfonate alone or in combination with dispersion compounds.....	106
Figure 3-11: Confocal microscopy images of <i>Pseudomonas aeruginosa</i> bacteria after treatment with erythromycin alone or in combination with dispersion compounds.....	107
Figure 3-12: Erythromycin structure	108
Figure 4-1: Histogram of image pixel intensity on the x-axis and frequency on the y-axis.....	147
Figure 4-2: Steps for connected volume filtration algorithm.....	148
Figure 4-3: “.info” file for COMSTAT.....	149
Figure 4-4: COMSTAT user interface in MatLab	150
Figure 4-5: PHLIP user interface	151
Figure 4-6: COMSTAT2-Beta program interface in ImageJ.....	152
Figure 4-7: Illustration of connected-biofilm bacteria grown on top of an uneven surface and grown on top of the imaging substratum	153
Figure 4-8: “.info” file for STAINIFICATION.....	154
Figure 4-9: Screen shot of an Excel [®] file of data saved by STAINIFICATION.....	155
Figure 4-10: Screen shot of an Excel [®] file of the user chosen processing parameters saved by STAINIFICATION.....	156

Figure 4-11: Two windows of the STAINIFICATION program	157
Figure 4-12: Steps for using STAINIFICATION first window.....	158
Figure 4-13: Steps for using STAINIFICATION second window	159
Figure 4-14: Comparison of thresholding methods	160
Figure 4-15: Comparison of before and after colocalization adjustment is applied	161
Figure 4-16: Quantification steps for connected-biofilm bacteria and unconnected bacteria in COMSTAT or COMSTAT2-Beta.....	162
Figure 4-17: Steps required by STAINIFICATION to save “.tif” image sequences of the processed images	163
Figure 4-18: <i>Pseudomonas aeruginosa</i> confocal images used to demonstrate the utility of separating the connected-biofilm bacteria and the unconnected bacteria.....	164
Figure 4-19: <i>Pseudomonas aeruginosa</i> confocal images used to demonstrate the utility of separating the connected-biofilm bacteria and the unconnected bacteria for viability assessment	165
Figure 4-20: Quantification steps for connected-biofilm bacteria, unconnected bacteria, and matrix in COMSTAT or COMSTAT2-Beta	166
Figure 4-21: Quantification steps for connected-biofilm bacteria, unconnected bacteria, and a <i>flat</i> surface in COMSTAT or COMSTAT2-Beta	167
Figure 4-22: Four-slice images containing bacteria and surface components	168
Figure 4-23: Green-fluorescent <i>Staphylococcus aureus</i> biofilms grown on cultured human airway epithelial cells (Calu-3) stained with Cell Tracker Orange.....	169
Figure 4-24: Four-slice images containing bacteria and surface components with some overlap between bacteria and surface.....	170
Figure 4-25: Green-fluorescent <i>Neisseria gonorrhoeae</i> bacteria grown on transformed cervical epithelial cells with red-stained nuclei.....	171
Figure 4-26: Quantification steps for connected-biofilm bacteria, unconnected bacteria, matrix, and a <i>flat</i> surface in COMSTAT or COMSTAT2-Beta	172
Figure 5-1: Calibration curve of ciprofloxacin concentration versus corrected absorbance readings at 276 nm	201
Figure 5-2: The main effects plot of the effect the five factors have on the response variable yield (%).....	202
Figure 5-3: Surface plot of atomizer and solution concentration versus percent yield.....	203

Figure 5-4: Surface plot of inlet temperature and liquid flow versus percent yield	204
Figure 5-5: Surface plot of inlet temperature and solution liquid flow versus outlet temperature.	205
Figure 5-6: Aerosol size distribution by bin versus powder mass (blue = experimentally measured, red = single log normal fit)	206
Figure 5-7: Scanning electron microscopy image of Run 24	207
Figure 5-8: The main effects plot of the effect the five factors have on the response variable MMAD from the Copley Citdas software (Copley, Scientific, Nottingham, UK)	208
Figure 5-9: Surface plot of solution concentration and solution liquid flow versus MMAD from the Copley Citdas software.	209
Figure 5-10: Aerosol size distribution by bin versus powder mass (blue = experimentally measured, red = two log normal fit).....	210
Figure 5-11: Frequency particle size distribution curve	211
Figure 5-12: The main effects plot of the effect the five factors have on the response variable MMAD1	212
Figure 5-13: The main effects plot of the effect the five factors have on the response variable GSD1	213
Figure 5-14: The main effects plot of the effect the five factors have on the response variable MMAD2.....	214
Figure 5-15: Surface plot of the significant parameters solution concentration and solution liquid flow versus MMAD2.....	215
Figure 5-16: Surface plot of inlet temperature and atomizer rate versus MMAD2; the interaction of inlet temperature and atomizer significantly affected MMAD2.....	216
Figure 5-17: Surface plot of atomizer rate and solution concentration versus MMAD2.....	217
Figure 5-18: The main effects plot of the effect the five factors have on the response variable GSD2.....	218
Figure 5-19: The main effects plot of the effect the five factors have on the response variable FPF< 4.46 μm	219
Figure 5-20: Surface plot of solution concentration and the parameter solution liquid flow versus FPF<4.46 μm	220
Figure 5-21: The main effects plot of the effect the five factors have on the response variable FPF< 2.82 μm	221

Figure 5-22: The main effects plot of the effect the five factors have on the response variable fine particle fraction (FPD)222

Figure 5-23: Surface plot of pH and the parameter inlet temperature versus FPD.....223

CHAPTER 1

INTRODUCTION

1.1 *Pseudomonas aeruginosa* in Cystic Fibrosis Patients

Cystic fibrosis (CF) is a genetic disease where the lungs are highly susceptible to bacterial infections. Common infections are caused by *Pseudomonas aeruginosa*, *Burkholderia cepacia* complex, *Haemophilus influenza*, *Staphylococcus aureus*, methicillin resistant *Staphylococcus aureus*, and *Stenotrophomonas maltophilia*.¹ These infections affect about 70,000 people worldwide with approximately 1,000 new cases annually.² It is believed about ten million unaffected carriers have the defective CF transmembrane conductance regulator gene and could potentially pass the defect to offspring.² In 1955, most children with CF died prior to attending school. Now the median life expectancy has increased due to many advances in detection and treatment.¹

Pseudomonas aeruginosa (*P. aeruginosa*) commonly form infections in the lungs of cystic fibrosis patients. As cystic fibrosis patients age, *P. aeruginosa* becomes the prevalent bacterial species in the lungs, infecting about 80% of patients (Figure 1-1).¹ When the patient is young, the infections are acute and treatable with antibiotic therapy. As the patient ages, the infection becomes chronic and cannot be eliminated with antibiotics. During this time, *P. aeruginosa* transitions from a non-mucoid phenotype (acute infection, limited exopolysaccharide present) to a mucoid phenotype (chronic infection, viscous alginate-like exopolysaccharide present).³⁻⁴ When patient lung samples are positive for mucoid *P. aeruginosa*, this is the number one indicator of morbidity and mortality among the patients.³ These bacterial infections directly impact the median life expectancy of CF patients being only 37 years.¹

CF patients are more susceptible to bacterial infections than healthy people due to alterations in the lungs. With the loss of function of the cystic fibrosis conductance regulator protein, regulation of ions is not conducted properly. This leads to

microenvironments with changes in ion concentrations.⁵ The change in salt concentrations may prevent innate antimicrobial agents from being active in the lungs.⁵ Disruption of chloride ion transport in the CF lung assists in development of thick, dehydrated mucus that disrupts the airway surface liquid and mucociliary clearance.⁶ Limiting this natural defense mechanism of the lungs leads to a stagnant environment that promotes formation of new, organized communities of bacteria called biofilms. During inflammatory response to these infections, hydrogen peroxide release has been shown to stimulate *P. aeruginosa* conversion from the non-mucoid phenotype to mucoid, chronic phenotype.⁷ The mucoid bacteria require iron for metabolism and thrive in the CF environment with increased iron.³ The CF lungs also have increased nitrate and nitrite, which enable anaerobic biofilm growth in the presence of oxygen limitation within thick CF mucus.⁸ Decreased magnesium, which is sequestered by extracellular DNA in the lung mucus, triggers biofilm formation and aids bacteria in limiting membrane permeability against antibiotic therapy.⁹⁻¹⁰

1.2 Antibiotic Treatments

Cystic fibrosis patients receive long-term, aggressive antibiotic treatments to combat *P. aeruginosa* lung infections. Currently, the initial antibiotic therapy in patients chronically colonized with *P. aeruginosa* is nebulized tobramycin (TOBI[®]) in the United States and colistin methanesulfonate in Europe. As an alternative, other inhaled antibiotics, such as amikacin, aztreonam (Cayston[®]), or colistin, may be prescribed.¹¹⁻¹² The Cystic Fibrosis Foundation reported substantial benefits to be found with tobramycin inhaled antibiotic and moderate to small benefits with other inhaled antibiotics, including colistin, gentamicin, and ceftazidime.¹³

Early market inhaled therapies were focused on time-consuming nebulization. The time required for nebulization of TOBI[®] has been successfully reduced from 15

minutes to 4 minutes per treatment, with the introduction of a new nebulizer (PARI eFlow rapid).¹⁴ To further reduce the administration time, dry powder formulations are being investigated in clinical trials. Dry powder formulations have the advantages over nebulization of having more efficient deposition and faster, more convenient administration for patients. Current formulations in clinical trials contain the antibiotics tobramycin or ciprofloxacin. The TOBI[®] Podhaler[®], also known as tobramycin inhalation powder (TIP[®]), is currently approved in Europe as a dry powder formulation. It is in Phase III clinical trials in the United States and was shown to decrease administration time by 70% or 13 hours per treatment cycle of 28 days.¹⁵ Bayer's Cipro Inhale[®] is a dry powder ciprofloxacin-containing formulation currently in Phase III clinical trials.¹⁶

With early infections, patients will be prescribed an inhaled antibiotic and possibly also an oral antibiotic. Oral fluoroquinolones, such as ciprofloxacin and levofloxacin, are commonly prescribed for outpatient care.¹² The Cystic Fibrosis Foundation reported substantial benefits with the use of macrolide oral antibiotics since they have an additional benefit of decreasing inflammation.¹³ When lung function further deteriorates, intravenous antibiotics are prescribed and typically patients are admitted to the hospital for two or three weeks of treatment.¹² While these aggressive therapies alleviate some acute symptoms caused by the lung infection, the chronic infection is not completely eradicated.¹⁷

Similar to clinical results, many researchers have focused on applying combinations of antibiotics against *P. aeruginosa* biofilms, but have had limited success in inhibiting or eradicating biofilms.¹⁸⁻¹⁹ Prior to antibiotic treatments being commonly administered to CF patients, preserved lung tissue from patients colonized with mucoid *P. aeruginosa* showed colonization in the tracheobronchial regions of the lungs. After aggressive antibiotic therapy, lung explants from patients showed *P. aeruginosa* colonization in the alveolar region of the lungs, rather than the tracheobronchial

regions.¹⁷ Therefore, when antibiotics are not effective at eradicating all of the *P. aeruginosa* bacteria in the respiratory zone, the bacteria relocate to the conductive zone. Thus, it is important that the antibiotic treatment fully eradicate the bacteria. Aaron et al. tested the effectiveness of two- and three-antibiotic combinations against biofilms using 10 different antibiotics. Only 1 out of 53 combinations (tobramycin and meropenem) with two antibiotics were effective against biofilms. Only 5 out of 41 combinations with three antibiotics were bactericidal.¹⁸

Antibiotic therapies are ineffective clinically for two main reasons. The first is that clinicians focus on the antibiotic susceptibility of the free-swimming bacteria present in patient sputum samples to determine antibiotic prescriptions. The biofilm bacteria can be 100 times more tolerant to the antibiotic(s) than free-swimming bacteria. There is no direct correlation between free-swimming bacteria and biofilm bacteria susceptibility.¹⁸⁻¹⁹ The second is that bacteria within a biofilm have more antibiotic resistance mechanisms than free-swimming bacteria.^{9, 20-22}

1.3 Antibiotic Resistance Mechanisms

Biofilm bacteria form in many bacterial species for added protection. Biofilm bacteria have all the traditional resistance mechanisms of free-swimming bacteria, including modification of the antibiotic target site, efflux pumps, use of alternative metabolic pathways to avoid antibiotic target, and release of enzymes that destroy the antibiotic.²² Bacteria within biofilms also have additional resistance mechanisms. Biofilms consist of bacteria that attach to a surface and develop a community of bacteria within a protective matrix.²³ There are three general steps for biofilm evolution (Figure 1-2).²⁴ First, the free-swimming bacteria attach to a surface, such as glass or tissue. These bacteria use flagella to swim in the liquid medium and use pili and lectins to attach to a surface.²⁵⁻²⁶ As bacteria attach to the surface, small microcolonies or communities of

bacteria develop with a viscoelastic matrix surrounding the bacteria. The bacteria inside the biofilm may make up 10% of the biofilm, while the matrix may make up 90% of the biofilm.²⁷ The matrix is structurally supported by polysaccharides, alginate, and DNA in a three-dimensional architecture with dense regions, pores, and water channels.²⁸⁻²⁹ This early stage of biofilm formation affords extra protection to the bacteria compared to their free-swimming counterparts. In 26 out of 36 instances, the first layer of bacteria that attached to a surface within 2 hours had reduced antibiotic susceptibilities compared to free-swimming bacteria.¹⁸

Over time, the bacteria enter the second stage of mature biofilm growth. Depending on growth conditions, the mature biofilms can develop as a flat lawn of biofilm, ripples of biofilm, or as towers of biofilm.³⁰⁻³¹ In mature biofilms, the first line of defense is the biofilm matrix. The architecture of the matrix varies greatly; it depends on the bacterial species and strain as well as the growth conditions. There are multiple microenvironments within the matrix that differ in pH, oxygen concentration, nutrient concentration, and bacterial cell density.³² The matrix contains polysaccharides (1-2%), proteins and enzymes (<1-2%), DNA and RNA from lysed bacterial cells (<1-2%), water (up to 97%), and possibly ions.²⁸ The matrix structure depends primarily on hydrated polysaccharides that are relatively water soluble with large molecular masses, resulting in viscous aqueous solutions. In *P. aeruginosa*, the most common polysaccharides are polysaccharide synthesis locus (Psl) that is composed of repeating D-mannose, D-glucose, and L-rhamnose, the glucose-rich polysaccharide (Pel), and alginate.³³ Psl is required for initial biofilm adherence to a surface and plays important roles in cell to cell interactions and cell to surface interactions. Psl holds the bacterial cells together in the matrix.³³ Pel is important for biofilm formation at air-liquid interfaces and for maintaining the biofilm structure; however it is not vital for biofilm adherence to a surface.³³ Mucoid strains of *P. aeruginosa* produce alginate, which consists of nonrepetitive monomers of D-mannuronic acid and L-guluronic acid (Figure 1-3).³³

Alginate increases the viscosity of the biofilm, forms a gel, and binds water to keep the biofilm hydrated.³⁴ Hydrogen bonds and electrostatic interactions are the primary forms for maintaining the biofilm matrix. Physical entanglement, repulsive forces, van der Waals interactions, and ionic forces also aid in the structural integrity of the matrix.^{27, 35}

It has been demonstrated that negatively charged alginate and DNA within the matrix can bind cationic antibiotics, such as aminoglycosides and cyclic polypeptides, and lead to poor penetration of the antibiotics.^{9, 36} Abdi-Ali et al. investigated the penetration of various antibiotics at a concentration of 64 µg/mL in a pH 7.5 buffered solution through 1% alginate that was isolated from a mucoid *P. aeruginosa* strain. The polycationic aminoglycosides, gentamicin and amikacin, attained 73% and 59% penetration, respectively, after allowing 24 hours for diffusion. The zwitterionic fluoroquinolones, ciprofloxacin, had 90% penetration. The single positively-charged macrolides, azithromycin and erythromycin, had 100% penetration for both antibiotics.³⁶ Kumon et al. investigated the penetration of various antibiotics at the concentration of 1 µg/mL in buffered phosphate solution (pH 7) through 1% alginate that was isolated from a mucoid *P. aeruginosa* strain. Polycationic aminoglycosides, gentamicin and tobramycin, had no penetration through the alginate after 24 hours. Polycationic cyclic polypeptides, polymyxin B and colistin, also had no penetration through the alginate after 24 hours. The single positively-charged macrolides, azithromycin, clarithromycin, and erythromycin, had full penetration through the alginate. The zwitterion fluoroquinolones, ofloxacin and ciprofloxacin, had 95-100% penetration through the alginate. The negatively charged beta-lactams, carbenicillin, piperacillin, ceftazidime, and imipenem, had full penetration through the alginate.³⁷ Walters et al. recorded the penetration of tobramycin and ciprofloxacin in pH 7.2 buffered solution through 48-hour old *P. aeruginosa* biofilms. Treatment with 10 µg/mL polycationic tobramycin took 12 hours to have measureable penetration and after 36 hours only had 30% penetration into the biofilm. Treatment with 1 µg/mL zwitterionic ciprofloxacin began penetrating the

biofilm within an hour and had 100% penetration by 8 hours.³⁸ Therefore, polycationic aminoglycoside and cyclic polypeptide antibiotics may have penetration limitations into the negatively charged matrix, while zwitterionic fluoroquinolones, positively-charged macrolides, and negatively-charged beta-lactams do not have penetration limitations.

Within the matrix, a biofilm community can have nutrient and oxygen gradients that lead to different rates of bacterial growth. King et al. observed different bacterial growth rates caused by oxygen limitations reduced the effectiveness of antibiotics.³⁹ Different antibiotic classes are effective against bacteria with high or low metabolic activity (Table 1-1). With high metabolic activity, bacteria are replicating and able to adapt to antibiotic treatments. With low metabolic activity, the bacteria are slowly replicating or may become dormant and less able to adapt to antibiotic treatments. Aminoglycosides, fluoroquinolones, and macrolides are effective against bacteria with high metabolic activity within the biofilm since the bacteria need to be synthesizing proteins or DNA to be effected.⁴⁰ Aminoglycosides inhibit bacterial protein synthesis by binding to the 30S ribosomal subunit.⁴⁰ The aminoglycosides antibiotics are able to cross the outer membrane of gram-negative bacteria through an energy-independent process of disrupting Mg²⁺ bridges.⁴⁰ Fluoroquinolones inhibit topoisomerases, which are the enzymes that supercoil and relax DNA.⁴⁰ Macrolide antibiotics inhibit protein synthesis by reversibly binding to the 50S ribosomal subunit for protein synthesis. Unlike the other macrolides, erythromycin is able to fully prevent, rather than just alter, the assembly of the 50S subunit.⁴⁰ Cyclic polypeptides are effective against bacteria with low metabolic activity in the biofilm.⁴⁰ Cyclic polypeptides are amphipathic compounds that act similar to a detergent to alter the permeability of the inner membrane of gram-negative bacteria.⁴⁰ The antibiotics interact with the lipopolysaccharide on the gram-negative bacteria outer membrane to cross the membrane to its target.⁴⁰

Bacteria within the biofilm also have a communication system (quorum sensing) to aid in adaptation to antibiotic treatment. Shih and Huang observed removal of quorum

sensing communication between bacteria reduced biofilm maturation and made the biofilm more susceptible to lower concentrations of antibiotics compared to a biofilm with quorum sensing.²¹ Finally, a population of persister cells may develop. Fauvart et al. observed persister cells were able to survive aggressive antibiotic therapy and were able to grow when the antibiotic treatment was removed. This newly grown population was later sensitive to the antibiotic, indicating the persister cells were not intrinsically resistant to the antibiotic treatment.²⁰

Finally, the bacteria within the biofilm reach the detachment stage where they have the ability to disperse out of the biofilm.^{25, 41} Dispersion is particularly problematic in health care since it allows for recolonization of bacterial infections in patients when antibiotic treatment is stopped.⁴¹

1.4 Alternative Approaches

Efforts have been made to develop vaccines to prevent *P. aeruginosa* infections and to develop treatment enhancers that inhibit inactivating enzymes or prevent bacterial attachment. Ideally, a vaccine could be used to prevent the chronic biofilm infection. The lipopolysaccharide vaccines Pseudogen[®] and Aerugen[®] were not successful in Phase III clinical trials.⁴²⁻⁴³ However, more recently a flagella-based vaccine has shown promise in Phase III clinical trials with 51% protection from chronic *Pseudomonas aeruginosa* infections.⁴⁴

Beyond vaccines, treatments have been developed to bypass antibiotic resistance mechanisms. Beta lactam antibiotics are commonly used as intravenous treatments. However, beta lactamase enzymes are released by bacteria within biofilms to inactivate the antibiotic. AstraZeneca has a Phase III beta lactamase inhibitor and cephalosporin combination strategy to be completed in 2014 in Europe and Japan and in 2016 in China. This combination approach is not being filed in the United States.⁴⁵ Another alternative

approach is to prevent bacterial attachment of lectins, which are bacterial outer membrane proteins that attach to lung epithelia. Fucose and galactose lectin inhibitors were inhaled by cystic fibrosis patients, which led to significant decreases of *P. aeruginosa* in patient sputum.⁴⁶

Researchers have been investigating other alternative approaches that include efflux pump inhibitors, quorum sensing inhibitors, type III secretion prevention, iron chelators, matrix disruptors, biofilm dispersion agents, and phage therapy.⁴⁷⁻⁴⁸ Efflux pumps are used as antibiotic resistance mechanisms by both free-swimming bacteria and biofilm bacteria to remove antibiotics from bacterial cells. Coban et al. demonstrated that an efflux pump inhibitor, MC-207110, significantly reduced fluoroquinolone resistance *in vitro* in biofilms.⁴⁷ Quorum sensing is used as a communication system in biofilm bacteria to resist antibiotic treatment. Furanones have been observed to interfere with quorum sensing and to increase bacterial clearance from lungs in mice.⁴⁹ Type III secretions are appendages used by bacteria to identify and deliver cytotoxins into host cells. Frank et al. demonstrated an anti-PcrV antibody, which is aimed against a central protein in the type III secretion system, neutralized the *P. aeruginosa* infection.⁵⁰ Iron is important in bacterial metabolism and release of virulence factors. Gallium nitrate has been shown to reduce the ability of biofilms to resist antibiotic treatments by interfering with iron metabolism.⁵¹ Researchers are also investigating ways to disrupt the matrix since the matrix maintains the structural integrity of the biofilm. Matrix disruption by the enzyme alginate lyase has been shown to enhance the antibiotic effectiveness on bacteria within biofilms.⁵² Biofilm dispersion agents cause bacteria to leave the protective biofilm and, in the process, weaken the biofilm matrix. Compounds, such as nutrients, oxygen, or nitric oxide, have been shown to cause bacteria to disperse out of biofilms.⁵³⁻⁵⁶ Finally, phage therapy is used to infect the bacteria with a virus and cause cell lysis. Phages can produce polysaccharide depolymerases to degrade the matrix and can reduce bacterial counts by viral infection and cell lysis.⁵⁷⁻⁵⁸ Purification of the phage products,

known as lysins, can be used to create cell lysis with small quantities. Nelson et al. observed nanogram quantities of lysins could be used to reduce bacterial numbers by 6 log units in seconds.⁴⁸

1.4.1 Compounds that Cue Bacterial Dispersion

Dispersion is a natural progression of biofilm maturation. It involves active participation of bacteria as they react to environmental cues.⁵⁹ Dispersion allows bacteria to release out of the biofilm when interior environmental conditions may be unfavorable; nutrient gradients are common in biofilms, such that depletion of the nutrient carbon source can lead to starvation. The three main steps for dispersion are communication through quorum sensing, transition from nonmotile to motile bacteria, and enzymatic degradation of the biofilm matrix to afford an escape route.³² Bacteria within the biofilm use quorum sensing through release of small acyl homoserine molecules to initiate dispersion.³² Bacteria within the biofilm transition from being nonmotile to motile to escape from the biofilm. Gene expression for pili (attachment appendages) has been observed to decrease as the bacteria release from the substratum surface and from the matrix.⁵⁵ Gene expression for flagella has been observed to increase as the bacteria become motile.⁵⁵ The bacteria must detach from the matrix and degrade portions of the matrix to escape from the biofilm. Therefore, *P. aeruginosa* produces alginate lyase to create a path to leave the matrix. This also weakens the matrix structure by reducing the alginate connections and makes the biofilm less stable.⁵⁹⁻⁶⁰ Many researchers are investigating dispersion as a method to disrupt biofilms. A wide variety of compounds are able to disperse the bacteria out of the biofilm, including environmental conditions, external stressors, enzymes, and internal signals.

Environmental conditions, such as oxygen⁵⁶, nutrients⁵⁵, and pH⁶¹, have been observed to trigger dispersion. Thromann et al. observed when biofilms were grown in

flow cells for 16 hours and the flow was stopped for 5 minutes that 80% of the biofilm bacteria mass was dispersed. It was determined that the major trigger for dispersion was the decrease in oxygen associated with the stopped flow.⁵⁶ Sauer et al. observed the nutrient compounds glucose, sodium citrate, sodium glutamate, and sodium succinate induced dispersion in flow cells.⁵⁵ Chen and Stewart reported a pH shift from 6.4 to 2.9 or from 6.4 to 11.2 also induced dispersion.⁶¹

A variety of external stressors have been found to cause dispersion. External stressors include simple salts⁶¹, chelating agents⁶¹⁻⁶², surfactants^{61, 63}, nitric oxide⁵³, and synthetically-derived compounds.⁶⁴ Chen and Stewart reported simple salts NaCl, CaCl₂, MgCl₂, and NH₂Cl all induced dispersion.⁶¹ The chelating agents ethylenediaminetetraacetic acid (EDTA) and Dequest 2006 and the surfactants sodium dodecyl sulfate (SDS), Tween 20, and Triton X-100 all caused greater than 25% of biofilm protein to be removed.⁶¹ Boles et al. observed a biosurfactant, rhamnolipids, mediated detachment of *P. aeruginosa* bacteria from biofilms.⁶³ Nitric oxide induced dispersion even at sublethal nanomolar doses.⁵³ 2-aminoimidazole-derived compounds have been shown to both inhibit and disperse biofilms.⁶⁴

Pertinent enzymes for dispersion include lysozyme⁶¹ and alginate lyase⁵². Bacteriophages with enzymatic activity also cause dispersion.⁶⁵ Enzymes can be naturally occurring or bioengineered.^{61, 65-66} Lysozyme is part of the innate immune system and has been shown to reduce the biofilm protein by 40%.⁶¹ Alginate lyase is naturally secreted by *Pseudomonas aeruginosa* to enable the bacteria to make a path out of the biofilm during dispersion.^{52, 66} Alkawash et al. observed alginate lyase degraded the exopolysaccharide in the matrix produced by mucoid *P. aeruginosa* biofilms.⁵² Lu and Collins engineered an enzymatic bacteriophage that could degrade the matrix and simultaneously infect the bacterial cells with a virus to cause cell lysis.⁶⁵

Internal signals also play a role in biofilm dispersion. Internal signals include a gene shown to affect chemotaxis⁶⁷, fatty acid molecule synthesis⁶⁸, and autoinducing

peptide release.⁶⁹ Morgan et al. identified the gene BdlA was essential for regulating chemotaxis and thus dispersion.⁶⁷ Davies and Marques used a small fatty acid molecule, cis-2-decenoic acid, which is naturally produced by *P. aeruginosa*, to disperse biofilms of both gram-negative bacteria and gram-positive bacteria.⁶⁸ Boles and Horswill reported the autoinducing peptide AIP-I reduced the biofilm by 91% within 48 hours of AIP-I addition.⁶⁹

1.4.2 Combining Antibiotics with Compounds that Cue

Dispersion

Clinically, antibiotics and dispersion compounds have not been combined for patient treatments. However, researchers have investigated combining antibiotics with dispersion compounds to reduce viability of *in vitro* biofilms. To combat antibiotic resistance mechanisms of the biofilm, it is important to combine dispersion compounds with antibiotics; the dispersion compounds weaken the matrix integrity and cause bacteria to leave the protective environment while the antibiotic kills the escaping bacteria and the bacteria within the weakened biofilm structure. Chen and Stewart reported the surfactant, 1000 µg/mL SDS, dispersed and killed bacteria. SDS treatment alone reduced the biofilm protein by 79% and reduced the viable bacteria by 37%. Combining 1000 µg/mL SDS with 200 µg/mL chloramphenicol reduced the biofilm protein by 91% and reduced the viable bacteria by 97% compared to an untreated control.⁶¹ Banin et al. investigated chelator-induced dispersal and killing of *P. aeruginosa* biofilms. They reported synergistic killing with 50 mM of the iron chelator EDTA and 50 µg/mL of the antibiotic gentamicin.⁶² Barraud et al. observed 500 nM nitric oxide significantly enhanced the efficacy of 100 µM tobramycin against *P. aeruginosa* biofilms.⁵³ Rogers et al. reported 32 µg/mL of a 2-aminoimidazole-derived compound enhanced the antibiotic effectiveness of novobiocin at 1 µM against

Staphylococcus epidermidis biofilms, novobiocin at 0.1 μM against *Staphylococcus aureus* biofilms, and tobramycin at 10 μM against *P. aeruginosa* biofilms.⁶⁴ Lamma and Griswold observed synergistic killing of *P. aeruginosa* biofilms with 1000 $\mu\text{g/mL}$ alginate lyase and 500 $\mu\text{g/mL}$ tobramycin.⁶⁶ Alkawash et al. observed co-administration of 20 U/mL alginate lyase with 64 $\mu\text{g/mL}$ gentamicin significantly reduced viable *P. aeruginosa* biofilm bacteria.⁵²

1.4.3 Nutrient Dispersion

Bacterial nutrient compounds show promise for causing dispersion since they are inexpensive additives that could be easily added to existing treatments. Early studies have focused on the chemotaxis effect of nutrients on bacteria.⁷⁰⁻⁷¹ Moulton and Montie showed glucose, amino acids, and organic acids attracted *P. aeruginosa* bacteria to swim toward the nutrients.⁷¹ It has been observed that gene clusters involved in pili and twitching motility needed for dispersion were similar to chemotaxis proteins.⁷² As the dispersion occurs, gene expression for pili, hair-like appendages used for attachment, decreases and gene expression for flagella motility increases.⁵⁵ Sauer et al. showed the nutrient compounds glucose, sodium citrate, sodium succinate, and sodium glutamate caused dispersion.⁵⁵ The theory behind nutrient dispersion is that the bacteria remain in the biofilm as a survival mechanism where they are protected from the external environment. Upon addition of nutrients, the external environment is high in nutrient concentration. The bacteria release from within the biofilm to consume these nutrients, since within the biofilm nutrient concentration gradients can lead to starvation of some bacteria in the biofilm.^{55, 59} Once released from the biofilm, the bacteria may be more susceptible to antibiotics,⁶³ although this has not been proven to date.

1.5 In Vitro Systems to Study Biofilms

Biofilms can be studied in open systems or closed systems. The four most common open systems consist of a flow cell, rotating disk biofilm reactor, Centers for Disease Control (CDC) reactor, and drip flow biofilm reactor. Closed systems consist of a static biofilm grown on agar or use of 96-well plates, the Minimum Biofilm Eradication Concentration assay, and chambered coverglass.

The most common open system is a flow cell that allows for continuous media or treatments to be administered to the bacteria.^{55, 62, 73} Large quantities of sterile media are fed horizontally through the flow cell, which typically has a flat coverglass bottom for real-time microscopic imaging of biofilm growth.⁶² Spent media leaves the flow cell and can be collected for evaluation of dispersed bacteria. With a flow cell, confocal microscopy can be used to visualize bacterial dispersion.⁵⁵ The biofilm bacteria are commonly quantified for total mass or bacterial viability using appropriate stains.^{62, 73} The biofilm bacteria and the dispersed bacteria can also be quantified by plating the bacteria and counting the colonies that grow.^{55, 62} The second open system is the rotating disk reactor. It has large quantities of sterile media flow into the top of the device and the spent media flows out of the bottom of the reactor. Within the reactor are coupons (flat disks) of 1.25 cm round Teflon disks for growing the biofilms.⁷⁴ At the bottom of the reactor a stir bar rotates to cause shear in the system, which can be greater than the shear achieved in a flow cell.⁷³ The CDC reactor is similar to the rotating disk reactor. It has media flow into the top of the reactor and spent media flows out the bottom of the reactor. This reactor allows for more sampling by having eight coupon holders. Each holder contains three coupons, which can be plastic, metal, or ceramic.⁷⁵ Like the rotating disk reactor, a magnetic stir bar rotates to cause shear in the system, which can be greater than the shear achieved in a flow cell.⁷³ Bacteria can be quantified by plating the bacteria or by staining and imaging via confocal microscopy.^{62, 76-77} Finally, a drip flow reactor uses large quantities of sterile media that are dripped onto a surface for

biofilm growth. The low shear is created as the drip travels down the inclined surface, promoting biofilm growth at the air-liquid interface.⁷⁸ Spent media can be collected as with the other reactors. Biofilm bacteria and dispersed bacteria can be quantified by plating the bacteria and counting the colonies.^{77, 79}

The simplest closed batch system is the static biofilm grown on agar.⁷⁷ The biofilm inoculum is saturated filter paper that gets set on top of the agar. A glass coupon is set on top of the filter paper. The nutrients come from the agar and the biofilm grows on the underside of the coupon. The biofilm bacteria can be quantified by plating and counting the colonies.⁷⁷ A 96-well plate or microtiter assay has been used to more easily assess many treatments simultaneously.^{68, 80} Biofilms are grown in the bottom of the wells and then treatments can be added to the wells of biofilms to be tested. With the 96-well plate assay, quantification is typically done via absorbance readings or plating the bacteria and counting colonies.^{73, 80-81} A special microtiter assay is the Minimum Biofilm Eradication Concentration (MBEC) assay.⁸² It consists of a 96-well plate with a lid containing 96 plastic pegs that fit into the wells for biofilm growth. The peg lid can be transferred to a 96-well plate to apply treatments to the biofilms. The bacteria can be quantified with absorbance readings or by plating the bacteria.⁸²⁻⁸⁴ Finally, the chambered coverglass is used to grow batch cultures of biofilms for confocal microscopy analysis. A single chambered coverglass can have multiple wells, which allows for comparison of different treatments. The bacteria can be qualitatively assessed in confocal images and can be quantified for mass or viability if appropriately stained.⁸⁵⁻⁸⁶

Open systems have the advantage over closed systems of developing denser biofilms due to the media flow and constant access of the bacteria to replenished nutrient media.^{62, 73, 85, 87} The open systems can be used to investigate biofilm growth on a variety of substratum materials, especially in the CDC reactor since it has the most coupon substratum holders.⁷⁵ However, all of the coupons in the rotating disk reactor and CDC reactor are exposed to the same growth media. Therefore, they cannot be used to assess

varying treatments (ie. antibiotics) against the biofilms in a single reactor.⁷⁵ Flow cells and drip flow reactors are also more difficult to use to assess varying treatments since a flow cell or drip flow reactor, media, and pump are needed per treatment. These systems also require more space in an incubator compared to the closed systems. The closed system has the advantage over the open systems of being used to investigate varying treatments in a single system.^{82-83, 87} The closed systems also do not require large quantities of growth media. However, since the systems do not have shear from media flow, the biofilms are generally less dense than those from open systems.^{62, 73, 85, 87}

1.6 Quantification of Biofilms

Biofilms are commonly quantified by three methods. The first is using absorbance readings for high-throughput quantification, which is the least sensitive, but least time-consuming of the three methods. The second is plate counting, which is the standard method for microbiologists. Plate counting is sensitive to 100 colonies.⁸⁸ The third is using confocal microscopy to capture images of biofilms that can be quantified with computer software. This method is sensitive to single bacterial cells.

Absorbance readings at 650 nm can be used to represent bacterial density. Free-swimming bacterial densities are uniform and proportional to absorbance readings.⁸⁹ Biofilm bacteria must be disrupted via sonication to create a uniform suspension prior to taking absorbance readings.⁸² This method is used routinely since it requires few materials and time. It is used commonly in microtiter and the MBEC assays.^{82, 90} Absorbance readings are used to quantify total bacteria, rather than viable bacteria.⁸⁹ Therefore, to further investigate viability it is common for researchers to use plate counting.

Plate counting, which is the gold standard in microbiology, can refer to pour plating, spread plating, or drop plating. All three of these methods have been shown to

be comparable to quantify viable colonies.⁹¹ In all cases, agar plates are created in petri dishes and the bacteria are counted. The spread and drop plate methods are the most common. Spread plating requires larger volumes of bacteria for enumeration. A bacterial sample is serially diluted 10-fold multiple times. For each dilution, 100 μ L of the sample is pipetted to an agar plate and spread with glass beads. For example, to enumerate eight dilutions, a total of eight agar plates will be needed per sample. Agar plates are inverted and incubated for 24 hours. After 24 hours, the agar plates are counted. The highest concentration plate that has 30-300 colonies gets recorded.^{88, 92} The drop plate method uses the same concept, but requires lower volumes. A single agar plate is inverted and eight quadrants are drawn on the underside. After the bacteria are serially diluted, a 10 μ L aliquot of each dilution is transferred to a quadrant on the agar plate. This drop remains and is not spread on the plate. For example, to enumerate eight dilutions, a total of one agar plate will be needed per sample. Agar plates are inverted and incubated for 24 hours. After 24 hours, the agar plates are counted. The highest concentration quadrant that has 3-30 colonies gets recorded.^{88, 92}

Confocal laser scanning microscopy (CLSM) is non-destructive, allowing real-time imaging of biofilms. Confocal images comprise a series of 2D images that can be rendered to generate 3D images with high resolution.⁹³ Stains can be used to label various components within the biofilm, including cells, proteins, polysaccharides, extracellular DNA, metabolic enzymes, or intracellular DNA. The most common live/dead stain used for bacterial viability is the BacLight Live/Dead kit with syto 9 green live fluorescent stain and propidium iodide red dead fluorescent stain.⁹⁴ It is also common for bacteria to be genetically-engineered to have fluorescent proteins for detection of total bacteria. These are most commonly green fluorescent proteins or red fluorescent proteins, which eliminate the need for using a stain to label the bacteria.³⁰ Computer software programs, such as ImageJ/Fiji or COMSTAT, can be used to quantify components in the confocal images.⁹⁵⁻⁹⁶ COMSTAT is the most commonly used

program in the biofilm field.^{30, 54, 62, 67, 96} Common quantification parameters are the total biofilm biomass, maximum thickness, average thickness, surface area, and substratum coverage.^{30, 54, 62, 67} The biomass or surface area parameters can be used to quantify the percent live or dead bacteria when viability stains are used. These allow researchers to compare biofilm architecture³⁰, identify biofilm dispersion⁶⁷, and evaluate viability after antimicrobial treatment.³⁰

1.7 Objectives

New clinical approaches are needed to improve the effectiveness of antibiotic treatments in cystic fibrosis patients. Researchers have demonstrated that dispersion compounds can enhance the activity of antibiotics. However, researchers have not combined nutrient dispersion compounds with antibiotics. Nutrient dispersion compounds are enticing co-therapies since they are simple, inexpensive additives that are generally regarded as safe. We hypothesize that treatments of antibiotics with nutrient dispersion compounds will reduce live bacteria in *P. aeruginosa* biofilms *in vitro*. Analysis of these new potential treatment strategies requires the ability to analyze both the dispersed bacterial population in addition to the biofilm population. Therefore, we aimed to develop algorithms to aid in bacterial viability analysis. Furthermore, we investigated formulating antibiotics and nutrient dispersion compounds into dry powder aerosols with optimized aerodynamic properties, which could lead to a treatment strategy for cystic fibrosis patients or other patients with *P. aeruginosa* infections in their lungs.

Objective 1: To identify compounds that enhance the dispersion and eradication of *in vitro Pseudomonas aeruginosa* biofilms

Specific Aim 1.1: To determine the time it takes for *P. aeruginosa* bacteria to disperse from a biofilm after treatment with nutrient dispersion compounds

Specific Aim 1.2: To determine the dispersion activity of xylitol, which may mimic nutrient dispersion, on *P. aeruginosa* bacterial biofilms

Specific Aim 1.3: To identify combinations of dispersion and antibiotic compounds that improve elimination of young and mature *P. aeruginosa* biofilms

Objective 2: To improve confocal microscopy quantification of biofilms

Specific Aim 2.1: To quantify biofilm bacteria and free-swimming bacteria to enhance analysis of bacterial viability

Specific Aim 2.2: To quantify biofilm bacteria grown on top of an uneven surface

Objective 3: To formulate a dry powder aerosol containing a dispersion and antibiotic compound via spray drying

Specific Aim 3.1: To investigate the effects of formulation and processing parameters on the yield, aerodynamic diameter, geometric standard deviation, fine particle fractions, and fine particle dose of dry powder aerosols to optimize aerodynamic properties

Table 1-1: Relevant mode of action and limitations for antibiotics of interest.

Antibiotic	Ciprofloxacin	Tobramycin & Amikacin	Colistin & Polymyxin B	Erythromycin
Class ⁴⁰	Fluoroquinolone	Aminoglycoside	Cyclic Polypeptide	Macrolide
Mode of Action ⁴⁰	Affect nucleic acid (inhibit DNA gyrase)	Act on cell wall (inhibit protein synthesis)	Act on membrane (alter permeability)	Act on cell wall (inhibit protein synthesis)
Biofilm Bacteria Population ^{40,120}	High metabolic activity	High metabolic activity	Low metabolic activity	High metabolic activity
Charge Effects (Algiate Limiting Penetration) ³⁶⁻³⁸	Minimal limitation	Limited penetration	Limited penetration	No limitation
Mg²⁺ Influence ^{9,97}	Has not been shown to have an effect	Limits outer membrane uptake	Limits outer membrane uptake	Has not been shown to have an effect

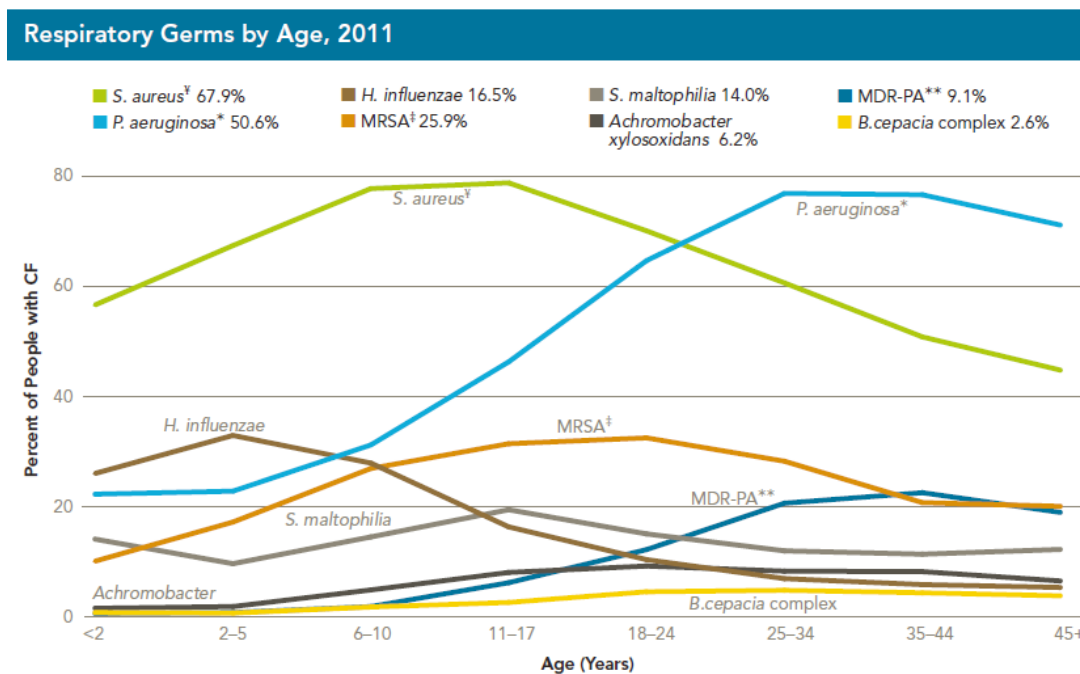


Figure 1-1: Cystic fibrosis patients have a variety of respiratory infections throughout their lives; most notably, *P. aeruginosa* becomes the prevalent bacterial species as the patient gets older; reprinted with permission from the Cystic Fibrosis Foundation.¹

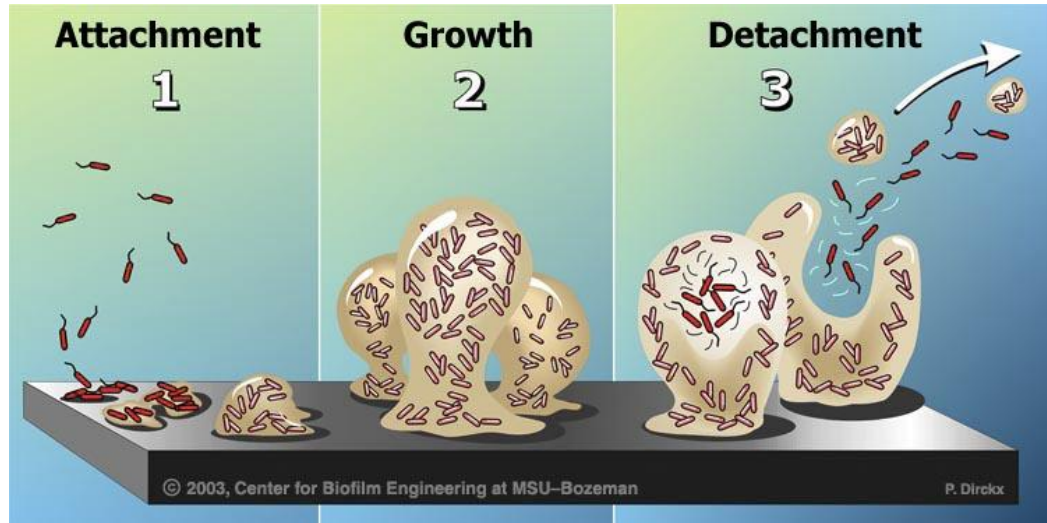


Figure 1-2: Three stages of biofilm evolution; free-swimming bacteria attach to a surface, grow into mature biofilms, and then bacteria are able to detach or disperse from within the biofilm; reprinted with permission from the Center for Biofilm Engineering.²⁴

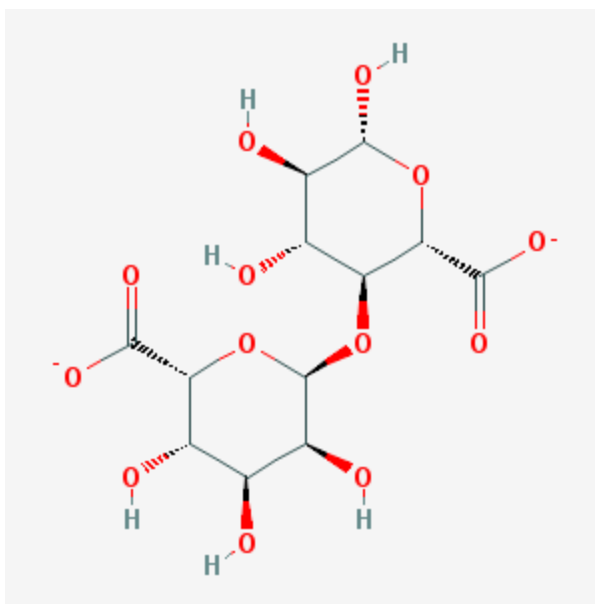


Figure 1-3: Structure of alginate, which consists of repeating connections of mannuronic acid and guluronic acid.⁹⁸

CHAPTER 2
HIGH-THROUGHPUT SCREENING OF DISPERSION COMPOUNDS
AND ANTIBIOTICS AGAINST YOUNG *PSEUDOMONAS*
AERUGINOSA BIOFILMS

2.1 Introduction

P. aeruginosa biofilms can be studied in a variety of systems, including open flow cells and closed batch systems. Most commonly flow cell chambers are used to develop biofilms under the stress of media flow. This method is known to grow thick biofilms; however it is limited by the number of samples that can be assessed simultaneously.^{55, 62, 81} Therefore many researchers use microtiter 96-well plates or the Minimum Biofilm Eradication Concentration (MBEC) assay to grow batch cultures of biofilms to investigate many samples.^{68, 80, 83, 99} The MBEC assay is most commonly used to examine the effectiveness of antimicrobial treatments,^{83-84, 100} although it has also been used to investigate bacterial dispersion.^{65-66, 101}

The MBEC assay consists of a 96-well plate where free-swimming bacteria reside within the wells with a peg lid where biofilm bacteria attach and grow as a community (Figure 2-1).⁸² Since these two bacterial populations can be quantified separately, dispersion can be assessed. Researchers have shown dispersion can be observed as a simultaneous increase in free-swimming bacteria and decrease in biofilm bacteria.^{55, 67} It is important to note that an increase in bacteria can occur due to bacteria replicating or due to the reversible attachment and detachment of bacteria to the biofilm.⁵⁹ The bacteria in the MBEC assay can be quantified quickly using high-throughput absorbance readings.^{82, 89-90, 101} Further quantification may be achieved with plate counting of bacteria, which has better sensitivity than absorbance readings but is labor intensive.^{88, 91-}

The MBEC assay can be used with absorbance readings to determine the minimum inhibitory concentration (MIC) that is observed to inhibit the growth of free-swimming bacteria and to determine the minimum biofilm eradication concentration (MBEC) that is observed to inhibit the growth of bacteria within a biofilm. Table 2-1 shows reported MIC and MBEC values for the fluoroquinolone, ciprofloxacin, aminoglycosides, amikacin and tobramycin, and cyclic polypeptides, polymyxin B and colistin. The concentrations needed to inhibit bacterial growth are dependent on bacterial age and growth conditions.^{9, 19, 83-84, 102-104} Ceri et al. grew *Pseudomonas aeruginosa* under the same growth conditions for 4 hours or 9 hours in the MBEC assay. The MIC values increased by about 1 order of magnitude for *Pseudomonas aeruginosa* grown for 9 hours compared to bacteria grown 4 hours.⁸³⁻⁸⁴ The MBEC values increased by 1 to 2 orders of magnitude for *Pseudomonas aeruginosa* biofilms grown 5 hours longer.⁸³⁻⁸⁴ In addition to growth age, the growth media significantly affects MBEC. Mulcahy et al. observed media supplemented with 20 μ M magnesium, rather than 2 mM magnesium, required an order of magnitude higher concentration of polymyxin B or colistin to inhibit biofilm growth.⁹

In this study, we used absorbance readings and plate counts to investigate dispersion in the MBEC device. Six antibiotic compounds were investigated (ciprofloxacin hydrochloride, amikacin disulfate, tobramycin sulfate, polymyxin B sulfate, colistin sulfate, and colistin methanesulfonate) since they are commonly used against *P. aeruginosa* biofilms.¹²⁻¹³ The fluoroquinolone, ciprofloxacin, is zwitterionic at pH 7 (Figure 2-2A).¹⁰⁵ The aminoglycosides, amikacin and tobramycin, are polycationic at pH 7 (Figure 2-2B-C).¹⁰⁶⁻¹⁰⁷ The cyclic polypeptides, polymyxin B and colistin, are polycationic at pH 7 (Figure 2-3A-B).¹⁰⁸ The cyclic polypeptide prodrug colistin methanesulfonate is polyanionic at pH 7 (Figure 2-3C); the prodrug hydrolyzes to the active antibiotic form, colistin.¹⁰⁸ The dispersion compounds investigated were sodium citrate, succinic acid, glutamic acid, and xylitol. The organic acids, sodium citrate

(Figure 2-4A) and succinic acid (Figure 2-4B), are polyanionic at pH 7.¹⁰⁹ The amino acid, glutamic acid (Figure 2-4C), is zwitterionic at pH 7. Xylitol (Figure 2-4D) is unionized at pH 7. The nutrient compounds sodium citrate, succinic acid, and glutamic acid were chosen because they were observed to have chemotaxis attraction for bacteria and to disperse bacteria.^{55,71} Upon dispersion, enzymes that degrade the biofilm matrix are released and thus weaken the biofilm structure. It is important to note that sodium citrate and succinic acid have other mechanisms of action. Sodium citrate is a nutrient dispersion compound that has the additional ability to permeabilize the outer membranes of bacteria, to act as a chelator, and to weaken the biofilm structure.^{55,123} Xylitol, which had not been previously investigated as a dispersion compound, was included since it also has the ability to decrease the amount of matrix component in the biofilm structure⁷⁶. Furthermore, it was investigated as a nutrient dispersion compound since it mimics being a nutrient for bacteria. Xylitol is initially taken up by the bacteria as a nutrient carbon source, increasing expression of metabolic activity genes.¹¹⁰ However, *P. aeruginosa* cannot metabolize xylitol and with time it accumulates as a xylitol phosphate that inhibits growth at large concentrations.¹¹¹ Xylitol is also an osmotic agent, which may hydrate the biofilm and, in doing so, modify the matrix structure.¹¹²

2.2 Materials and Methods

2.2.1 Materials

Nutrient Agar, Nutrient Broth, and Hinton Mueller Broth were purchased from Becton, Dickinson, and Company (Sparks, MD). Glycerol, amikacin disulfate, tobramycin sulfate, colistin sulfate, colistin methanesulfonate, polymyxin B sulfate, xylitol, and glutamic acid were purchased from Sigma Aldrich (St. Louis, MO). Sodium citrate dihydrate and sodium chloride were purchased from Research Products International Corp. (Mt. Prospect, IL). Ciprofloxacin hydrochloride and succinic acid

were from MP Biomedicals LLC (Solon, OH). Purified water was obtained from a NanoPure Infinity Ultrapure Water System (Barnstead Int., Dubuque, IA).

2.2.2 Bacterial Strain and Culture Conditions

The freeze-dried mucoid *Pseudomonas aeruginosa* strain BAA-47 (American Type Culture Collection, ATCC, Manassas, VA) was rehydrated per ATCC's recommended methods.¹¹³ Briefly, the glass vial was heated with a flame and the glass was cracked with cold water and pliers. Sterile nutrient broth (0.3 mL), which was autoclaved (Amsco Scientific, Tucson, AZ) on the liquid cycle at 121°C for 15 minutes, was added to the vial to suspend the freeze-dried bacterial pellet. The suspension was transferred to a glass test tube with 6 mL sterile nutrient broth, mixed by inverting, and incubated (VWR, West Chester, PA, 37°C and 70% relative humidity) for 24 hours. A mixture of 80% glycerol in sterile water was used for storing the bacteria. This mixture was used to create a final 50:50 suspension of glycerol and rehydrated bacteria. Each cryovial was filled with 0.25 mL of bacterial suspension. In the future, it is recommended to put at most 0.2 mL volume in cryovials since, once the bacteria thaws, it cannot be refrozen. Twenty samples were stored in liquid nitrogen and the remainder of the samples were stored in a -80°C freezer. It is recommended to keep bacteria stored below -50°C.¹¹⁴

Experiments were started from a thawed cryovial of bacteria and maintained on agar slants. Agar slants were prepared by transferring 10 mL mixed nutrient agar into 15 mL test tubes, autoclaving the filled test tubes, and placing them at a 45° angle while the agar hardened at room temperature. A nutrient agar slant was inoculated with a streak of bacteria from the thawed cryovial across the agar surface using an inoculating loop. The agar slant was incubated stationary at 37°C overnight and then stored in a refrigerator for

up to two weeks.¹¹⁴ Any bacteria maintained on nutrient agar slants were only passaged up to two generations to minimize mutations accumulating in the strain.¹¹⁴

From the nutrient agar slant, a lawn of bacteria were streaked onto nutrient agar in a petri dish (Figure 2-5).¹¹⁵ Using an inoculation loop, bacteria were transferred to the petri dish and wiped across the surface to cover 1/3 of the surface area. A fresh inoculating loop was used to dilute the bacteria by spreading a portion of the bacteria on the agar petri dish across another 1/3 of the agar surface. Finally a fresh inoculating loop was again used to dilute the bacteria by spreading a portion of the previously diluted bacteria across the remaining 1/3 of the agar surface. The agar plate was inverted and incubated at 37°C overnight. Three colonies were isolated from the agar plate and suspended in 5 mL sterile Hinton Mueller broth and incubated stationary at 37°C for 24 hours. The bacterial suspension was diluted to visually match a 0.5 McFarland turbidity standard (Fisher Scientific, Fair Lawn, NJ). Then 3 mL of the diluted suspension was transferred to 27 mL fresh Hinton Mueller broth. Twenty two milliliters of this final dilution were added to the trough of the Minimum Biofilm Eradication Concentration (MBEC) assay (Innovotech, Edmonton, Alberta, Canada).^{82, 100} The peg lid of the assay was placed on top of the trough and sealed with two layers of Parafilm™. Then the assay system was incubated (37°C) on a rocking table (VWR, West Chester, PA, 10° angle and 3 rocks per minute) for 24 hours.

2.2.3 Biofilm Growth Controls

After 24 hours, biofilm growth controls were quantified via absorbance readings or plate counting. The peg lid was removed from the trough, transferred briefly to a 96-well plate with 200 µL sterile water per well to rinse any loosely adhered bacteria from the peg lid, and then the lid was transferred to a 96-well plate with 200 µL sterile Hinton Mueller broth per well. The plate was sealed with Parafilm™, zipped closed in a plastic

bag to prevent water from entering, and sonicated with an ultrasonic bath (VWR, West Chester, PA) for 10 minutes to disrupt the biofilm bacteria from the peg lid into the wells of broth. For absorbance readings quantification, the peg lid was discarded and the 96-well plate with broth and bacteria was sealed with a flat lid and two layers of Parafilm™. The plate was incubated stationary at 37°C for 24 hours. After 24 hours, the absorbance readings of the bacteria in the wells were read at 650 nm using a SpectraMax Plus 384 (Molecular Devices, Sunnyvale, CA). A broth control plate was also read with the average absorbance readings of Hinton Mueller broth being 0.040 ± 0.003 . This broth control was subtracted from the bacteria plate readings. Significant differences ($p < 0.05$) of the absorbance readings by column ($n=8$) and by row ($n=12$) were investigated using Minitab 15 (Minitab Inc, State College, PA) via ANOVA with the Tukey Test to verify consistent biofilm growth in the assay. The Tukey Test was used to compare the absorbance readings of all columns and of all rows with an overall error rate of 5%.

For plate counting, after 24 hours of growing the biofilms on the peg lid, the lid was removed from the assay trough and the pegs were rinsed in a 96-well plate with 200 μ L sterile water per well to rinse any loosely adhered bacteria from the peg lid. Using sterile pliers, three pegs were moved from the peg lid and transferred to wells in a 96-well plate with 200 μ L sterile Hinton Mueller broth. The peg lid was discarded and the 96-well plate with broth and bacteria was sealed with a flat lid, Parafilm™, and a plastic bag. The plate was sonicated for 10 minutes to disrupt the biofilm bacteria from the peg lid into the wells of broth. The bacteria in the wells were serially diluted ten-fold across seven orders of magnitude and then spot plated to enumerate the number of colony forming units (CFU) per mL.⁹² Briefly, a black marker was used to draw eight pie quadrants on the bottom of an agar petri dish. Each quadrant was labeled 0 to 7 to indicate the dilution of the quadrant. Ten microliters from each dilution was transferred to the quadrant and the petri dish was left in the biocabinet for at least 5 minutes to prevent streaking of the drop. After 5 minutes, the petri dish was inverted and incubated

at 37°C for 24 hours. After 24 hours, the colonies were counted by finding the most concentrated quadrant with 3 to 30 separate colonies. Significant differences ($p < 0.05$) of the colony counts were quantified using Minitab 15 (Minitab Inc, State College, PA) via ANOVA with the Tukey Test. The Tukey Test was used to compare the biofilm controls for different MBEC assay plates with an overall error rate of 5%. Beyond statistical analysis, the average colony counts between samples had to have a difference of two orders of magnitude to be significant due to the sensitivity of the plate counting method. Results were reported as mean \pm standard deviation for $n=3$.

2.2.4 Biofilm Treatments

For the dispersion screening study, biofilms were treated for 0.5, 1, 2, 4, 8, 12, and 24 hours with 10 mM sodium citrate, succinic acid, or glutamic acid in media or 75 mM xylitol or sodium chloride in media for screening the dispersion compounds. The time points were chosen based on common time points investigated with antibiotic time studies. Two hundred microliters per treatment (compound dissolved in Hinton Mueller broth with a phosphate buffer at 37°C and pH 7.1) was transferred to each well with $n=3$ per treatment. The phosphate buffer was created with 2.995 g sodium monobasic phosphate and 9.083 g potassium dibasic phosphate, which were added to 400 mL Hinton Mueller broth and sterile filtered. The peg lid with biofilm growth was placed on the 96-well plate with the treatments. The plates were sealed with two layers of Parafilm™ and incubated stationary at 37°C for the allotted time. After the allotted treatment time, free-swimming bacteria and biofilm bacteria were quantified by plate counting. After treatment, aliquots from the 96-well plates were serially diluted as sixteen 10-fold dilutions for the first five time points and as twenty four 10-fold dilutions for the last two time points and spot plated to quantify CFU/mL of free-swimming bacteria. After treatment, the peg lid of the assay was transferred to a 96-well plate with fresh Hinton

Mueller broth and sonicated for 10 minutes to disrupt the biofilm bacteria from the peg lid into the wells of broth. As with the free-swimming bacteria, aliquots for each treatment were serially diluted and spot plated to quantify the CFU/mL of biofilm bacteria. Significant differences ($p < 0.05$) of the colony counts were determined using Minitab 15 (Minitab Inc, State College, PA) via ANOVA with the Dunnett Test. The Dunnett Test was used to compare the colony counts for each treatment against the untreated control with an overall error rate of 5%. Beyond statistical analysis, the average colony counts between samples had to have a difference of two orders of magnitude to be significant due to the sensitivity of the plate counting method.

For the MBEC assay screening, biofilms grown for 24 hours were treated for 24 hours with either antibiotic alone, dispersion compound alone, or a combination of antibiotic and dispersion compound. Controls included a positive, untreated control and a negative, sterility control where pegs were removed from the lid prior to placing the lid on the treatment 96-well plate so no bacteria were present. The antibiotics were investigated across the minimum inhibitory concentration (MIC) and the minimum biofilm eradication concentration (MBEC). The dispersion compounds were tested at 10 mM for sodium citrate, succinic acid, and glutamic acid and at 75 mM for xylitol. The compounds were dissolved in Hinton Mueller broth at 37°C and 200 μ L of each treatment were transferred via pipette into three wells of the MBEC 96-well plate. After treatment, the plates were sealed with two layers of Parafilm™ and incubated for 24 hours. The sample size was $n=16$ for the untreated control and sterility control, $n=8$ for the antibiotic controls of tobramycin sulfate, amikacin disulfate, colistin sulfate, and colistin methanesulfonate, $n=7$ for the antibiotic control of polymyxin B sulfate, $n=6$ for co-treatments with tobramycin sulfate, amikacin disulfate, polymyxin B sulfate, colistin sulfate, and colistin methanesulfonate, $n=4$ for the antibiotic control of ciprofloxacin hydrochloride, and $n=3$ for the co-treatments with ciprofloxacin hydrochloride and the nutrient dispersion compounds. High-throughput quantification was completed with

absorbance readings at 650 nm using a SpectraMax Plus 384 (Molecular Devices, Sunnyvale, CA). This wavelength was chosen by the manufacturers to be within the visible light spectra and to avoid wavelengths where antibiotics may have absorbance.¹¹⁶ Bacterial growth was classified as absorbance readings greater than 0.1. Incidence of growth was defined as the percent of treatment wells that had absorbance readings greater than 0.1.

Further investigation of colistin methanesulfonate combinations with sodium citrate and xylitol were quantified with eight serial dilutions and plate counting. Controls included the untreated control, 32 $\mu\text{g}/\text{mL}$ colistin methanesulfonate treatment alone, and 100 $\mu\text{g}/\text{mL}$ colistin methanesulfonate treatment alone. Sodium citrate at 10 mM co-treatment was investigated at both antibiotic concentrations and 75 mM xylitol co-treatment was investigated with 100 $\mu\text{g}/\text{mL}$ antibiotic. The sample size was $n=6$ for the untreated control, $n=6$ for the antibiotic controls, and $n=3$ for all other treatments. Significant differences ($p<0.05$) of the colony counts were determined using Minitab 15 (Minitab Inc, State College, PA) via ANOVA with the Tukey Test. The Tukey Test was used to compare the colony counts for all treatments with an overall error rate of 5%. Beyond statistical analysis, the average colony counts between samples had to have a difference of two orders of magnitude to be significant due to the sensitivity of the plate counting method.

2.3 Results

2.3.1 Peg Biofilm Growth Controls

The MBEC device grew biofilms consistently across all pegs with an overall average absorbance reading of 0.97 ± 0.13 . The absorbance readings was not found to be significantly different by assay column ($p=0.072$, Table 2-2, Figure 2-6) or by assay row ($p=0.059$, Table 2-3, Figure 2-7). To verify the biofilm growth was consistent between

different MBEC assays, three pegs were quantified via plate counting. For each time point in the dispersion screening (t=0.5, 1, 2, 4, 8, 12, and 24 hour assays), the biofilm growth was consistent with an overall average biofilm growth of 7.6 ± 0.5 log(CFU)/mL (p=0.057, Table 2-4).

2.3.2 Dispersion Screening

Biofilm bacteria (Figure 2-8A) and free-swimming bacteria (Figure 2-8B) were quantified for colony counts (CFU/mL) after 0.5, 1, 2, 4, 8, 12, and 24 hours of treatment with the dispersion compounds. Both biofilm bacteria (Table 2-5) and free-swimming bacteria (Table 2-6) did not have significantly different growth compared to the untreated controls up to 4 hours after treatment. After 8 hours of glutamic acid treatment, biofilm bacteria (12.6 ± 0.8 log(CFU/mL)) were increased in growth compared to the untreated control (10.5 ± 0.6 log(CFU/mL)). Dispersed bacteria also increased in growth after 8 hours of treatment with either glutamic acid (13.3 ± 1.6 log(CFU/mL)) compared to the untreated control (10.7 ± 1.2 log(CFU/mL)).

Dispersion was observed as a simultaneous decrease in biofilm bacteria and increase in free-swimming bacteria after 12 hours of treatment with sodium citrate, succinic acid, or xylitol. At 12 hours of treatment, sodium citrate (8.4 ± 0.2 log(CFU/mL)), succinic acid (8.8 ± 0.0 log(CFU/mL)), glutamic acid (8.3 ± 0.4 log(CFU/mL)), and xylitol (9.1 ± 0.4 log(CFU/mL)) resulted in significantly lower bacterial counts for biofilm bacteria compared to the untreated control (12.4 ± 0.1 log(CFU/mL)). Sodium chloride (10.7 ± 0.6 log(CFU/mL)) did not significantly reduce biofilm bacterial counts. At the same time, 12 hour treatments with sodium citrate (25.3 ± 0.2 log(CFU/mL)), succinic acid (27.4 ± 0.2 log(CFU/mL)), or xylitol (27.5 ± 0.3 log(CFU/mL)) led to significantly higher bacterial counts for free-swimming bacteria compared to the untreated control (20.3 ± 0.1 log(CFU/mL)). Sodium chloride ($27.7 \pm$

0.0 log(CFU/mL)) after 12 hours of treatment also led to increased free-swimming bacteria. Treatment with glutamic acid after 12 hours led to a decrease in biofilm bacteria, but not a simultaneous increase in free-swimming bacteria. This suggests dispersion was not initiated at 12 hours, but the significant decrease in biofilm bacteria indicates dispersion occurred near this time point.

After 24 hours most treatments led to biofilm bacteria growth being similar to the untreated control, while the free-swimming bacteria were higher than the untreated control. Treatment with sodium citrate significantly increased the biofilm bacteria (12.8 ± 0.9 log(CFU/mL)) compared to the untreated control (7.7 ± 0.4 log(CFU/mL)) and significantly increased the free-swimming bacteria (19.4 ± 0.1 log(CFU/mL)) compared to the untreated control (9.8 ± 0.1 log(CFU/mL)). Treatment with succinic acid, glutamic acid, xylitol, or sodium chloride led to increased free-swimming bacterial growth, but not increased biofilm bacteria growth compared to the untreated controls. At 12 hours and 24 hours all treatments led to significantly more free-swimming bacteria compared to biofilm bacteria, which may imply growth was preferred as individual free-swimming bacteria over community biofilm bacteria. From 12 hours to 24 hours, biofilm bacteria remain constant for treatments that caused dispersion. This may indicate the dispersed bacteria at 12 hours remain dispersed at 24 hours. The untreated control and sodium chloride biofilm bacteria decreased at the 24 hour time point, which may indicate nutrient depletion. Likewise, free-swimming bacteria decreased after 24 hours compared to after 12 hours for all treatments, except glutamic acid, which may indicate nutrient depletion.

2.3.3 Minimum Biofilm Eradication Concentration (MBEC) Assay Screening

2.3.3.1 Treatment Effects on Free-swimming Bacteria

For all untreated controls and dispersion treatments alone, 100% incidence of *P. aeruginosa* free-swimming bacteria growth was observed (Table 2-7). The sterility controls had 0% incidence of free-swimming bacteria growth (Table 2-7). For all antibiotic treatments, except with tobramycin sulfate, free-swimming bacteria were not found to grow in any wells including the lowest antibiotic concentration tested (Tables 2-8 to 2-13). Combination treatments did not enhance bacterial killing as the incidence of growth for co-treatments were the same as for the antibiotic alone. For treatment with tobramycin sulfate, free-swimming bacteria had 100% incidence of bacterial growth in the presence of 0.35 µg/mL antibiotic and 0% growth for the other concentrations tested (Table 2-10). Combination treatments did not enhance bacterial killing as the incidence of growth for co-treatments were the same as for the antibiotic alone.

2.3.3.2 Treatment Effects on Biofilm Bacteria

Dispersion compounds alone or untreated controls had 100% incidence of growth for *P. aeruginosa* biofilms, indicating no biofilm bacterial death (Table 2-7). The sterility controls had 0% incidence of biofilm growth, indicating the assay was not contaminated with bacteria (Table 2-7).

2.3.3.3 Co-treatment with Fluoroquinolone Against Biofilms

Ciprofloxacin hydrochloride (Figure 2-9A, Table 2-8) was ineffective alone at 0.97 µg/mL and 50 µg/mL antibiotic concentrations, resulting in 100% incidence of biofilm growth. Increasing the concentration to 510 µg/mL, 0% incidence of biofilm

growth was observed. Co-treatment with dispersion compounds did not enhance biofilm bacteria killing. Combination treatment with sodium citrate, succinic acid, glutamic acid, or xylitol did not enhance bacterial killing since the incidence of growth values for co-treatments were the same for the antibiotic alone. At 0.97 $\mu\text{g/mL}$ and 50 $\mu\text{g/mL}$ antibiotic concentrations, 100% incidence of growth was observed. At 510 $\mu\text{g/mL}$ antibiotic concentration, 0% incidence of growth was observed.

2.3.3.4 Co-treatment with Aminoglycosides Against Biofilms

Treatment with amikacin disulfate (Figure 2-9B, Table 2-9) alone was ineffective at reducing *P. aeruginosa* biofilm growth at concentrations of 32 $\mu\text{g/mL}$, 508 $\mu\text{g/mL}$, and 970 $\mu\text{g/mL}$ since biofilms had 100% incidence of growth. Amikacin disulfate treatment reduced the incidence of growth for biofilms when combined with sodium citrate, succinic acid, or glutamic acid. Co-treatment with sodium citrate reduced the incidence of growth from 100% to 17% at 970 $\mu\text{g/mL}$ amikacin disulfate. Co-treatment with succinic acid or glutamic acid led to reduced biofilm growth at antibiotic concentrations of 508 $\mu\text{g/mL}$ or 970 $\mu\text{g/mL}$. Succinic acid co-treatment led to 33% incidence of growth at both antibiotic concentrations. Glutamic acid co-treatment led to 50% incidence of growth at both antibiotic concentrations. Treatment with xylitol did not enhance the effectiveness of amikacin disulfate since 100% incidence of biofilm growth was observed at all three antibiotic concentrations tested.

Treatment with tobramycin sulfate (Figure 2-10A, Table 2-10) alone was ineffective against *P. aeruginosa* biofilms at 0.35 $\mu\text{g/mL}$ and 19 $\mu\text{g/mL}$, leading to 100% incidence of biofilm growth. Increasing the concentration to 190 $\mu\text{g/mL}$ reduced the incidence of biofilm growth to 75%. Combining tobramycin sulfate above 0.35 $\mu\text{g/mL}$ with any of the dispersion compounds reduced the incidence of biofilm growth. Co-treatment with sodium citrate at either 19 or 190 $\mu\text{g/mL}$ tobramycin sulfate was very

effective in eradicating the biofilm bacteria, resulting in 0% incidence of growth.

Succinic acid was also effective, reducing the incidence of growth from 100% to 67% with 19 $\mu\text{g/mL}$ tobramycin sulfate and reducing the incidence of growth from 75% to 0% with 190 $\mu\text{g/mL}$ tobramycin sulfate. Co-treatment of glutamic acid and 19 $\mu\text{g/mL}$ tobramycin sulfate decreased the incidence of growth to 17% and 190 $\mu\text{g/mL}$ tobramycin sulfate decreased the incidence of growth to 0%. Like the sodium citrate co-treatment, the xylitol and tobramycin co-treatment led to 0% incidence of biofilm growth for 19 $\mu\text{g/mL}$ and 190 $\mu\text{g/mL}$ antibiotic concentrations.

2.3.3.5 Co-treatment with Cyclic Polypeptides Against Biofilms

Treatment with polymyxin B sulfate (Figure 2-10B, Table 2-11) alone was ineffective at 4 $\mu\text{g/mL}$ with 100% incidence of biofilm growth and was more effective at 51 $\mu\text{g/mL}$ with only 57% incidence of biofilm growth. Combining polymyxin B sulfate with sodium citrate resulted in 0% incidence of biofilm growth at both antibiotic concentrations. Co-treatment with succinic acid was not as effective since the incidence of biofilm growth was reduced to only 50% at both antibiotic concentrations. Co-treatment with glutamic acid was ineffective at 4 $\mu\text{g/mL}$ with 100% incidence of biofilm growth, but was effective at 51 $\mu\text{g/mL}$ with 0% incidence of biofilm growth. Combining polymyxin B sulfate with xylitol led to 0% incidence of biofilm growth at both antibiotic concentrations.

Treatment with colistin sulfate (Figure 2-11A, Table 2-12) alone was ineffective at both 32 $\mu\text{g/mL}$ and 100 $\mu\text{g/mL}$, resulting in 100% incidence of biofilm growth. Increasing the concentration to 1000 $\mu\text{g/mL}$ reduced the incidence of growth to 0%. Combining colistin sulfate with any dispersion compound did not reduce biofilm growth since the incidence of growth values were the same as the antibiotic alone.

Treatment with colistin methanesulfonate (Figure 2-11B, Table 2-13) alone was ineffective at 32 $\mu\text{g}/\text{mL}$ with 100% incidence of biofilm growth. Increasing the antibiotic concentration reduced the incidence of biofilm growth to 63% at 100 $\mu\text{g}/\text{mL}$ colistin methanesulfonate and to 13% at 1000 $\mu\text{g}/\text{mL}$ colistin methanesulfonate. Co-treatment with sodium citrate or succinic acid reduced the incidence of growth to 17% at 32 $\mu\text{g}/\text{mL}$ colistin methanesulfonate and fully reduced the incidence of growth to 0% at both 100 $\mu\text{g}/\text{mL}$ and 1000 $\mu\text{g}/\text{mL}$ colistin methanesulfonate. Glutamic acid co-treatment decreased the incidence of biofilm growth to 17% at both 32 $\mu\text{g}/\text{mL}$ and 100 $\mu\text{g}/\text{mL}$ antibiotic concentrations and to 0% at 1000 $\mu\text{g}/\text{mL}$ antibiotic concentration. Xylitol co-treatment was the most effective with 0% incidence of biofilm growth at all antibiotic concentrations tested.

2.3.3.6 Further Investigation of Colistin Methanesulfonate with Sodium Citrate and Xylitol

The biofilm bacteria remaining on the pegs and the free-swimming bacteria remaining in the wells of the MBEC assay were regrown on agar plates for further analysis of the promising combinations colistin methanesulfonate with sodium citrate or xylitol (Table 2-14). For biofilm bacteria (Figure 2-12A), the 32 $\mu\text{g}/\text{mL}$ colistin methanesulfonate control ($8.3 \pm 0.7 \log(\text{CFU}/\text{mL})$) was not effective compared to the untreated control ($9.6 \pm 0.6 \log(\text{CFU}/\text{mL})$). Biofilm bacteria were more susceptible to the higher concentration of 100 $\mu\text{g}/\text{mL}$ colistin methanesulfonate alone ($5.4 \pm 0.4 \log(\text{CFU}/\text{mL})$), which resulted in a significant reduction in live biofilm bacteria compared to the untreated control. Free-swimming bacteria (Figure 2-12B) were more susceptible to the 32 $\mu\text{g}/\text{mL}$ colistin methanesulfonate antibiotic control ($6.7 \pm 0.7 \log(\text{CFU}/\text{mL})$) compared to the untreated control ($11.6 \pm 0.8 \log(\text{CFU}/\text{mL})$). Increasing the antibiotic control concentration to 100 $\mu\text{g}/\text{mL}$ led to significant free-swimming

bacterial death ($4.6 \pm 0.3 \log(\text{CFU/mL})$) compared to the $32 \mu\text{g/mL}$ antibiotic control and the untreated control.

For bacteria in biofilms, combining $32 \mu\text{g/mL}$ colistin methanesulfonate with sodium citrate made the bacteria susceptible to the antibiotic ($6.3 \pm 0.6 \log(\text{CFU/mL})$), leading to a significant reduction in live biofilm bacteria compared to the untreated control and the antibiotic control. The largest effects were observed with either sodium citrate or xylitol and $100 \mu\text{g/mL}$ colistin methanesulfonate combinations ($< 2 \log(\text{CFU/mL})$). The live biofilm bacteria were reduced by at least 3 orders of magnitude compared to the antibiotic control for either combination and the live bacteria were below the limit of 100 colony forming units for plate counting.

For free-swimming bacteria, sodium citrate co-treatment with $32 \mu\text{g/mL}$ colistin methanesulfonate ($7.0 \pm 0.2 \log(\text{CFU/mL})$) or $100 \mu\text{g/mL}$ colistin methanesulfonate ($3.9 \pm 0.4 \log(\text{CFU/mL})$) did not enhance the free-swimming bacterial killing compared to the antibiotic controls. Likewise co-treatment with xylitol and $100 \mu\text{g/mL}$ colistin methanesulfonate ($3.7 \pm 0.4 \log(\text{CFU/mL})$) did not enhance the free-swimming bacterial killing compared to the antibiotic control. Sodium citrate or xylitol in combination with $100 \mu\text{g/mL}$ colistin methanesulfonate were equally as effective at reducing biofilm growth.

The untreated controls for biofilm bacteria ($9.6 \pm 0.9 \log(\text{CFU/mL})$) had less live bacteria than those for free-swimming bacteria ($11.6 \pm 0.8 \log(\text{CFU/mL})$), suggesting a preference for the planktonic mode of bacterial growth. The biofilm bacteria co-treatments of $100 \mu\text{g/mL}$ colistin methanesulfonate with sodium citrate or xylitol ($< 2 \log(\text{CFU/mL})$) resulted in less live bacteria than the free-swimming bacteria in the presence of the antibiotic or co-treatment, indicating antibiotic killing and bacterial dispersion led to the decrease in bacterial counts.

2.4 Discussion

2.4.1 Peg Biofilm Growth Controls

The MBEC assay was reproducible for *P. aeruginosa* biofilm growth on all pegs with no significant difference being found for the assay columns or rows. This was consistent with literature reports of biofilms grown reproducibly by row.^{83, 100} The overall average biofilm growth was $7.6 \pm 0.5 \log(\text{CFU/mL})$, which was consistent with Ceri et al. having an overall average of $7.2 \pm 0.4 \log(\text{CFU/mL})$ for *P. aeruginosa*.⁸³

2.4.2 Dispersion Screening

In this study we were the first to investigate nutrient dispersion compounds in the MBEC assay. The nutrient compounds 10 mM sodium citrate, succinic acid, and glutamic acid were chosen because they were observed to have chemotaxis attraction for bacteria and to disperse bacteria from biofilms.^{55, 71} Xylitol was tested at 75 mM (12 mg/mL) since xylitol requires a higher concentration to cause a change to the biofilm structure and this concentration was safely assessed in mice.^{76, 117} Sodium chloride at 75 mM was investigated for the effect of molar strength on bacterial viability; it was tested at the highest molar concentration used in this study.

Sodium citrate and succinic acid caused bacterial dispersion by 12 hours of treatment, which was observed as a simultaneous decrease in biofilm bacteria and increase in free-swimming bacteria (Figure 2-8). Glutamic acid likely caused dispersion around the 12 hour time point as well since significant biofilm bacteria reduction was observed, although a simultaneous increase in free-swimming bacteria was not observed at that exact time. This may indicate dispersion occurred prior to the 12 hour time point; dispersed bacteria have the ability to reversibly reenter the biofilm. Thus, a significant decrease could still be seen in the biofilm bacteria while the free-swimming bacteria population is not significantly increased. Sauer et al. found nutrient dispersion with

sodium citrate, sodium succinate, and sodium glutamate to occur within 120 minutes using a flow cell system.⁵⁵ Moulton and Montie observed the sodium ion did not affect the chemotaxis attraction.⁷¹ Lu and Collins demonstrated that when using the closed MBEC assay system, dispersion with bacteriophages required 5 to 10 hours to disperse bacteria.⁶⁵ When flow is stopped to create a batch system or when a closed system is used, young biofilms initially gain biomass and disperse later.⁵⁹ This was consistent with our findings where live biofilm bacteria growth increased until 8 hours and then decreased at the 12 hour time point.

Sodium chloride was included to investigate molar strength effects on bacterial dispersion and viability. It was not found to cause dispersion or bacterial death at 75 mM since it did not significantly reduce the biofilm bacteria compared to the untreated control. This was consistent with Moulton and Montie observing the sodium ion did not affect the chemotaxis attraction.⁷¹ Our results were also consistent with Winslow and Dolloff reporting that bacteria were not killed at this sodium chloride concentration.¹¹⁸

In this study, we were also the first to investigate xylitol as a dispersion compound. Ammons et al. reported the ability of xylitol treatment to weaken the biofilm structure by reducing the quantity of matrix present in confocal microscopy images.⁷⁶ Since dispersion also weakens the biofilm structure, we investigated its ability to disperse *P. aeruginosa* bacteria from biofilms. We observed xylitol caused bacterial dispersion by 12 hours of treatment with a simultaneous decrease in biofilm bacteria and increase in free-swimming bacteria like the sodium citrate and succinic acid treatments (Figure 2-8). Unlike sodium citrate and succinic acid, xylitol is not a nutrient dispersion compound since it has not been shown to provide a nutrient source for *P. aeruginosa* growth.¹¹² Beyond dispersion, xylitol was also investigated since it may aid additionally in the treatment of cystic fibrosis patients. Zabner et al. found 304 mM xylitol may reduce the Cl⁻ concentration in the airway surface liquid and enhance bacterial killing, which would be advantageous for cystic fibrosis patients.¹¹²

At 12 hours and 24 hours all treatments led to significantly more free-swimming bacteria compared to biofilm bacteria, implying growth was preferred as individual free-swimming bacteria over community biofilm bacteria. Our findings were consistent with Sauer et al. that showed more free-swimming bacteria were present than biofilm bacteria after dispersion occurred.⁵⁵ This may have implications for treatment strategies of cystic fibrosis patients since free-swimming bacteria are more susceptible to antibiotics than biofilm bacteria.¹⁸

2.4.3 MBEC Screening

In this study, we investigated the ability of nutrient dispersion compounds to enhance the effectiveness of antibiotics on *P. aeruginosa* bacteria within the MBEC assay. Six antibiotic compounds were investigated (ciprofloxacin hydrochloride, amikacin disulfate, tobramycin sulfate, polymyxin B sulfate, colistin sulfate, and colistin methanesulfonate) since they are commonly used against *P. aeruginosa* biofilms.¹²⁻¹³ The antibiotics were tested at concentrations spanning the reported MIC and MBEC values.^{8, 18, 75-76, 92-94} Co-treatments included the dispersion compounds sodium citrate, succinic acid, glutamic acid, or xylitol.

As expected free-swimming bacteria did not grow in the presence of antibiotic concentrations above the MIC value.^{9, 19, 83-84} Antibiotic and dispersion compound co-treatments did not reduce free-swimming bacteria growth compared to the antibiotic alone. This was expected since the dispersion compound was incorporated to entice the biofilm bacteria to leave the biofilm to evade the additional biofilm bacteria resistance mechanisms.

For biofilm bacteria, ciprofloxacin hydrochloride treatment alone required a higher concentration to reduce biofilm growth than previously reported.⁸³ This was reasonable since in this previous study by Ceri et al. the biofilms were grown for 4 hours,

compared to 24 hours in our current study. It has been shown by various researchers that older *P. aeruginosa* biofilms require higher antibiotic concentrations.^{83-84, 104} Ceri et al. observed that growing biofilms for an additional 5 hours increased antibiotic tolerance by an order of magnitude.⁸³⁻⁸⁴ Bacteria in biofilms may be more tolerant of ciprofloxacin hydrochloride treatment since oxygen limitation and low metabolic activity within the biofilm reduces the effectiveness of the antibiotic.³⁸ Providing nutrient compounds should encourage metabolic activity and dispersion and thus would be expected to increase the antibiotic's effectiveness.^{38, 40, 55} However since Walters et al. observed ciprofloxacin can easily penetrate 48-hour old *P. aeruginosa* biofilms within 8 hours, the bacteria likely induced antibiotic resistance mechanisms, such as efflux pumps, as metabolic activity was increased prior to dispersion occurring.^{38, 40} Thus co-treatments with ciprofloxacin hydrochloride may be more effective if the antibiotic were added at a later time, after dispersion occurred.

The aminoglycoside amikacin disulfate (Figure 2-6B) treatment alone led to biofilms growing in the presence of antibiotic concentrations greater than or equal to 970 $\mu\text{g/mL}$, which was consistent with the reported minimum biofilm eradication antibiotic concentration value being greater than 512 $\mu\text{g/mL}$.⁸⁴ Therefore, this study did not identify the MBEC. Co-treatment with sodium citrate, succinic acid, and glutamic acid reduced the incidence of biofilm. Solely based on chemical structure, potentially a salt formed between the positively charged antibiotic and negatively charged dispersion compounds, which could enhance penetration of the polycationic aminoglycoside through the negatively charged biofilm matrix.³⁶⁻³⁷ Since there was not complete biofilm bacteria eradication, a portion of the biofilm bacteria were able to adapt and grow in the presence of the co-treatment. Amikacin is effective against metabolically active bacteria, thus the addition of nutrient dispersion compounds would be expected to increase the effectiveness of the antibiotic.⁴⁰ However, simultaneous application of nutrient compounds and amikacin disulfate may allow for adaptation of metabolically active

bacteria, such as release of modifying enzymes or reduced membrane permeability.^{40, 119} This adaptation may be assisted by growth in Hinton Mueller broth, which has 13 $\mu\text{g/mL}$ Mg^{2+} that has been observed to reduce the outer membrane permeability for antibiotic uptake of aminoglycosides.⁹

The aminoglycoside tobramycin sulfate (Figure 2-10A) alone had reduced incidence of biofilm growth at 190 $\mu\text{g/mL}$. Our findings for the antibiotic alone were consistent with tobramycin sulfate requiring a lower antibiotic concentration than amikacin disulfate to reduce biofilm bacteria viability.⁸⁴ Combination treatments with sodium citrate and xylitol showed the most promise with no biofilm growth observed after treatment with only 19 $\mu\text{g/mL}$ antibiotic. Sodium citrate and xylitol have two mechanisms of action in common. They both disperse bacteria and further disrupt the biofilm structure.^{55, 76} Co-treatments with succinic acid and glutamic acid decreased incidence of biofilm growth, but did not eliminate biofilm growth. Succinic acid and glutamic acid both disperse bacteria, but do not have the ability to further disrupt the biofilm structure. Therefore the ability of sodium citrate or xylitol to further disrupt the biofilm structure plays an important role in the success of the combination treatment. As with amikacin, the polycationic tobramycin may have formed a salt with the negatively charged dispersion compounds to enhance antibiotic penetration; polycationic aminoglycoside have been reported to have limited biofilm penetration.³⁶⁻³⁷ Co-treatments with succinic acid and glutamic acid had biofilm growth suggesting adaptation occurred in the presence of the co-treatments. Tobramycin sulfate is effective against bacteria with high metabolic activity.⁴⁰ As with amikacin disulfate treatment, co-treatments with succinic acid and glutamic acid may have allowed for adaptation of metabolically active bacteria by release of modifying enzymes or reduction of membrane permeability.^{40, 119} This adaptation may be assisted by growth in Hinton Mueller broth, which has 13 $\mu\text{g/mL}$ Mg^{2+} that has been observed to reduce the permeability of the bacterial outer membrane for antibiotic uptake of aminoglycosides.⁹

Treatment with the cyclic polypeptide polymyxin B sulfate (Figure 2-10B) alone was the most effective antibiotic tested. Co-treatments with sodium citrate and xylitol eliminated biofilm growth with only the antibiotic MIC concentration of 4 $\mu\text{g/mL}$.¹⁹ Sodium citrate and xylitol have the ability to disperse bacteria and to further disrupt the biofilm structure.^{46,68} This appears to have been particularly successful with cyclic polypeptides, requiring only a small concentration of antibiotic to kill the bacteria. Cyclic polypeptides are most effective against bacteria with low metabolic activity inside the biofilm.¹²⁰ Thus, dispersion and disruption of the biofilm structure likely disrupted the biofilm matrix and enabled more antibiotic access to the interior biofilm bacteria with lower metabolic activity and less ability to adapt to treatments. Polymyxin B sulfate with succinic acid or glutamic acid treatment reduced the biofilm growth, but did not eliminate the biofilms. This suggests adaptation of metabolically active bacteria reduced antibiotic uptake, possibly via reducing membrane permeability. In addition, the Mg^{2+} concentration in Hinton Mueller broth has been observed to reduce the outer membrane permeability for antibiotic uptake of cyclic polypeptides.^{9,97}

Colistin sulfate (Figure 2-11A) did not show synergistic biofilm killing with dispersion compounds at the concentrations tested. The antibiotic treatment alone was consistent with the reported antibiotic concentration range needed to eradicate biofilms.⁹ Colistin sulfate has been shown to act quickly, killing bacteria within 15 minutes.¹²¹ Thus the bacteria may have adapted to antibiotic treatment prior to the time dispersion would have been initiated.

The cyclic polypeptide colistin methanesulfonate (Figure 2-11B) alone had reduced incidence of biofilm growth at 1000 $\mu\text{g/mL}$ antibiotic, which is consistent with reported ranges of MBEC values.⁹ Co-treatment with xylitol was the most promising combination followed by sodium citrate and succinic acid and then by glutamic acid, suggesting biofilm structure modification may play an important role in disrupting the biofilms beyond the effects of nutrient dispersion.^{55,76} The prodrug colistin

methanesulfonate hydrolyzes to the active colistin form.¹²² This delayed antibiotic action likely led to synergistic killing since dispersion was able to occur prior to the drug hydrolyzing into the active form. It has been reported to take 4 hours to hydrolyze 1/8 of colistin methanesulfonate to colistin.¹²²

Overall, sodium citrate and xylitol showed the most promise as co-treatments with aminoglycosides and cyclic polypeptides. Xylitol was shown in this study to cause dispersion and also has been observed by others to modify the biofilm structure.⁷⁶ It also has the ability to act as an osmotic agent, which could hydrate the biofilm and affect its structure; however this was not investigated currently.¹¹² Sodium citrate causes dispersion and has the additional ability to permeabilize the outer membranes of bacteria, to act as a chelator, and to weaken the biofilm structure.^{55, 123} Furthermore, sodium citrate is the most negatively charged dispersion compound; forming a salt with the polycationic antibiotics may have aided antibiotic penetration through the matrix.⁹⁸ (CITE) Succinic acid causes dispersion and has the added ability to permeabilize the outer membranes of bacteria.^{55, 123} Succinic acid may also form a salt with the antibiotics to aid penetration through the matrix; however it has less ionizable groups than sodium citrate.⁹⁸ Glutamic acid acts as a dispersion compound and is zwitterionic at pH 7, which may have aided penetration of polycationic antibiotics, but not to the extent as the polyanionic organic acids.^{55, 98} Xylitol does not have ionizable groups to aid in antibiotic penetration. This suggests that dispersion and further weakening of the biofilm structure were vital to xylitol and sodium citrate being successful in more combinations than succinic acid and glutamic acid.

2.4.4 Further Studying Colistin Methanesulfonate with Sodium Citrate or Xylitol

The promising treatments of colistin methanesulfonate with sodium citrate or xylitol were further investigated via plate counting, which is a more sensitive technique for quantifying bacteria growth compared to absorbance readings (Figure 2-12).⁸⁸ With plate counting, the live bacteria are quantified. The number of live biofilm bacteria can be reduced due to bacterial death, due to dispersed bacteria leaving the biofilm, or a combination of both. As expected, treatment at the MIC value of 32 µg/mL colistin methanesulfonate had little effect on biofilm bacteria, while it significantly decreased the growth of free-swimming bacteria compared to the untreated control. This is consistent with Mulcahy et al. reporting free-swimming bacteria were more susceptible to colistin than their biofilm counterparts.⁹ For both biofilm bacteria and free-swimming bacteria, as the antibiotic concentration was increased the bacterial growth decreased. This trend of increasing colistin concentration across 32 µg/mL and 100 µg/mL resulting in less live bacteria was reported by Li et al.¹²¹

For bacteria in biofilms, combining 32 µg/mL colistin methanesulfonate with sodium citrate significantly reduced the live bacteria present compared to the antibiotic control. This was expected since a decrease in biofilm bacteria is consistent with bacteria dispersing out of the biofilm.⁵⁵ Furthermore, as bacteria disperse out of the biofilm, the protective matrix material is weakened due to enzymatic degradation.⁶⁰ Thus the bacteria within the biofilm may also be more susceptible to the antibiotic treatment. The free-swimming bacteria were equally affected by the antibiotic control treatment and the co-treatment with sodium citrate. This was expected since the sodium citrate was added to enhance dispersion of the biofilm bacteria and not to have an added benefit for killing free-swimming bacteria. This is consistent with our findings that sodium citrate did not kill the free-swimming bacteria in our dispersion screening study and is consistent with

Sauer et al. observing that nutrient dispersion compounds did not reduce the viability of dispersed bacteria.⁵⁵

For bacteria within the biofilm, combining 100 µg/mL colistin methanesulfonate with sodium citrate or with xylitol significantly reduced the live bacteria to below the sensitivity limit for plate counting.⁹¹ This reduction in live bacteria is consistent with a higher quantity of bacteria dispersing out of the biofilm. Furthermore, since the sodium citrate co-treatment with 100 µg/mL colistin methanesulfonate had a greater reduction in live bacteria than the co-treatment with 32 µg/mL colistin methanesulfonate, this suggested biofilm bacteria were also killed with the co-treatment, rather than only dispersion playing a role in decreasing the live bacterial counts. This synergistic killing of bacteria is consistent with Rogers et al. observing synergistic killing of bacteria with conventional antibiotics and a synthetic aminoimidazole dispersion compound.⁶⁴ As previously seen in our studies, co-treatment with 100 µg/mL colistin methanesulfonate and sodium citrate or xylitol did not enhance killing of free-swimming bacteria. Therefore sodium citrate and xylitol did not affect free-swimming bacteria viability, which is consistent with our findings in our dispersion screening study. This is also consistent with Sauer et al. reporting that nutrient dispersion compounds did not reduce the viability of free-swimming bacteria in liquid culture and with Zabner et al. reporting that xylitol did not reduce the viability of bacteria in nasal lavage liquid.^{55, 112}

2.5. Conclusions

In this study, dispersion compounds were shown to enhance biofilm bacteria killing with aminoglycosides amikacin disulfate and tobramycin sulfate and cyclic polypeptides polymyxin B sulfate and colistin methanesulfonate. Co-treatment of 100 µg/mL colistin methanesulfonate with 10 mM sodium citrate or 75 mM xylitol significantly reduced the live biofilm bacteria present beyond the antibiotic control,

indicating both enhanced antibiotic action and a preference for bacteria to disperse and remain out of the biofilm after 24 hours of treatment. In addition, we observed that xylitol acts as a dispersion compound. It was found that xylitol and the nutrient dispersion compounds sodium citrate and succinic acid enticed bacterial dispersion after 12 hours of treatment in the closed MBEC assay.

Table 2-1: Concentrations of antibiotics used spanned the minimum inhibitory concentration (MIC) reported to inhibit free-swimming bacteria and the minimum biofilm eradication concentration (MBEC) reported to inhibit biofilm bacteria growth.

Antibiotic	MIC, $\mu\text{g/mL}$	MBEC, $\mu\text{g/mL}$
Ciprofloxacin ^{83-84, 103}	0.25 (4 hr), 1 (9 hr), 1.5 (31.5 hr)	4 (4hr), >256 (31.5 hr)
Amikacin ⁸³⁻⁸⁴	2 (4 hr), 32 (9 hr)	16 (4 hr), >512 (9 hr)
Tobramycin ⁸³⁻⁸⁴	0.5 (4 hr), 14 (9 hr)	2 (4 hr), 112 (9 hr)
Polymyxin B ^{9, 19}	4-63 (24 hr)	640-2560 (24 hr)
Colistin ^{9, 19}	10-32 (24 hr)	320-2560 (24 hr)

Reported as concentration in $\mu\text{g/mL}$ (time bacteria were given to grow in hours).

Table 2-2: Absorbance readings by column of bacteria suspended in Hinton Mueller broth after 24 hours of growth in the MBEC assay.

Column	Absorbance Readings at 650 nm
1	0.87 ± 0.13
2	1.0 ± 0.12
3	0.95 ± 0.14
4	1.01 ± 0.10
5	1.07 ± 0.08
6	1.01 ± 0.11
7	0.98 ± 0.07
8	0.99 ± 0.13
9	0.96 ± 0.15
10	0.92 ± 0.10
11	1.02 ± 0.09
12	0.87 ± 0.23

Results reported as mean \pm standard deviation for n=8.

Table 2-3: Absorbance readings by row of bacteria suspended in Hinton Mueller broth after 24 hours of growth in the MBEC assay.

Row	Absorbance Readings at 650 nm
1	0.92 ± 0.14
2	1.04 ± 0.12
3	0.91 ± 0.06
4	1.02 ± 0.12
5	0.93 ± 0.07
6	1.03 ± 0.12
7	0.93 ± 0.12
8	0.98 ± 0.21

Results reported as mean \pm standard deviation for n=12.

Table 2-4: Biofilm growth controls (log(CFU/mL)) for the dispersion screening assay plates at each time point tested.

Assay Plate	Biofilm Growth, log(CFU/mL)
Overall	7.6 ± 0.5
0.5 Hour	8.0 ± 0.2
1 Hour	7.3 ± 0.5
2 Hour	8.0 ± 0.1
4 Hour	7.9 ± 0.9
8 Hour	7.2 ± 0.1
12 Hour	7.7 ± 0.2
24 Hour	7.4 ± 0.3

Prior to any treatment, biofilms were tested for consistent 24-hour biofilm growth.

Results are reported as mean ± standard deviation for n=3 pegs of biofilm growth

Table 2-5: Biofilm bacteria growth (log(CFU/mL)) for dispersion screening study.

	Biofilm Growth, log(CFU/mL)						
	0.5 Hour	1 Hour	2 Hour	4 Hour	8 Hour	12 Hour	24 Hour
Untreated Control	6.6 ± 0.1	6.0 ± 0.3	7.0 ± 0.1	7.2 ± 0.1	10.5 ± 0.6	12.4 ± 0.1	7.7 ± 0.4
Sodium Citrate	6.5 ± 0.0	5.3 ± 0.1	6.7 ± 0.2	7.3 ± 0.3	10.8 ± 0.6	8.4 ± 0.2*	12.8 ± 0.9*
Succinic Acid	6.6 ± 0.2	5.9 ± 0.1	6.6 ± 0.2	7.2 ± 0.7	11.0 ± 0.8	8.8 ± 0.0*	8.3 ± 0.5
Glutamic Acid	6.5 ± 0.0	5.6 ± 0.1	6.7 ± 0.2	7.6 ± 0.3	12.6 ± 0.8*	8.3 ± 0.4*	7.9 ± 0.2
Xylitol	6.5 ± 0.0	5.6 ± 0.4	6.7 ± 0.3	7.7 ± 0.1	11.5 ± 0.6	9.1 ± 0.4*	8.3 ± 0.7
Sodium Chloride	6.5 ± 0.1	6.3 ± 0.5	6.6 ± 0.1	7.4 ± 0.1	11.7 ± 0.6	10.7 ± 0.6	8.2 ± 0.6

*Significant compared to the untreated control

Significant difference required a statistical significance ($p < 0.05$) and at least 2 log(CFU/mL) decrease in biofilm growth.

Table 2-6: Free-swimming bacteria growth (log(CFU/mL)) for dispersion screening study.

	Free-swimming Bacteria Growth, log(CFU/mL)						
	0.5 Hour	1 Hour	2 Hour	4 Hour	8 Hour	12 Hour	24 Hour
Untreated Control	7.3 ± 0.1	7.1 ± 0.1	7.3 ± 0.1	8.0 ± 0.3	10.7 ± 1.2	20.3 ± 0.1	9.8 ± 0.1
Sodium Citrate	7.3 ± 0.03	6.9 ± 0.0	6.9 ± 0.2	8.1 ± 0.1	11.2 ± 2.3	25.3 ± 0.2*	19.4 ± 0.1*
Succinic Acid	7.1 ± 0.1	6.9 ± 0.2	7.0 ± 0.1	7.9 ± 0.4	10.0 ± 1.0	27.4 ± 0.2*	14.2 ± 0.2*
Glutamic Acid	7.1 ± 0.2	7.0 ± 0.2	6.8 ± 0.3	8.1 ± 0.1	13.3 ± 1.6*	19.8 ± 0.5	18.9 ± 0.6*
Xylitol	7.1 ± 0.4	6.5 ± 0.4	6.5 ± 0.1	8.1 ± 0.2	12.3 ± 1.9	27.5 ± 0.3*	13.5 ± 0.8*
Sodium Chloride	6.9 ± 0.3	6.8 ± 0.3	7.2 ± 0.2	8.0 ± 0.2	9.7 ± 0.6	27.7 ± 0.0*	13.3 ± 1.1*

*Significant compared to the untreated control

Significant difference required a statistical significance ($p < 0.05$) and at least 2 log(CFU/mL) decrease in biofilm growth.

Table 2-7: Incidence of free-swimming bacteria and biofilm bacteria growth for untreated control, sterility control, and dispersion compound treatments alone in Minimum Biofilm Eradication Concentration (MBEC) assay screening study.

Treatment Group	Incidence of Free-swimming Bacteria Growth, %	Incidence of Biofilm Bacteria Growth, %
Untreated Control	100	100
Sterility Control	0	0
Sodium Citrate	100	100
Succinic Acid	100	100
Glutamic Acid	100	100
Xylitol	100	100

P. aeruginosa biofilms were grown for 24 hours and left untreated or treated with dispersion compounds for another 24 hours.

Free-swimming bacteria that released from the biofilm and were located in the wells of the assay were assessed.

Incidence of growth was defined as percent of wells with absorbance readings at 650 nm greater than 0.1.

Table 2-8: Incidence of free-swimming bacteria and biofilm bacteria growth for Minimum Biofilm Eradication Concentration (MBEC) assay screening study with ciprofloxacin hydrochloride alone or in combination with dispersion compounds.

Treatment Group	Incidence of Free-swimming Bacteria Growth, %	Incidence of Biofilm Bacteria Growth, %
Ciprofloxacin Hydrochloride		
0.97 µg/mL	0	100
50 µg/mL	0	100
510 µg/mL	0	0
Ciprofloxacin Hydrochloride & Sodium Citrate		
0.97 µg/mL	0	100
50 µg/mL	0	100
510 µg/mL	0	0
Ciprofloxacin Hydrochloride & Succinic Acid		
0.97 µg/mL	0	100
50 µg/mL	0	100
510 µg/mL	0	0
Ciprofloxacin Hydrochloride & Glutamic Acid		
0.97 µg/mL	0	100
50 µg/mL	0	100
510 µg/mL	0	0
Ciprofloxacin Hydrochloride & Xylitol		
0.97 µg/mL	0	100
50 µg/mL	0	100
510 µg/mL	0	0

P. aeruginosa biofilms were grown for 24 hours and treated with antibiotic alone or with dispersion compounds for another 24 hours.

Free-swimming bacteria that released from the biofilm and were located in the wells of the assay were assessed.

Incidence of growth was defined as percent of wells with absorbance readings at 650 nm greater than 0.1.

Table 2-9: Incidence of free-swimming bacteria and biofilm bacteria growth for Minimum Biofilm Eradication Concentration (MBEC) assay screening study with amikacin disulfate treatment alone or in combination with dispersion compounds.

Treatment Group	Incidence of Free-swimming Bacteria Growth, %	Incidence of Biofilm Bacteria Growth, %
Amikacin Disulfate		
32 µg/mL	0	100
508 µg/mL	0	100
970 µg/mL	0	100
Amikacin Disulfate & Sodium Citrate		
32 µg/mL	0	100
508 µg/mL	0	100
970 µg/mL	0	17
Amikacin Disulfate & Succinic Acid		
32 µg/mL	0	100
508 µg/mL	0	33
970 µg/mL	0	33
Amikacin Disulfate & Glutamic Acid		
32 µg/mL	0	100
508 µg/mL	0	50
970 µg/mL	0	50
Amikacin Disulfate & Xylitol		
32 µg/mL	0	100
508 µg/mL	0	100
970 µg/mL	0	100

P. aeruginosa biofilms were grown for 24 hours and treated with antibiotic alone or with dispersion compounds for another 24 hours.

Free-swimming bacteria that released from the biofilm and were located in the wells of the assay were assessed.

Incidence of growth was defined as percent of wells with absorbance readings at 650 nm greater than 0.1.

Table 2-10: Incidence of free-swimming bacteria and biofilm bacteria growth for Minimum Biofilm Eradication Concentration (MBEC) assay screening study with tobramycin sulfate treatment alone or in combination with dispersion compounds.

Treatment Group	Incidence of Free-swimming Bacteria Growth, %	Incidence of Biofilm Bacteria Growth, %
Tobramycin Sulfate		
0.35 µg/mL	100	100
19 µg/mL	0	100
190 µg/mL	0	75
Tobramycin Sulfate & Sodium Citrate		
0.35 µg/mL	100	100
19 µg/mL	0	0
190 µg/mL	0	0
Tobramycin Sulfate & Succinic Acid		
0.35 µg/mL	100	100
19 µg/mL	0	67
190 µg/mL	0	0
Tobramycin Sulfate & Glutamic Acid		
0.35 µg/mL	100	100
19 µg/mL	0	17
190 µg/mL	0	0
Tobramycin Sulfate & Xylitol		
0.35 µg/mL	100	100
19 µg/mL	0	0
190 µg/mL	0	0

P. aeruginosa biofilms were grown for 24 hours and treated with antibiotic alone or with dispersion compounds for another 24 hours.

Free-swimming bacteria that released from the biofilm and were located in the wells of the assay were assessed.

Incidence of growth was defined as percent of wells with absorbance readings at 650 nm greater than 0.1.

Table 2-11: Incidence of free-swimming and biofilm bacteria growth for Minimum Biofilm Eradication Concentration (MBEC) assay screening study with polymyxin B sulfate treatment alone or in combination with dispersion compounds.

Treatment Group	Incidence of Free-swimming Bacteria Growth, %	Incidence of Biofilm Bacteria Growth, %
Polymyxin B Sulfate		
4 µg/mL	0	100
51 µg/mL	0	57
Polymyxin B Sulfate & Sodium Citrate		
4 µg/mL	0	0
51 µg/mL	0	0
Polymyxin B Sulfate & Succinic Acid		
4 µg/mL	0	50
51 µg/mL	0	50
Polymyxin B Sulfate & Glutamic Acid		
4 µg/mL	0	100
51 µg/mL	0	0
Polymyxin B Sulfate & Xylitol		
4 µg/mL	0	0
51 µg/mL	0	0

P. aeruginosa biofilms were grown for 24 hours and treated with antibiotic alone or with dispersion compounds for another 24 hours.

Free-swimming bacteria that released from the biofilm and were located in the wells of the assay were assessed.

Incidence of growth was defined as percent of wells with absorbance readings at 650 nm greater than 0.1.

Table 2-12: Incidence of free-swimming bacteria and biofilm bacteria growth for Minimum Biofilm Eradication Concentration (MBEC) assay screening study with colistin sulfate treatment alone or in combination with dispersion compounds.

Treatment Group	Incidence of Free-swimming Bacteria Growth, %	Incidence of Biofilm Bacteria Growth, %
Colistin Sulfate		
32 µg/mL	0	100
100 µg/mL	0	100
1000 µg/mL	0	0
Colistin Sulfate & Sodium Citrate		
32 µg/mL	0	100
100 µg/mL	0	100
1000 µg/mL	0	0
Colistin Sulfate & Succinic Acid		
32 µg/mL	0	100
100 µg/mL	0	100
1000 µg/mL	0	0
Colistin Sulfate & Glutamic Acid		
32 µg/mL	0	100
100 µg/mL	0	100
1000 µg/mL	0	0
Colistin Sulfate & Xylitol		
32 µg/mL	0	100
100 µg/mL	0	100
1000 µg/mL	0	0

P. aeruginosa biofilms were grown for 24 hours and treated with antibiotic alone or with dispersion compounds for another 24 hours.

Free-swimming bacteria that released from the biofilm and were located in the wells of the assay were assessed.

Incidence of growth was defined as percent of wells with absorbance readings at 650 nm greater than 0.1.

Table 2-13: Incidence of free-swimming bacteria and biofilm bacteria growth for Minimum Biofilm Eradication Concentration (MBEC) assay screening study with colistin methanesulfonate treatment alone or in combination with dispersion compounds.

Treatment Group	Incidence of Free-swimming Bacteria Growth, %	Incidence of Biofilm Bacteria Growth, %
Colistin Methanesulfonate		
32 µg/mL	0	100
100 µg/mL	0	63
1000 µg/mL	0	13
Colistin Methanesulfonate & Sodium Citrate		
32 µg/mL	0	17
100 µg/mL	0	0
1000 µg/mL	0	0
Colistin Methanesulfonate & Succinic Acid		
32 µg/mL	0	17
100 µg/mL	0	0
1000 µg/mL	0	0
Colistin Methanesulfonate & Glutamic Acid		
32 µg/mL	0	17
100 µg/mL	0	17
1000 µg/mL	0	0
Colistin Methanesulfonate & Xylitol		
32 µg/mL	0	0
100 µg/mL	0	0
1000 µg/mL	0	0

P. aeruginosa biofilms were grown for 24 hours and treated with antibiotic alone or with dispersion compounds for another 24 hours.

Free-swimming bacteria that released from the biofilm and were located in the wells of the assay were assessed.

Incidence of growth was defined as percent of wells with absorbance readings at 650 nm greater than 0.1.

Table 2-14: Bacteria growth (log(CFU/mL)) of biofilm bacteria and free-swimming bacteria after treatment with colistin methanesulfonate (CM) alone or in combination with sodium citrate or xylitol determined using the plate counting method.

	Bacteria Growth, log(CFU/mL)	
	Biofilm Bacteria	Free-swimming Bacteria
Untreated Control	9.6 ± 0.9	11.6 ± 0.8
32 µg/mL CM	8.3 ± 0.7	6.7 ± 0.7
32 µg/mL CM & Sodium Citrate	6.3 ± 0.6	7.0 ± 0.2
100 µg/mL CM	5.4 ± 0.4	4.6 ± 0.3
100 µg/mL CM & Sodium Citrate	**	3.9 ± 0.4
100 µg/mL CM & Xylitol	**	3.7 ± 0.4

** <2 Log (CFU/mL)

P. aeruginosa biofilms were grown for 24 hours in the MBEC assay and treated for 24 hours

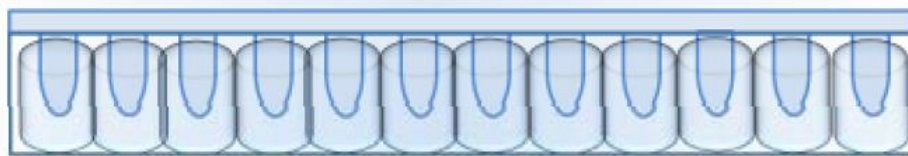


Figure 2-1: Minimum Biofilm Eradication Concentration assay consists of a 96-well plate with a lid that contains 96 plastic pegs protruding from the lid and into the wells; biofilms grow on the pegs of the lid and dispersed bacteria grow in the well; reprinted with permission from Innovotech.⁸²

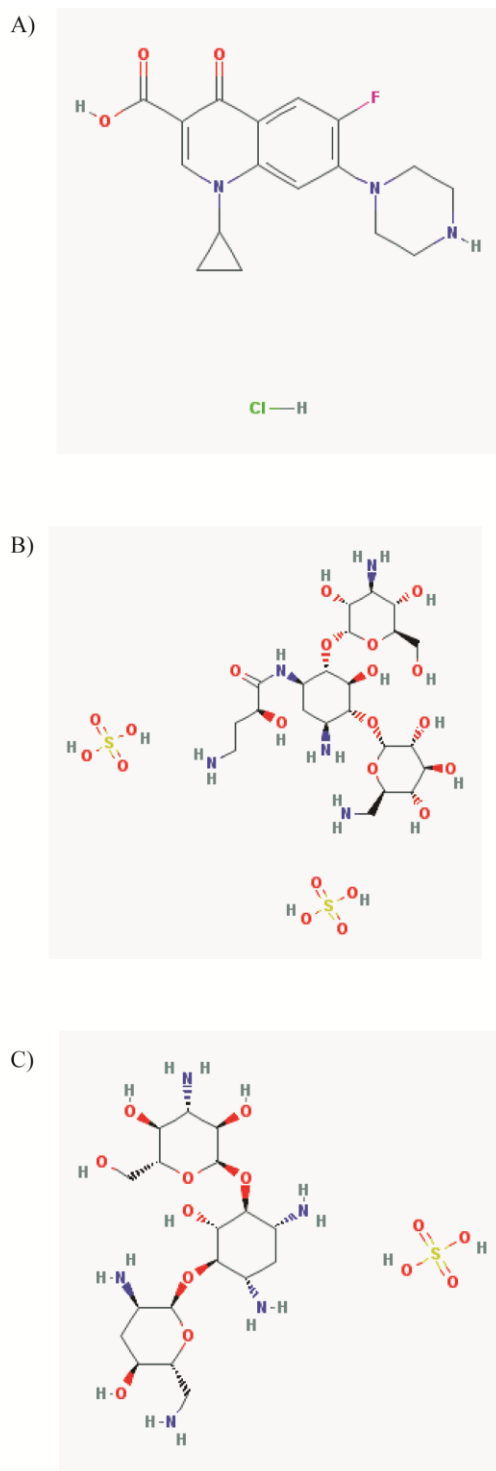
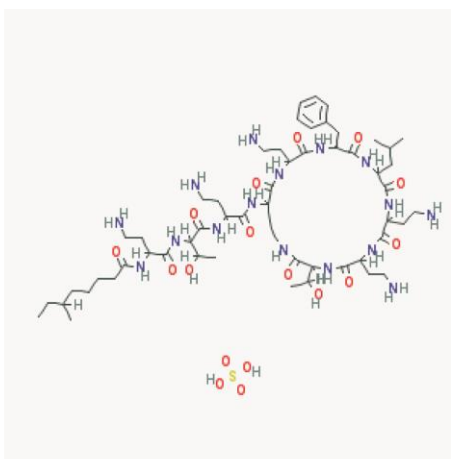
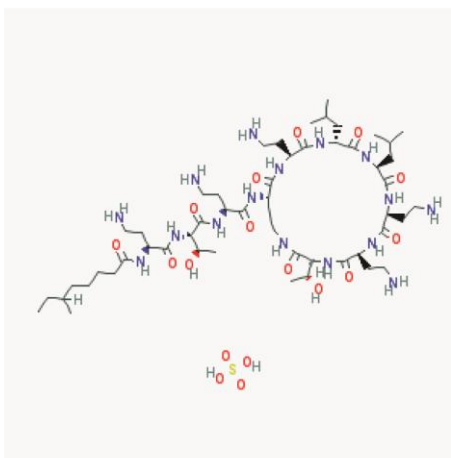


Figure 2-2: Structures of fluoroquinolones and aminoglycosides antibiotics; A) ciprofloxacin hydrochloride structure (ciprofloxacin $pK_a1=6.0$, $pK_a2=8.8$);^{98, 105, 119} B) amikacin disulfate structure (amikacin $pK_a1=6.9$, $pK_a2=8.1$, $pK_a3=8.7$, $pK_a4=10.1$);^{98, 106, 120} C) tobramycin sulfate (tobramycin $pK_a1=6.6$, $pK_a2=7.3$, $pK_a3=7.3$, $pK_a4=7.5$, $pK_a5=8.4$).^{98, 107, 121}

A)



B)



C)

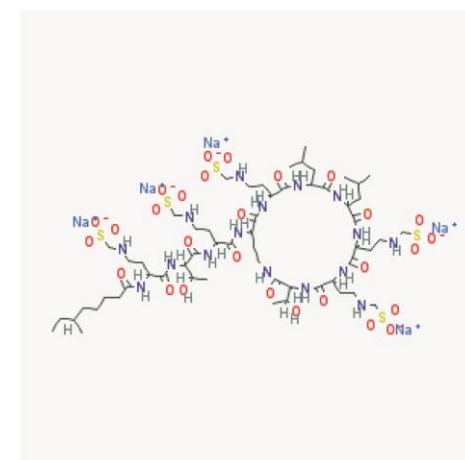


Figure 2-3: Structures of cyclic polypeptide antibiotics, A) polymyxin B sulfate,⁹⁸ B) colistin sulfate,⁹⁸ C) colistin methanesulfonate,⁹⁸ polymyxin and colistin both have five pK_a values close to 10; colistin methanesulfonate is negatively charged and hydrolyzes to the active colistin form.¹⁰⁸

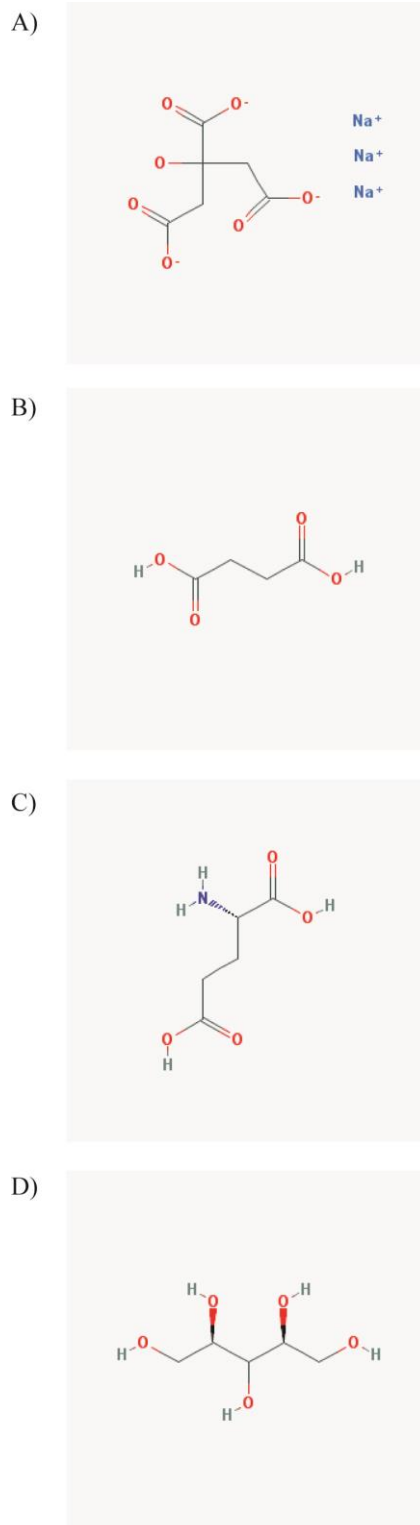


Figure 2-4: Structures of dispersion compounds; A) sodium citrate ($pK_{a1}=3.1$, $pK_{a2}=4.8$, $pK_{a3}=6.4$), B) succinic acid ($pK_{a1}=4.2$, $pK_{a2}=5.6$), C) glutamic acid ($pK_{a1}=2.3$, $pK_{a2}=4.3$, $pK_{a3}=9.7$), D) xylitol.^{98, 109}

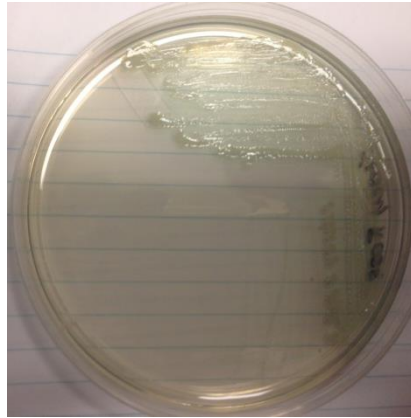


Figure 2-5: Image of a streaked lawn of *Pseudomonas aeruginosa* bacteria; bacteria were diluted across the surface of an agar plate to isolate individual colonies for beginning experiments.

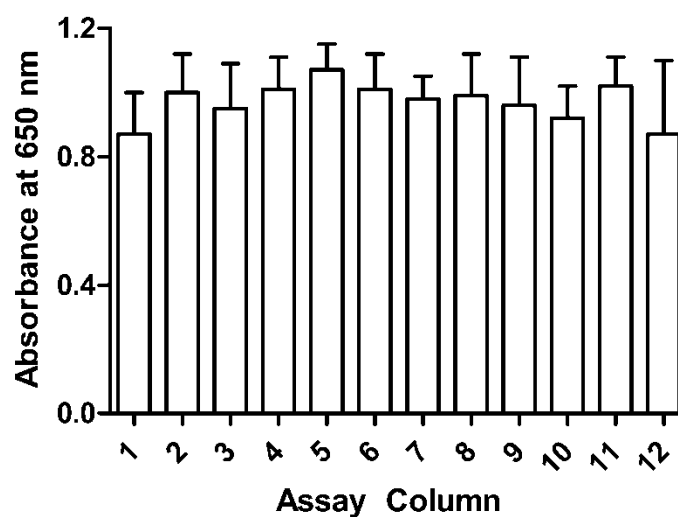


Figure 2-6: Absorbance readings of *Pseudomonas aeruginosa* biofilm bacteria grown 24 hours in Hinton Mueller broth by MBEC assay column, which were the columns of the 96-well plate; to take absorbance readings of the biofilm bacteria, peg lids were sonicated for 10 minutes so biofilm bacteria was disrupted and collected in wells of a 96-well plate with 200 μ L Hinton Mueller broth per well, absorbance of Hinton Mueller broth alone was 0.040 ± 0.003 .

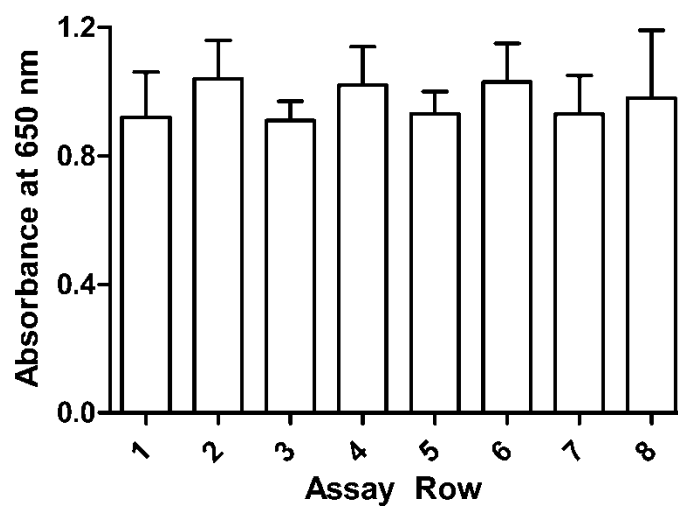
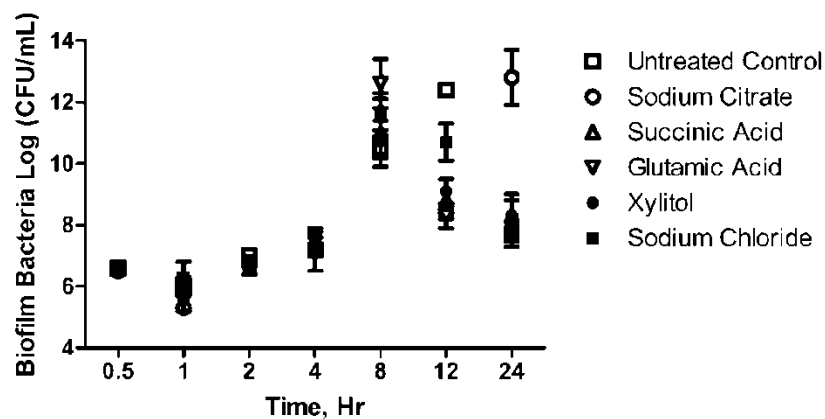


Figure 2-7: Absorbance readings of *Pseudomonas aeruginosa* biofilm bacteria grown 24 hours in Hinton Mueller broth by MBEC assay row, which were the rows of the 96-well plate; to take absorbance readings of the biofilm bacteria, peg lids were sonicated for 10 minutes so biofilm bacteria was disrupted and collected in wells of a 96-well plate with 200 μ L Hinton Mueller broth per well, absorbance of Hinton Mueller broth alone was 0.040 ± 0.003 .

A)



B)

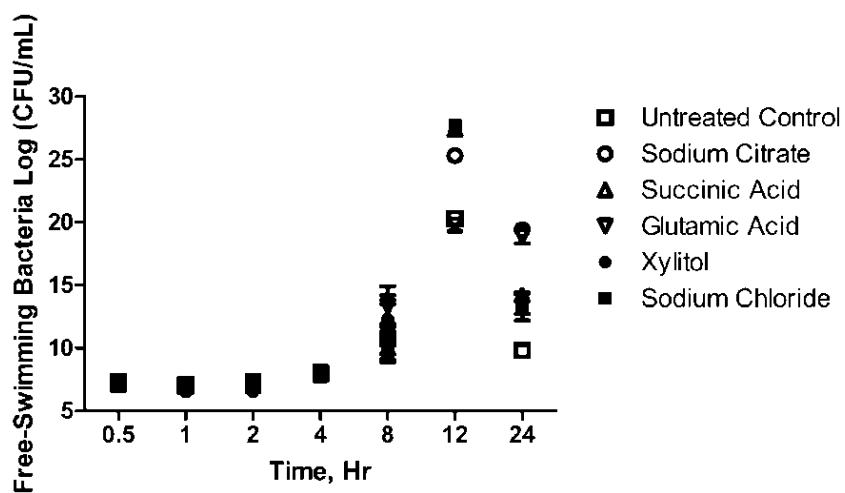
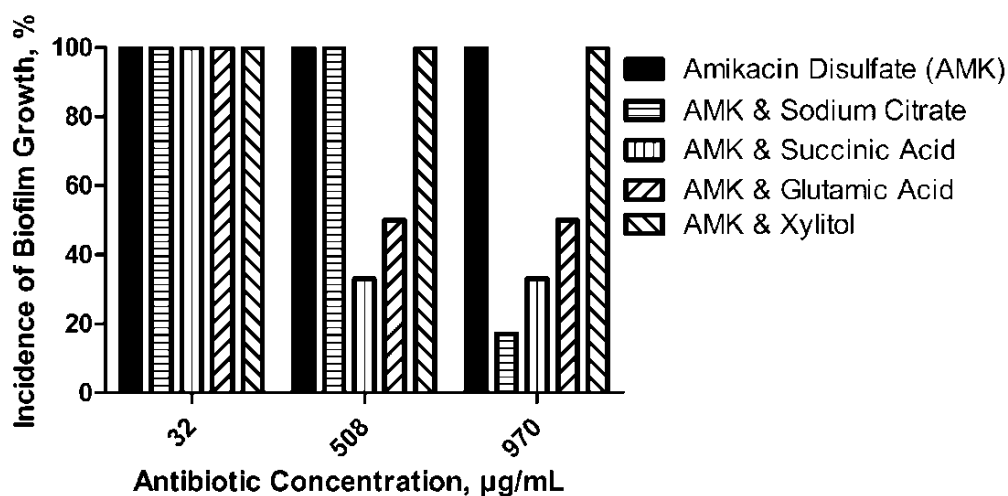
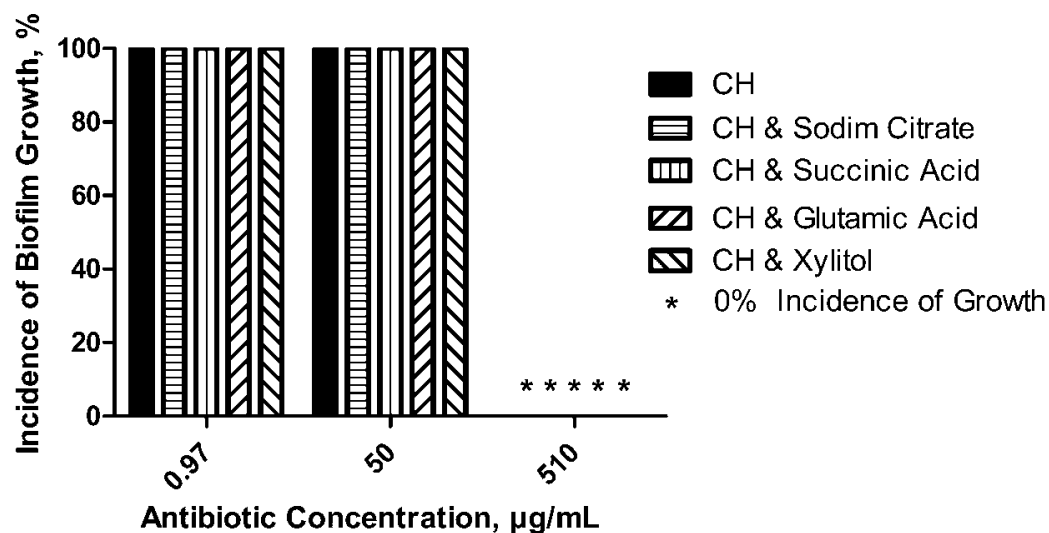


Figure 2-8: Bacteria growth (log(CFU/mL)) of *P. aeruginosa* bacteria versus time; A) biofilm bacteria and B) free-swimming bacteria were grown for 24 hours in the MBEC assay and left untreated or treated with 10 mM sodium citrate, succinic acid, or glutamic acid or 75 mM xylitol or sodium chloride for up to 24 hours, untreated control (open square) important for comparison to treatments.

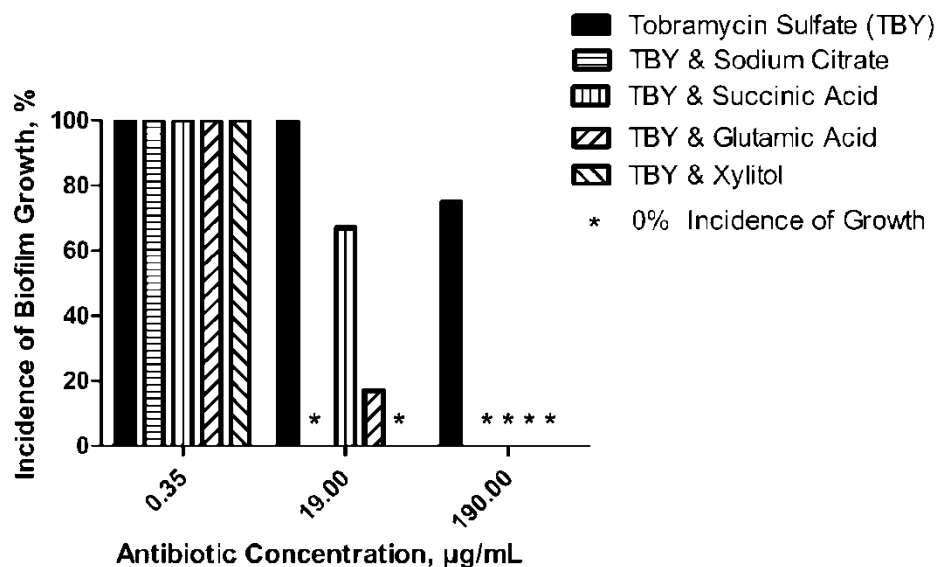
A)



B)

Figure 2-9: Incidence of biofilm growth versus antibiotic concentration for MBEC screening study; *P. aeruginosa* biofilms were grown for 24 hours and treated with antibiotics alone or in combination with dispersion compounds for 24 hours; incidence of growth was defined as percent of wells with absorbance at 650 nm greater than 0.1; incidence of growth for biofilm bacteria for the antibiotic A) ciprofloxacin hydrochloride (CH), MIC 1 $\mu\text{g/mL}$,⁸³ MBEC > 256 $\mu\text{g/mL}$,¹⁰³ B) amikacin disulfate (AMK), MIC 32 $\mu\text{g/mL}$,⁸⁴ MBEC > 512 $\mu\text{g/mL}$.⁸⁴

A)



B)

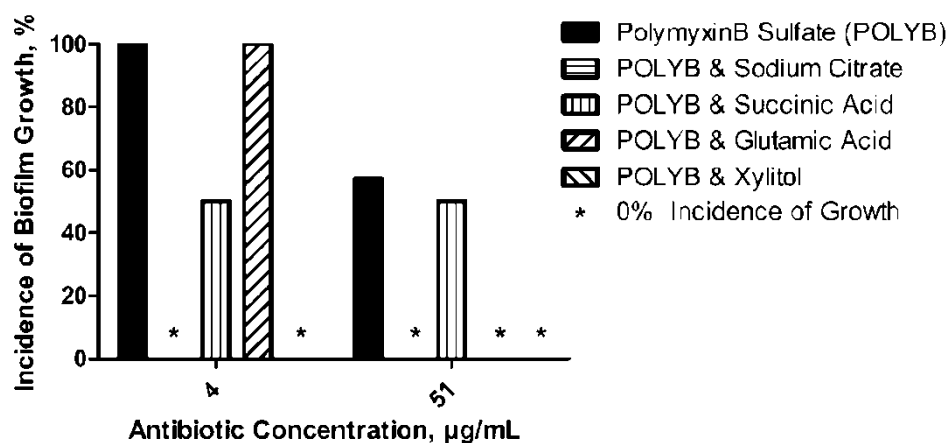
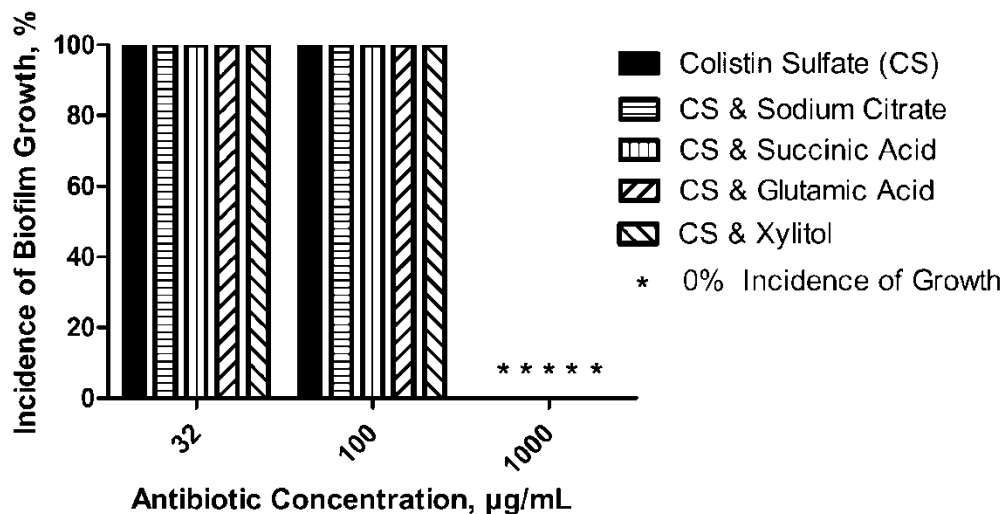


Figure 2-10: Incidence of biofilm growth versus antibiotic concentration for MBEC screening study; *P. aeruginosa* biofilms were grown for 24 hours and treated with antibiotics alone or in combination with dispersion compounds for 24 hours; incidence of growth was defined as percent of wells with absorbance at 650 nm greater than 0.1; incidence of growth for biofilm bacteria for the antibiotic A) tobramycin sulfate (TBY), MIC 0.5 µg/mL,⁸³ MBEC 112 µg/mL;⁸⁴ B) polymyxin B sulfate (POLYB), MIC 4 µg/mL,¹⁹ MBEC 640 µg/mL.⁹

A)



B)

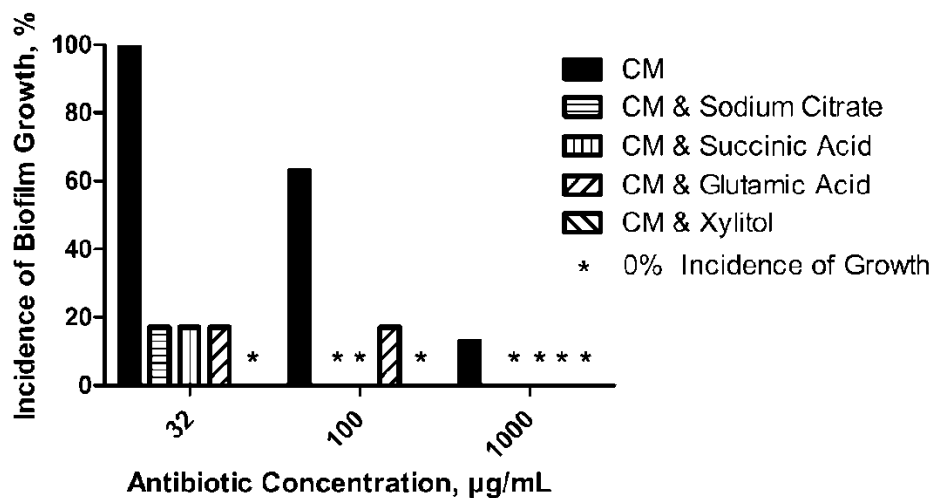


Figure 2-11: Incidence of biofilm growth versus antibiotic concentration for MBEC screening study; *P. aeruginosa* biofilms were grown for 24 hours and treated with antibiotics alone or in combination with dispersion compounds for 24 hours; incidence of growth was defined as percent of wells with absorbance at 650 nm greater than 0.1; incidence of death for biofilm bacteria for the antibiotic A) colistin sulfate (CS); B) colistin methanesulfonate (CM); Colistin MIC 32 $\mu\text{g/mL}$,¹⁹ MBEC 320-2560 $\mu\text{g/mL}$.⁹

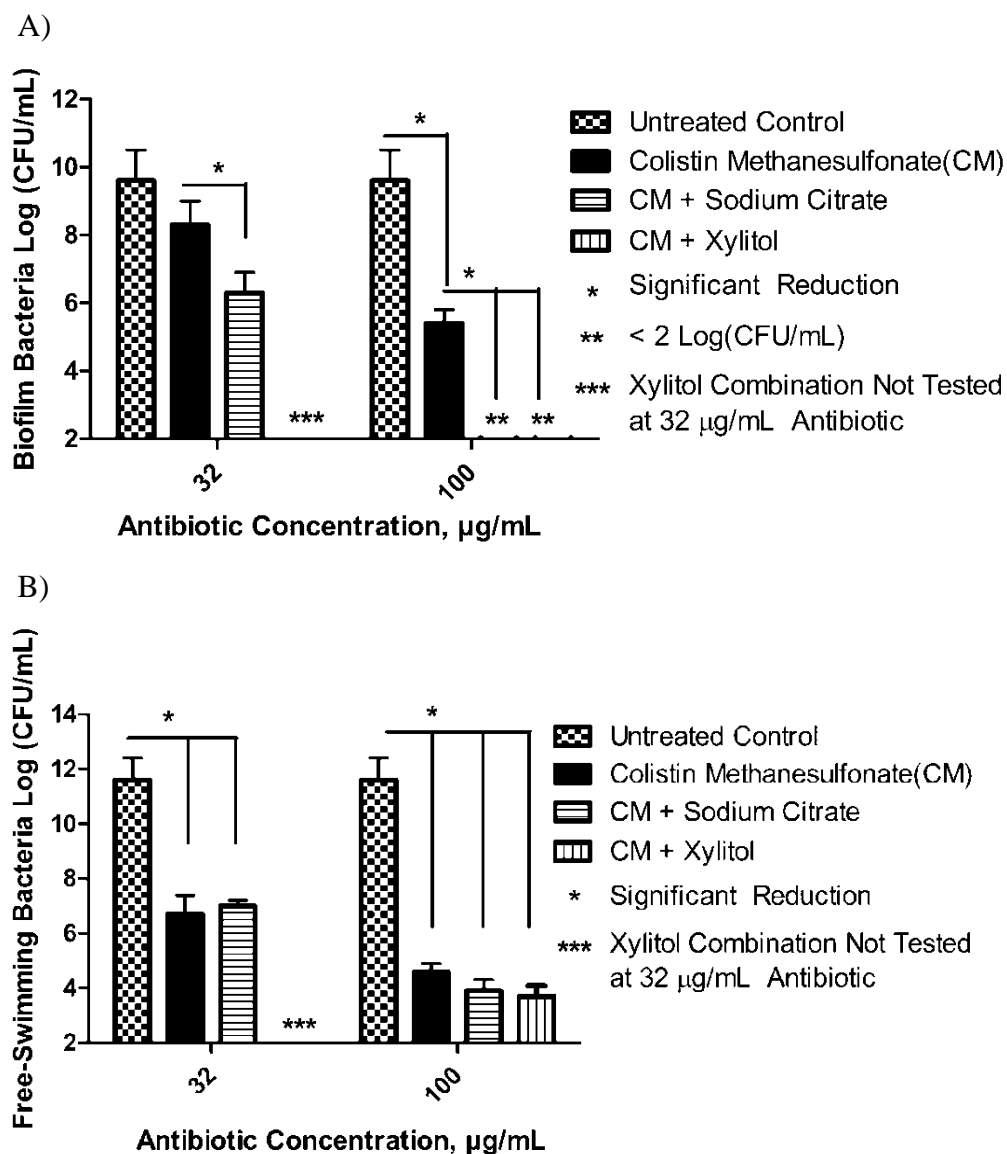


Figure 2-12: Bacteria growth (log(CFU/mL)) of biofilm bacteria and free-swimming bacteria versus antibiotic concentration; *P. aeruginosa* biofilms were grown for 24 hours in the MBEC assay and then treated for 24 hours; controls included the untreated control, the 32 $\mu\text{g/mL}$ colistin methanesulfonate (CM) antibiotic control, and the 100 $\mu\text{g/mL}$ CM antibiotic control. Combination treatments included 32 $\mu\text{g/mL}$ or 100 $\mu\text{g/mL}$ CM with 10 mM sodium citrate and 100 $\mu\text{g/mL}$ CM with 75 mM xylitol; biofilm bacteria were sonicated for 10 minutes and then serially diluted and spot plated for colony forming unit quantification; free-swimming bacteria were serially diluted and spot plated for colony forming unit quantification; significant reduction represented at least a 2 order magnitude reduction in the average log(CFU/mL) and statistically significant reduction using ANOVA with $\alpha=0.05$.

CHAPTER 3
DISPERSION ENHANCES CONVENTIONAL ANTIBIOTIC
ACTIVITY AGAINST MATURE *PSEUDOMONAS AERUGINOSA*
BIOFILMS¹

3.1 Introduction

Biofilm age has been shown to significantly affect antibiotic tolerance in biofilm bacteria. Aaron et al. defined 2-hour-old biofilm cultures as adherent bacteria, while 4-hour-old biofilm cultures were considered young biofilms.¹⁸ The mucoid *P. aeruginosa* adherent bacteria and young biofilms had the same susceptibility to antibiotics in 26 out of 36 instances, although in 10 out of 36 instances adherent bacteria had similar antibiotic susceptibilities compared to the free-swimming bacteria.¹⁸ Thus, even the first layer of adherent bacteria that attach within 2 hours of growth begin to mimic the young biofilm bacteria. It has been shown that older *P. aeruginosa* biofilms require higher minimum biofilm eradication concentrations (MBEC) of antibiotics to prevent biofilm regrowth.^{83-84, 104} For young biofilms, Ceri et al. found that an order of magnitude higher MBEC was needed to prevent *P. aeruginosa* biofilm regrowth for 9-hour-old biofilms compared to 4-hour-old biofilms.⁸³⁻⁸⁴ Tré-Hardy et al. demonstrated that *P. aeruginosa* isolates from cystic fibrosis patients that were grown as mature biofilms (grown more than 24 hours) were found to be less susceptible to antibiotics than young biofilms (grown up to 24 hours).¹²⁴ Since more mature biofilms are more difficult to eradicate, they better represent the biofilms in the cystic fibrotic lung. When cystic fibrosis patients are diagnosed with chronic *P. aeruginosa* infections, aggressive antibiotic treatments do not eradicate the biofilms.¹⁷

¹ Parts of this chapter have been reprinted from Sommerfeld Ross, S.; Fiegel, J., Nutrient dispersion enhances conventional antibiotic activity against *Pseudomonas aeruginosa* biofilms. *International Journal of Antimicrobial Agents* **2012**, *40* (2), 177-181 with permission from Elsevier.

To investigate more mature biofilms, a variety of growth methods can be used. The MBEC assay is typically used for high-throughput screening with quantification of bacteria focused on absorbance readings or plate counting.^{82-83, 91, 101, 125} Less frequently, confocal microscopy may be used to quantify the biofilm bacteria grown on the peg lids, which enables better sensitivity for viability assessment.⁸² However, this can be time-consuming since the pegs need to be manually removed from the device and this can be difficult to quantify via confocal microscopy since the surface of the pegs are not flat. Standard confocal quantification software does not quantify biofilms grown on an uneven surface, thus the quantification would be manual and time-consuming.⁹⁶ Therefore, more mature models investigated by confocal microscopy are commonly done in flow cells.^{55, 62, 73, 96} Biofilms in flow cells grow on a flat surface and can be automatically quantified for viability.^{94, 96, 126} However, flow cells do not represent the cystic fibrotic lung well, since in the lungs mucociliary clearance is disrupted and leads to a more stagnant environment.⁶

Therefore, this chapter focuses on using a Lab-Tek[®] chambered coverglass with stress applied by an orbital shaker instead of media flow. Since this is a low shear system, it better represents the cystic fibrotic lung. This system also retains the advantage of automatic quantification of confocal images since the coverglass bottom is flat. In addition, this chapter follows growth of 4-day-old mature biofilms with media that represents the cystic fibrotic lung containing 8 μM iron.¹²⁷

3.2 Materials and Methods

3.2.1 Materials

Difco nutrient agar and nutrient broth were purchased from Becton, Dickinson, and Company (Sparks, MD). Glycerol, amikacin disulfate, tobramycin sulfate, erythromycin, colistin sulfate, colistin methanesulfonate, polymyxin B sulfate, and magnesium sulfate were purchased from Sigma Aldrich (St. Louis, MO). Sodium citrate dihydrate and succinic acid were from Research Products International Corp. (Mt. Prospect, IL) and MP Biomedicals LLC (Solon, OH), respectively. Morpholinepropanesulfonic (MOPS) free acid (10X) and dipotassium phosphate (0.132 M) were purchased from Teknova (Hollister, CA). Ferrous sulfate heptahydrate was purchased from Fisher Scientific (Fair Lawn, NJ). Purified water was obtained from a NanoPure Infinity Ultrapure Water System (Barnstead Int., Dubuque, IA).

3.2.2 Bacterial Strain and Culture Conditions

Experiments were started from a thawed cryovial of bacteria and maintained on agar slants. Agar slants were prepared by transferring 10 mL mixed nutrient agar into test tubes, autoclaving the filled test tubes, and placing them at a 45° angle while the agar hardened at room temperature. A nutrient agar slant was inoculated with a streak of bacteria from the thawed cryovial across the agar surface using an inoculating loop. The agar slant was incubated stationary at 37°C overnight and then stored in a refrigerator for up to two weeks.¹¹⁴ Any bacteria maintained on nutrient agar slants were only passaged up to two generations to minimize mutations accumulating in the strain.¹¹⁴

The mucoid *Pseudomonas aeruginosa* strain BAA-47 (American Type Culture Collection, Manassas, VA) was streaked on an agar plate to isolate colonies. Three colonies were cultured overnight in nutrient broth (37°C). The absorbance readings of the bacterial suspension was read at 600 nm using a SpectraMax Plus 384 (Molecular

Devices, Sunnyvale, CA). The culture was diluted with fresh broth to a cell concentration of approximately 10^8 CFU/mL. 250 μ L of media (50 mL of 10X MOPS free acid, 5 mL of 0.132 M dipotassium phosphate, 6.4 mg of magnesium sulfate, and 1.14 mg of ferrous sulfate heptahydrate in 500 mL of purified water with final adjusted pH 7.3) was added to Lab-Tek 8 well chambered coverglass wells. 100 μ L of bacterial suspension at approximately 10^8 CFU/mL was then added to each well. The plate was then sealed with two layers of Parafilm™ and incubated at 37°C, 5% CO₂ and 80% relative humidity on an orbital shaker table (190 rpm, VWR, West Chester, PA) for 4 days. This batch device was chosen to provide low shear stress on the biofilm, thereby better mimicking the impaired mucociliary clearance in the CF lung. This system also allowed for visualization of the biofilm grown on the glass substratum by confocal microscopy.

3.2.3 Biofilm Treatments

Biofilms were treated on day four with either antibiotic alone, dispersion compound alone, or a combination of antibiotic and dispersion compound (Table 3-1). The antibiotics were tested at their solubility limit in water. Tobramycin sulfate was also tested at a concentration of 1.8 mg/mL, which was determined from the reported mean sputum concentration achievable (1237 μ g/g sputum),¹²⁸ assuming a sputum density of 1.5 g/mL.¹²⁹ The compounds were dissolved in water at 37°C and transferred via pipette into three wells of the Lab-Tek chambered coverglass. Water was added to the untreated controls such that all wells contained 400 μ L of fluid. After treatment, the chambered coverglass plates were sealed with Parafilm™ and incubated for 24 hours on an orbital shaker. For each treatment the sample size was n=3, except for the polymyxin B sulfate with sodium citrate co-treatment where n=5, polymyxin B sulfate control, amikacin disulfate control, and amikacin co-treatments with sodium citrate or succinic acid where

n=6, and untreated control samples with n=18. Some samples had larger sample sizes since colistin methanesulfonate was studied at a later date and the other treatments were used as additional controls.

3.2.4 Live/Dead Staining and Confocal Imaging

Prior to imaging via confocal microscopy, the media was replaced with 400 μ L of fresh media to remove free-swimming bacteria. A LIVE/DEAD *BacLight*[™] Bacterial Viability Kit (Invitrogen, Eugene, OR) was used to stain the cells remaining in the biofilm as per the kit directions. Briefly, each well was stained with 2 μ L of a mixture containing 3.34 mM syto 9 (to stain both live and dead cells green) and 19.97 mM propidium iodide (to stain cells with damaged membranes red). With this kit, dead bacteria are observed under fluorescence as either red or yellow (colocalized red and green) cells.

Images of the biofilms were obtained using a Zeiss LSM 510 confocal laser scanning microscope (Carl Zeiss, Jena, Germany). Syto 9 was excited with the 488 nm argon laser and the emission was collected with a band pass 505-530 nm filter. Propidium iodide was excited with the 543 nm HeNe laser and the emission was collected with the long pass 560 nm filter. Z-stack image sequences were obtained via a Plan-Neofluar 40x/1.3 oil objective. For comparisons of images, the pinhole was set to 1 Airy Unit with an optimal size of < 1 μ m, which led to the z-step size of 0.48 μ m.

3.2.5 Image Quantification and Statistical Analysis

Images were rendered using Volocity (PerkinElmer, Waltham, MA). For each Lab-Tek well, three images were taken about the center of the well with one image randomly to the right of the center, one image randomly to the left of the center, and one image randomly above the center. Random images were taken to avoid bias. General imaging regions were assigned to prevent overlap of the random images. Confocal images were quantified using our program STAINIFICATION (see Chapter 4). For a single treatment well, the sum of the live bacteria area and sum of the dead bacteria area from three images were used to calculate the percent live (Equation 3-1). At least three Lab-Tek wells were assessed per treatment.

$$\% \text{ Live} = \frac{\text{sum}(\text{Channel 2 bacteria area})}{(\text{sum}(\text{Channel 1 bacteria area}) + \text{sum}(\text{Channel 2 bacteria area}))} * 100\% \quad \text{Equation 3-1}$$

Images were segmented with a threshold intensity value of 45 to uniformly separate bacterial fluorescence from background noise (Figure 3-1). Significant differences ($p < 0.05$) between the percent live of different treatment groups were determined using Minitab 15 (Minitab Inc, State College, PA) via ANOVA with the Tukey Test. The Tukey Test is used to compare all treatments to each other while maintaining an overall error rate of 5%.

3.3 Results

3.3.1 Growth Controls

Biofilms were prepared separately six times to assess reproducibility of growth. Three representative images were selected for visualization. The untreated controls were not visually different from one another (Figure 3-2). STAINIFICATION was used to

quantify both the biofilm bacteria and the free-swimming bacteria (Table 3-2). Since the media was rinsed prior to staining, the free-swimming bacteria exposed to the treatments were removed. The free-swimming bacteria that were stained and imaged represented bacteria that dispersed from the biofilm during imaging. Overall, the biofilm bacteria were $73.5\% \pm 9.4\%$ live with the six separate untreated control samples not significantly different from each other for percent live bacteria ($p=0.277$). Overall, the free-swimming bacteria were $85.2\% \pm 4.8\%$ live with the six separate untreated control samples not being significantly different from each other for percent live bacteria ($p=0.058$). There was not a significant difference between the percent live bacteria within the biofilm and the percent live bacteria that dispersed from the biofilm.

3.3.2 Investigating Combination Treatments

The effects of treatments on the percent live biofilm bacteria were quantified with our program STAINIFICATION. The free-swimming bacteria again were not investigated.

3.3.2.1 Controls

Controls consisted of untreated samples, dispersion treatments alone, and antibiotic treatments alone. Untreated *P. aeruginosa* biofilms grew as a flat community (flat lawn, Figure 3-3A) of primarily live bacteria ($73.5 \pm 9.4\%$, Table 3-3). The dispersion controls of sodium citrate, succinic acid, and xylitol led to biofilms that were denser than the untreated controls (Figure 3-3B-3D). All three treatments had more biofilm growth, but did not significantly change the percent live bacteria ($p>0.05$). The dispersion control of glutamic acid alone resulted in biofilms that were visually sparser than the untreated control (Figure 3-3E).

Five of the seven antibiotics tested (amikacin disulfate, tobramycin sulfate (1.8 mg/mL), polymyxin B sulfate, colistin sulfate, and colistin methanesulfonate) significantly reduced the percent live bacteria in the biofilms compared to the untreated controls. Erythromycin and tobramycin sulfate (6.3 mg/mL) treatments exhibited no significant effect on viability (Table 3-3).

Two aminoglycosides investigated, amikacin disulfate and tobramycin sulfate (1.8 mg/mL), significantly reduced the viable bacteria. Treatment with amikacin disulfate resulted in a less bacteria as a flat community (sparse lawn) with $48.4 \pm 12.0\%$ live bacteria (Figure 3-4A). Treatment with tobramycin sulfate (1.8 mg/mL) resulted in biofilms with lower viability ($18.6 \pm 6.3\%$ live), visually observed as a lawn of live bacteria with clumps of dead bacteria (Figure 3-4B). Tobramycin sulfate (6.3 mg/mL) treatment did not significantly reduce the viable bacteria ($61.5 \pm 4.4\%$ live) compared to the untreated controls. Biofilms treated with 6.3 mg/mL tobramycin sulfate were visually similar to the untreated control (Figure 3-4C).

The cyclic polypeptides polymyxin B sulfate, colistin sulfate, and colistin methanesulfonate were effective in reducing percent live bacteria compared to the untreated controls. Polymyxin B sulfate reduced the live bacteria population to $28.1 \pm 8.0\%$, resulting in a thick lawn of dead bacteria (Figure 3-4D). Colistin sulfate reduced the bacteria viability ($21.7 \pm 1.2\%$ live) and visually appeared to have a change in biofilm architecture with clumps of dead bacteria (Figure 3-4E). Colistin methanesulfonate treatment decreased the total bacteria within the wells (Figure 3-4F) and significantly reduced the percent live remaining after treatment ($33.8 \pm 3.2\%$ live) compared to the untreated control.

Biofilms treated with the macrolide, erythromycin, displayed minimal death ($62.6 \pm 8.4\%$ live), but a significant morphology change observed as a clumped architecture (Figure 3-4G).

3.3.2.2 Co-treatment with Aminoglycosides

P. aeruginosa biofilms were treated with amikacin disulfate alone or in combination with one of four dispersion compounds (Figure 3-5). Treatment of amikacin disulfate with sodium citrate reduced the total amount of bacteria (Figure 3-5B) and decreased the live bacteria to $8.7 \pm 7.6\%$ after treatment (Table 3-3). Combination treatment with succinic acid resulted in more bacteria (Figure 3-5C) and a decrease in percent live bacteria ($42.1 \pm 19.8\%$) compared to the untreated control and dispersion compound control (Table 3-2). However, the percent live bacteria after treatment with succinic acid was not statistically significant compared to the antibiotic control. Treatment of amikacin disulfate with xylitol or with glutamic acid did not significantly reduce the percent live bacteria after treatment compared to the antibiotic or untreated controls (Table 3-3). Co-treatment with xylitol led to biofilms growing as a thicker lawn of bacteria with both more live and dead bacteria than the antibiotic control (Figure 3-5D). Co-treatment with glutamic acid led to a denser lawn of biofilm that also had more live and dead bacteria present compared to the antibiotic control (Figure 3-5E).

Combination treatment of *P. aeruginosa* biofilms with 1.8 mg/mL tobramycin sulfate and sodium citrate significantly increased the viable bacteria compared to the antibiotic control ($35.8 \pm 2.1\%$ live compared to $18.6 \pm 6.3\%$). The biofilm resulted in a lawn of live and dead bacteria with less dead clumped architecture than the antibiotic control (Figure 3-6A and 3-6B). Co-treatment with succinic acid did not significantly reduce the percent live bacteria compared to the antibiotic alone (Table 3-3). However, the biofilms did develop denser lawns of bacteria with more live and dead bacteria present (Figure 3-6C).

Co-treatment of *P. aeruginosa* biofilms with 6.3 mg/mL tobramycin sulfate and sodium citrate, succinic acid, or glutamic acid did not result in significant bacterial death compared to the antibiotic control (Table 3-3). The percent live bacteria was, however, significantly reduced when compared to the untreated control. Co-treatment with sodium

citrate (Figure 3-7B) or succinic acid (Figure 3-7C) led to sparser biofilms than the antibiotic control, and co-treatment with xylitol (Figure 3-7D) or glutamic acid (Figure 3-7E) resulted in biofilms visually similar to the antibiotic control.

3.3.2.3 Co-treatment with Cyclic Polypeptides

While polymyxin B sulfate treatment alone ($28.1 \pm 8.0\%$) shows promise against biofilms, co-treatments did not result in further reduction in the percent live bacteria (Table 3-3). However, differences in architecture were observed for biofilms treated with both polymyxin B sulfate and dispersion compounds. Co-treatment of biofilms with polymyxin B sulfate and sodium citrate or glutamic acid resulted in clumps of dead bacteria (Figure 3-8B and 3-8E). Treatment with succinic acid or xylitol led to biofilms of sparse lawns containing both live and dead bacteria (Figure 3-8C and 3-8D).

The percent live bacteria after co-treatment with colistin sulfate and any of the dispersion compounds were not significantly different than the percent live bacteria for the antibiotic control (Table 3-3). All biofilms treated with co-treatments were visually similar to the antibiotic control, containing clumped biofilm of mainly dead cells (Figure 3-9).

Colistin methanesulfonate treatment alone ($33.8 \pm 3.2\%$; Figure 3-10) greatly reduced the amount of bacteria present in the biofilm and decreased the percent live bacteria after treatment. Synergistic eradication of *P. aeruginosa* biofilms occurred when colistin methanesulfonate was combined with sodium citrate ($5.6 \pm 2.9\%$). Biofilms treated with colistin methanesulfonate and sodium citrate were visually similar to the antibiotic alone with minimal bacteria present (Figure 3-10B). Co-treatment with succinic acid resulted in increased bacteria present and with similar percent live bacteria to the antibiotic control ($22.2 \pm 12.8\%$ vs $33.8 \pm 3.2\%$). Co-treatment with xylitol or

glutamic acid led to biofilms that were visually similar to the antibiotic control and the percent live bacteria were not significantly reduced (Figure 3-10C and 3-10D).

3.3.2.4 Co-treatment with a Macrolide

Erythromycin treatment provided synergistic killing of biofilms with sodium citrate ($8.6 \pm 6.3\%$ live cells with co-treatment versus $62.6 \pm 8.4\%$ for erythromycin alone, Table 3-3). This combination resulted in biofilms with a clumped architecture of mainly dead bacterial cells (Figure 3-11B). Co-treatment with succinic acid led to denser biofilm formation (Figure 3-11C), but no significant difference in percent live bacteria compared to the antibiotic control ($37.8 \pm 22.6\%$ versus $62.6 \pm 8.4\%$). Co-treatment with xylitol or glutamic acid did not decrease the percent live bacteria compared to the untreated control (Table 3-3) and both resulted in lawns of bacteria with clumped architecture (Figures 3-11D and 3-11E).

3.4 Discussion

3.4.1 Growth Controls

The biofilm growth was reproducible for six separate controls with $73.5\% \pm 9.4\%$ live bacteria. The free-swimming bacteria were assessed to determine if dispersion was consistent with samples as well. Prior to imaging, the sample wells were rinsed and new media was added with fluorescent stain. Therefore, the free-swimming bacteria that were stained represented bacteria that dispersed after the rinse step. Dispersion is a natural part of biofilm evolution.^{25,41} The free-swimming bacteria that dispersed were also reproducible for percent live bacteria, which was $85.2\% \pm 4.8\%$ live bacteria.

3.4.2 Investigating Combination Treatments

This study focused on using dispersion compounds to entice bacteria out of the biofilm, which simultaneously weakens the biofilm structure and could make the bacteria more susceptible to antibiotics.^{59-60, 64} Only the bacteria within the biofilm were investigated for viability.

The nutrient dispersion compounds sodium citrate and succinic acid were tested at 10 mM to be similar to the studies conducted by Sauer et al.⁵⁵ Glutamic acid was tested at 0.6 mM due to solubility limitations in the Lab-Tek system. However, amino acids and organic acids between 10^{-2} and 10^{-4} M have been shown to cause chemotaxis attraction in *P. aeruginosa* bacteria.⁷¹ Xylitol was tested at 75 mM (12 mg/mL) since xylitol requires a higher concentration to cause a change to the biofilm structure and this concentration was safely assessed in mice.^{76, 117} Treatments with sodium citrate and succinic acid led to increased biofilm growth, which was expected since the addition of nutrient dispersion compounds provided a carbon source for the bacteria to consume. Both compounds are used as nutrient sources, increasing expression of metabolic activity genes.⁵⁵ Xylitol treatment also led to denser biofilms. This is consistent with *P. aeruginosa* growing in the presence of xylitol at concentrations below 200-400 mg/mL.^{76, 100} Xylitol is initially taken up by the bacteria as a nutrient carbon source, increasing expression of metabolic activity genes.¹¹⁰ However, *P. aeruginosa* cannot metabolize xylitol and, with time, it accumulates as a xylitol phosphate that inhibits growth at high intracellular concentrations.¹¹¹ Glutamic acid treatment did not result in denser biofilms at the 10^{-4} M concentration. While this concentration can cause chemotaxis in *P. aeruginosa*, it may be below an optimal level for increasing metabolism and increasing biofilm growth in our studies.⁷¹

Six antibiotic compounds were investigated (amikacin disulfate, tobramycin sulfate, polymyxin B sulfate, colistin sulfate, colistin methanesulfonate, and erythromycin) since they are commonly used against *P. aeruginosa* biofilms. The

concentrations investigated were at or above the minimum biofilm eradication concentrations (MBEC) reported to reduce viability of young biofilms grown for 4-24 hrs since mature 4-day-old biofilms should not be eradicated at these concentrations.^{83-84, 125} Aminoglycosides (amikacin and tobramycin) are effective against bacteria with high metabolic activity.¹³⁰ Cyclic polypeptides (polymyxin B and colistin) are effective against bacteria with low metabolic activity within the biofilms.¹³¹ Macrolides (erythromycin) require bacteria to be metabolically active to be effective.¹³⁰ In our study, treatments of antibiotic alone showed aminoglycosides and cyclic polypeptides were effective at reducing biofilm viability, indicating the biofilm consists of bacteria with both low and high metabolic activity. It has been reported that aminoglycosides and cyclic polypeptides can have limited penetration through matrix components, particularly for mature biofilms.³⁶⁻³⁷ Since we did not observe full eradication, the polycationic antibiotics may have had some penetration limitation. However, the macrolide, erythromycin, also did not fully eradicate the bacteria in our study; it has been reported that macrolides have little to no penetration limitations into the matrix.³⁶⁻³⁷ Therefore, it cannot be said conclusively if penetration limitations played a role in this study.

Amikacin disulfate was less effective than tobramycin sulfate at similar concentrations, which is consistent with Harrison et al. reporting a higher MBEC needed for amikacin.⁸⁴ Tobramycin sulfate at 1.8 mg/mL concentration was more efficient at reducing the percent live bacteria than tobramycin sulfate at 6.3 mg/mL. At this relatively higher antibiotic concentration, the bacteria may have reacted earlier to the threat by adaptation. The relatively lower concentration may not have triggered the adaptation on the same time-scale. A common resistance mechanism to tobramycin sulfate is the release of modifying enzymes.¹¹⁹ Release of modifying enzymes would reduce the effectiveness of the tobramycin treatment, which is consistent with our observed reduced efficiency of the 6.3 mg/mL tobramycin sulfate treatment. Macrolides have been observed to require higher concentrations than aminoglycosides to eradicate

bacteria within biofilms.³⁶ Our results were consistent with this since erythromycin was not effective at a mass or molar concentration double that of amikacin disulfate.

With this mature biofilm system, biofilms were viable at the highest concentrations tested on the young biofilms in Chapter 2. This is consistent with the trend of older biofilms requiring higher antibiotic concentrations to be inhibited or killed than young biofilms.⁸³⁻⁸⁴ Biofilms grown for 9 hours compared to 4 hours required an order of magnitude higher antibiotic concentration to prevent biofilm regrowth.⁸³⁻⁸⁴ The mature biofilms were also less susceptible to combination treatments than the young biofilms in Chapter 2. Sodium citrate was the only dispersion compound to aid in antibiotic effectiveness for the mature biofilms. Xylitol, which had been effective against young biofilms, did not enhance the antibiotic killing against mature biofilms. Succinic acid and glutamic acid treatment had aided the biofilm killing against young biofilms, although they had not been as effective compared to sodium citrate and xylitol. Succinic acid and glutamic acid were not effective co-treatments against mature biofilms.

The sodium citrate, succinic acid, and xylitol treatment concentrations were the same for the young and mature biofilm studies. Since sodium citrate did not enhance antibiotic effectiveness with all antibiotics against mature biofilms and since succinic acid and xylitol did not enhance the antibiotic effectiveness of any of the antibiotics against the mature biofilms, this suggests that biofilm age plays a significant role for dispersion as well. This is consistent with Xu et al. observing 24-hour-old biofilms dispersed 34% of the biofilm mass compared to 6-hour-old biofilms dispersing 80% of the biofilm mass with the same concentration of dispersion compound.¹³² An increase in dispersion compound concentration may be needed to synergistically kill mature biofilms with antibiotics. This is consistent with Xu et al. demonstrating that an increase in dispersion concentration increased the biofilm mass that was dispersed.¹³²

In the current study, sodium citrate treatment enhanced bacterial metabolism as observed by the increase in total biofilm mass after treatment. Amikacin is effective

against metabolically active bacteria by shutting down protein synthesis; therefore the addition of sodium citrate to the treatment enhanced the eradication ability of amikacin.⁴⁰ Dispersion of bacteria out of the biofilm may have disrupted the biofilm structure, enabling more antibiotic to enter the biofilm structure.⁵⁹⁻⁶⁰ The negatively-charged citrate may have formed a salt with polycationic amikacin, which would aid the antibiotic in penetrating the biofilm matrix.^{98, 106}

Tobramycin sulfate treatments did not enhance antibiotic effectiveness. Tobramycin at 6.3 mg/mL with co-treatments were not significantly different from the antibiotic control. Tobramycin at 1.8 mg/mL with sodium citrate treatment resulted in a significant increase in percent live bacteria. Modifying enzymes could be responsible for ineffective killing with a relatively higher antibiotic concentration. Modifying enzymes could also be responsible for the antagonistic relationship at a relatively lower antibiotic concentration since metabolic activity increase from the nutrient compound could lead to release of the enzymes. Miller et al. have shown that aminoglycosides respond differently to resistance mechanisms developed by the bacteria.¹¹⁹ They observed that a reduction in bacterial membrane permeability and the release of modifying enzymes accounted for about 90% of the aminoglycoside resistance. The effectiveness of amikacin and tobramycin were both affected by reduced permeability. However, tobramycin resistance was increased in the presence of 9 out of 11 modifying enzymes, while amikacin resistance was increased in the presence of only 3 out of 11 modifying enzymes.¹¹⁹ Our results are consistent with the release of tobramycin inactivating enzymes, suggesting that tobramycin's effectiveness may have been significantly reduced by modifying enzymes even at a concentration that was 6-fold higher than that of amikacin. Furthermore, tobramycin is known to be highly susceptible to inactivating enzymes. Amikacin is a semisynthetic aminoglycoside specifically modified to be less susceptible to inactivating enzymes.⁴⁰ Inactivating enzymes were not quantified in this

study; however in the future it will be helpful to investigate the enzymatic activity with assays.¹³³

Cyclic polypeptides have been shown to effectively kill bacteria in the interior of the biofilm.¹³¹ Therefore, bacteria need to disperse for the co-treatment to be effective. Colistin sulfate and polymyxin B sulfate have been shown to kill bacteria within 20 minutes.^{97, 121} Treating with the antibiotic at the same time as the dispersion compound likely led to bacteria adapting to the antibiotic treatment prior to the dispersion occurring. The growing cells on the exterior of the biofilm have been shown to adapt to treatment by reducing membrane permeability.^{40, 131} Thus, simply increasing metabolic activity with use of the nutrient compound would not be expected to further reduce bacterial viability.

Co-treatment with colistin methanesulfonate and sodium citrate significantly reduced the live bacteria after treatment compared to the antibiotic alone. The prodrug colistin methanesulfonate takes time to hydrolyze to the active colistin form; it was reported to take 4 hours to hydrolyze 1/8 of colistin methanesulfonate to colistin.¹²² This delayed antibiotic action likely led to synergistic killing since dispersion was able to occur prior to the drug hydrolyzing into the active form. Dispersion of bacteria out of the biofilm may have weakened the biofilm structure to enable antibiotic penetration within the biofilm.

Erythromycin inhibits bacterial growth through inhibition of protein synthesis, especially at high concentrations.⁴⁰ Thus, erythromycin requires bacterial cells to be metabolically active to be effective. The promotion of bacterial metabolic activity with the addition of sodium citrate likely enhanced the synergistic activity of the compounds. Sodium citrate also has the largest negative charge, which may have aided the penetration of positively charged erythromycin (Figure 3-12) into the biofilm.⁹⁸

3.5 Conclusions

The most promising combination treatments against mature biofilms included amikacin disulfate, colistin methanesulfonate, and erythromycin with sodium citrate. Succinic acid and xylitol had been effective dispersion compounds to be used with antibiotics against young biofilms in the high-throughput screening (Chapter 2), but were not effective at the same concentrations against mature biofilms. Thus biofilm age plays an important role on dispersion compounds and antibiotics synergistically killing *P. aeruginosa* biofilms. The concentrations may need to be increased to be effective against more mature biofilms. Glutamic acid was tested at a lower concentration and may require a higher concentration to be effective with antibiotics against the mature biofilms as well.

Table 3-1: Concentrations of antibiotic and dispersion compounds tested.

Antibiotic	Concentration (mg/mL)	Concentration (mM)	Dispersion Compounds	Concentration (mM)
Amikacin disulfate	1.0	1.3	Sodium Citrate	10
Tobramycin sulfate	1.8, 6.3	1.3, 4.4	Succinic acid	10
Polymyxin B sulfate	2.5	1.8	Xylitol	75
Colistin sulfate	1.0	1.9	Glutamic acid	0.6
Colistin methanesulfonate	2.2	0.6		
Erythromycin	2.0	2.7		

Table 3-2: Percent live biofilm bacteria and percent live free-swimming bacteria of untreated growth controls.

	Live Biofilm Bacteria, %	Live Free-swimming Bacteria, %
Overall	73.5 ± 9.4	85.2 ± 4.8
Tray 1	77.7 ± 0.9	87.6 ± 1.8
Tray 2	65.5 ± 19.4	87.8 ± 0.8
Tray 3	67.5 ± 6.9	81.7 ± 5.4
Tray 4	71.7 ± 3.1	87.1 ± 0.8
Tray 5	76.2 ± 10.4	87.7 ± 0.3
Tray 6	83.1 ± 1.2	88.4 ± 1.9

Pseudomonas aeruginosa bacteria were grown in a Lab-Tek chambered coverglass tray.

Biofilm bacteria were grown for 4 days followed by 1 day of growth after fresh media was replaced.

Free-swimming bacteria were those that dispersed from the biofilm after a rinse step and fresh media addition.

Sample n=3 for each Lab-Tek chambered coverglass tray.

Table 3-3: Percent live biofilm bacteria quantified with STAINIFICATION after 1 day of treatment with antibiotics alone or in combination with dispersion compounds.

Sample	Live Biofilm Bacteria, %
Untreated controls	73.5 ± 9.4
Dispersion compound only controls	
sodium citrate	79.2 ± 1.3
succinic acid	80.0 ± 1.0
xylitol	67.0 ± 2.0
glutamic acid	78.4 ± 3.6
Amikacin disulfate (1.0 mg/mL)	
	48.4 ± 12.0 *
with citrate	8.7 ± 7.6 * ^
with succinic acid	42.1 ± 19.8 *
with xylitol	60.7 ± 10.0
with glutamic acid	58.4 ± 4.7
Tobramycin sulfate (1.8 mg/mL)	
	18.6 ± 6.3 *
with citrate	35.8 ± 2.1 * ^
with succinic acid	23.5 ± 5.1 *
Tobramycin sulfate (6.3 mg/mL)	
	61.5 ± 4.4
with citrate	45.0 ± 12.0 *
with succinic acid	47.6 ± 21.6 *
with xylitol	56.4 ± 0.9
with glutamic acid	49.2 ± 9.4 *
Polymyxin B sulfate (2.5 mg/mL)	
	28.1 ± 8.0 *
with citrate	33.1 ± 4.5 *
with succinic acid	34.0 ± 4.3 *
with xylitol	31.9 ± 2.0 *
with glutamic acid	31.8 ± 3.0 *

Table 3-3: Continued.

Sample	Live Biofilm Bacteria, %
Colistin sulfate (1 mg/mL)	21.7 ± 1.2 *
with citrate	15.5 ± 1.8 *
with succinic acid	17.6 ± 2.2 *
with xylitol	12.8 ± 1.8 *
with glutamic acid	22.0 ± 2.1 *
Colistin methanesulfonate (2.2 mg/mL)	33.8 ± 3.2 *
with citrate	5.6 ± 2.9 * ^
with succinic acid	22.2 ± 12.8 *
with xylitol	27.9 ± 6.8 *
with glutamic acid	36.5 ± 1.7 *
Erythromycin (2.0 mg/mL)	62.6 ± 8.4
with citrate	8.6 ± 6.3 * ^
with succinic acid	37.8 ± 22.6 *
with xylitol	60.5 ± 10.6
with glutamic acid	64.6 ± 4.7

* significant compared to untreated control (p<0.05)

^ significant compared to antibiotic control and dispersion control (p<0.05)

Pseudomonas aeruginosa biofilms were grown for 4 days in Lab-Tek chambered coverglass.

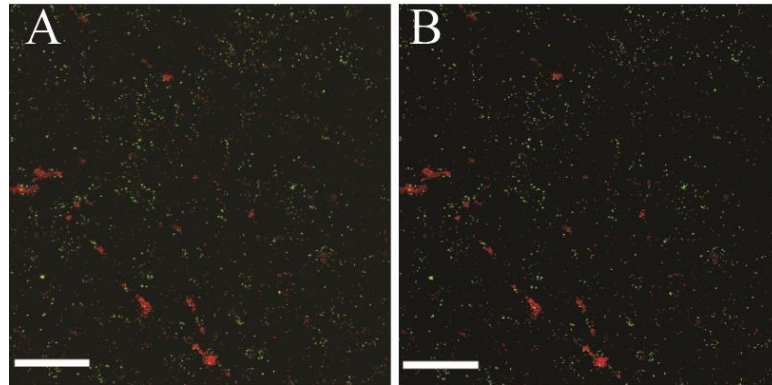


Figure 3-1: Confocal microscopy images of *Pseudomonas aeruginosa* biofilms; images were segmented with a threshold intensity value of 45; after thresholding, the images were visually similar to the original confocal image; example of an A) original confocal image and B) image after thresholding; bacteria were stained with syto 9 and propidium iodide; aerial view, scale bar = 45 μm .

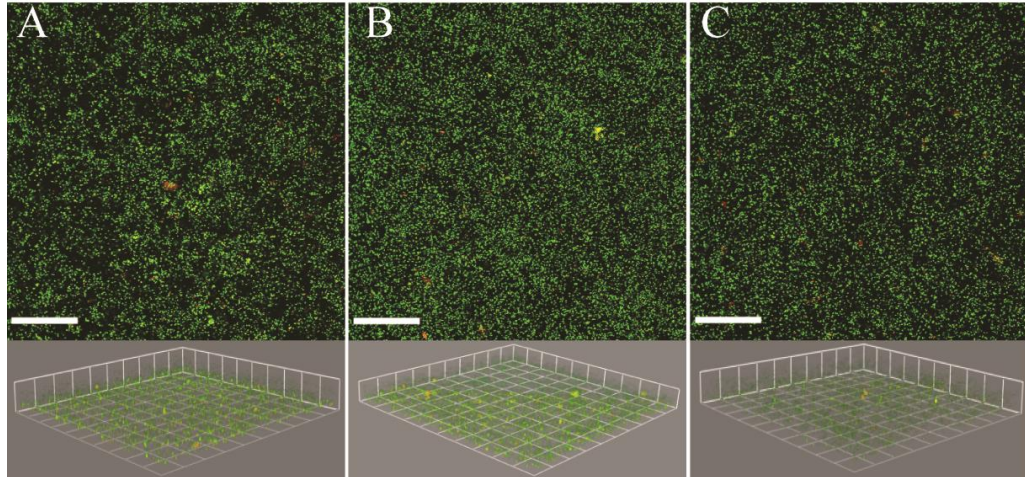


Figure 3-2: Three representative untreated controls for *Pseudomonas aeruginosa* biofilm growth; A-C) All untreated controls were visually similar to one another; stained with syto 9 and propidium iodide; green=live bacteria, red=dead bacteria; Top: aerial view, scale bar = 45 μm ; Bottom: side view, each square = 23.1 μm on each side.

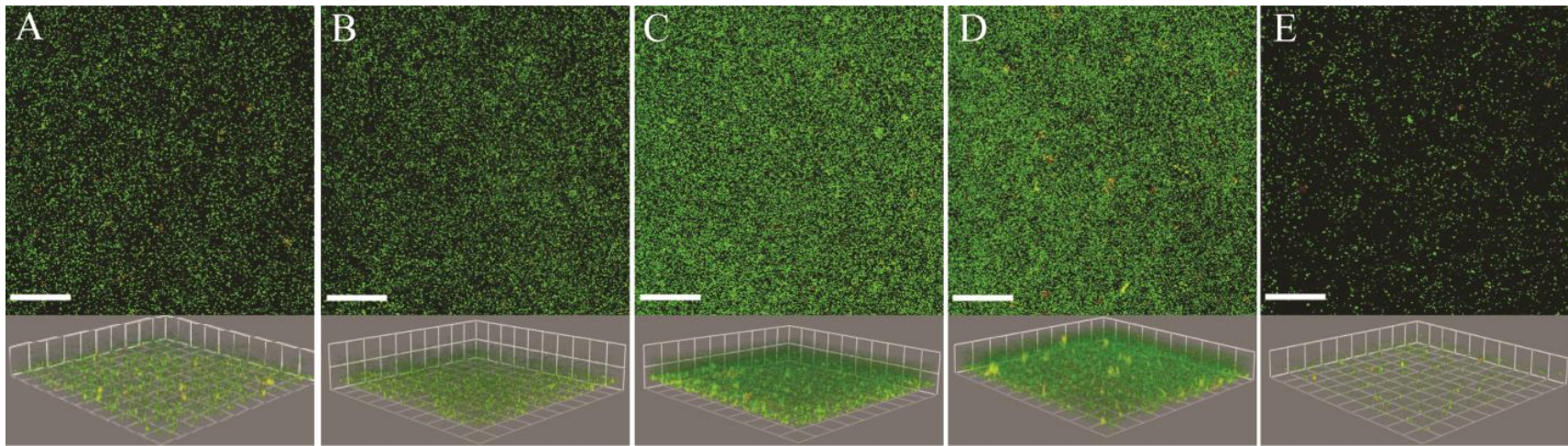


Figure 3-3: Confocal microscopy images of the untreated control and dispersion compound treated *Pseudomonas aeruginosa* bacteria; confocal images of *P. aeruginosa* biofilms A) left untreated or treated with aqueous solutions containing one of four dispersion compounds: B) sodium citrate, C) succinic acid, D) xylitol, and E) glutamic acid; stained with syto 9 and propidium iodide; green=live bacteria, red=dead bacteria; top: aerial view, scale bar = 45 μm ; bottom: side view, each square = 23.1 μm on each side.

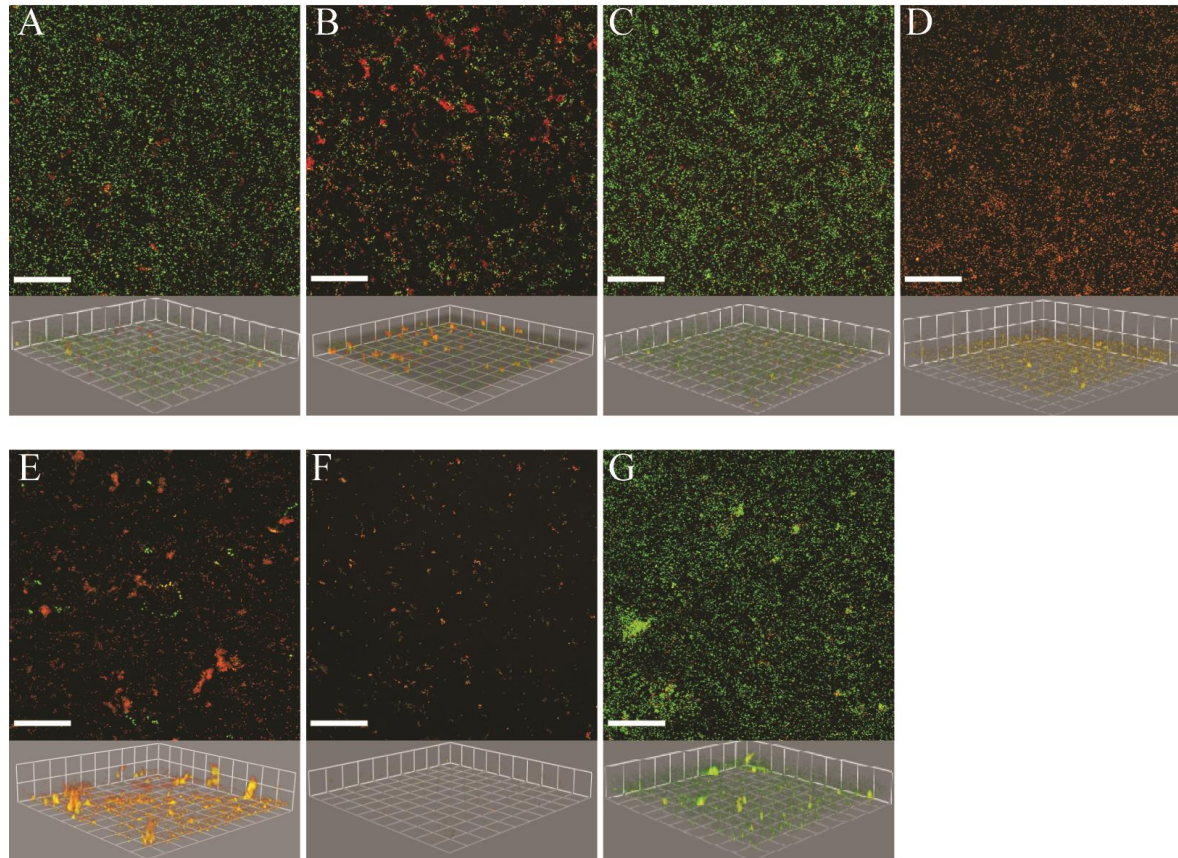


Figure 3-4: Confocal images of biofilms after treatment with antibiotics, A) amikacin disulfate, B) tobramycin sulfate (1.8 mg/mL), C) tobramycin sulfate (6.3 mg/mL), D) polymyxin B sulfate, E) colistin sulfate, F) colistin methanesulfonate, and G) erythromycin; bacteria were stained with syto 9 and propidium iodide; green=live bacteria, red=dead bacteria; top: aerial view, scale bar = 45 μm ; bottom: side view, each square = 23.1 μm on each side.

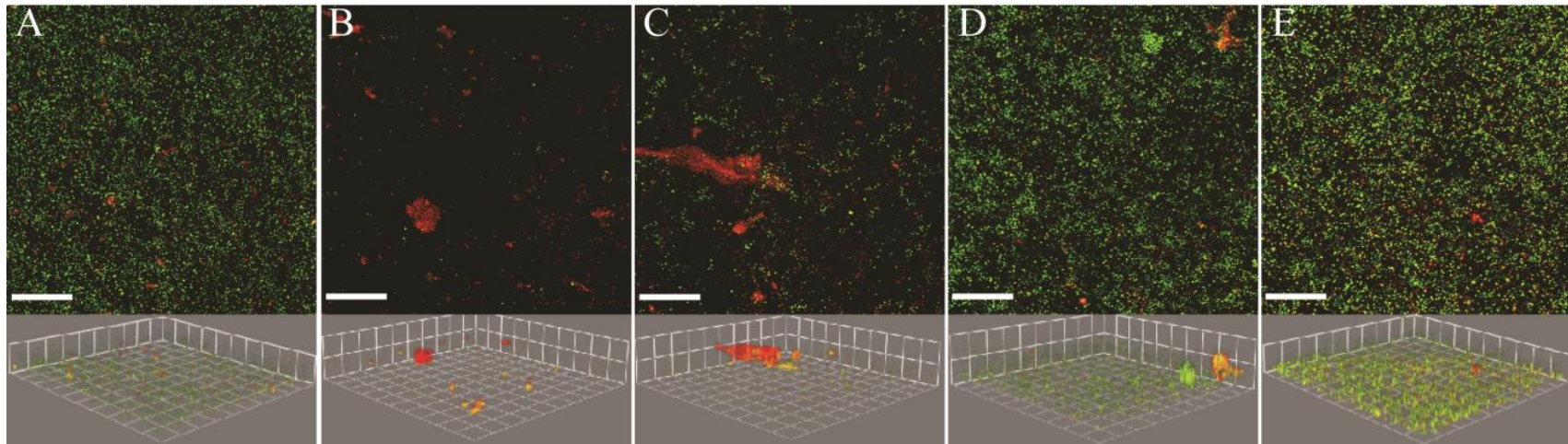


Figure 3-5: Confocal microscopy images of *Pseudomonas aeruginosa* bacteria after treatment with amikacin disulfate alone or in combination with dispersion compounds; amikacin disulfate exhibited a synergistic effect on eradication of *P. aeruginosa* biofilms with the nutrient dispersion compound sodium citrate; confocal images of *P. aeruginosa* treated with aqueous solutions containing A) amikacin disulfate, B) amikacin disulfate with sodium citrate, C) amikacin disulfate with succinic acid, D) amikacin disulfate with xylitol, and E) amikacin disulfate with glutamic acid; stained with syto 9 and propidium iodide; green=live bacteria, red=dead bacteria; top: aerial view, scale bar = 45 μm ; bottom: side view, each square = 23.1 μm on each side.

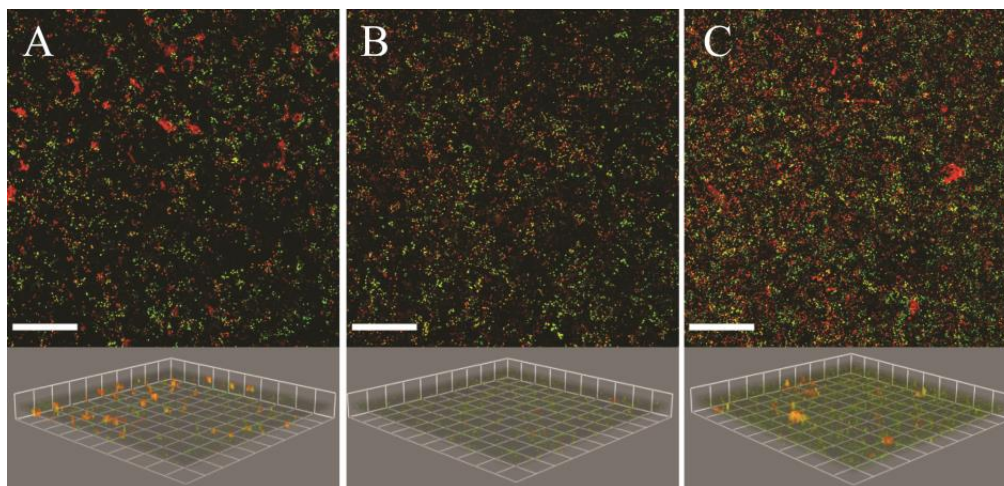


Figure 3-6: Confocal microscopy images of *Pseudomonas aeruginosa* bacteria after treatment with 1.8 mg/mL tobramycin sulfate alone or in combination with dispersion compounds; co-treatments of tobramycin sulfate (1.8 mg/mL) with dispersion compound sodium citrate led to biofilms with more live bacteria compared to the antibiotic control; confocal images of *P. aeruginosa* biofilms treated with aqueous solutions containing A) tobramycin sulfate (1.8 mg/mL), B) tobramycin sulfate (1.8 mg/mL) with sodium citrate and C) tobramycin sulfate (1.8 mg/mL) with succinic acid; stained with syto 9 and propidium iodide; green=live bacteria, red=dead bacteria; top: aerial view, scale bar = 45 μm ; bottom: each square = 23.1 μm on each side.

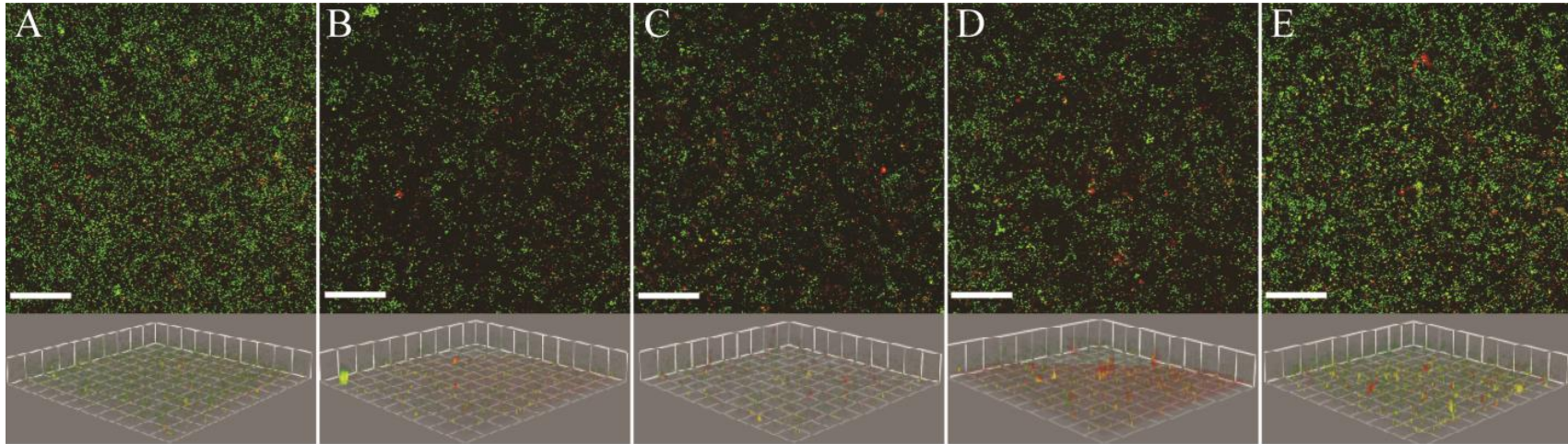


Figure 3-7: Confocal microscopy images of *Pseudomonas aeruginosa* bacteria after treatment with 6.3 mg/mL tobramycin sulfate alone or in combination with dispersion compounds; co-treatments of tobramycin sulfate (6.3 mg/mL) with dispersion compounds were minimally effective at reducing the live bacteria remaining within *P. aeruginosa* biofilms; confocal images of *P. aeruginosa* biofilms treated with aqueous solutions containing A) tobramycin sulfate (6.3 mg/mL), B) tobramycin sulfate (6.3 mg/mL) with sodium citrate, C) tobramycin sulfate (6.3 mg/mL) with succinic acid, D) tobramycin sulfate (6.3 mg/mL) with xylitol, and E) tobramycin sulfate (6.3 mg/mL) with glutamic acid; stained with syto 9 and propidium iodide; green=live bacteria, red=dead bacteria; top: aerial view, scale bar = 45 μm ; bottom: side view, each square = 23.1 μm on each side.

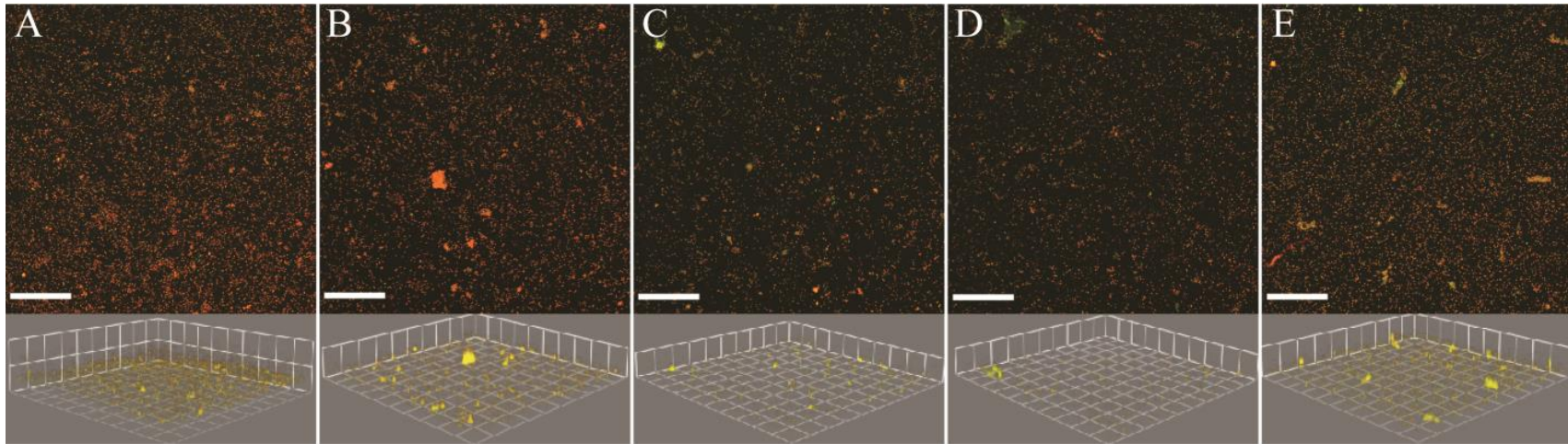


Figure 3-8: Confocal microscopy images of *Pseudomonas aeruginosa* bacteria after treatment with polymyxin B sulfate alone or in combination with dispersion compounds; treatment of *P. aeruginosa* biofilms with polymyxin B sulfate in combination with a dispersion compound did not provide synergistic killing; confocal images of *P. aeruginosa* biofilms treated with aqueous solutions containing A) polymyxin B sulfate, B) polymyxin B sulfate with sodium citrate, C) polymyxin B sulfate with succinic acid, D) polymyxin B sulfate with xylitol, and E) polymyxin B sulfate with glutamic acid; stained with syto 9 and propidium iodide; green=live bacteria, red=dead bacteria; top: aerial view, scale bar = 45 μm ; bottom: side view, each square = 23.1 μm on each side.

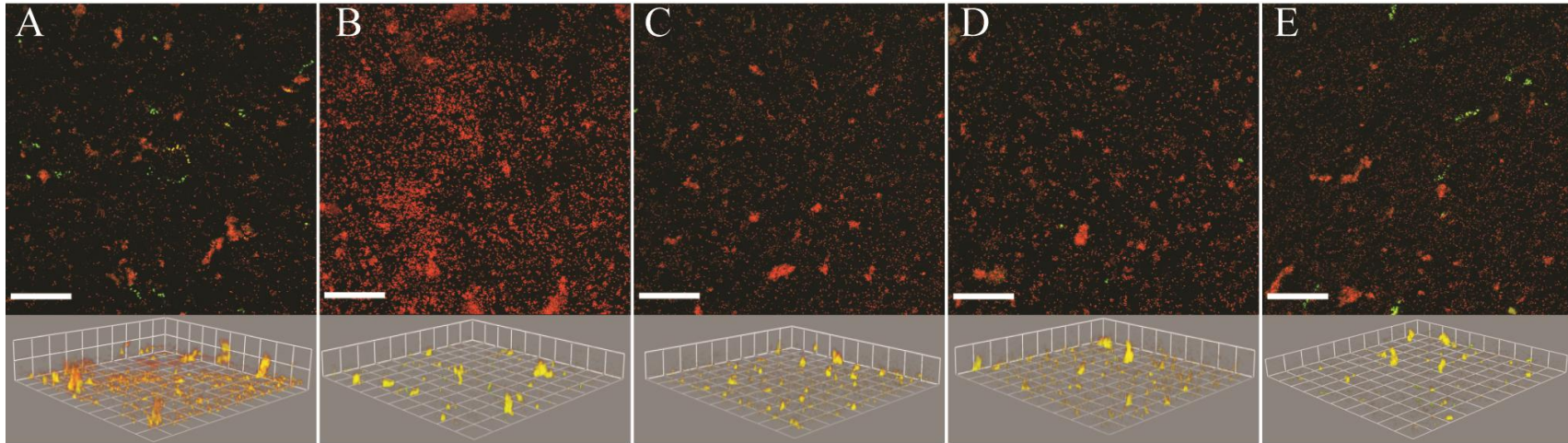


Figure 3-9: Confocal microscopy images of *Pseudomonas aeruginosa* bacteria after treatment with colistin sulfate alone or in combination with dispersion compounds; treatment of *P. aeruginosa* biofilms with colistin sulfate was effective at reducing the percent live bacteria after treatment, while co-treatments were not significantly different from the antibiotic treatment alone; confocal images of *P. aeruginosa* biofilms treated with aqueous solutions containing A) colistin sulfate, B) colistin sulfate with sodium citrate, C) colistin sulfate with succinic acid, D) colistin sulfate with xylitol, and E) colistin sulfate with glutamic acid; stained with syto 9 and propidium iodide; green=live bacteria, red=dead bacteria; top: aerial view, scale bar = 45 μm ; bottom: side view, each square = 23.1 μm on each side.

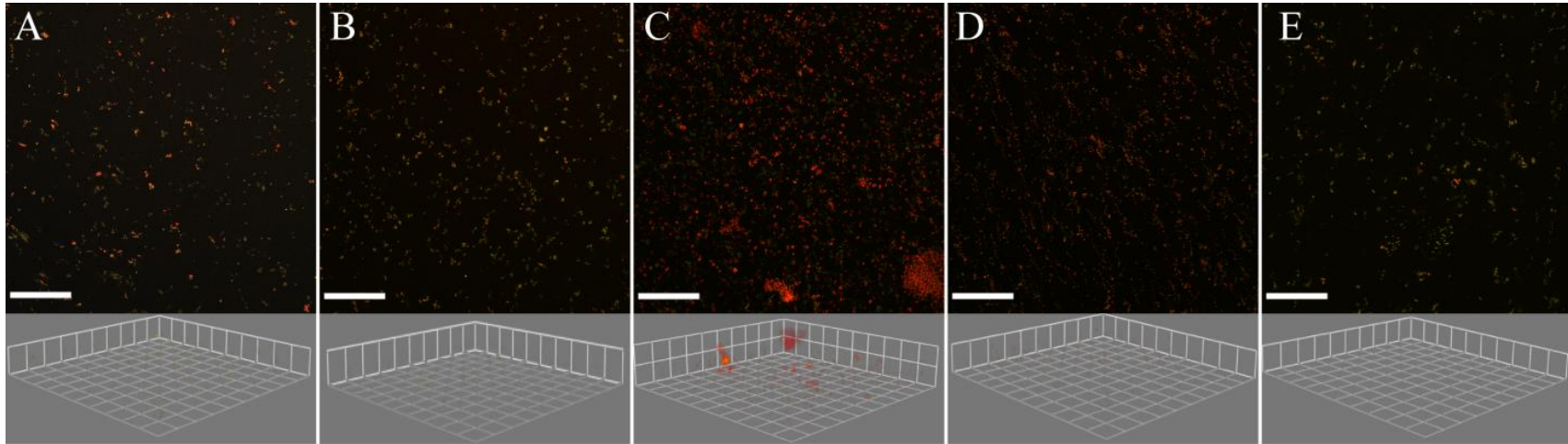


Figure 3-10: Confocal microscopy images of *Pseudomonas aeruginosa* bacteria after treatment with colistin methanesulfonate alone or in combination with dispersion compounds; colistin methanesulfonate synergistically killed *P. aeruginosa* bacteria in combination with the dispersion compound sodium citrate; confocal images of *P. aeruginosa* biofilms treated with aqueous solutions containing A) colistin methanesulfonate, B) colistin methanesulfonate with sodium citrate, C) colistin methanesulfonate with succinic acid, D) colistin methanesulfonate with xylitol, and E) colistin methanesulfonate with glutamic acid; stained with syto 9 and propidium iodide; green=live bacteria, red=dead bacteria; top: aerial view, scale bar = 45 μm ; bottom: each square = 23.1 μm on each side.

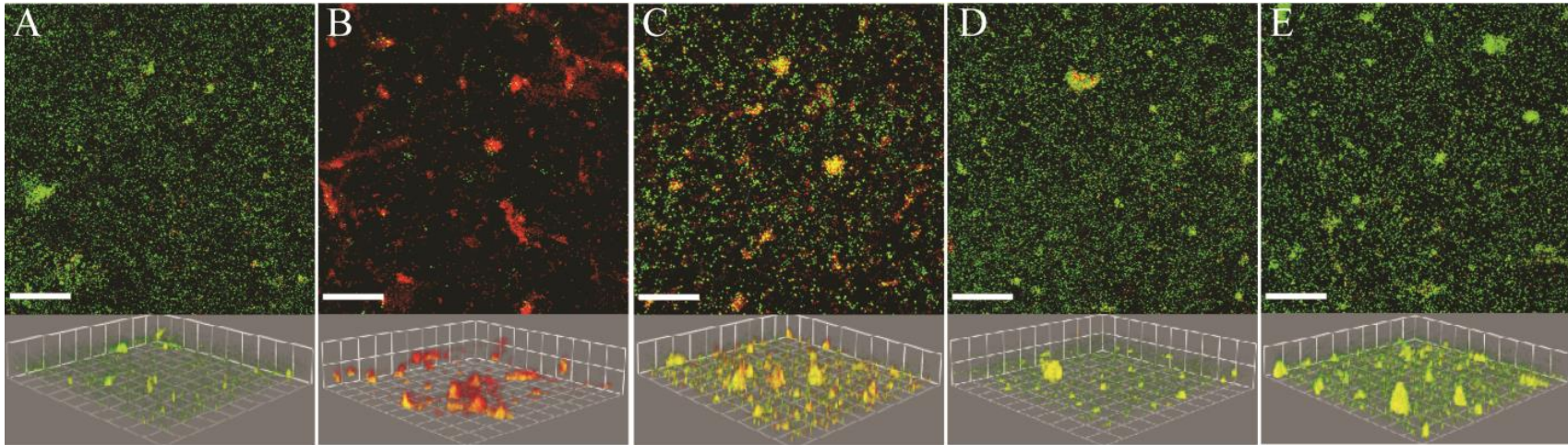


Figure 3-11: Confocal microscopy images of *Pseudomonas aeruginosa* bacteria after treatment with erythromycin alone or in combination with dispersion compounds; erythromycin and sodium citrate synergistically decreased the percentage of live bacteria remaining within *P. aeruginosa* biofilms after co-treatment; confocal image of *P. aeruginosa* biofilms treated with aqueous solutions containing A) erythromycin, B) erythromycin with sodium citrate, C) erythromycin with succinic acid, D) erythromycin with xylitol, and E) erythromycin with glutamic acid; stained with syto 9 and propidium iodide; green=live bacteria, red=dead bacteria; top: aerial view, scale bar = 45 μm ; bottom: side view, each square = 23.1 μm on each side.

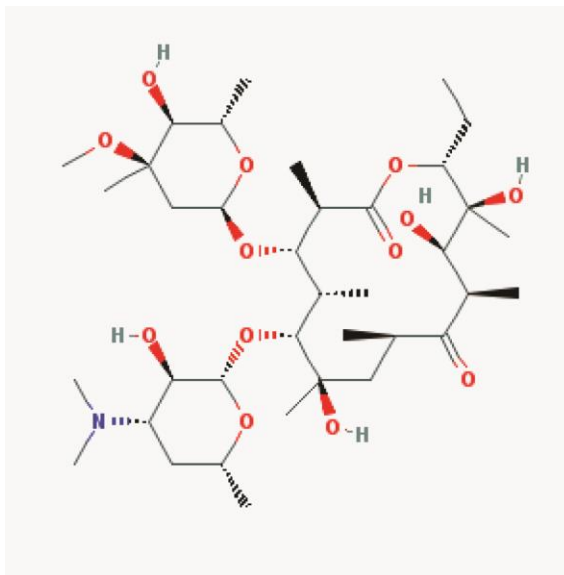


Figure 3-12: Erythromycin structure ($pK_a=8.9$).⁹⁸

CHAPTER 4
INTRODUCING A NOVEL QUANTIFICATION PROGRAM
STAINIFICATION FOR BIOFILM CONFOCAL IMAGE ANALYSIS²

4.1 Introduction

Confocal laser scanning microscopy (CLSM) is commonly used to investigate biofilms. CLSM is a non-destructive method that allows for real-time imaging of biological systems with high resolution (200 nm).⁹³ The major limitations are the time and cost of image acquisition.⁹³ Imaging of fluorescently-labeled bacteria, proteins polysaccharides, DNA, and enzymes, at different planes of the biofilm lead to 3D image sequences for analysis.⁹³ These images can then be used for both qualitative and quantitative comparison for evaluating biofilm architecture, biofilm development on different growth substratum materials, and bacterial viability.^{62, 134-135}

Programs to quantify CLSM images of biofilms require two main steps. The first step is to threshold the image, which allows for separation of bacteria fluorescence from background noise. A threshold intensity between 1 and 256 for an 8 bit image is used to define the separating value; intensities in the image below the threshold value are considered background noise and intensities in the image equal to or above the threshold value are considered objects of interest.¹³⁶⁻¹³⁷ Figure 4-1A shows an ideal histogram of pixel intensity values versus frequency. The ideal histogram has a large background noise peak and a smaller object of interest peak. The threshold intensity that would best separate the two intensity populations occurs at the minimum between the two peaks. After thresholding, all pixels in the image will be reassigned a value of either 1 or 0 to create a binary image. The resulting binary thresholded image has a value of 1

² Parts of this chapter have been reprinted from Sommerfeld Ross, S.; Reinhardt, J. M.; Fiegel, J., Enhanced analysis of bacteria susceptibility in connected biofilms. *Journal of Microbiological Methods* **2012**, *90* (1), 9-14 with permission from Elsevier.

reassigned to all object of interest pixels and a value of 0 reassigned to all background noise pixels. With an intensity histogram in Figure 4-1A, a user can easily manually determine a threshold value. However, when an intensity histogram has peaks that are not well-separated, do not follow Gaussian distribution, or have multiple modes, the thresholding can be more difficult to determine (Figure 4-1B). A user can manually choose threshold values and compare the original image to the thresholded image to determine a threshold value by trial and error. Or more commonly, automated thresholding algorithms are used. The National Institute of Health's ImageJ program has 17 automated thresholding algorithm options.⁹⁵ The Otsu algorithm is the automated thresholding option that has been incorporated into biofilm-specific quantification programs, like COMSTAT and PHLIP.^{96, 136, 138-139} The Otsu algorithm maximizes the variance between the object of interest fluorescence and the background noise fluorescence.¹³⁶ Therefore, it can be used to automatically determine a threshold intensity value from non-ideal intensity histograms. Since confocal images contain sequences of 2D images, an Otsu threshold can be found for each 2D image. Either each Otsu threshold can be applied to its respective image (Otsu local thresholding) or one Otsu threshold (Otsu global thresholding), such as a maximum or median, can be applied to all of the images in the sequence. Current biofilm-specific software only allows for Otsu global thresholding.^{96, 138-139}

The second step in quantifying CLSM images is to separate connected-biofilm bacteria and unconnected bacteria. Confocal images for biofilm studies typically contain bacteria within the biofilm and bacteria outside of the biofilm that are fluorescently labeled with the same probe.^{96, 140} Whether using standard nucleic acid stains or working with internally fluorescently probed bacteria, such as GFP-bacteria, both bacterial populations will appear the same color in the confocal images.¹⁴⁰ To separate these populations, Heydorn et al. developed the connected volume filtration (CVF) algorithm.⁹⁶ The CVF algorithm starts at the substratum image slice where the bacteria attach to a

surface. For CVF it is important to have a flat imaging substratum, such as glass, to be able to quantify the biofilm. The algorithm compares pixels between the first two image slices. If pixels of interest on slice two are located in the same position directly above pixels of interest on slice one, then these pixels are considered biofilm bacteria pixels (Figure 4-2A). Any pixel deemed biofilm bacteria on slice two then has an eight neighborhood connection completed to allow for horizontal biofilm growth (Figure 4-2B). If pixels of interest are located in any of the 8 surrounding pixel locations, then these pixels are considered biofilm bacteria pixels. The comparison between slices for vertical biofilm growth and the eight neighborhood connection for horizontal biofilm growth are continued until the final image slice.⁹⁶ The biofilm bacteria retained are called connected-biofilm bacteria since the CVF algorithm assumes the bacteria grow in close proximity (within the z-step slice size from CLSM acquisition). Any pixels of interest that are not connected to the substratum slice through the CVF algorithm are considered unconnected bacteria, which can be dispersed or free-swimming bacteria. With current software, it is common for the unconnected bacteria pixels to be excluded from analysis.⁹⁶

Thresholding and CVF are used in the most common quantification software COMSTAT⁹⁶ and in the software PHLIP.¹³⁸ The original COMSTAT program was developed in MatLab and provided many quantification parameters for users.⁹⁶ The software PHLIP is not used commonly, however the publications on the theory of PHLIP address limitations in COMSTAT.¹³⁸ A newer version of COMSTAT called COMSTAT2-Beta is now available with improvements.^{96, 139}

Table 4-1 lists comparisons between COMSTAT, PHLIP, and COMSTAT2-Beta.^{96, 138-139} COMSTAT can read “.tif” sequences of images with “.info” text files that provide information such as the number of images in the sequence, the calibration information for the x and y directions ($\mu\text{m}/\text{pixel}$), and the z-step slice size (μm) (Figure 4-3). This requires users to save their CLSM images as “.tif” sequences and to generate

“.info” files, which is more time-consuming than saving the native CLSM formats. However, this does not limit the program to specific brands of confocal microscopes to generate specific CLSM formats. The user interface in MatLab requires users to type commands into the MatLab window (Figure 4-4). COMSTAT only has a manual thresholding option. The CVF algorithm, which was developed by the makers of COMSTAT, is used on each image sequence separately. A colocalization parameter is not available in COMSTAT. This is a limitation since the most common viability stains for biofilms are based on nucleic acid stain permeability. One stain is membrane permeable (usually green) and thus can stain all cells, while one stain is impermeable (usually red). Therefore, colocalization of both color stains in the images can be common and when quantified these pixels will be counted for both color channels. After quantification, COMSTAT data is saved as individual “.txt” files for each parameter quantified.⁹⁶ This requires additional processing steps for the user if they desire to have all data in a single file.

PHLIP has a separate program for converting CLSM images into eXtensible Markup Language (XML) files to assist in creating a standard format for CLSM images. Like COMSTAT, the PHLIP quantification program was developed in MatLab as well. The program provides the user with many options (Figure 4-5). Beyond manual thresholding, PHLIP also has an automated Otsu threshold option. The computer program automatically finds an optimal Otsu threshold value for the entire image stack. Developers of PHLIP acknowledged a limitation in COMSTAT’s CVF algorithm. COMSTAT completes CVF for a single image channel. However, bacteria can be stained with multiple color stains and thus it is advantageous to complete CVF for all bacteria color channels together. Since colocalization is common in biofilm research, the PHLIP program quantifies the fraction of pixels that are colocalized. The quantified data can be saved as text files or as HTML files that automatically format the data and generate plots.¹³⁸

COMSTAT2-Beta was developed in ImageJ to provide a free platform for users, compared to MatLab that requires a license. This program directly opens the native Zeiss CLSM “.lsm” files. However, it cannot read “.tif” sequences with “.info” files, which is what COMSTAT users are familiar with. The user interface is easy to use and intuitive (Figure 4-6). Like PHLIP, the thresholding options are manual or Otsu global. For Otsu global thresholding, one optimal value is used for the entire image sequence. The CVF algorithm is still completed on single image channels rather than multiple channels together. There is not a colocalization algorithm. The data is still saved as “.txt” files for each parameter quantified.^{96, 139}

This chapter introduces a new CLSM biofilm quantification program STAINIFICATION that addresses limitations to COMSTAT and COMSTAT2-Beta, including user interface, thresholding, CVF, colocalization, and image saving. A novel colocalization adjustment option is provided to automatically prevent double counting of colocalized pixels. We also introduce a modified CVF algorithm that allows quantification of biofilms grown on an uneven surface. This has led to two novel quantification parameters. A modified substratum coverage calculation enumerates the percent of the uneven substratum covered by connected-biofilm bacteria. For bacteria that can enter the surface, such as intracellular bacteria, we can now quantify the percent bacteria or volume of bacteria associated with the surface.

4.2 Materials and Methods

4.2.1 Development of STAINIFICATION

MatLab R2009b was used with the Image Processing Toolbox to develop STAINIFICATION. MatLab was used since it has many internal functions and has the ability to create stand-alone executable files. The disadvantage to using MatLab is the software cost. STAINIFICATION, while developed in MatLab, does not require

MatLab to be run since a stand-alone executable file was created. COMSTAT source code was used to enable reading “.tif” and “.info” files and to complete CVF for separating connected-biofilm bacteria and unconnected bacteria.^{96, 139, 141}

Code from other programmers was used to read in image files, to complete separation of connected-biofilm bacteria from unconnected bacteria (standard in the field), and to save the data to an Excel[®] file. To develop STAINIFICATION, source code from COMSTAT was used to read in “.tif” image sequences with the calibration “.info” file.⁹⁶ The LSM File Toolbox from Peter Li was used to read in “.lsm” image sequences.¹⁴² Since it is standard in common quantification programs, source code for the connected volume filtration from COMSTAT was used to separate connected-biofilm bacteria and unconnected bacteria.⁹⁶ It was modified to quantify bacteria grown on an uneven surface. Scott Hirsch provided xlsxwrite code, which I modified, to save data in STAINIFICATION.¹⁴³

4.2.1.1 Thresholding

Thresholding in CLSM images is used to separate the bacteria fluorescence from background noise. Otsu threshold, the automatic thresholding option available in COMSTAT2-beta and in PHLIP, maximizes the variance between the bacteria fluorescence and the background noise fluorescence.^{96, 136, 138-139}

4.2.1.2 Colocalization Adjustment Algorithm for Bacteria

STAINIFICATION’s novel colocalization adjustment algorithm is an option to prevent double counting of pixels with use of nucleic acid membrane integrity stains for bacterial viability. The colocalization adjustment algorithm identifies colocalized pixels and removes the membrane permeable signal (see Appendix). For example, most commonly a green fluorescent membrane permeable stain and red fluorescent membrane

impermeable stain are used. A colocalized pixel appears yellow. With the colocalization adjustment algorithm, pixels that are colocalized will only retain the red membrane impermeable signal and the green membrane permeable signal will be removed. Colocalized pixels are assumed to have disrupted membranes and thus be classified as dead bacteria.

The algorithm uses the binary thresholded channel images as input. Binary images are also known as logical parameters since they contain values of 1 or 0. Assuming a green membrane permeable stain and red membrane impermeable stain, the variables ChannelRedThresholdLogic and ChannelGreenThresholdLogic sequences are compared at each pixel location. For each pixel that contains a value of 1 for both image sequences, only the red channel will retain the value of 1 and the green channel value will be changed to 0. Otherwise the values at a given pixel remain the same.

4.2.1.3 Applying Connected Volume Filtration to Multiple Channels

STAINIFICATION uses COMSTAT's connected volume filtration (CVF) algorithm on all bacteria color channels to separate connected-biofilm bacteria and unconnected bacteria. The binary thresholded sequence variables ChannelRedThresholdLogic and ChannelGreenThresholdLogic are compared. If either variables ChannelRedThresholdLogic or ChannelGreenThresholdLogic or if both have a value of 1 for a given pixel, then a value of 1 is given to that pixel location in the variable Connect. Otherwise a value of 0 is given to the pixel location in the variable Connect. COMSTAT's CVF is applied to the Connect variable.

It is important to use the recommended slice size for optimal resolution on the microscope (set confocal pinhole to 1 Airy unit, optimal step size is $\frac{1}{2}$ the pinhole size in

μm).¹³⁷ It is not ideal to have slice sizes greater than the size of the bacteria being investigated when using connected volume filtration.

4.2.1.4 Maintaining the Connected and Unconnected

Bacterial Populations

STAINIFICATION uses CVF algorithm on all bacteria color channels to separate connected-biofilm bacteria and unconnected bacteria. Unlike COMSTAT which only saves the connected-biofilm bacteria image pixels, STAINIFICATION maintains both the connected-biofilm bacteria and unconnected bacteria image pixels.

To maintain these bacterial populations, a comparison of the CVF output (which indicates connection) and the bacteria images after thresholding (which indicates bacteria present) are compared. In the CVF algorithm, 1 represents connected-biofilm bacteria and 0 represents either unconnected bacteria or background noise. If CVF has a value of 1 and the bacteria thresholded image has a value of 1 for a pixel location, then that pixel is classified as connected-biofilm bacteria. If CVF has a value of 0 and the bacteria thresholded image has a value of 1 for a pixel location, then that pixel is classified as unconnected bacteria. If both CVF and the bacteria thresholded image have a value of 0, then the pixel is background noise.

This comparison algorithm (see Appendix) compared each pixel in the color channel after thresholding and after colocalization adjustment (if applicable). The variables AllRedPixels or AllGreenPixels were compared with the CVF matrix variable filt_images. If both the color channel and the connected volume filtration matrix had a value of 1 for a particular pixel location, then a value of 1 was placed in that pixel location for the variable ConnectedBiofilmRedPixel or ConnectedBiofilmGreenPixel. If the color channel had a value of 1, but the CVF matrix had a value of 0 at a particular pixel location, then a value of 1 was placed in that pixel location for the variable

UnconnectedBacteriaRedPixel or UnconnectedBacteriaGreenPixel. Otherwise, a 0 was placed in the pixel location.

4.2.1.5 Quantifying Bacterial Viability

The percent dead and live bacterial populations can be quantified using STAINIFICATION. After colocalization adjustment where applicable and CVF, the connected-biofilm bacteria were quantified for viability by

$$\text{Live Connected Biofilm, \%} = \frac{\text{ConnectedBiofilmGreenPixel}}{(\text{ConnectedBiofilmGreenPixel} + \text{ConnectedBiofilmRedPixel})} *$$

100%

Equation 4-1

$$\text{Dead Connected Biofilm, \%} = \frac{\text{ConnectedBiofilmRedPixel}}{(\text{ConnectedBiofilmGreenPixel} + \text{ConnectedBiofilmRedPixel})} *$$

100%

Equation 4-2

Connected-biofilm bacteria were quantified for overall viability in the entire image sequence and for each image slice (see Appendix). Likewise, the same calculations were done for the unconnected bacteria.

4.2.1.6 Saving “.tif” Image Sequences

STAINIFICATION saves “.tif” image sequences of processed images (see Appendix). The “.tif” image sequences were created by multiplying the binary image files (ConnectedBiofilmRedPixel, ConnectedBiofilmGreenPixel, UnconnectedBacteriaRedPixel, and UnconnectedBacteriaGreenPixel) by the original

bacteria image with gray scale values between 1 and 256 for 8-bit images (OriginalBacteria). The “.tif” image sequences can be visualized with 3D rendering software, such as Volocity® (PerkinElmer, Waltham, MA).

4.2.1.7 Quantifying Bacteria on an Uneven Surface

4.2.1.7.1 Surface Quantification Parameters

For biofilms grown on a flat surface, the substratum coverage or percent of the flat surface that is covered by bacteria, is given by

$$\text{Substratum, \%} = B_0 / (\text{pixelx} * \text{pixely}) * 100\% \quad \text{Equation 4-3}$$

where B_0 is the number of bacteria pixels on the first image layer, pixelx is the number of pixels in the x-direction, and pixely is the number of pixels in the y-direction. The original substratum coverage in COMSTAT takes into account all bacteria growing on the imaging substratum.⁹⁶

To account for attachment to an irregular surface, a modified connected volume filtration (MCVF) algorithm was developed. The MCVF is used to find the modified substratum coverage, which is equated to the percent bacteria pixels on the first image slice that surround the irregular surface and bacteria pixels directly above a surface pixel (Figure 4-7). The bacteria on the first image slice represent bacteria adhered to the device imaging substratum (Figure 4-7 far right). Beyond this, our modified substratum coverage includes the bacteria above the fluorescent / reflective uneven surface. The algorithm assumes that bacteria and surface cannot occupy the same pixel location. Mathematically the modified substratum coverage is given by

$$\text{Modified Substratum, \%} = (B_0 + B^*) / (\text{pixelx} * \text{pixely}) * 100\% \quad \text{Equation 4-4}$$

where B_0 is the number of bacteria pixels on the first image layer, B^* is the number of connected-biofilm bacteria pixels directly above a surface pixel, $pixelx$ is the number of pixels in the x-direction, and $pixely$ is the number of pixels in the y-direction. Unlike the original substratum coverage algorithm, the modified substratum coverage considers the uneven surface and any imaging substratum surrounding the surface as the overall substratum of interest. Therefore bacteria above the uneven surface or the flat imaging substratum are considered in the quantification.

The colocalization of bacteria and the surface was quantified for percent bacteria associated with surface and volume of bacteria associated with surface.

$$Bacteria\ Associated\ with\ Surface, \% = \frac{BacteriaColocalizedwithSurface}{TotalBacteria} * 100\%$$

Equation 4-5

$$Volume\ Bacteria\ Associated, \mu m^3 = BacteriaColocalizedwithSurface * pixelx * pixely * pixelz$$

Equation 4-6

where $pixelz$ is the z-step size in μm .

4.2.1.7.2 Surface Code

To analyze the connected-biofilm bacteria and surface components in a single pass, the Uneven Surface Scripts (see Appendix) began with self-defined binary image sequences Bacteria and Surface. The number of pixels in the image columns, number of pixels in the image rows, total number of pixels, micron per pixel calibration information, and the z-step size were written in the code. Once the image and calibration information

were established, then the modified connected volume filtration (MCVF) was used to retain the connected-biofilm bacteria grown on an uneven surface in the variable `ConnectedBiofilmBacteriaPixel`. The original CVF algorithm assumes that any bacteria pixel on the first image slice or flat substratum is considered connected-biofilm bacteria.⁹⁶ This assumption still holds true in our MCVF algorithm, which would account for bacteria growing around the irregular surface within the biofilm growth device. In addition, the MCVF algorithm assumes that any bacteria pixel in the same location directly above a surface pixel on a previous image slice is also considered a connected-biofilm bacteria pixel. The MCVF algorithm was used to identify bacteria growing on the flat substratum around the irregular surface and bacteria growing on top of an uneven surface. These bacteria pixels were stored in the variable `BiofilmConnectedtoSurface`. Then any bacteria pixels colocalized with the surface pixels (stored in variable `BacteriaColocalized`) were eliminated for the modified substratum coverage calculation since bacteria internalized within the surface were not included in this calculation. The variable `BiofilmConnectedtoSurfaceforSubstratum` represented the $(B_0 + B^*)$ pixels and was used to quantify the modified substratum coverage (Equation 4-4).

The MCVF algorithm included an eight neighborhood connection on the variable `BiofilmConnectedtoSurface` to allow for horizontal biofilm growth. For each value of 1 in the variable `BiofilmConnectedtoSurface`, an eight neighborhood connection was completed for the specified pixel location in the Bacteria image. The eight neighborhood connection identified surrounding pixels in the eight locations around the pixel. If any of those pixel locations contained a value of 1, then a value of 1 was saved in the same pixel location for variable `HorizontalGrowthForBacteriaAttachedtoBStart`. To prevent double counting of the bacteria attached to the surface, a comparison of each pixel location in the variables `BiofilmConnectedtoSurface` and `HorizontalGrowthForBacteriaAttachedtoBStart` was completed. If a value of 1 was found

in either group or in both groups for a single pixel location, then this pixel location was given the value of 1 in the variable BasisforSubstratum. Otherwise, a value of zero was given to the pixel location.

An index variable called StartIndex was created to determine which image slices had values of 1 present in the variable BiofilmConnectedtoSurface. Then CVF was completed for each image slice according to the variable StartIndex starting with the BasisforSubstratum image and comparing to the binary Bacteria image. This comparison included pixel-by-pixel comparison between image slices to allow for vertical biofilm growth and eight neighborhood connections to allow for horizontal biofilm growth. For any pixel location that contained a 1 in the variable BiofilmAttachedtoBiofilm, the value was kept in the variable Storage. To prevent over counting pixels, a comparison was done between the variables BiofilmConnectedtoSurface, BasisforSubstratum, and Storage. If a value of 1 was found in a pixel location for any of these three variables, then the output (variable filt_images) was given a value of 1 for the specific pixel location. The filt_images variable was used to quantify the connected-biofilm bacteria (variable ConnectedBiofilmBacteriaPixel) both associated with the surface and growing on top of the surface.

The bacteria pixels that were located in the same location as the surface pixels (variable BacteriaColocalized) were used to quantify the total number of pixels and the percentage of bacteria pixels that were associated with the surface (variables NumberofBacteriaandSurfaceSamePixel and PercentBacteriaAssociatedwithSurface respectively). This is a new quantification option for assessing bacteria internalized or associated with the edge of a surface.

The Surface binary image sequence was not subjected to CVF and was directly quantified. While the emphasis was on connected-biofilm bacteria and surface quantification of this code, the Uneven Surface Scripts also contain code to separate connected-biofilm bacteria and unconnected bacteria populations, which was previously

discussed. For all quantified bacteria and surface pixels, the number of pixels and area were calculated for the overall image stack and for each slice in the stack. Calculated data were saved in an Excel[®] file. Image “.tif” sequences were generated for visualization of ConnectedBiofilmBacteria, UnconnectedBacteria, OverallBacteria, Surface, BacteriaAssociatedWithSurface, and ModifiedSubstratumCoverageBacteria.

4.2.2 *Pseudomonas Aeruginosa* Biofilm Growth

Pseudomonas aeruginosa biofilms were investigated with this computer program because they are relevant to cystic fibrosis infections and because the bacteria grow in close proximity, which means the connected volume filtration algorithm can be used. Experiments were started from a thawed cryovial of mucoid *Pseudomonas aeruginosa* BAA-47 (American Type Culture Collection, Manassas, VA) bacteria and maintained on agar slants. From the nutrient agar slant a lawn of bacteria was streaked onto nutrient agar in a petri dish.⁹¹ The agar plate was inverted and incubated at 37°C overnight. Three colonies were isolated from the agar plate and suspended in 5 mL sterile nutrient broth and incubated stationary at 37°C for 24 hours. The bacterial suspension was diluted to visually match a 0.5 McFarland turbidity standard. The biofilm growth media consisted of 4.30 g potassium phosphate monobasic, 2.70 g sodium phosphate dibasic, 6.04 mg magnesium sulfate, 137.50 mg glutamic acid (Sigma Aldrich, St. Louis, MO), and 1.55 mg ferrous sulfate heptahydrate (Fisher Scientific, Fair Lawn, NJ) dissolved in 500 mL nanopurified water (Barnstead International, Dubuque, IA) at a final adjusted pH of 6.9. The biofilms were grown in glass bottom 96-well plates (Whatman, Piscataway, NJ). Each well contained 100 µL biofilm growth media and 20 µL bacterial suspension. The plates were sealed with two layers of Parafilm[™] and incubated at 37°C and 70% relative humidity on an orbital shaker table (190 rpm, 24 hrs; VWR model 1000, West Chester, PA). For treatment studies, the biofilm growth media was supplemented with 20

μ l nutrient broth per well, ciprofloxacin hydrochloride (556 or 927 μ g/mL) was added to the treatment wells, and the plates were incubated for another 24 hours.

Prior to imaging via confocal microscopy, each well was stained with 3 μ L of 0.8 mM green-fluorescent Syto 9 (Invitrogen, Eugene, OR) to stain all cells and with 2 μ L of 5 μ M red-fluorescent Sytox Red (Invitrogen, Eugene, OR) to stain cells with disrupted membranes. The Zeiss LSM 510 inverted confocal laser scanning microscope (Carl Zeiss, Jena, Germany) was used to detect the green and red fluorescence from the stains. Syto 9 was excited with the argon 488 nm laser and the emission fluorescence was collected with the band pass filter of 505-530 nm. Sytox Red was excited with the HeNe2 633 nm laser and emission fluorescence was collected with the long pass 650 nm filter. Images were obtained via a Plan-Neofluar 40x/1.3 oil objective with a z-step of 2.0 μ m or 20x objective with a z-step of 5.0 μ m.

4.2.3 *Staphylococcus Aureus* Bacteria Grown on Cultured

Human Airway Epithelial Cells

Staphylococcus aureus biofilms were investigated with this computer program because they are relevant to cystic fibrosis infections and because the bacteria grow in close proximity, which means the connected volume filtration algorithm can be used. Dr. Kiedrowski from Dr. Alexander Horswill's laboratory (The University of Iowa, Department of Microbiology) provided confocal images for quantification. Polarized, antibiotic-free cultured human airway epithelial cells (Calu-3) were prepared following the methods of Starner et al. and Karp et al.¹⁴⁴⁻¹⁴⁵ Calu-3 cells were stained with CellTracker Orange (Invitrogen, Eugene, OR). Green-fluorescent *Staphylococcus aureus* at 10^8 CFU/mL in phosphate buffer were added to the apical surface of the cells and grown 24 hours. The Nikon Eclipse E600 microscope with Radiance 2010 image capturing (Biorad, Hercules, CA) was used to acquire images.

4.2.4 *Neisseria Gonorrhoeae* Bacteria Grown on Cervical Tissue

Neisseria gonorrhoeae biofilms were investigated with this computer program because the bacteria grow in close proximity, which means the connected volume filtration algorithm can be used, and we wanted to demonstrate quantification of intracellular bacteria. It is important to note that this bacteria is not relevant to cystic fibrosis infections. Dr. Falsetta Wood of Dr. Micheal Apicella's laboratory (The University of Iowa, Department of Microbiology) provided confocal images for quantification. Primary cervical cells were grown with *Neisseria gonorrhoeae* in continuous-flow chambers and imaged via confocal microscopy as previously reported by Falsetta et al.¹⁴⁶ Briefly, primary cervical cells were provided by the University of Iowa Hospitals and Clinics, Iowa City, IA, from cervical biopsies and immortalized by the method of Klingelhurtz et al.¹⁴⁷ Tissue was cultured on collagen-coated coverslips until confluent at 37°C and 5% CO₂ (2 days) and were stained with Cell Tracker Orange (Invitrogen, Eugene, OR) prior to introducing bacteria. Green-fluorescent *Neisseria gonorrhoeae* bacteria was grown in continuous-flow chambers adapted for tissue growth at 37°C and 5% CO₂ statically for 1 hour and with 180 µL/min flow for 48 hours. The Nikon PCM-2000 confocal system (Nikon, Melville, NY) was used to acquire images.

4.3 Results and Discussion

The computer program STAINIFICATION was developed to address limitations in COMSTAT and COMSTAT2-Beta (Table 4-1). The image format read by the program is the same as with COMSTAT, which makes it easy for current users to transition to this new program.⁹⁶ The “.info” files are the same as with COMSTAT except for an additional section that requests the fluorescent color for each image channel

(1=red, 2=green, 3=blue, 0=empty) (Figure 4-8). STAINIFICATION was developed with a user-friendly interface with two simple windows. Like COMSTAT2-Beta, STAINIFICATION has a manual thresholding option and an Otsu global thresholding option. Furthermore, a novel Otsu local option is available. As mentioned by the developers of PHLIP, it is advantageous to apply CVF to all color channels with bacteria.¹³⁸ Therefore STAINIFICATION applies this modification. A colocalization algorithm is included to prevent double counting pixels for quantification of bacteria viability with common nucleic stains. Saving data was improved by generating a single Excel[®] file with all quantified data in sheet 1 (Figure 4-9). Furthermore, all processing decisions were recorded in sheet 2 of the Excel[®] file (Figure 4-10).

4.3.1 STAINIFICATION User Friendly Interface

STAINIFICATION was developed with a user-friendly interface to aid biofilm researchers in quantifying confocal images (Figures 4-11A and B). The first window allows users to identify the color channels used for confocal image acquisition. These may be individual colors, a combination of two color channels, or all three color channels of red, green, and blue (Figure 4-12A). The user then clicks the 'Add File(s)' button to import ".tif/tiff" image sequences with ".info" files (Figure 4-12B). Like COMSTAT, many sequences can be loaded at one time. Finally the user indicates the files have been uploaded (Figure 4-12C). Then the second window opens and requires the user to complete three segments. Users select a thresholding method to separate the pixels of interest from background noise (Figure 4-13A). Either a manually determined threshold intensity value can be input for each color channel, a global Otsu threshold can be automatically computed for each color channel, or a local Otsu threshold can be automatically computed for each image slice within each color channel. Once the threshold is established, the user associates a color channel with a physical trait of the

image. Biofilm researchers may use fluorescent stains to investigate bacteria, a component of the protective matrix, or a surface (Figure 4-13B). Finally the quantification analysis is chosen (Figure 4-13C). The options include connected-biofilm bacteria and unconnected bacteria, connected biofilm bacteria, unconnected bacteria, and a matrix component, or connected-biofilm bacteria, unconnected bacteria, and surface with the further decision of applying colocalization adjustment (CA) or not applying CA. A final option of connected-biofilm bacteria, unconnected bacteria, a matrix component, and surface without CA is available.

4.3.2 Confocal Image Thresholding

Thresholding of CLSM images is a vital step in image quantification, and yet, many do not understand its importance. Depending on the threshold value chosen, the quantified data can vary. Therefore, it is important to be precise to reproducibly threshold the CLSM images. STAINIFICATION has three thresholding options.

Like COMSTAT, a manual threshold may be entered by the user. Through trial and error the user can compare the original image to the image after thresholding. If the threshold value is too low, excess pixels will be seen in the thresholded image compared to the original image. If the threshold value is too high, the thresholded image will be missing pixels of interest compared to the original image. The manual threshold chosen by the user is accurate, but may not be reproducible between operators. Furthermore, the manual threshold value entered is applied to the entire image sequence. All images in the sequence may not be well represented by the threshold entered, especially if fluorescence changes with image depth.

To reduce human bias and ensure reproducibility, two automated thresholding options are also available in STAINIFICATION. Both automated options are based on Otsu thresholding, which is the most common automatic thresholding option used in

biofilm-specific quantification programs, such as COMSTAT2-Beta.^{96, 139} In COMSTAT2-Beta, the optimal Otsu threshold value is found for the substratum (first) image slice and applied to all images in the sequences. STAINIFICATION finds the optimal Otsu threshold per image slice and applies the median value to all images in the slice for the Otsu global option. The median value was chosen over the substratum global value to allow for a difference in Otsu values throughout the image sequence. Like with the manual threshold, the global Otsu threshold applies a single threshold value to the entire image sequence. This may not be ideal if images have large changes in fluorescence with time or image depth.

STAINIFICATION is unique in having an Otsu local option. In the Otsu local option, each optimal Otsu threshold is applied to its respective image slice. To show the utility of these approaches, a *Pseudomonas aeruginosa* biofilm treated with ciprofloxacin hydrochloride (Figure 4-14A) was thresholded with COMSTAT's Otsu (Figure 4-14B), STAINIFICATION'S Otsu global (Figure 4-14C), or STAINIFICATION's Otsu local (Figure 4-14D). After COMSTAT's Otsu values are applied (Table 4-2, red channel: 57, green channel: 85), it can be seen that compared to the original image there was loss of biofilm after thresholding. Thus quantification after this automated threshold would underestimate the amount of biofilm present. Using a median global Otsu in STAINIFICATION (Table 4-2, red channel: 28, green channel: 29) instead of the global Otsu based on the substratum results in an image similar to the original image. Thus more biofilm pixels were retained. Visually the STAINIFICATION global (Figure 4-14C) and local (Figure 4-14D) were similar to the original image. The local Otsu values (Table 4-2) show the optimal Otsu threshold values decrease with image slice. It is common for fluorescence to decrease with depth in a sample.⁹³ The local Otsu uses the optimal Otsu thresholds found per slice and thus accounts for a decrease in fluorescence. Any time there is a decrease in fluorescence with image depth, COMSTAT's Otsu thresholds found for the substratum image slice will result in a loss of biofilm pixels.

4.3.3 Colocalization Adjustment

STAINIFICATION implements a novel automatic colocalization adjustment algorithm to prevent double counting of pixels for viability assessment with membrane integrity nucleic acid stains. Syto 9 membrane permeable green stain and Sytox Red membrane impermeable red stain were used to investigate a *Pseudomonas aeruginosa* biofilm treated with 556 µg/mL ciprofloxacin hydrochloride. The image after Otsu thresholding (Figure 4-15A) shows a biofilm with mainly yellow coloring in the center of the image. Bacteria surrounding this portion of the image are more difficult to distinguish as red, green, or yellow. The impermeable red stain can only enter cells with disrupted membranes. The permeable green stain can enter all cells, although it can also be reduced by the red stain signal. Therefore, not all cells with disrupted membranes have both signals. Thus, an algorithm was needed to prevent double counting of colocalized pixels as both dead and live for analysis. Colocalized yellow pixels were identified by the colocalization algorithm. For these pixels the red signal was maintained and the green signal was eliminated (Figure 4-15B), making it easier to visually determine live and dead bacteria pixels. Decreasing the color choices from red, green, and yellow to just red and green improved the qualitative identification of bacteria with intact or disrupted membranes, enabling for faster comparison of the live and dead populations. This algorithm assumes that if a red signal is present, the bacteria's membrane was disrupted and should be identified as a dead bacteria pixel. This assumption should be used with proper staining techniques since over-staining with membrane impermeable stains such as propidium iodide can create a leaky membrane and falsely stain the cells red.¹⁴⁸

4.3.4 Connected-Biofilm Bacteria and Unconnected Bacteria

COMSTAT and COMSTAT2-Beta automatically quantify biofilm bacteria by default using the CVF algorithm.^{96, 139} Unconnected bacteria are not automatically quantified.^{96, 139} To enumerate that population using COMSTAT programs, the CLSM images must be run through the computer program again to quantify total bacteria with CVF de-selected (Figure 4-16). Then a manual post-calculation step subtracts the biofilm data from the total bacteria data, yielding unconnected bacteria data. STAINIFICATION uses CVF to quantify connected-biofilm bacteria. Instead of discarding the unconnected bacteria pixels, STAINIFICATION maintains these pixels for simultaneous quantification. Therefore, the CLSM images only need to be run through STAINIFICATION once. In addition, STAINIFICATION also saves images of the processed images so the outcome can be visualized (Figure 4-17).

Generally only the original CLSM image (Figure 4-18A) is published, however separating the bacterial populations for visualization allows researchers to better qualitatively assess results from their experiments. STAINIFICATION is unique as it can be used to generate images of total bacteria after thresholding (Figure 4-18B), connected-biofilm bacteria (Figure 4-18C), and unconnected bacteria (Figure 4-18D). The two bacterial populations can be pseudo-colored and merged back into a single image (Figure 4-17E) to provide the spatial location of unconnected bacteria in relation to connected-biofilm bacteria. This can provide insight into biofilm architecture and the natural transition of connected-biofilm bacteria to disperse and become unconnected bacteria.

The utility of qualitative and quantitative analysis of STAINIFICATION was shown with *Pseudomonas aeruginosa* biofilms treated with 927 µg/mL ciprofloxacin hydrochloride (Figure 4-19A). Applying Otsu thresholding and colocalization adjustment (Figure 4-19B), the total bacteria population contained 31.0% live and 69.0% dead bacteria (Table 4-3). The total bacteria were separated into connected-biofilm

(Figure 4-19C) and unconnected (Figure 4-19D) bacteria populations. The connected-biofilm bacteria contained 43.5% dead bacteria. The unconnected bacteria contained 97.3% dead bacteria. The unconnected bacteria were more susceptible to antibiotics, but were not eradicated. This is important since these bacteria have the ability to recolonize and perpetuate infection. The percentage of live and dead bacteria in both the connected-biofilm and unconnected bacterial populations were quantified with and without the colocalization adjustment algorithm (Table 4-3). The data were quantified for the overall image stack and for each of the 11 images in the sequence. The colocalization algorithm reduced double counting of the colocalized pixels to reduce underestimation of the dead bacteria. Without the colocalization adjustment, the overall dead connected-biofilm bacteria were underestimated by 9.8%. The unconnected bacteria were underestimated by 0.3%. Current software programs without colocalization adjustment would provide a conservative estimate of the dead population. The connected-biofilm bacteria were more susceptible to the antibiotic than would have been induced without the colocalization adjustment. The biofilm-bacteria had more colocalized pixels than the unconnected bacteria. This may be due to biofilm components, like the protective matrix, trapping the syto 9 stain.¹⁴⁹ STAINIFICATION could be used to quantify both the connected-biofilm and unconnected bacteria to investigate the effectiveness of antimicrobial treatments, adaptation to antimicrobials, and durability of persistent bacteria.

4.3.5 Quantifying Connected-Biofilm Bacteria,

Unconnected Bacteria, and a Matrix Component

STAINIFICATION has an analysis option of quantifying the connected-biofilm, unconnected bacteria, and a matrix component in a single pass through of the CLSM image. This was included to save time in image analysis, which may encourage researchers to quantify bacteria and matrix components in the future. COMSTAT and

COMSTAT2-Beta can be used to quantify all of these components.^{96, 139} However, the CLSM image needs to be passed through the program twice (Figure 4-20). First with CVF, the connected-biofilm bacteria can be quantified. Then with CVF de-selected, the total bacteria and the matrix component can be quantified. With a post-calculation, the unconnected bacteria can be found.

4.3.6 Quantifying Connected-Biofilm Bacteria, Unconnected Bacteria, and Surface

STAINIFICATION includes an analysis option of quantifying the connected-biofilm, unconnected bacteria, and a surface component upon which bacteria are grown all in a single pass through of the CLSM image. This saves time in image analysis, which may encourage researchers to quantify bacteria and surface components in the future. If the surface is flat, COMSTAT and COMSTAT2-Beta can be used to quantify all of these components.^{96, 139} However, the CLSM image needs to be passed through the program twice (Figure 4-21). First with CVF, the connected-biofilm bacteria can be quantified. Then with CVF de-selected, the total bacteria and surface can be quantified. With a post-calculation, the unconnected bacteria can be found.

4.3.6.1 MCVF is Needed to Quantify Bacteria Grown on an Uneven Surface

COMSTAT and COMSTAT2-Beta cannot be used to quantify connected-biofilm and unconnected bacteria when grown on an uneven surface; it is common for tissue growth not to be uniform.¹⁵⁰⁻¹⁵² STAINIFICATION uses a modified CVF algorithm (MCVF) to enable quantification of connected-biofilm bacteria grown on an uneven surface (Figure 4-7). The original CVF algorithm requires the first image to be flat in order to quantify all connected-biofilm bacteria on the surface. Therefore, using CVF only the biofilm on the right would be quantified. The MCVF algorithm indexes all

locations where bacteria pixels are located above surface pixel. These index points are used to apply CVF and comparisons are made to prevent double counting of pixels. Therefore, MCVF can be used to quantify all biofilm grown on the uneven surface.

STAINIFICATION is unique since it has the MCVF to quantify the connected-biofilm bacteria and unconnected bacteria. COMSTAT and COMSTAT2-Beta cannot quantify both of these items. However, COMSTAT and COMSTAT2-Beta can be used to quantify the surface with CVF de-selected and thus can be used to confirm STAINIFICATION's surface results. A test image was developed to show the utility of MCVF. This test image contains an uneven surface with connected-biofilm bacteria. The surface pixels (S) start on the first image slice and extend to the second image slice and a portion starts on the second image slice and extends to the third image slice (Figure 4-22A). This uneven surface could be tissue, medical, or industrial materials. For quantification, the surface must either be fluorescently labeled or reflective for use of reflective confocal. Connected-biofilm bacteria (B and B^*) grow from the second image slice to the fourth image slice.

The surface binary image (Figure 4-22B) has values of 1 in the locations where the S pixels are located. Assuming calibration values of $0.5 \mu\text{m}/\text{pixel}$ in the x and y directions and a z-step of $1 \mu\text{m}$, the total area of the labeled surface was found to be $11.0 \mu\text{m}^2$ with $6.0 \mu\text{m}^2$ irregular surface on the first slice, $4.5 \mu\text{m}^2$ irregular surface on the second slice, and $0.5 \mu\text{m}^2$ irregular surface on the third slice (Table 4-4). Using COMSTAT with CVF de-selected, these areas were verified as they correlated to 60.0% surface coverage on the first slice, 45.0% on the second slice, 5.0% on the third slice, and no coverage on the final slice. The surface was not required to be continuously connected or to be initiated from a flat device imaging substratum. This is particularly useful for tissue grown on membranes or reflective curved metals.¹⁵¹⁻¹⁵²

To quantify the connected-biofilm bacteria (B and B^*) the MCVF algorithm was used (Figure 4-22C). The B_0 value was zero for this example since no bacteria were

located on the first image slice. Indexed bacteria pixels (Figure 4-21A, B^* , Figure 4-22D) were those found in the same pixel location directly above a surface pixel (S). Indexed bacteria were found on slice 2 and slice 3. As expected, our script output showed there were 33 connected-biofilm bacteria pixels total with none on the first slice, 8 on the second slice, 12 on the third slice, and 13 on the fourth slice (Table 4-4). This was equal to a total connected-biofilm bacteria area of $8.3 \mu\text{m}^2$ with $0 \mu\text{m}^2$ connected-biofilm bacteria on the first slice, $2.0 \mu\text{m}^2$ connected-biofilm bacteria on the second slice, $3.0 \mu\text{m}^2$ connected-biofilm bacteria on the third slice, and $3.3 \mu\text{m}^2$ connected-biofilm bacteria on the fourth slice. Since this example had only connected-biofilm bacteria and no unconnected bacteria, COMSTAT was able to be used with CVF de-selected to quantify the total bacteria in the image. This was used to confirm the connected-biofilm area calculations of 0% on the first slice, 20% on the second slice, 30% on the third slice, and 32.5% on the fourth slice. COMSTAT with CVF returns 0% connected-biofilm bacteria.

Our MCVF algorithm is novel since it allows for quantification of the biofilm bacteria on top of the uneven surface. Table 4-5 compares CVF and MCVF when starting at image slice 1, slice 2, and slice 3 of Figure 4-22A. The original CVF uses a single imaging substratum slice to define connected-biofilm bacteria on the imaging substratum ($B_0 = B + B^*$) and includes connected-biofilm bacteria on the slices above in quantification. When beginning at slice 1, the value of B_0 was zero since no bacteria were present on the first slice. If slice 1 were eliminated and analysis was started at slice 2, the value of B_0 was 8 ($B + B^*$). The connected-biofilm bacteria were connected from the B_0 pixels, resulting in 31 total pixels. Similar to Figure 4-7, only bacteria on the right side of Figure 4-22A slices 2 through 4 were quantified with CVF. The two bacteria pixels on the left in slice 3 were not connected to any B_0 pixels and therefore were not quantified. This shows the limitation of using CVF, since it misses some connected-biofilm pixels. If both slices 1 and 2 were eliminated and quantification was started at

slice 3, the value of B_0 was 12 ($B + B^*$) all on slice 3. All pixels on slice 4 would be connected to the B_0 pixels, resulting in a total of 25 connected-biofilm bacteria pixels.

The MCVF uses the B_0 and B^* values to define the surface substratum slice instead of a single imaging substratum. Bacteria above the B_0 and B^* pixels were connected the same as with the original CVF. When beginning at slice 1, the value of B_0 was zero since no bacteria were present on the first slice and the value of B^* was 14 from all the B^* pixels on the image slices above. Upon connecting bacteria from B_0 and B^* , a total of 33 connected-biofilm bacteria pixels were quantified. If slice 1 were eliminated and analysis was started at slice 2, the value of B_0 was 8 ($B_0 = B + B^*$) for all the bacteria pixels on slice 2. The value of B^* was 6 from the pixels on slice 3. Quantifying all connected-biofilm bacteria pixels from the B_0 values on slice 2 and B^* values on slice 3, a total of 33 connected-biofilm bacteria pixels were found. This was the same number of connected-biofilm bacteria pixels for when analysis was started on the first image slice. The MCVF quantified all connected-biofilm bacteria present, regardless of the irregular surface. Unlike using CVF, the MCVF did not neglect the two bacteria pixels on the left of slice 3. Finally, if both slices 1 and 2 were eliminated and analysis was started at slice 3, the value of B_0 was 12 ($B_0 = B + B^*$) for all the bacteria pixels on slice 3. All pixels on slice 4 would be connected to the B_0 pixels, resulting in a total of 25 connected-biofilm bacteria pixels. Therefore, the only way MCVF and CVF result in the same number of connected-biofilm bacteria pixels was when the starting image slice contained all B^* pixels.

4.3.6.2 Two Novel Parameters: Modified Substratum Coverage and Surface Association

The substratum coverage, defined as the percent coverage of bacteria on the first image slice, is a common quantification parameter quantified via COMSTAT.^{30, 54, 96, 153}

Our modified substratum coverage, which contains the bacteria on the first image slice

around a surface and the bacteria on the uneven surface, was found to be 35.0% from 14 B* pixels present on the 4x10 image size (Figure 4-22A). Using COMSTAT, the substratum coverage would be 0% since no bacteria were on the first image slice. Therefore this new modified substratum coverage can be used to quantify the percentage of the substratum that is covered with connected-biofilm bacteria when bacteria are grown on an uneven surface.

The utility of the modified substratum coverage parameter is demonstrated with *Staphylococcus aureus* biofilms grown on cultured human airway epithelial cells (Calu-3) (Figure 4-23A). The original image shows green fluorescent bacteria on red membrane-stained tissue. COMSTAT's substratum coverage parameter, which quantified bacteria on the first image slice (Figure 4-23B) resulted in 0.2% bacteria covering the first image (Table 4-6). Furthermore since COMSTAT uses CVF to quantify bacteria from the first image slice and cannot quantify connected-biofilm bacteria on top of an uneven surface, only 24,250 connected-biofilm pixels were found using COMSTAT (Table 4-6, Figure 4-23C). STAINIFICATION, which uses a MCVF algorithm to quantify connected-biofilm bacteria on the tissue, found 126,081 total connected-biofilm bacteria pixels (Table 4-6, Figure 4-23D). Comparing Figures 4-23C and D show that COMSTAT only retained about 20% of the pixels and mainly on the right of the image. STAINIFICATION enables researchers to quantify the bacteria on the tissue surface, rather than just on the first image slice (Figure 4-23E). STAINIFICATION was used to find the modified substratum coverage of 9.7% (Table 4-6). Therefore STAINIFICATION provides a new analytical tool to quantify connected-biofilm bacteria grown on an uneven surface that cannot be quantified using current software.

Bacteria are able to grow on top of a surface and sometimes also within a surface. Colocalization of pixels for fluorescently labeled bacteria and surface pixels have been observed.¹⁴⁶ We have developed an algorithm to quantify these colocalized pixels. The pixels that contain both the bacteria and surface pixels in the same location were

classified as surface associated bacteria pixels. The test image in Figure 4-24A includes six surface associated bacteria pixels (SA) in the first image slice and two surface associated bacteria pixels (SA) in the second slice. It is important to note that the modified substratum coverage remained at 35.0% (as in the test image in Figure 4-22A) since SA pixels were not included in the calculation (Table 4-7). The modified substratum coverage quantifies bacteria above the surface and not the bacteria within the surface.

However, quantification of the SA pixels alone could be of interest to researchers investigating internalization of bacteria into the uneven surface, such as intracellular bacteria in tissue.¹⁵⁰ On the first slice there were six SA pixels, which correlated to 100% of the six bacteria pixels on the first image slice being associated with the surface. On the second slice there were two SA pixels and eight connected-biofilm bacteria pixels ($B + B^*$), which correlated to 20% of the bacteria on the image slice being associated with the surface. Overall there were 8 SA pixels and 33 connected-biofilm bacteria pixels ($B + B^*$), which meant 19.5% of the total bacteria were associated with the surface. The volume of bacteria associated with the surface was also calculated. The first slice had $1.5 \mu\text{m}^3$ bacteria associated with surface, the second slice had $0.5 \mu\text{m}^3$ bacteria associated with surface, and a total of $2.0 \mu\text{m}^3$ bacteria associated with surface.

Figure 4-25A visualizes *Neisseria gonorrhoeae* biofilms grown on transformed cervical epithelial cells with the nuclei stained for the surface. Biofilms grown on tissue were chosen to demonstrate the utility of the MCVF and modified substratum coverage since it is common for tissue growth not to be uniform.¹⁵⁰⁻¹⁵² Table 4-8 shows quantified data for the overall 51-slice image sequence and for the first 5 image slices. The number, area (μm^2), and percent area (%) of nuclei stained surface were quantified without any CVF or MCVF. Using MCVF, the number, area (μm^2), and percent area (%) of connected-biofilm bacteria pixels were quantified. COMSTAT without CVF for analysis of the nuclei stained surface resulted in the same percent area per image slice as when

using our algorithms. COMSTAT without CVF quantified the total bacteria (connected-biofilm and unconnected bacteria) in the image, which was the same as the connected-biofilm bacteria (Table 4-8) and the unconnected bacteria (not shown) quantified by our scripts. Since bacteria were internalized and found on the first image layer, COMSTAT with CVF did result in quantified data similar to our scripts. The area of bacteria per image slice was underestimated by 0.1% on the second image slice and by 0.2% on slices 3 through 5 with COMSTAT compared to with our MCVF algorithm due to connected-biofilm bacteria being omitted from calculation when on the uneven surface. Without internalized bacteria, COMSTAT with CVF would significantly underestimate the connected-biofilm bacteria present.

Figure 4-25B includes the 0.6% of total bacteria that were associated with the nuclei surface, which is equivalent to 35,489.8 μm^3 volume. Progressing from the first image slice, less bacteria were associated with the nuclei for each successive image slice (Table 4-8). This new quantification parameter not only allows researchers to quantify colocalization of bacteria with a surface, but also allows identification of the spatial location of the interactions.

4.3.7 Quantifying 4 Components Simultaneously: Connected-Biofilm Bacteria, Unconnected Bacteria, a Matrix Component, and Surface Material

The final analysis option in STAINIFICATION is to quantify the connected-biofilm bacteria, unconnected bacteria, a matrix component, and a surface component with one pass through of a CLSM image. STAINIFICATION can quantify all components regardless of the irregularity of the surface. COMSTAT and COMSTAT2-Beta can be used to quantify all of these components as well only if the surface is flat.⁹⁶

¹³⁹ The CLSM image needs to be passed through the program twice (Figure 4-26). First,

with CVF de-selected, the total bacteria, the matrix component, and surface can be quantified. Then with CVF, the biofilm bacteria can be quantified. With a post-calculation, the unconnected bacteria can be found.

4.4 Conclusions

STAINIFICATION is available for researchers to analyze connected-bacteria, unconnected bacteria, matrix, and an irregular surface upon which bacteria are grown in confocal microscopy images in a more time efficient manner. STAINIFICATION has a user friendly interface to make image analysis straight forward. STAINIFICATION has novel thresholding and quantification abilities. A local Otsu threshold is a new option in biofilm-specific quantification programs. A colocalization adjustment option is available to prevent double counting of colocalized pixels when assessing bacteria viability with membrane integrity nucleic acid stains. The utility of thresholding and colocalization adjustments were demonstrated with *Pseudomonas aeruginosa* biofilms. The modified connected volume filtration algorithm allows connected-biofilm bacteria to be quantified on an uneven surface. Furthermore, the parameters of modified substratum coverage and percent or volume bacteria associated with surface have been introduced. The utility of these new quantification parameters and the MCVF algorithm were demonstrated with *Staphylococcus aureus* biofilms grown on cultured human airway epithelial cells and *Neisseria gonorrhoeae* biofilms grown on transformed cervical epithelial cells.

Table 4-1: Comparison of COMSTAT,⁹⁶ PHLIP,¹³⁸ COMSTAT2-Beta,^{96, 139} and STAINIFICATION.

COMSTAT (MatLab-based)	
Image formats	".tif" and ".info"
Thresholding	Manual
CVF	Each image channel separately
Colocalization	N/A
Saved data	".txt" files per quantification parameter
PHLIP (MatLab-based)	
Image formats	Custom format
Thresholding	Manual and Otsu global
CVF	Multiple image channels together
Colocalization	Fraction colocalization quantified
Saved data	Text files and HTML with plots generated
COMSTAT2-Beta (ImageJ-based)	
Image formats	Zeiss ".lsm"
Thresholding	Manual and Otsu global
CVF	Each image channel separately
Colocalization	N/A
Saved data	".txt" files per quantification parameter
STAINIFICATION (MatLab-based)	
Image formats	".tif" and ".info"
Thresholding	Manual and Otsu (global and local)
CVF	Multiple image channels together
Colocalization	Adjustment algorithms
Saved data	".xls" files for all data in one sheet

Table 4-2: Comparison of Otsu threshold values between STAINIFICATION local, COMSTAT global (substratum-based), and STAINIFICATION global (median-based).

STAINIFICATION Local Otsu Values		
Slice	Red Channel Threshold	Green Channel Threshold
Substratum	57	85
Slice 2	51	45
Slice 3	56	29
Slice 4	50	29
Slice 5	37	22
Slice 6	28	21
Slice 7	23	31
Slice 8	20	34
Slice 9	20	28
Slice 10	20	20
Slice 11	20	20

COMSTAT Global Otsu (Substratum)	
Red Channel Threshold	Green Channel Threshold
57	85

STAINIFICATION Global Otsu (Median)	
Red Channel Threshold	Green Channel Threshold
28	29

Table 4-3: STAINIFICATION quantification of dead and live connected-biofilm bacteria and unconnected bacteria with or without colocalization adjustment (CA).

	Dead Connected- Biofilm, %		Live Connected- Biofilm, %		Dead Unconnected Bacteria, %		Live Unconnected Bacteria, %	
	No CA	With CA	No CA	With CA	No CA	With CA	No CA	With CA
Overall	33.7	43.5	66.3	56.5	97	97.3	3	2.7
Slice 1	45.1	66.5	54.9	33.5	0.0	0.0	0.0	0.0
Slice 2	26.0	34.8	74.0	65.2	93.3	93.5	6.7	6.5
Slice 3	18.2	22.1	81.8	77.9	70.7	71.2	29.3	28.8
Slice 4	28.7	37.1	71.3	62.9	75.3	76.4	24.7	23.6
Slice 5	29.9	36.6	70.1	63.4	83.9	84.9	16.1	15.1
Slice 6	40.7	47.9	59.3	52.1	94.9	95.6	5.1	4.4
Slice 7	65.8	76.6	34.2	23.4	99.3	99.4	0.7	0.6
Slice 8	68.1	80.7	31.9	19.3	99.8	99.8	0.2	0.2
Slice 9	61.5	72.8	38.5	27.2	99.7	99.8	0.3	0.2
Slice 10	44.5	52.3	55.5	47.7	99.5	99.6	0.5	0.4
Slice 11	32.8	37.9	67.2	62.1	99.1	99.2	0.9	0.8

CA=Colocalization Adjusted

Table 4-4: Quantification of surface, connected-biofilm bacteria, and modified substratum coverage for Test Image 1.

	Surface			Connected-Biofilm Bacteria			Modified Substratum Coverage, %
	Number of Pixels	Area, μm^2	Area, %	Number of Pixels	Area, μm^2	Area, %	
Overall	44	11.0	27.5	33	8.3	20.6	35.0
Slice 1	24	6.0	60.0	0	0.0	0.0	
Slice 2	18	4.5	45.0	8	2.0	20.0	
Slice 3	2	0.5	5.0	12	3.0	30.0	
Slice 4	0	0.0	0.0	13	3.3	32.5	

The number of pixels, area (μm^2), and area (%) were enumerated for surface and connected-biofilm bacteria using a single pass through our scripts.

The modified substratum coverage, calculated using Equation 4-4, represents the bacteria on top of the uneven surface.

Table 4-5: Comparison of original connected volume filtration (CVF) and modified connected volume filtration (MCVF) for quantifying connected-biofilm bacteria.

Beginning at Slice Number:	Using CVF	Using MCVF
	Number of Connected-Biofilm Bacteria Pixels	Number of Connected-Biofilm Bacteria Pixels
1	0	33
2	31	33
3	25	25

Analysis was started at image slice 1, image slice 2, or image slice 3 for comparison.

Table 4-6: Quantified data for *Staphylococcus aureus* biofilms grown on cultured human airway epithelial cells (Calu-3).

COMSTAT (CVF-based)		STAINIFICATION (MCVF-based)	
Substratum Coverage, %	Number of Connected-Biofilm Bacteria Pixels	Modified Substratum Coverage, %	Number of Connected-Biofilm Bacteria Pixels
0.2	24250	9.7	126081

COMSTAT was used to quantify substratum coverage (Equation 4-3), which enumerated the percent of the first image slice covered by bacteria.

The substratum algorithm used the first imaging layer as the basis of the substratum calculation.

COMSTAT was also used to quantify the total number of connected-biofilm bacteria pixels using connected volume filtration.

STAINIFICATION was used to quantify the modified substratum coverage (Equation 4-4), which enumerated bacteria grown on the cells.

The modified substratum algorithm used the cells as the basis of the substratum coverage.

STAINIFICATION was also used to quantify the total number of connected-biofilm bacteria pixels using modified connected volume filtration.

Table 4-7: Quantification for modified substratum coverage and the bacteria associated with the surface for Test Image 2.

	Modified Substratum Coverage, %	Bacteria Associated with Surface		
		Number of Pixels	Volume, μm^3	Percent Bacteria, %
Overall	35.0	8	2.0	19.5
Slice 1		6	1.5	100.0
Slice 2		2	0.5	20.0
Slice 3		0	0.0	0.0
Slice 4		0	0.0	0.0

The modified substratum coverage, calculated from Equation 4-4, represents the bacteria on top of the uneven surface, but does not include bacteria colocalized with the surface.

The number of pixels, volume (μm^3), and percent of bacteria associated with the surface (%) were enumerated for the bacteria associated with the surface using a single pass through our scripts and Equation 4-5 and Equation 4-6.

Table 4-8: Quantified data for *Neisseria gonorrhoeae* biofilms grown on transformed cervical epithelial cells.

	<u>Surface</u>			<u>Connected-Biofilm Bacteria</u>			<u>Bacteria Associated with Surface</u>		
	Number of Pixels	Area, μm^2	Area, %	Number of Pixels	Area, μm^2	Area, %	Number of Pixels	Volume, μm^3	Percent Bacteria Associated with Surface, %
Overall	76837	118716.9	0.6	1804992	2788801.1	13.5	11485	35489.8	0.6
Slice 1	17002	26268.9	6.5	107187	165609.2	40.9	2890	8930.4	2.7
Slice 2	13184	20369.9	5.0	116785	180438.5	44.5	2255	6968.2	1.9
Slice 3	10225	15798.1	3.9	121900	188341.5	46.5	1580	4882.4	1.3
Slice 4	8178	12635.4	3.1	123441	190722.4	47.1	1169	3612.3	0.9
Slice 5	6744	10419.8	2.6	121824	188224.0	46.5	966	2985.0	0.8

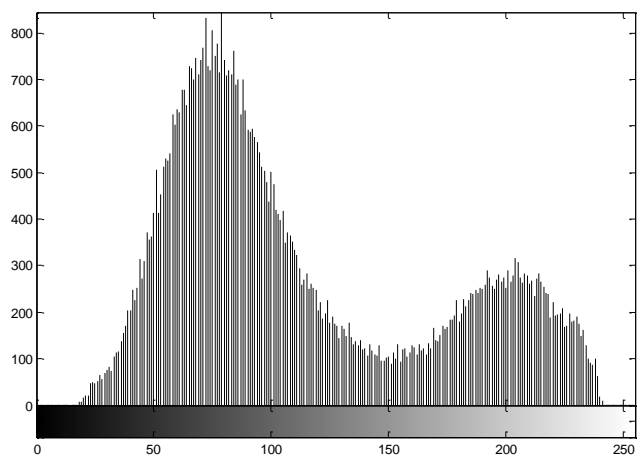
The entire image sequence contained 51 image slices.

Data is shown for the overall image sequence and for each of the first five image slices.

The number of pixels, area (μm^2), and area (%) were enumerated for surface and connected-biofilm bacteria using a single pass through our scripts.

The number of pixels, volume (μm^3), and percent of bacteria associated with the surface (%) were enumerated for the bacteria associated with the surface using a single pass through our scripts.

A)



B)

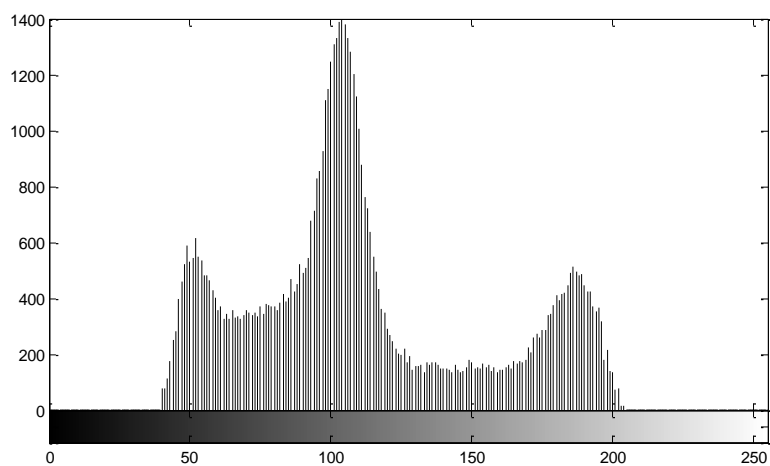


Figure 4-1: Histogram of image pixel intensity on the x-axis and frequency on the y-axis; A) well-separated intensity histogram of background noise pixels (left) and object of interest pixels (right); B) more typical intensity histogram that is not well separated.

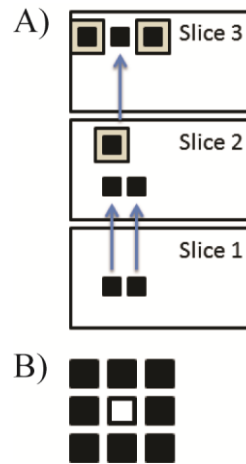
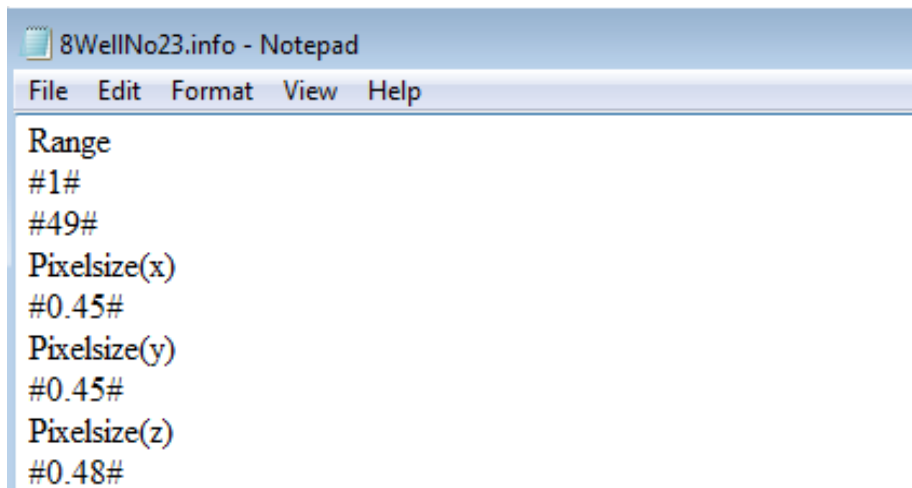


Figure 4-2: Steps for connected volume filtration algorithm; A) top view of three image slices; connected volume filtration compares pixels between slices to allow for vertical growth of biofilms (blue arrows) and completes an eight neighborhood connection around these pixels to allow for horizontal growth of biofilms (boxed squares); B) eight neighborhood connection allows biofilm growth to spread from a center pixel to any of the eight pixel locations surrounding the pixel.



```
8WellNo23.info - Notepad
File Edit Format View Help
Range
#1#
#49#
Pixelsize(x)
#0.45#
Pixelsize(y)
#0.45#
Pixelsize(z)
#0.48#
```

Figure 4-3: “.info” file for COMSTAT; this file contains the number of image slices, the x-direction calibration information in $\mu\text{m}/\text{pixel}$, the y-direction calibration information in $\mu\text{m}/\text{pixel}$, and the z-step size in μm for each image stack.

```

MATLAB 7.9.1 (R2009b) Service Pack 1
File Edit Debug Desktop Window Help
Current Folder: E:\Fiegl Lab Graduate Research\Stainification Batch Processing May 2011\Stainification\COMSTAT\TestImage\Bacteria
Shortcuts How to Add What's New
New to MATLAB? Watch this Video, see Demos, or read Getting Started.
Technical University of Denmark
*****
The program found 1 ".info" files in the current directory E:\Fiegl Lab Graduate Research\Stainification Batch Processing May 2011\Stainification\COMSTAT\TestImage\Bacteria
All the image stacks are listed above.
Enter the number of the first image stack that you want to analyze (1-1) > 1
Enter the number of the last image stack that you want to analyze (1-1) > 1
Setting of threshold values : The threshold value for each image stack must be known
From image stack number 1 to image stack number > 1
Enter threshold value > 1
Threshold values have been set.
*****
* COMSTAT v.1 2000 written by Arne Heydorn *
* Molecular Microbial Ecology Group *
* Technical University of Denmark *
*****
Image Analysis Tools:
1. Biomass (um^3/um^2)
2. Area occupied by bacteria in each layer (also executes 3)
3. Thickness distribution & average thickness
4. Identification and area distribution of microcolonies at the substratum
5. Volumes of microcolonies identified at the substratum (also executes 4)
6. Fractal dimension (Minkowski sausage) of each microcolony identified at the substratum (also executes 4)
7. Fractal dimension (slope of the cross correlation function) in the x and y direction of each image in the stack
8. Dimensionless roughness coefficient (also executes 3)
9. Distribution of diffusion distances and maximum diffusion distance
10. Surface area and surface to volume ratio (also executes 1)
11. Maximum thickness of the biofilm
12. Backlight Live/Dead Analysis
A report.txt file will be generated containing all results from the selected image analysis tools.
Separate .txt files for each of the selected tools will also be generated. Note that if a .txt file
with the same name already exists, the results of the analysis will be added to the end of this file.
All the .txt files can be opened in eg. MS Excel, MATLAB or NotePad
Additional options:
21. Save the thresholded and filtered images in a new folder "Filtered_images"
22. Show images during program execution
23. Smacking. Correction for a non-flat first image
24. Do not use connected volume filtration (used by default)
25. Save the result text files with comma as decimal symbol instead of point (used by default)
*****
Select the desired tools and options (1-25) (e.g. 1,3,4,21) > |
Start | Waiting for input

```

Figure 4-4: Screen shot of COMSTAT user interface in MatLab;⁹⁶ the program is started with the command 'Comstat' and then the user enters processing options.

```

Workspace | Command
*****
***      Automated determination of thresholds      ***
*****

[a]: start automatic determination of threshold
[b]: set thresholds manually in GUI
([e]xit)

Select from above >> a

      -- Automatic determination of threshold levels --

This operation may take a few minutes, please wait...

Done!
GUI starting...
GUI done...

      -- Threshold levels for each stack --

Sample 1 - 2 Channel Test - 1 stacks
2 channel(s): red, green
  001 - mytstack:
      red: 67, green: 68

Press any key to continue...

Do you require connected volume filtration? [y/n] ([e]xit) >> y

      -- Single channel operations --

1 - biovolume
2 - substratum Coverage
3 - area to volume ratio
4 - Spatial spreading of biovolume
5 - Thickness and roughness [last image must be coverslip]
6 - fractal dimension in 2D (still in testing phase)

Enter a list of operations (separated by commas), [a]ll, [n]one, [e]xit >>

```

Figure 4-5: Screen shot of PHLIP user interface;¹³⁸ PHLIP provides the user with many options for analysis.

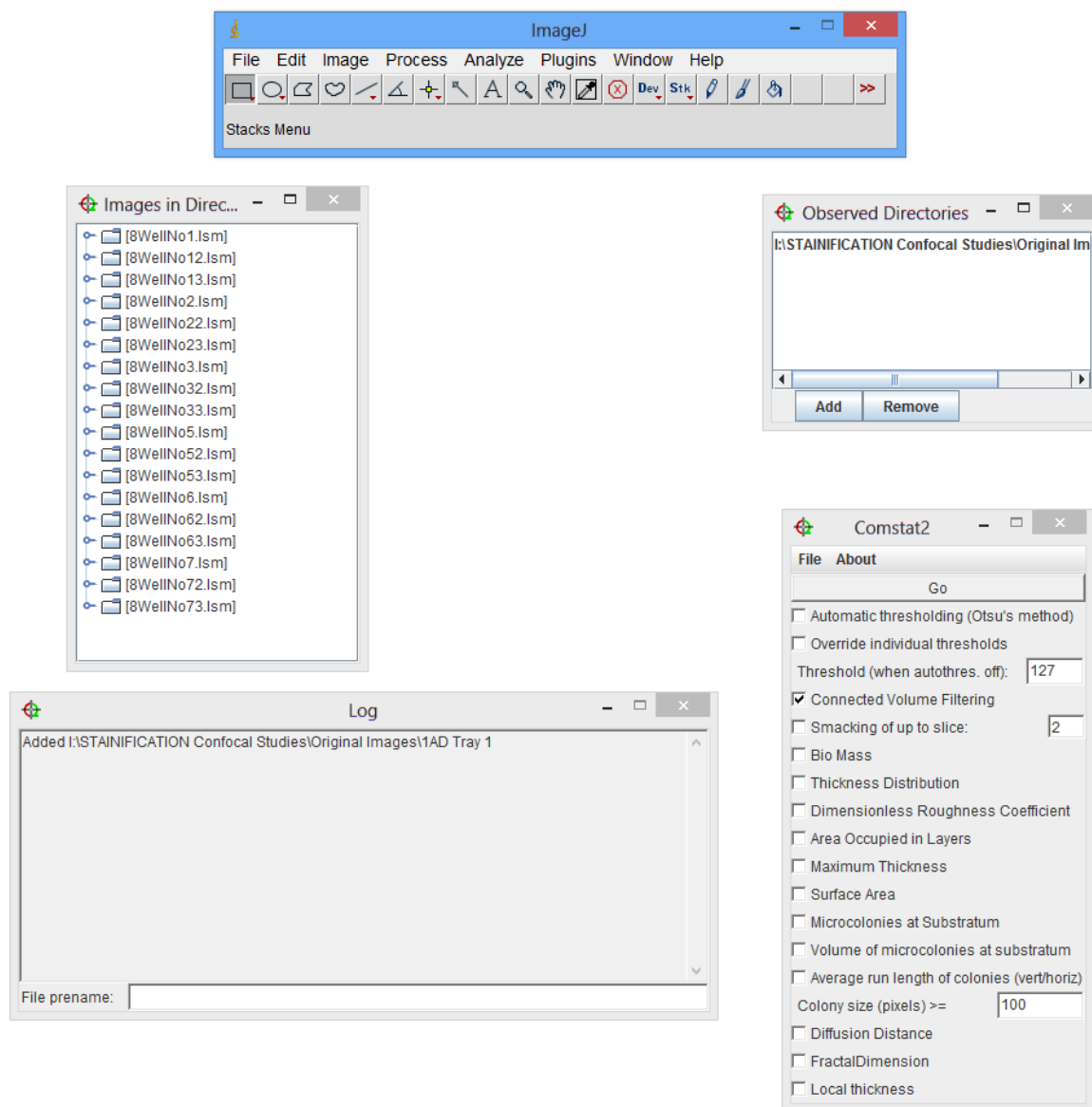


Figure 4-6: Screen shot of COMSTAT2-Beta program interface in ImageJ.^{96, 139}

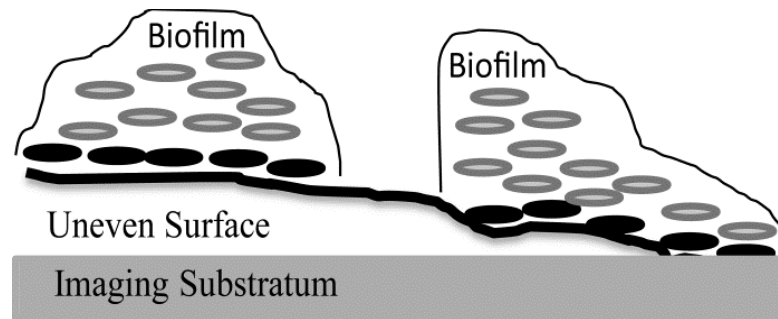
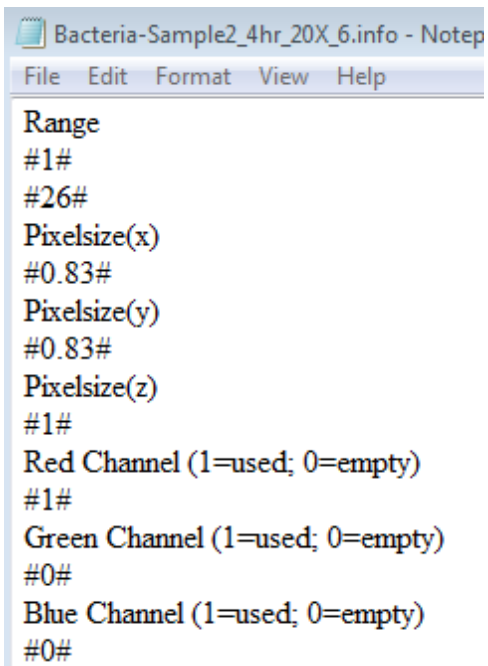


Figure 4-7: Illustration of connected-biofilm bacteria grown on top of an uneven surface and grown on top of the imaging substratum; STAINIFICATION uses a modified connected volume filtration (MCVF) algorithm developed from Heydorn et al.'s connected volume filtration (CVF) algorithm;⁹⁶ the original CVF quantifies connected-biofilm bacteria from the first image slice (imaging substratum); therefore, CVF can quantify the biofilm on the right; since the biofilm grows on an uneven surface, the biofilm portion on the left is missed with the CVF algorithm; using MCVF, all biofilm is quantified; this algorithm indexes the locations where bacteria are located above the surface (black bacteria); from these indexed locations, the CVF algorithm is applied; at the end, a comparison is done between all quantified biofilm to prevent double counting of pixels; therefore, MCVF allows for quantification of biofilm grown on an uneven surface.



```
Bacteria-Sample2_4hr_20X_6.info - Notep
File Edit Format View Help
Range
#1#
#26#
Pixelsize(x)
#0.83#
Pixelsize(y)
#0.83#
Pixelsize(z)
#1#
Red Channel (1=used; 0=empty)
#1#
Green Channel (1=used; 0=empty)
#0#
Blue Channel (1=used; 0=empty)
#0#
```

Figure 4-8: “.info” file for STAINIFICATION; this file requires three additional lines of information; for each channel, the fluorescent stain color is identified (1=color used, 0=empty).

The screenshot shows an Excel spreadsheet titled "Threshold Table.xlsx" with the following data:

	A	B	C	D	E	F	G	
1	E:\Analysis Files\20XCiproTreatmentLastWell Again.lsm							
2		Red Biofilm, %	Green Biofilm, %	Area Red Biofilm, um ²	Area Green Biofilm, um ²	Volume Red Biofilm, um ³	Volume Green Biofilm, um ³	Sub
3	Overall	33.7	66.3	72839.9	143037.9	364927.8	716619.8	
4	1	45.1	54.9	20910.2	25441.5	104759.9	127461.9	
5	2	26.0	74.0	11691.4	33259.7	58574.1	166631.3	
6	3	18.2	81.8	7624.3	34374.4	38197.9	172215.8	
7	4	28.7	71.3	6685.0	16621.4	33491.9	83273.1	
8	5	29.9	70.1	6254.0	14637.7	31332.4	73334.6	
9	6	40.7	59.3	5948.8	8678.8	29803.7	43480.6	
10	7	65.8	34.2	4998.7	2592.4	25043.5	12988.1	
11	8	68.1	31.9	3571.2	1671.6	17891.5	8374.9	
12	9	61.5	38.5	2501.3	1567.4	12531.4	7852.4	
13	10	44.5	55.5	1553.4	1935.1	7782.8	9694.6	
14	11	32.8	67.2	1101.6	2257.9	5518.8	11312.3	
15								

Figure 4-9: Screen shot of an Excel[®] file of data saved by STAINIFICATION; data is quantified for the overall image sequence and for each image slice.

	A	B	C	D	E	F
1	E:\Analysis Files\20XCiproTreatmentLastWell Again.lsm					
2						
3	Channel 1: Red			Threshold Method Used		
4	Channel 2: Green			Otsu Local		
5						
6				RedChannelThreshold	GreenChannelThreshold	
7	Analysis Option Used			57	85	
8	Biofilm Only: Non-Membrane			51	45	
9	Live Bacteria: Green			56	29	
10	Dead Bacteria: Red			50	29	
11				37	22	
12				28	21	
13				23	31	
14				20	34	
15				20	28	
16				20	20	
17				20	20	

Figure 4-10: Screen shot of an Excel[®] file of the user chosen processing parameters saved by STAINIFICATION.

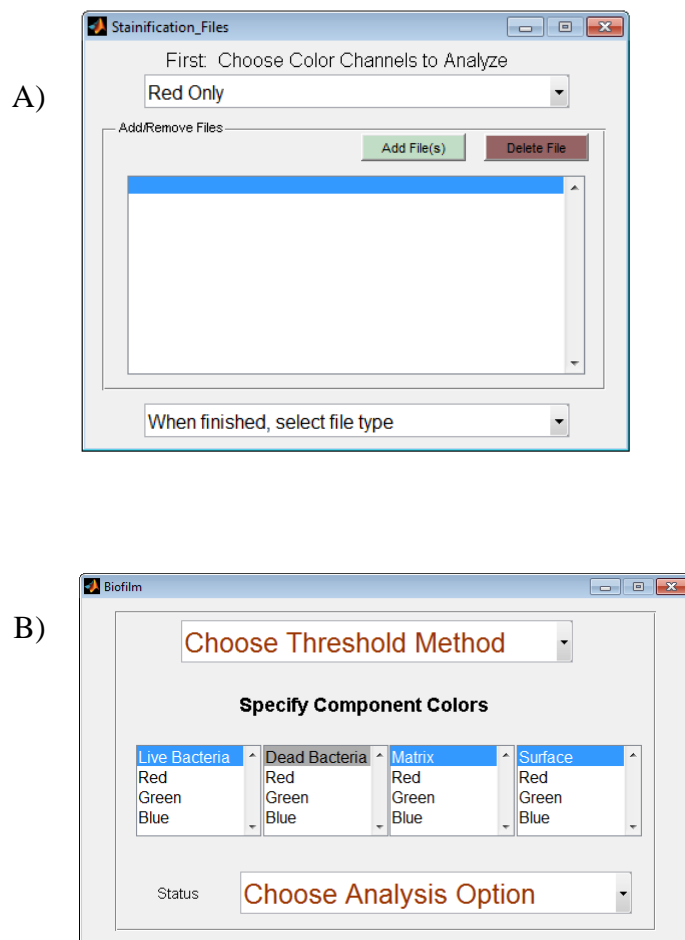


Figure 4-11: Two windows of the STAINIFICATION program; A) the first window is used for loading image sequences; B) the second window is used for selecting processing options.

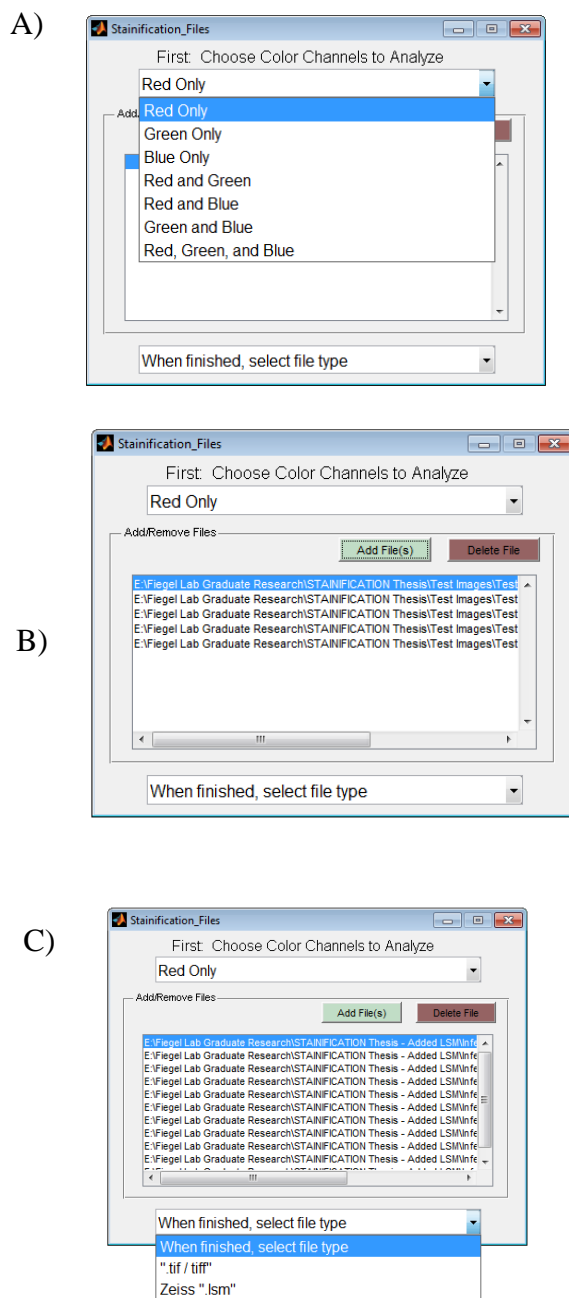


Figure 4-12: Steps for using STAINIFICATION; A) the user selects the color channels collected in the CLSM images; B) the user chooses files to analyze; for each “.tif” image sequence loaded (image1.tif, image2.tif, image3.tif) an “.info” file with the same base name (image.info) is needed; C) when finished loading images, the user selects that the “.tif” have been loaded.

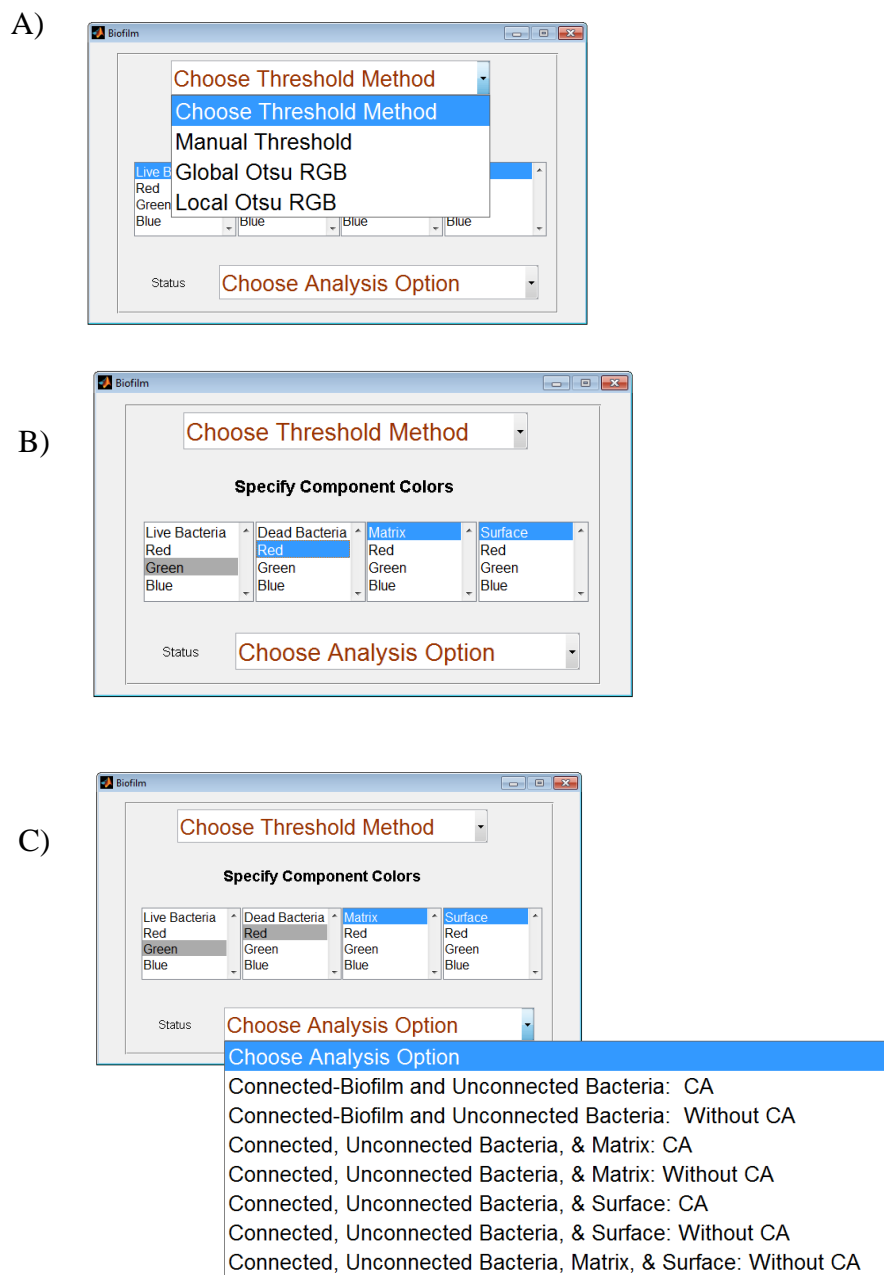


Figure 4-13: Steps for using STAINIFICATION; A) the second window opens and the user selects the threshold option of manual, Otsu global (median-based), or Otsu local (per image slice); B) the user connects color channels to physical properties of the biofilms, including live bacteria, dead bacteria, matrix, or surface; if a component is not stained, the user does not select a color; C) finally the user selects the analysis option for the components of interest, which may include connected-biofilm bacteria, unconnected bacteria, matrix, or surface; a colocalization adjustment (CA) algorithm option is available as well.

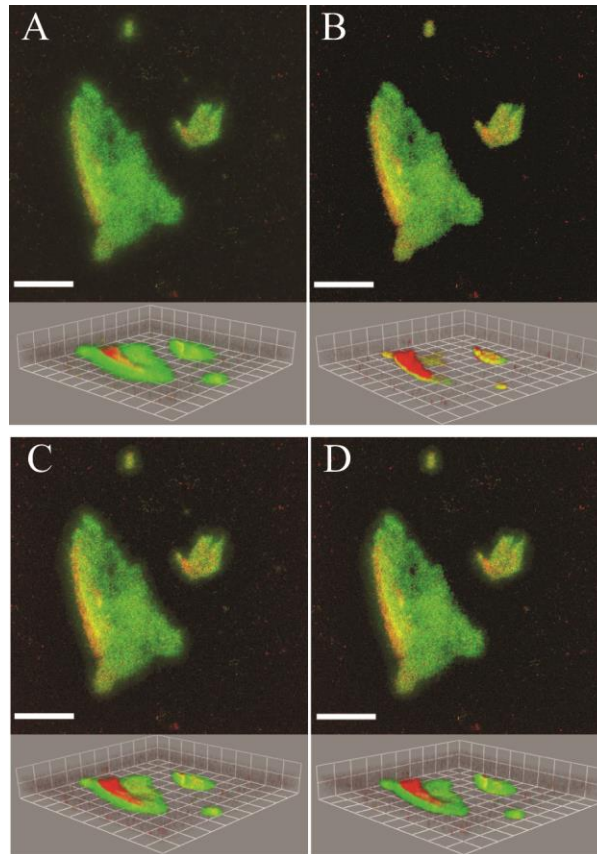


Figure 4-14: Comparison of thresholding methods; A) original 20X magnification confocal image of *Pseudomonas aeruginosa* bacteria treated with 927 $\mu\text{g}/\text{mL}$ ciprofloxacin hydrochloride antibiotic, B) image after Otsu global thresholding in COMSTAT that uses the optimal Otsu found on the substratum slice (red channel: 57, green channel: 85), C) image after Otsu global thresholding in STAINIFICATION that uses the median optimal Otsu found for the entire image series (red channel: 28, green channel: 29), D) image after Otsu local thresholding in STAINIFICATION that uses the optimal Otsu for each slice; stained with syto 9 and Sytox Red; green=live bacteria, red=dead bacteria, yellow=colocalized dead bacteria; top: composite aerial view, scale bar = 90 μm ; bottom: side view, each side of the square = 45.2 μm .

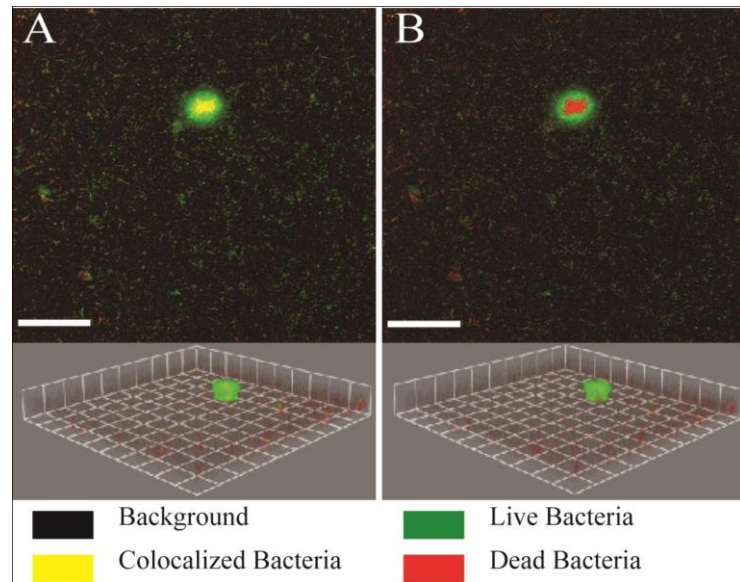


Figure 4-15: Comparison of before and after colocalization adjustment is applied; colocalization adjustment algorithm allows for easy visualization of live (green) bacteria and dead (red) bacteria, while eliminating the ambiguity of the yellow colocalized pixels; when colocalization occurs, the colocalization adjustment maintains the red fluorescent signal, while eliminating the green signal; *Pseudomonas aeruginosa* biofilms were treated with 556 $\mu\text{g}/\text{mL}$ ciprofloxacin hydrochloride and stained with syto 9 and Sytox Red; A) 20X magnification confocal image after Otsu local thresholding, B) implementing colocalization adjustment to image (A); green=live bacteria, red=dead bacteria, yellow=colocalized dead bacteria; top: composite aerial view, scale bar = 90 μm ; bottom: side view, each side of the square = 45.2 μm .

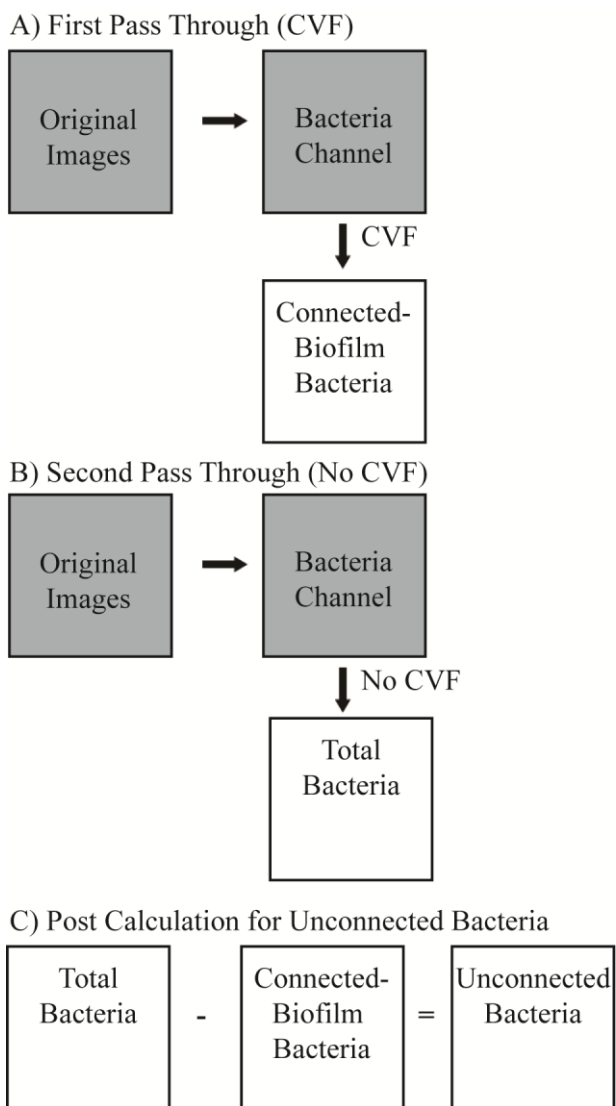


Figure 4-16: Quantification steps for connected-biofilm bacteria and unconnected bacteria in COMSTAT or COMSTAT2-Beta; A) the CLSM image is sent through the program with CVF to quantify the connected-biofilm bacteria; B) the CLSM image is sent through the program again with CVF de-selected to quantify the total bacteria; C) a post-calculation is needed to quantify the unconnected bacteria.

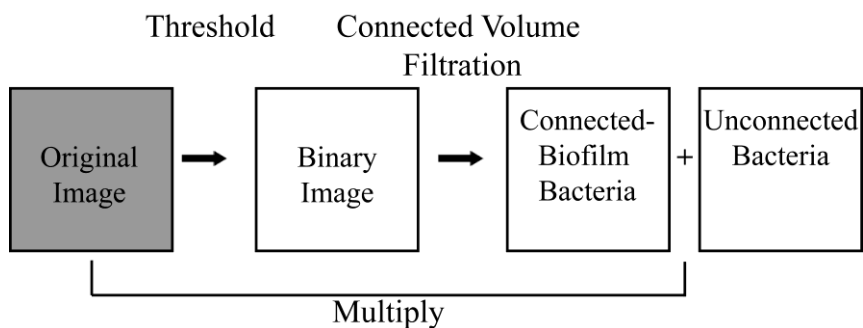


Figure 4-17: Steps required by STAINIFICATION to save “.tif” image sequences of the processed images; after thresholding the original image, a binary image sequence is generated for the bacteria; this binary sequence is separated into connected-biofilm bacteria and unconnected bacteria using connected volume filtration;⁹⁶ these binary image sequences of connected-biofilm bacteria and unconnected bacteria were multiplied by the original image sequence to generate the processed image sequences.

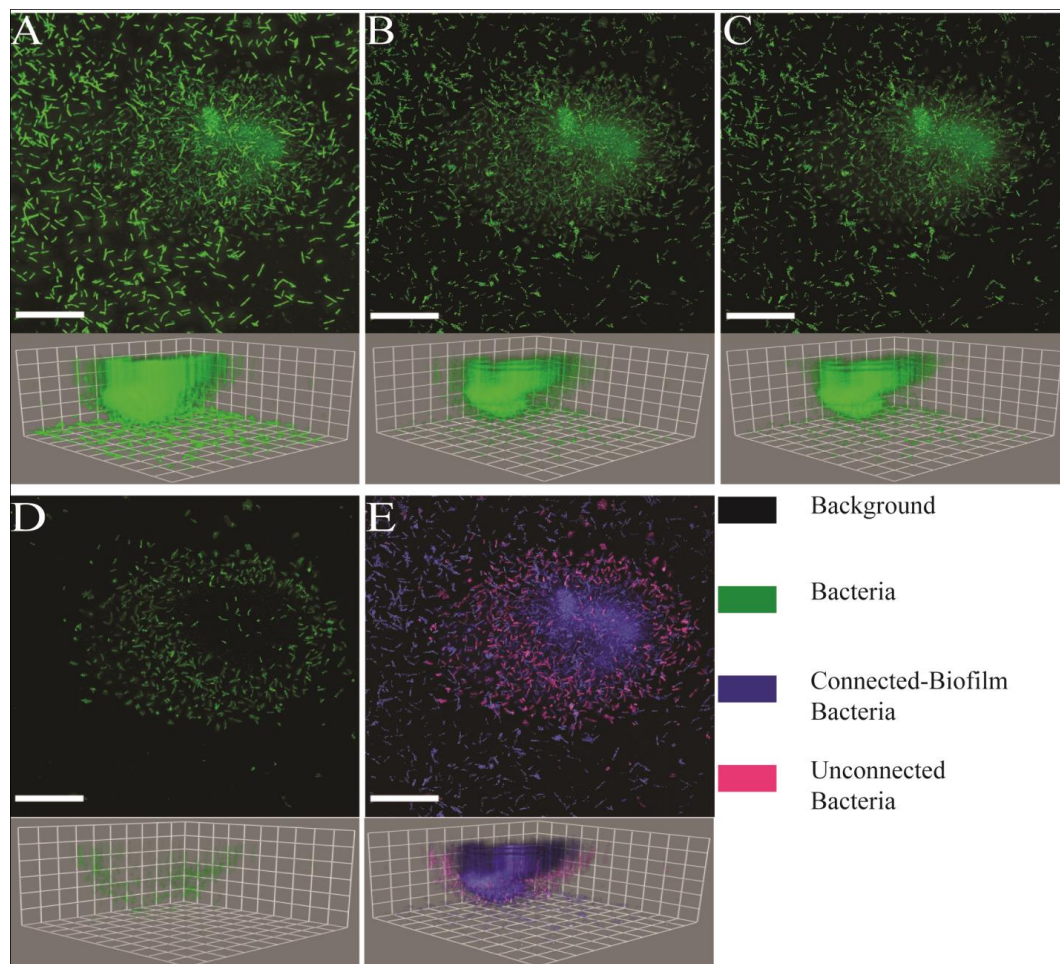


Figure 4-18: *Pseudomonas aeruginosa* confocal images used to demonstrate the utility of separating the connected-biofilm bacteria and the unconnected bacteria; STAINIFICATION can be used to visualize processed CLSM images after thresholding and separation of bacteria by connected volume filtration;⁹⁶ A) original confocal image of *Pseudomonas aeruginosa* biofilm stained with syto 9 at 40X magnification, B) image after Otsu local thresholding, C) connected-biofilm bacteria only image, D) unconnected bacteria only image, E) merged image of connected-biofilm bacteria (blue) and unconnected bacteria (pink); top: aerial view, scale bar = 44 μm ; bottom: side view, each side of the square = 22.6 μm .

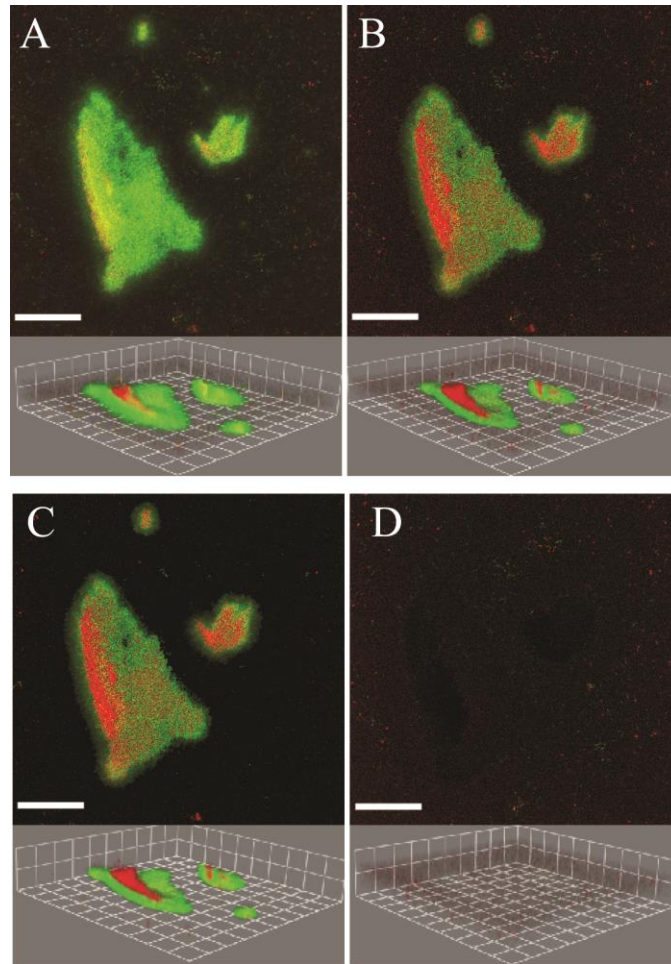


Figure 4-19: *Pseudomonas aeruginosa* confocal images used to demonstrate the utility of separating the connected-biofilm bacteria and the unconnected bacteria for viability assessment; quantification of connected-biofilm bacteria separately from unconnected bacteria is vital for quantification of viability; A) original 20X magnification confocal image of *Pseudomonas aeruginosa* bacteria treated with 927 $\mu\text{g}/\text{mL}$ ciprofloxacin hydrochloride antibiotic, B) image after Otsu local threshold and colocalization adjustment, C) connected-biofilm bacteria only from image B (43.5% dead), D) unconnected bacteria only (97.3 % dead), stained with syto 9 and Sytox Red; green=live bacteria, red=dead bacteria, yellow=colocalized dead bacteria; top: aerial view, scale bar = 90 μm ; bottom: side view, each side of the square = 45.2 μm .

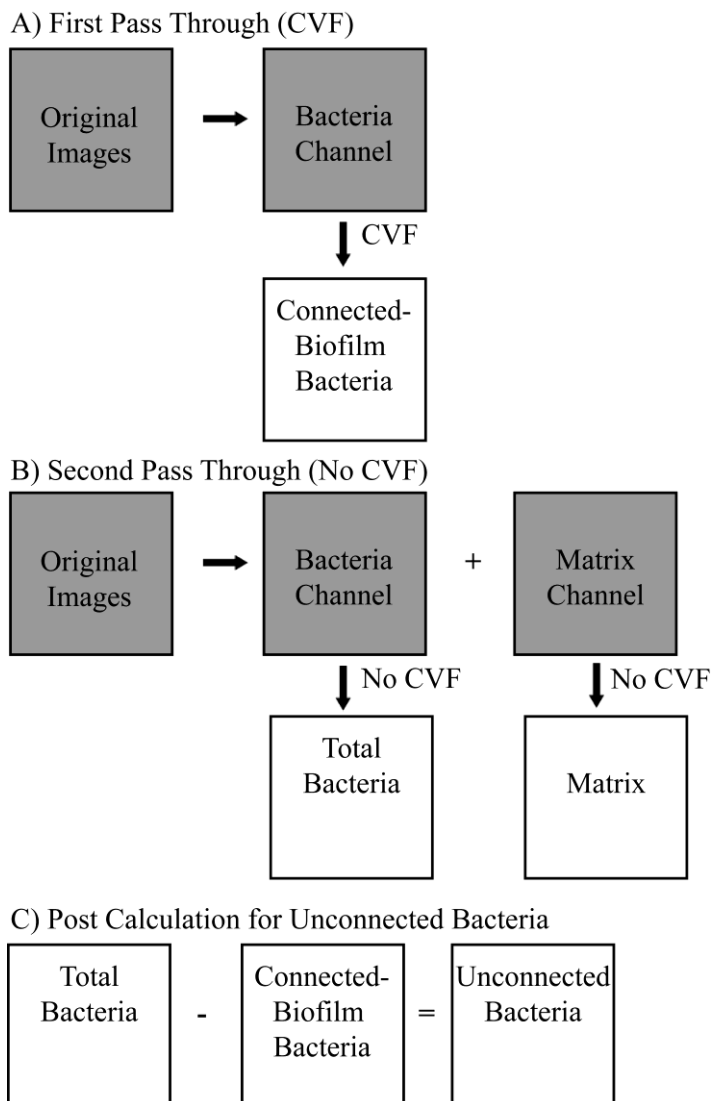


Figure 4-20: Quantification steps for connected-biofilm bacteria, unconnected bacteria, and matrix in COMSTAT or COMSTAT2-Beta; A) the CLSM image is sent through the program with CVF to quantify the connected-biofilm bacteria; B) the CLSM image is sent through the program again with CVF de-selected to quantify the total bacteria and matrix; C) a post-calculation is needed to quantify the unconnected bacteria.

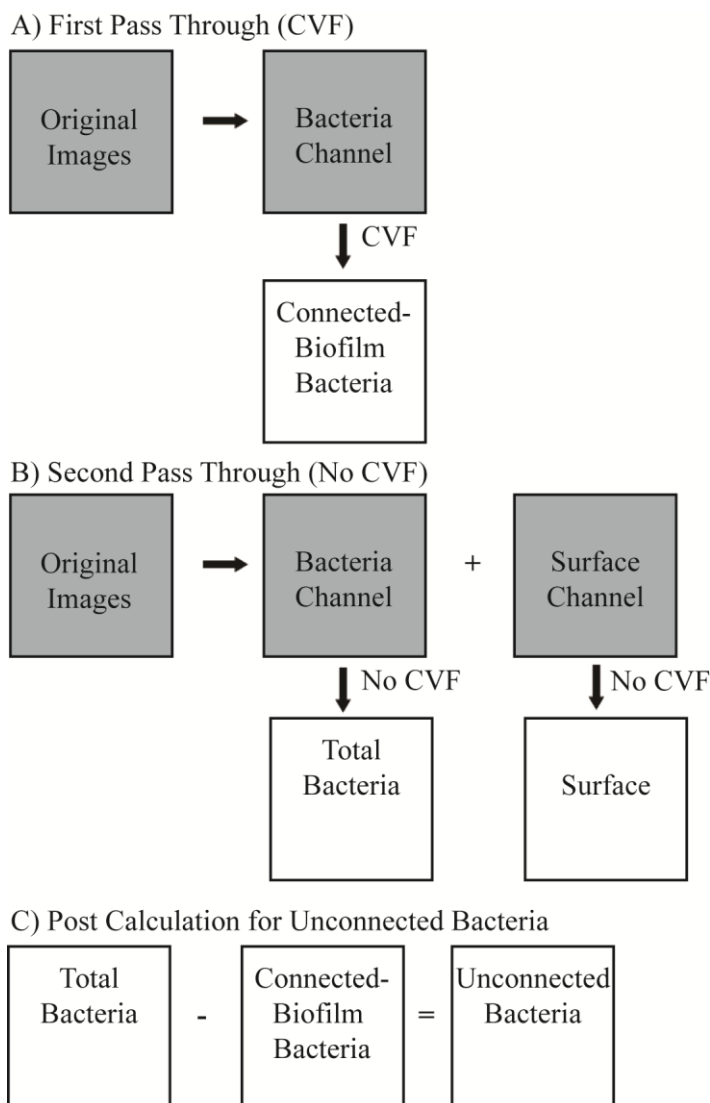


Figure 4-21: Quantification steps for connected-biofilm bacteria, unconnected bacteria, and a *flat* surface in COMSTAT or COMSTAT2-Beta; A) the CLSM image is sent through the program with CVF to quantify the connected-biofilm bacteria; B) the CLSM image is sent through the program again with CVF de-selected to quantify the total bacteria and a surface (must be flat); C) a post-calculation is needed to quantify the unconnected bacteria.

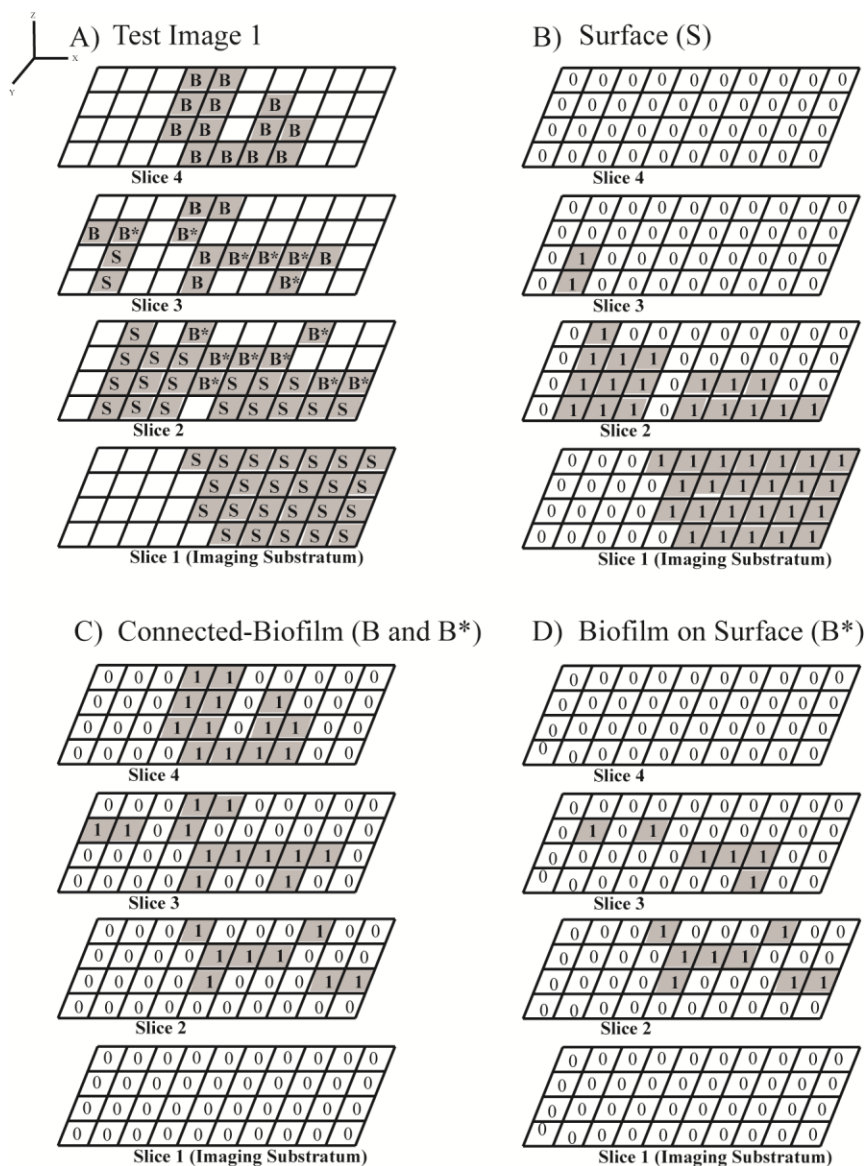


Figure 4-22: Four-slice images containing bacteria and surface components; A) Test Image 1 of connected-biofilm bacteria (B* and B) grown on top of an irregular surface (S); the indexed bacteria that were used for the modified substratum calculation (Equation 4-4) are depicted as B*; B) the binary image sequence of the surface from Test Image 1; C) the binary image sequence of the bacteria from Test Image 1; D) the binary image sequence of the indexed bacteria B*.

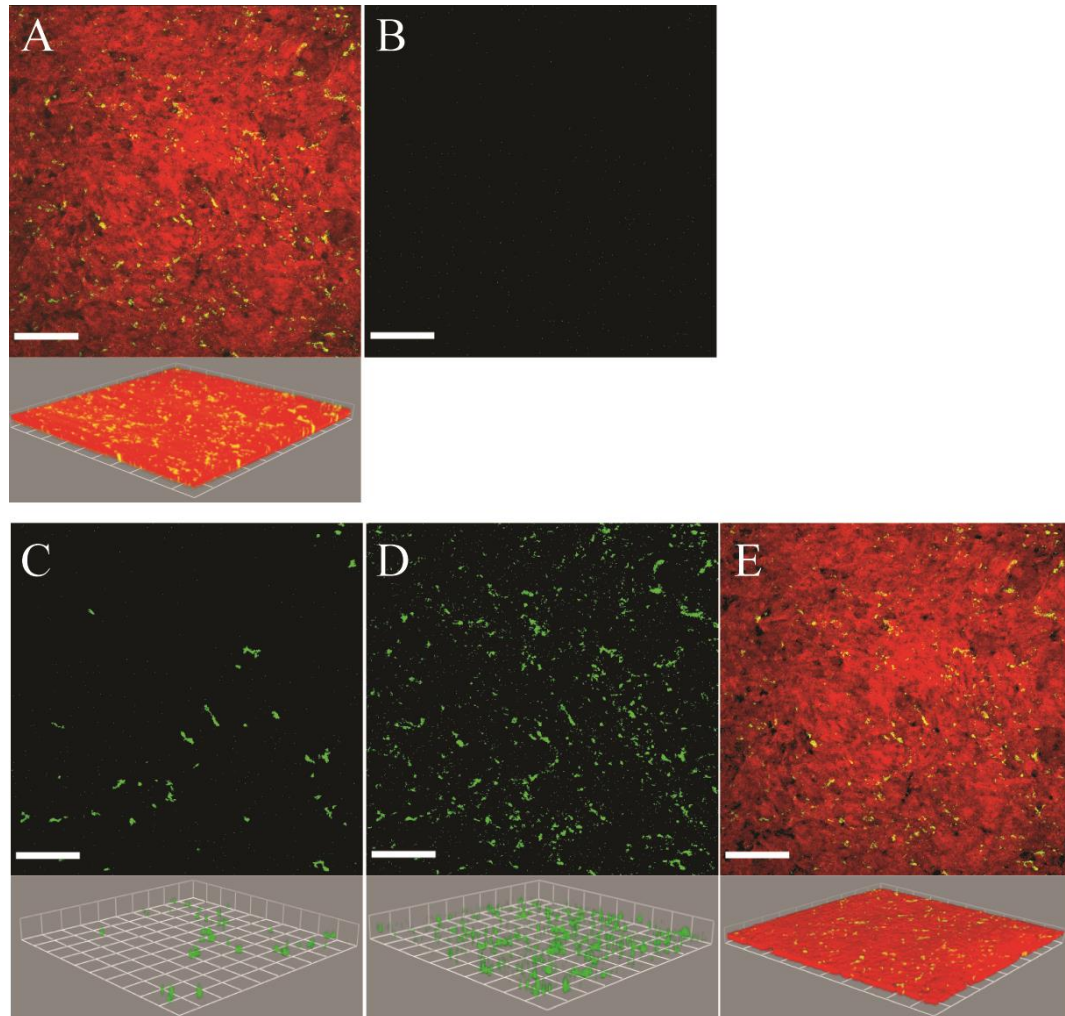


Figure 4-23: Green-fluorescent *Staphylococcus aureus* biofilms grown on cultured human airway epithelial cells (Calu-3) stained with Cell Tracker Orange; A) original confocal image with green bacteria on top of red tissue; B) bacteria on first image slice that were used to quantify 0.2% substratum coverage using COMSTAT (Equation 4-3);⁹⁶ C) connected-biofilm bacteria identified by COMSTAT's connected volume filtration algorithm; D) connected-biofilm bacteria identified by STAINIFICATION's modified connected volume filtration algorithm, which accounts for bacteria grown on the tissue; E) bacteria on cells that were used to quantify the 9.7% modified substratum coverage using STAINIFICATION (Equation 4-4); top: aerial view with scale bar of 70 μm ; bottom: side view with side of square equal to 38.2 μm ; the threshold values were 77 for surface and 49 for bacteria.

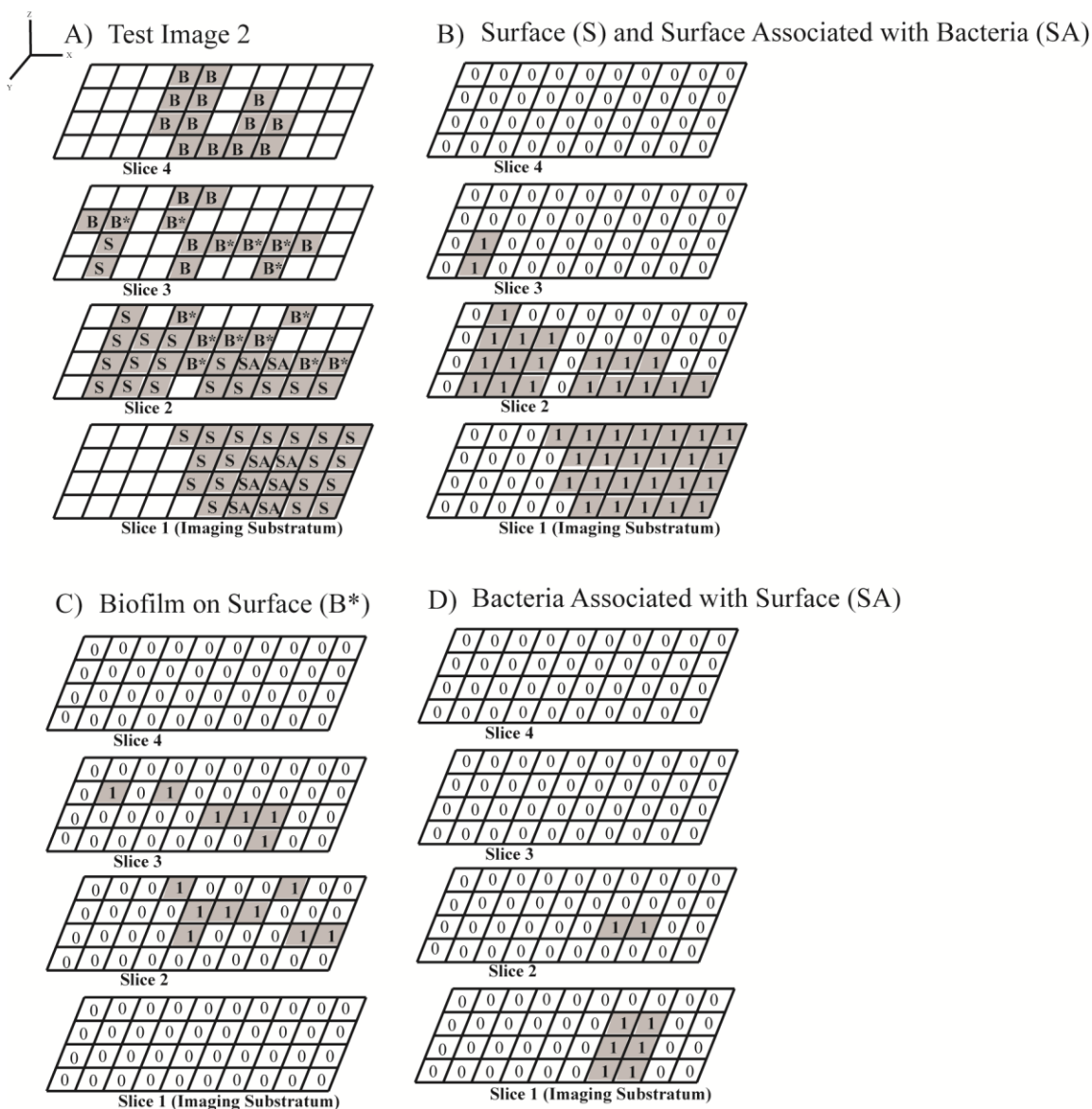


Figure 4-24: Four-slice images containing bacteria and surface components with some overlap between bacteria and surface; A) Test Image 2 of connected-biofilm bacteria (B* and B) grown on top of an irregular surface (S) with some bacteria and surface colocalized (SA); B) the binary image sequence of the surface from Test Image 2; C) the binary image sequence of the indexed biofilm bacteria on the surface B*. D) The binary image sequence of the bacteria associated or colocalized with the surface (SA); there are 6 surface associated bacteria pixels on the first image slice and 2 surface associated bacteria pixels on the second image slice; importantly, SA pixels do not affect the modified substratum coverage parameter.

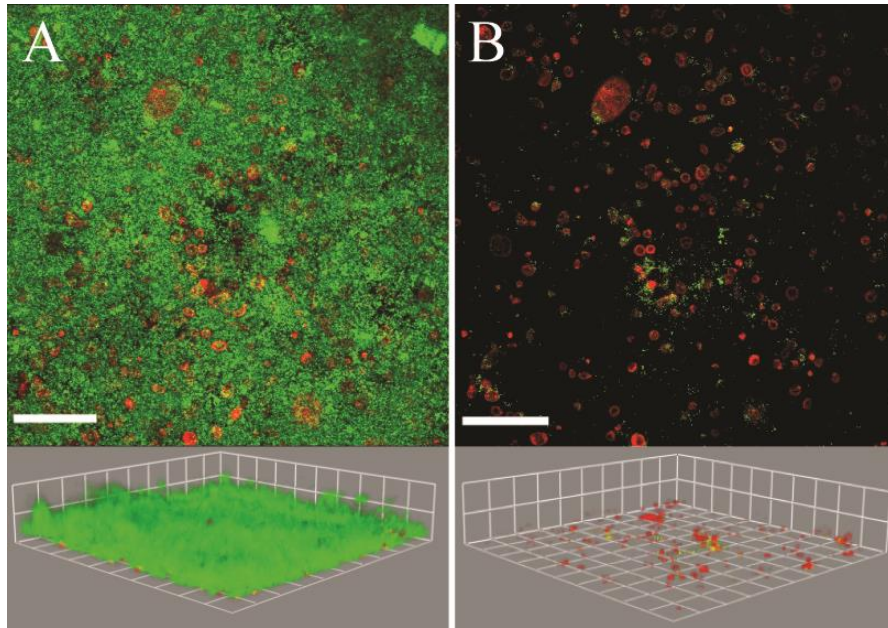


Figure 4-25: Green-fluorescent *Neisseria gonorrhoeae* bacteria grown on transformed cervical epithelial cells with red-stained nuclei; A) original confocal image with bacteria on top of nuclei; B) bacteria associated with the nuclei surface via colocalization; top: aerial view with scale bar of 120 μm ; bottom: side view with side of square equal to 61.7 μm ; the threshold values were 38 for surface and 37 for bacteria.

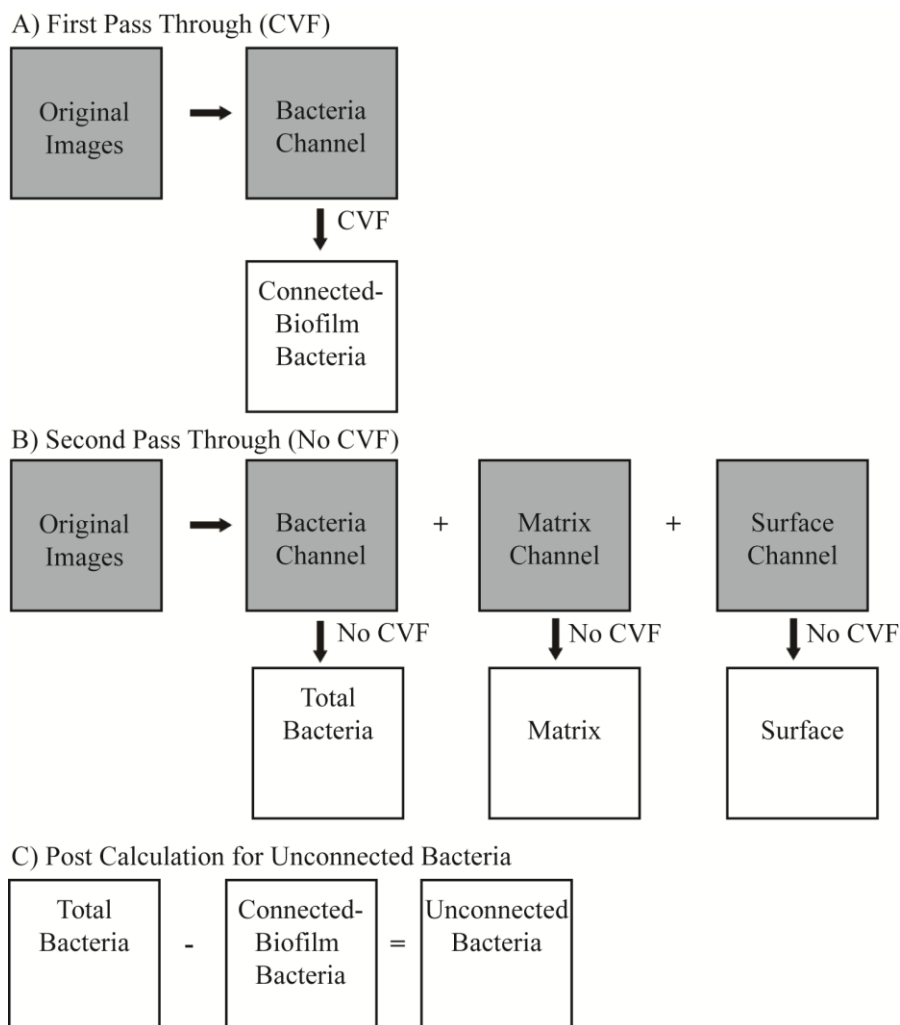


Figure 4-26: Quantification steps for connected-biofilm bacteria, unconnected bacteria, matrix, and a *flat* surface in COMSTAT or COMSTAT2-Beta; A) the CLSM image is sent through the program with CVF to quantify the connected-biofilm bacteria; B) the CLSM image is sent through the program again with CVF de-selected to quantify the total bacteria, matrix, and a surface (must be flat); C) a post-calculation is needed to quantify the unconnected bacteria.

CHAPTER 5
INVESTIGATING FORMULATION AND PROCESSING
PARAMETERS FOR SPRAY DRIED AEROSOLS

5.1 Introduction

The initial antibiotic therapy for cystic fibrosis patients with *Pseudomonas aeruginosa* infections is inhalation. Currently in the United States, nebulized tobramycin is most commonly prescribed.¹¹⁻¹² Nebulization of liquid formulations has many disadvantages including being time-consuming for administration and aerosol cleaning routines, requiring multiple treatments per day, and requiring multiple pieces of equipment for administration. With different pieces of equipment needed, including a power source, patients can have limited mobility for treatment outside of the home.^{15, 154} Thus, it can be difficult to ensure patient compliance outside of the hospital.

Dry powder inhalers have many advantages over nebulization. They provide a faster administration time. In Phase III clinical trials, TOBI[®] Podhaler[®], also known as tobramycin inhalation powder (TIP[®]), has been shown to decrease administration time by 70% or 13 hours per treatment cycle of 28 days.¹⁵⁵ There are fewer user-interfaced parts to a dry powder inhaler. Therefore, it takes less time to clean the device and the patient can be more mobile even if multiple daily treatments are needed. A power source is not needed with the dry powder inhaler when the patient's inhalation is able to actuate the device. Patients with severe lung function deterioration may be unable to actuate the device. Thus, dry powder aerosols reduce administration time and may improve patient compliance.¹⁵⁵⁻¹⁵⁶

Dry powder aerosols may be generated using a one-step process of spray drying. A liquid feed is atomized or sprayed into a hot drying chamber where the solvent is quickly evaporated. The dried powder is pulled by a vacuum from the aspirator, separated by a cyclone, and collected in a chamber. The powders generated by spray

drying can vary in physical properties depending on solution parameters in the spray dryer feed solution and processing parameters.¹⁵⁷ Common parameters investigated are feed solution concentration, composition, solvent/cosolvent choice, feed solution flow rate, inlet temperature, atomizer rate, and aspirator rate.¹⁵⁸⁻¹⁶² Since these parameters can affect the resulting powder, the parameters need to be optimized to obtain the desired powder characteristics.

Deposition in the tracheobronchial and alveolar regions of the lungs for cystic fibrosis patients is desired.¹⁷ Deposition of an aerosol in the lungs occurs from Brownian diffusion, sedimentation, and impaction of the powder. Brownian diffusion is based on random motion of particles in the alveolar region of the lungs where the air flow rate is low. Sedimentation relies on gravitational settling of particles primarily in the lower airways. Impaction of particles occurs when the momentum of the particle causes the particle to impact into the lung, rather than follow the air flow in the branching lungs. Impaction is more prevalent in the upper respiratory tract where the air flow rate is high. To deposit in the tracheobronchial and alveolar regions, aerosols should have aerodynamic diameters between 1 μm and 8 μm .¹⁶³ An aerodynamic diameter is the diameter of a spherical water droplet that has the same aerodynamic properties as the particle generated by spray drying. The aerodynamic diameter plays a role in powder impaction; most powder deposition, on a mass basis, occurs due to inertial impaction. The aerosol suspended in the air stream follows the change in air direction throughout the branching lungs. With this change in air direction, particles may impact with the lung surface due to particle momentum.¹⁶³ To study impaction, an *in vitro* lung model, such as the Andersen Cascade Impactor or Next Generation Impactor, can be used. Impactors are used to characterize powders for the important deposition parameters of mass median aerodynamic diameter (MMAD), fine particle fraction (fraction of powder below a specified aerodynamic diameter), and fine particle dose (mass of powder below 5 μm

aerodynamic diameter dosed in the *in vitro* model).¹⁵⁸⁻¹⁶² A geometric standard deviation (GSD) in combination with a MMAD describes the size distribution of the aerosol.¹⁶³⁻¹⁶⁵

In this chapter, we investigate the effects of solution and spray dryer processing parameters on the outcomes of yield, mass median aerodynamic diameter, geometric standard deviation, fine particle fractions, and fine particle dose. This proof-of-concept work uses leucine (flowability excipient), glutamic acid (dispersion compound), and ciprofloxacin hydrochloride (antibiotic) to demonstrate that dry powder aerosols can be generated with good flow properties for deposition. These parameter effects on the aerosol outputs will be used to guide future aerosol development of these combination treatments.

5.2 Materials and Methods

5.2.1 Materials

Ciprofloxacin hydrochloride (Cat 199020, lot 7446J) was from MP Biomedicals LLC (Solon, OH). L-glutamic acid (G8415, batch 129K0042), L-leucine non-animal source (L8912 batch 116K0042), silicone oil DC 200, and hexane mixture of isomers reagent 98.5% were purchased from Sigma Aldrich (St. Louis, MO). Hydrochloric acid (1 N) was purchased from VWR (West Chester, PA). Sodium hydroxide (2 N) was purchased from Fisher Scientific (Fair Lawn, NJ). Purified water was obtained from a NanoPure Infinity Ultrapure Water System (Barnstead Int., Dubuque, IA).

5.2.2 Central Composite Design

Spray drying is a one-step method to develop dry powder aerosols from solutions. A Buchi 190 spray drier (Flawil, Switzerland) was used to generate dry powder aerosols of ciprofloxacin, glutamic acid, and leucine from an aqueous solution. For each run, the

aqueous solution at room temperature was pumped into an atomizer nozzle, which used air flow to atomize the solution into droplets. The droplets entered a heated drying chamber where the water was evaporated within seconds. The resulting solid powder was pulled out of the drying chamber, through a cyclone to improve aerosol collection, and into a collection chamber at room temperature through use of an aspirator vacuum. The properties of the dry powder aerosols highly depend on formulation and spray dryer processing parameters.¹⁵⁷ Therefore, a central composite design of experiments was used to investigate formulation parameters (pH and solution concentration) and spray dryer processing parameters (inlet temperature, atomizer rate, and solution flow rate) on the yield, mass median aerodynamic diameter, fine particle fractions, and fine particle dose of the generated dry powder aerosols.

Dry powders were formulated with high drug loading (10 wt% excipient, L-leucine, and 90 wt% antibiotic, ciprofloxacin hydrochloride, and dispersion compound, glutamic acid). The constant parameters were the aspirator pressure of -30 mbar, which was the highest value attainable, and the ratio of 10% leucine, 2% antibiotic, and 88% dispersion compound based on mass. Previous work in our laboratory showed as little as 10 wt % leucine could improve powder flowability and deposition.¹⁶⁶ Leucine is commonly used to reduce adhesion between particles and to improve flowability in powders.¹⁵⁸⁻¹⁵⁹ The ratio of antibiotic to dispersion compound was based on 50 µg/mL ciprofloxacin hydrochloride significantly killing *Pseudomonas aeruginosa* biofilms and 20 mM glutamic acid dispersing *Pseudomonas aeruginosa* biofilms.^{55, 167}

Key formulation and process parameters were varied to optimize the physical properties of the spray dried powders. These parameters (Table 5-1) included the solution pH (3-11), solids concentration of the spray dried solution (0.025-0.725 wt %), spray dryer inlet temperature (155-195°C), atomizer air rate (150-750 L/hr), and solution flow rate (5-13 mL/min). A Buchi 190 spray drier (Flawil, Switzerland) was used for the 32 runs of the central composite design (Table 5-2). The factor pH was included since it is

not well studied in the literature, and it may have an effect on formulations with ionizable groups since pH can affect particle morphology and amino acid crystallinity during spray drying.^{130, 168} Leucine has pK_a values of 2.4 (acidic) and 9.6 (basic).¹⁰⁹ Glutamic acid has pK_a values of 2.3, 4.3, and 9.7.¹⁰⁹ Ciprofloxacin has pK_a values of 6.0 (acidic) and 8.8 (basic).¹⁶⁹ The pH was investigated from 3 to 11 to cover a wide range of pH values. Solids concentration was investigated since it was shown to be a significant parameter by our laboratory and by others, affecting aerosol development.^{166, 170-171} The range of concentrations was expanded beyond those previously investigated in our laboratory. The inlet temperature was included in this study since it affects the drying of the aerosols.¹⁷¹ The maximum temperature was determined by the maximum allowable temperature for the spray dryer. The minimum temperature was chosen to be high enough to prevent water from accumulating in the collection chamber for typical parameter settings, but low enough to potentially lead to failure by water collecting in the chamber (determined by spray drying water alone). Despite the inlet temperature being high, the dried aerosol will not reach these temperatures due to the cooling effect from evaporation.¹⁵⁷ The product is fed at room temperature, is exposed to an elevated temperature for a few seconds with simultaneous solvent evaporation, and is collected in a chamber at room temperature. If degradation of temperature-sensitive components did occur, it could potentially be verified with high-performance liquid chromatography. The atomizer rate was investigated since it has been shown by others to be a significant parameter affecting the physical properties of aerosols.^{157, 171} The range was determined by the minimum and maximum allowable rates on the spray dryer. The solution flow rate was included since it was previously shown by our laboratory to be an important parameter.¹⁶⁶

5.2.3 Particle Deposition

The Next Generation Impactor (NGI, MSP Corporation, Shoreview, MN) is an *in vitro* lung model developed specifically for the pharmaceutical industry to be used to quantify the mass median aerodynamic diameter, fine particle fractions, and fine particle dose. The eight trays of the NGI were coated with 3 vol % solution of silicone oil in hexanes to prevent reentrainment of particles. The hexane was allowed to evaporate in the fume hood for 15 minutes prior to use. The NGI was assembled with the trays, HCP5 vacuum pump, flow meter (DFM 2000), and critical flow controller (TPK 2000) (Copley Scientific, Nottingham, UK). The NGI neck piece with a 90 degree bend was added to the inlet of the NGI, which collects large particles similar to the mouth and neck for a human. A gelatin capsule was 2/3 filled with powder, closed, and placed in an Aerolizer[®] inhaler (Merck, Kenilworth, NJ). As the inhaler was being placed into the neck piece entrance, the two side buttons on the inhaler were pressed in to puncture the capsule. The NGI TPK 2000 was set to pull powder in at 60 L/min for 4 seconds, which is an inspiratory flow rate attainable by cystic fibrosis patients six years and older that do not have substantially reduced lung function.¹⁷² If the patient were unable to attain 60 L/min, then the *in vitro* lung would need to be assessed at a lower rate, such as 30 L/min. As the run was completed, the capsule rotated in the inhaler to aid in powder dispersion. After the run was completed, 10 mL of purified water was added to each of the eight trays. The cups were agitated on a vortex mixer (VWR, West Chester, PA) for ~10 seconds. For each tray, three aliquots (100 μ L each) were transferred to the 96-well plate. The 96-well plate also included controls for ciprofloxacin hydrochloride at 0.1 mg/mL and serially diluting eight times to a final concentration of 0.1 μ g/mL and with a water control. The 96-well polystyrene plate was scanned at 276 nm using the SpectraMax Plus 284 plate scanner (Molecular Devices, Sunnyvale, CA). Each powder was run through the NGI three times, except sample 6 (n=0), sample 11 (n=0), and sample 31 (n=1). Excel[®] software was used to create a calibration curve of absorbance versus ciprofloxacin

concentration (mg/mL) for each 96-well plate (Figure 5-1). The calibration curve was used to determine the ciprofloxacin concentration per NGI tray, which was multiplied by 10 mL to determine the total mass of ciprofloxacin per NGI tray.

The ciprofloxacin mass from the aerosols was used to investigate deposition. It was assumed that the ciprofloxacin was evenly distributed throughout all particle sizes. The ciprofloxacin mass per tray was entered into the Copley Citdas software (Copley Scientific, Nottingham, UK). With the rate of 60 L/min, which is achievable for children and adults with cystic fibrosis, the cutoff diameters for the NGI trays are shown in Table 5-3.¹⁷²⁻¹⁷³ Cutoff diameters represent bins of particle sizes collected. For example, tray 1 may have powders of aerodynamic diameter greater than or equal to 8.06 μm . Tray 2 may have powders of aerodynamic diameter between 4.46 μm and 8.05 μm . The cutoff diameters were used to find the aerodynamic diameters of the aerosols and the software reported the mass median aerodynamic diameter (MMAD) and geometric standard deviation (GSD). The aerodynamic diameter is derived from Stoke's Law and is given by

$$d_{aero} = d_{geo} \sqrt{\frac{\rho_{powder}}{\rho_{ref}} \frac{1}{\gamma}} \quad \text{Equation 5-1}$$

where d_{aero} is the aerodynamic diameter, d_{geo} is the geometric diameter, ρ_{powder} is the bulk density of the powder, γ is the shape correction factor that is equal to 1 for spherical particles, and ρ_{ref} is the density of water (1 g/cm³).¹⁶³ Copley Citdas software determines the GSD, from

$$GSD = \frac{d_{84\%}}{d_{50\%}} \quad \text{Equation 5-2}$$

where $d_{n\%}$ is the particle diameter at the n th percentile of the cumulative particle size profile.¹⁶³ The GSD is found using a linear fit on a log-probability plot. For bimodal distributions, a two log normal mode algorithm (Dr. Charles Stanier, The University of Iowa, Department of Chemical and Biochemical Engineering) in MatLab was applied to the ciprofloxacin mass data per NGI tray data. Dr. Stanier's code quantified the MMAD and GSD for each size distribution in the aerosol, generating MMAD1 and GSD1 and MMAD2 and GSD2.¹⁷⁴

Copley Citdas software was used to quantify the fine particle fractions and fine particle dose. The lung deposition of particles less than 4.46 μm ($\text{FPF} < 4.46 \mu\text{m}$) was found from the percent of powder on stages 3 and below on the NGI stage. $\text{FPF} < 4.46 \mu\text{m}$ is given by

$$\text{FPF} < 4.46 \mu\text{m} = \frac{m_{3-8}}{M} * 100\% \quad \text{Equation 5-3}$$

where m_{3-8} is the mass of powder on trays 3 through 8 and M is the total mass of powder on all eight trays assuming negligible loss to the NGI throat.¹⁷³ The lower lung deposition of particles less than 2.82 μm ($\text{FPF} < 2.82 \mu\text{m}$) was found from the percent of powder on stages 4 and below. $\text{FPF} < 2.82 \mu\text{m}$ is given by

$$\text{FPF} < 2.82 \mu\text{m} = \frac{m_{4-8}}{M} * 100\% \quad \text{Equation 5-4}$$

where m_{4-8} is the mass of powder on stages 4 through 8 and M is the total mass of powder on all eight trays assuming negligible loss to the NGI throat. The fine particle dose (FPD) was the mass of powder less than 5 μm that impacted in the NGI.¹⁷³ The

FPD is found by interpolating the particle distribution to the 5 μm particle size, since there is not a cutoff diameter at exactly 5 μm .

5.2.4 Scanning Electron Microscopy

Aluminum stubs with double-sided adhesive were used for scanning electron microscopy (SEM) imaging. Using a spatula, powder was tapped onto the adhesive and the excess powder was tapped off the stub. The stub was sputter coated (Emitech K550 sputter coater, Kent, England) with gold and palladium for three minutes to prevent charging of the powder. The samples were visualized with the Hitachi S-4800 SEM (Krefeld, Germany) with an accelerating voltage of 2 kV and a working distance of 5 μm .

5.2.5 Statistical Analysis

All design of experiment data were analyzed with Statgraphics[®] (Warrenton, VA) and MiniTab[®] (State College, PA). Statgraphics[®] was used to generate main effects plots and select optimized design parameters. Statgraphics[®] used ANOVA to analyze the central composite design of experiment to determine significant parameters ($p < 0.05$). MiniTab[®] was used to generate surface contour plots.

5.3 Results and Discussion

Table 5-4 shows the data for percent yield, outlet temperature, FPF $<$ 4.46 μm , FPF $<$ 2.82 μm , and FPD by experimental design run. Table 5-5 shows the data for MMAD. Run 6, which had the lowest atomizer rate of 150 L/hr, collected water in the product vessel, so no dry powder was collected. Run 11, which had the lowest solution concentration of 0.025 wt %, collected a few large, agglomerated particles.

5.3.1 Yield

The percent yields for the aerosols generated by spray drying ranged from 6.0% to 43.1% (Table 5-4). Bench top spray dryers rarely reach yields greater than 90% due to losses of powder sticking to the drying chamber; common yields in literature range from 8% to 84%.^{159, 161-162, 175} Figure 5-2 depicts the main effect plot for the design factors on the yield response. Main effects plots depict the average outcome value per factor value, which is used to investigate overall trends. In this study, the solution concentration and atomizer rate significantly affected the yield of dry powder aerosols, which is seen as a large positive effect on yield.

In Figure 5-2, increasing pH across 3 to 11 resulted in an increase in yield. Our results were consistent with Vanbever et al. who demonstrated an increase in pH from 4 to 7 increased the particle size for particles of albumin, lactose, and phosphatidylcholine dipalmitoyl; an increase in particle size results in an increase in yield.^{40, 162, 171, 176} Increasing the solution concentration across 0.025 wt% and 0.725 wt% increased the yield, which is a consistent trend found in literature.^{162, 166, 171, 175-176} A higher solution concentration resulted in larger particles. Larger particles result in a higher yield due to better collection of particles by the spray dryer cyclone.¹⁵⁷ Increasing the inlet temperature across 155°C to 195°C decreased the yield. This was consistent with Tewa-Tagne et al. observing a decrease in yield from an increase in inlet temperature of 140°C to 160°C for spray dried polymeric nanocapsules.¹⁶² Billion et al. also reported an inlet temperature increase from 130°C to 160°C for spray dried acetaminophen and oxalic acid resulted in a decrease in yield.¹⁷⁰ It is possible that increasing the temperature decreased moisture in the drying chamber, decreasing agglomeration of particles; fine particles may have formed, which are lost in the vacuum exhaust rather than collected via the cyclone and collection chamber.¹⁵⁷ Thus, an increase in fine particles lost to the exhaust would account for the decrease in yield. In our study, increasing the atomizer rate increased the yield. This was consistent with Tewa-Tagne et al. reporting an increase in atomization

increased the yield for polymeric nanocapsules and Wan et al. reporting an increase in atomization increased the yield for theophylline and hydroxypropylmethylcellulose spray dried product.^{162, 177} Increasing atomization results in larger spray dried droplets entering the drying chamber of the spray dryer. Thus, a larger particle size and a larger yield are expected with an increase in atomization.¹⁵⁷

Figure 5-3 displays a surface plot showing the factors which had a significant effect on yield: solution concentration ($p=0.002$) and atomizer rate ($p<0.001$). A surface plot shows the outcome result for each parameter value, rather than the average outcome value for each factor that a main effects plot depicts. Increasing the solution concentration and increasing the atomizer rate resulted in a high percent yield. In our study, increasing the solution flow rate increased the yield, which was consistent with Billion et al. demonstrating an increased in feed rate increased the yield for spray dried acetaminophen and oxalic acid.¹⁷⁰ Figure 5-4 is the surface plot for the significant interaction of inlet temperature and liquid flow rate ($p=0.015$). At the highest inlet temperature and the fastest solution flow rate, or at the lowest temperature and slowest solution flow rate, the percent yield was maximized. With the highest inlet temperature and the slowest solution flow rate or the lowest inlet temperature and fastest solution flow rate, the percent yield was minimized. Our results were consistent with Billion et al. who observed a similar surface plot for the interaction of inlet temperature and feed solution flow rate.¹⁷⁰ At the lowest temperature and fastest solution flow rate interaction, the outlet temperature should be the lowest (Figure 5-5). At the highest temperature and slowest solution flow rate, the outlet temperature should be the highest (Figure 5-5). Billion et al. emphasized the difference between the inlet and outlet temperature is important for developing dry powders. Depending on the temperature difference, powder that sticks to the drying chamber may be created and lower the yield.¹⁷⁰ Therefore, more cohesive powder may have formed in our system at the highest flow rate and lowest inlet temperature and at the lowest flow rate and highest inlet temperature.

5.3.2 Mass Median Aerodynamic Diameter, MMAD

Figure 5-6 shows size distribution data acquired from the Next Generation Impactor (NGI). The Copley Citdas software (Copley Scientific, Nottingham, UK) that comes with the NGI assumes a single log normal distribution of data. Therefore it calculated a single MMAD value (Table 5-5). However, it did not always calculate a geometric standard deviation (GSD). This implied that the distribution was not a single log normal distribution. A single log normal distribution would result in a linear line on a log-probability plot and this is used to calculate GSD.¹⁶³ A distribution with multiple separate modes would not result in a linear line on a log-probability plot, so a GSD cannot be quantified for an overall multimodal distribution with good separation. GSD would need to be quantified for each size distribution.¹⁶³ Figure 5-6 visually compares the impactor data (blue) with fit values (red) from the two log normal fit. The single log normal mode fit does not match the data well since the red fit values do not match the blue experimental data values. SEM was used to verify that a single size distribution was not generated (Figure 5-7). Two populations of particles were observed: small spherical particles and large, collapsed particles. Other researchers formulating with leucine have also used SEM to show multiple particle sizes in the resulting spray dried aerosols.^{160, 175, 178} This has also been shown with publication of deposition profiles.¹⁵⁹ Even though the distributions are not single log normal, researchers commonly report a single MMAD and no GSD value.^{159-160, 175-176}

To stay consistent with literature, we have evaluated the MMAD values obtained from the Copley Citdas software (Table 5-5). The MMAD values ranged from 3.0 μm to 3.9 μm , which is consistent with formulations containing leucine having MMAD values between 0.9 and 5.0 μm .^{159-160, 164-165, 175} Figure 5-8 shows the main effect plot for the factors on the MMAD response. Main effects plots depict the average outcome value per

factor value, which is used to investigate overall trends. The solution concentration parameter significantly affected the MMAD output, which can be seen as a large increase in MMAD with increasing solution concentration in Figure 5-8.

Inlet temperature, pH, atomizer rate, and solution flow rate did not significantly affect MMAD. Increasing pH had a minimal decrease on MMAD. Inlet temperature showed a maximum effect on MMAD. Literature reports conflicting results on the effect of inlet temperature on particle size. Tewa-Tagne et al. found increasing inlet temperature decreased the particle size of spray-dried nanocapsules, while Stahl et al. and Wan et al. found increasing inlet temperature increased the particle size for insulin and theophylline with hydroxypropylmethylcellulose, respectively.^{161-162, 177} In our system, initially increasing the inlet temperature may increase the particle size due to the formation of larger, collapsed particles. As the temperature is increased further, it may result in an outer skin forming on the exterior of the particles, which helps the particles retain the smaller, spherical shape.¹⁶¹ As the atomizer rate was increased, MMAD decreased, which is a consistent trend found in literature.^{160-162, 171, 179} Increasing the atomizer rate provides more energy to create smaller liquid droplets; these smaller droplets generate smaller particles.¹⁵⁷ As the solution flow rate increased, MMAD was increased, which was consistent with literature.^{161-162, 171, 176} A faster liquid solution flow rate provides more material in the droplet, which results in a larger particle size.¹⁵⁷ Figure 5-9 is the surface plot for the solution concentration factor. An increase in solution concentration significantly ($p=0.027$) increased MMAD, which is a consistent trend in literature.^{162, 166, 171, 176} As the solution concentration increases, more material is dried in the spray dried droplet, which results in a larger particle size.¹⁵⁷

To go beyond reporting a single MMAD without a GSD value in literature,^{160, 175-176} we applied a two log normal mode fit (Figure 5-10). The fit (red) matches the data (blue) more appropriately with the two log normal mode fit since the red fit values resemble the blue experimental data. Figure 5-11 shows the resulting MMAD (D_p on

graph) and GSD ($10^{\wedge}\text{logsigma}$ on graph) for each mode. The top of Figure 5-11 is the single mode fit, which is similar to the output from the Copley software. However, this fit does not describe the distribution well. A single MMAD and GSD implies a single particle distribution. The lower portion of Figure 5-11 shows the two log normal fit, which better represents the data since two particle distribution modes are present in the plot. All MMAD and GSD data for both modes are listed in Table 5-5.

The smaller size distribution, MMAD1, ranged from 0.43 μm to 1.84 μm . MMAD1 was not significantly affected by any factor. From the main effects plot, it can be seen that pH had a negligible effect on MMAD1 (Figure 5-12). At lower values, an increase in solution concentration increased MMAD1, which was expected.^{162, 166, 171, 176} As the solution concentration increased further, the MMAD1 was decreased. It is possible that at the higher solution concentrations, the particle size is increased beyond the MMAD1 size distribution. The inlet temperature had both positive and negative effects on MMAD1. Inlet temperature is known to affect particle size differently. Tewa-Tagne et al. found increasing inlet temperature decreased the particle size, while Stahl et al. and Wan et al. found increasing inlet temperature increased the particle size.^{161-162, 177} In our study, increasing the atomizer rate decreased MMAD1. This is consistent with increasing atomizer rate reducing the particle size.^{161-162, 171, 176, 179} As the solution flow rate was increased, MMAD1 decreased. This was not consistent with literature where an increase in solution flow rate was found to increase the particle size.^{161-162, 171, 176} However, since literature commonly reports a single MMAD, it is possible to have different effects on one size distribution over the other. MMAD1 may decrease with an increasing liquid flow since larger particles are being made beyond the MMAD1 size distribution. This is consistent with our data showing an increase in liquid flow resulted in an increase in MMAD2 size (Figure 5-14).

GSD1 values ranged from 1.5 to 14.0 and were larger than GSD2 values (Table 5-5). The larger value for GSD represents more spread or polydispersity in the distribution.

No factors significantly affected GSD1. In general, to reduce the value of GSD1, low pH and solution concentration and high inlet temperature, atomizer rate, and liquid flow would be desired (Figure 5-13). However, these still result in polydispersed particles.

The larger size distribution, MMAD2, ranged from 2.84 μm to 5.08 μm , which were within the desired MMAD range of 1 to 8 μm . Figure 5-14 depicts the main effect trends for the larger size distribution MMAD2. Solution concentration, the interaction between solution concentration and atomizer rate, and the interaction between inlet temperature and atomizer rate significantly affected MMAD2.

As pH was increased, MMAD2 increased. This was consistent with Vanbever et al. reporting an increase in pH resulted in an increase in particle size due to a change in particle morphology between albumin, lactose, and phosphatidylcholine dipalmitoyl with a change in pH.¹³⁰ As the solution concentration was increased, MMAD2 increased. This was consistent with the trend of increasing solution concentration increasing particle size.^{162, 166, 171, 176} A larger solution concentration results in a larger particle since more material is being dried in the particle.¹⁵⁷ Inlet temperature an optimal effect on MMAD2. As stated previously, literature has conflicting reports on the effect of inlet temperature. Tewa-Tagne et al. found increasing inlet temperature decreased the particle size, while Stahl et al. and Wan et al. found increasing inlet temperature increased the particle size.^{161-162, 177} As the atomizer rate was increased, MMAD2 decreased. This is a consistent trend found in literature.^{160-162, 171, 179} As the solution flow rate increased, MMAD2 was increased, which was consistent with literature.^{161-162, 171, 176} An increase in solution flow rate provides more material to be dried in the droplet, which results in a larger particle size.¹⁵⁷

Figure 5-15 is the surface plot of the significant parameters solution concentration ($p=0.002$) and liquid flow ($p=0.026$). Both parameters had a positive outcome on MMAD2. Figure 5-16 is the surface plot for the significant interaction of inlet temperature and atomizer rate ($p=0.035$). From this plot it can be seen that, to generate

particles with MMAD2 close to 5 μm , a low inlet temperature and low atomizer rate should be used. Whereas, to generate particles with MMAD2 close to 3.5 μm , a low inlet temperature and high atomizer rate or a high inlet temperature and low atomizer rate should be used. Stahl et al. reported a significant interaction between inlet temperature and atomizer on particle size for spray dried insulin.¹⁶¹ Figure 5-17 is the surface plot of the significant interaction of solution concentration and atomizer rate ($p=0.023$). The largest MMAD2 was achieved with a low atomizer rate and high solution concentration, since a low atomizer produces larger droplets and a higher solution concentration results in more material to be dried in the droplet.¹⁵⁷ Tewa-Tagne et al. reported a significant negative interaction between solution concentration and atomizer rate on the particle size of spray dried polymeric nanocapsules.¹⁶²

GSD2 values ranged from 0.7 to 2.8, indicating the powders were polydispersed. None of the factors significantly affected GSD2. The main effect trends for GSD2 follow the opposite trends for GSD1 (Figure 5-18 compared to Figure 5-13).

5.3.3 Fine Particle Fraction, FPF

The deposition of particles less than 4.46 μm ($\text{FPF} < 4.46 \mu\text{m}$) was on average between 56 and 70% (Table 5-4). It is desired to maximize the deposition. Other researchers with varying formulations containing leucine have reported lung deposition values from 18.7 to 82.5%.^{158, 160, 164-165, 180} Seville et al. observed formulations with leucine alone had FPF values which varied from 50 to 80%.¹⁷⁵ Prota et al., who formulated with 10% leucine and the drug naringin, reported lung deposition values from 40.2 to 54.3%.¹⁵⁹ Figure 5-19 depicts the main effect trends for the design factors on the $\text{FPF} < 4.46 \mu\text{m}$ response. The pH had a negligible effect on $\text{FPF} < 4.46 \mu\text{m}$. As the solution concentration or solution flow rate were increased, the $\text{FPF} < 4.46 \mu\text{m}$ decreased, which were the opposite trends of MMAD2. This made sense since increasing particle

size should decrease FPF $<$ 4.46 μm , which is consistent with literature.^{162, 171, 176} Figure 5-20 is the surface plot showing the effect of solution concentration on FPF $<$ 4.46 μm ($p=0.038$). This was consistent with literature that showed increasing solution concentration significantly increased MMAD, which would significantly decrease FPF.^{162, 166, 176} The inlet temperature had an optimum on FPF $<$ 4.46 μm with the opposite trend of MMAD2. Likewise, the atomizer rate increased, FPF $<$ 4.46 μm increased.

The deposition of particles less than 2.82 μm (FPF $<$ 2.82 μm) on average ranged from 35 to 46% (Table 5-4). Sou et al. reported deposition values between 10.6 and 61.0%¹⁶⁰. Figure 5-21 depicts the main effect trends for the design factors on FPF $<$ 2.82 μm response. The trends were similar as those for FPF $<$ 4.46 μm . However, no factors significantly affected the FPF $<$ 2.82 μm outcome. As the pH or atomizer rate were increased, the FPF $<$ 2.82 μm was increased. As the solution concentration or liquid flow were increased, the FPF $<$ 2.82 μm was decreased. At low inlet temperatures the FPF $<$ 2.82 μm decreased. At high inlet temperatures the FPF $<$ 2.82 μm increased.

5.3.4 Fine Particle Dose, FPD

On average, the powder FPD ranged from 0.29 to 0.97 mg (Table 5-4). Seville et al. reported a similar FPD of 0.6 mg with formulations of 10% leucine and 90% salbutamol and lactose.¹⁷⁵ Figure 5-21 depicts the main effect trends for the FPD response. Increasing the pH or inlet temperature decreased the FPD. The solution concentration, atomizer rate, or liquid flow had optimum values to maximize FPD. Figure 5-22 is the surface plot that shows the effect of pH on FPD ($p=0.028$). The lowest pH of 3 resulted in the highest FPD.

5.3.5 Optimization

Parameters were optimized for this system to produce polydispersed dry powder aerosols with MMAD values between 1 μm and 8 μm and with high deposition. It was desired to maximize the deposition, to minimize the polydispersity, and to aim for a target range of 1 μm to 8 μm for MMAD. With the aim of maximizing yield, FPFs, and FPD, minimizing GSD1 and GSD2, and aiming to have MMAD1 and MMAD2 within 1 μm to 8 μm , Table 5-6 shows the suggested parameter settings. The optimized parameters were the minimum pH of 3, mid-range solution concentration of 0.556 wt %, minimum inlet temperature of 155°C, mid-range atomizer rate of 447 L/hr, and minimum solution flow rate of 5 mL/min. This suggests further investigation below pH 3, below the inlet temperature of 155°C, and below the solution flow rate of 5 mL/min may be necessary to better optimize the process for this particular set of compounds.

5.4 Conclusions

Dry powder aerosols were developed with MMADs in the range of 1 μm to 8 μm and with high FPF and FPD values. This work proved the concept that dry powder aerosols with good flowability and deposition could be developed with high drug concentrations (90% drug) by incorporating leucine into the formulations. The parameters that had significant effects on yield, particle size, and deposition included solution concentration, atomizer rate, solution flow rate, pH, interaction of inlet temperature and solution flow rate, interaction of inlet temperature and atomizer rate, and interaction of solution concentration and atomizer rate. These parameters should be considered in further aerosol development. Solution concentration was the most important parameter, significantly increasing yield and MMAD2, while decreasing FPF < 4.46 μm . For future formulations, it may be advantageous to investigate the pH parameter below pH 3 to examine below the lowest pKa of formulation compounds and

to investigate a wider range of solution concentration since this was the most important parameter. The pH may effect particle morphology and thus ultimately effect particle size and deposition.

Table 5-1: Central composite design of experiment solution parameters (pH and solution concentration) and processing parameters (inlet temperature atomizer air or spraying air flow rate, and solution flow rate).

Design Point	pH	Solution Concentration, Wt %	Inlet Temperature, °C	Atomizer Rate, L/hr	Solution Flow Rate, mL/min
Axial	3	0.025	155	150	5
Cubic	5	0.200	165	300	7
Midpoint	7	0.375	175	450	9
Cubic	9	0.550	185	600	11
Axial	11	0.725	195	750	13

Table 5-2: Factor values for 32 runs in the central composite design.

Run	pH	Solution Concentration, Wt %	Inlet Temperature, °C	Atomizer Rate, L/hr	Solution Flow Rate, mL/min
1	5	0.550	185	300	11
2	11	0.375	175	450	9
3	7	0.375	175	450	9
4	9	0.550	185	600	11
5	9	0.550	165	300	11
6	7	0.375	175	150	9
7	5	0.550	165	600	11
8	9	0.200	185	600	7
9	7	0.375	175	450	9
10	7	0.375	175	450	9
11	7	0.025	175	450	9
12	7	0.375	175	450	9
13	7	0.375	175	450	9
14	9	0.550	185	300	7
15	5	0.550	185	600	7
16	9	0.200	185	300	11
17	7	0.375	175	450	9
18	5	0.200	165	600	7
19	5	0.200	185	600	11
20	7	0.375	175	450	13
21	9	0.200	165	300	7
22	3	0.375	175	450	9
23	5	0.550	165	300	7
24	5	0.200	165	300	11
25	9	0.550	165	600	7
26	7	0.375	175	750	9
27	7	0.375	195	450	9
28	9	0.200	165	600	11
29	7	0.375	155	450	9

Table 5-2: Continued

Run	pH	Solution Concentration, Wt %	Inlet Temperature, °C	Atomizer Rate, L/hr	Solution Flow Rate, mL/min
30	7	0.375	175	450	5
31	5	0.200	185	300	7
32	7	0.725	175	450	9

Table 5-3: Next Generation Impactor (MSP, Shoreview, MN) cutoff diameters for 60 L/min inhalation flow rate.

Tray	Cutoff Diameter, μm
1	8.06
2	4.46
3	2.82
4	1.66
5	0.94
6	0.55
7	0.34
8	0.00

Cutoff diameter represents bins of particle sizes, for example, tray 1 is particle sizes greater than 8.06 μm and tray 2 represents particle sizes between 4.46 μm and 8.05 μm .¹⁷³

Table 5-4: Responses (mean \pm standard deviation) of percent yield, outlet temperature, average fine particle fraction in percent (FPF) < 4.46, FPF < 2.82, and fine particle dose (FPD) by run with n=3, except Run 31 with n=1.

Run	Yield, %	Outlet Temperature, °C	FPF < 4.46 μ m, %	FPF < 2.82 μ m, %	FPD, mg
1	13.3	90	56 \pm 13	35 \pm 16	0.56 \pm 0.12
2	29.0	93	64 \pm 6	43 \pm 6	0.46 \pm 0.22
3	36.8	91	63 \pm 3	43 \pm 3	0.49 \pm 0.09
4	42.9	92	62 \pm 6	41 \pm 3	0.72 \pm 0.04
5	16.2	77	58 \pm 7	39 \pm 5	0.72 \pm 0.05
6	*	*	*	*	*
7	33.8	84	61 \pm 2	35 \pm 7	0.97 \pm 0.02
8	14.4	106	65 \pm 1	41 \pm 2	0.53 \pm 0.03
9	22.4	87	56 \pm 3	36 \pm 3	0.54 \pm 0.06
10	27.6	87	57 \pm 2	35 \pm 2	0.82 \pm 0.11
11	**	**	**	**	**
12	24.7	90	58 \pm 6	36 \pm 5	0.44 \pm 0.12
13	27.3	98	63 \pm 5	42 \pm 4	0.55 \pm 0.11
14	9.3	110	63 \pm 5	42 \pm 5	0.62 \pm 0.06
15	24.9	110	64 \pm 4	41 \pm 2	0.79 \pm 0.09

Table 5-4: Continued.

Run	Yield, %	Outlet Temperature, °C	FPF < 4.46 µm, %	FPF < 2.82 µm, %	FPD, mg
16	12.8	102	64 ± 7	44 ± 6	0.50 ± 0.08
17	21.1	99	64 ± 1	42 ± 1	0.57 ± 0.12
18	18.5	99	70 ± 1	45 ± 1	0.82 ± 0.06
19	31.4	100	66 ± 1	44 ± 1	0.70 ± 0.08
20	26.2	87	64 ± 2	42 ± 2	0.59 ± 0.04
21	11.9	99	65 ± 1	43 ± 2	0.74 ± 0.16
22	22.4	98	63 ± 2	42 ± 3	0.94 ± 0.10
23	18.4	97	62 ± 1	40 ± 2	0.59 ± 0.25
24	6.0	87	66 ± 2	43 ± 3	0.50 ± 0.39
25	43.1	110	67 ± 1	44 ± 2	0.29 ± 0.06
26	19.8	110	68 ± 1	44 ± 2	0.34 ± 0.06
27	25.9	121	67 ± 1	44 ± 3	0.42 ± 0.09
28	27.2	97	68 ± 1	45 ± 1	0.73 ± 0.04
29	29.5	96	65 ± 2	44 ± 2	0.70 ± 0.05
30	25.2	120	66 ± 2	44 ± 2	0.64 ± 0.20
31	6.2	124	67	46	0.72
32	40.8	107	65±2	43 ± 2	0.64 ± 0.12

*Water was collected in product vessel

** Mostly agglomerated, larger particles

Table 5-5: Dry powder aerosol central composite design of experiment responses (mean \pm standard deviation) of mass median aerodynamic diameter (MMAD), bimodal responses (MMAD1, GSD1, MMAD2, and GSD2) by run with n=3, except Run 31 was n=1 due to low yield.

Run	MMAD, μm (Copley)	MMAD1, μm	GSD1	MMAD2, μm	GSD2
1	3.9 \pm 1.1	1.4 \pm 0.8	9.2 \pm 7.5	5.1 \pm 0.6	1.8 \pm 0.6
2	3.4 \pm 0.5	1.4 \pm 0.8	7.9 \pm 5.6	4.4 \pm 0.7	1.6 \pm 0.7
3	3.3 \pm 0.3	1.8 \pm 0.0	14.0 \pm 5.3	4.8 \pm 0.6	1.7 \pm 0.6
4	3.4 \pm 0.4	0.4 \pm 0.0	1.7 \pm 0.1	4.7 \pm 0.7	1.9 \pm 0.7
5	3.7 \pm 0.5	0.9 \pm 0.8	3.9 \pm 3.9	5.1 \pm 0.7	2.0 \pm 0.7
6	*	*	*	*	*
7	3.6 \pm 0.3	0.5 \pm 0.0	1.5 \pm 0.0	4.3 \pm 0.2	1.8 \pm 0.2
8	3.3 \pm 0.1	0.5 \pm 0.0	1.6 \pm 0.0	4.3 \pm 0.1	1.8 \pm 0.1
9	3.9 \pm 0.3	0.5 \pm 0.0	1.6 \pm 0.0	5.1 \pm 0.2	2.0 \pm 0.2
10	3.8 \pm 0.2	0.4 \pm 0.1	1.7 \pm 0.2	4.9 \pm 0.1	1.9 \pm 0.1
11	**	**	**	**	**
12	3.8 \pm 0.5	0.5 \pm 0.0	1.5 \pm 0.1	4.9 \pm 0.4	2.0 \pm 0.4
13	3.4 \pm 0.3	0.9 \pm 0.8	3.4 \pm 3.2	4.5 \pm 0.4	1.8 \pm 0.4
14	3.4 \pm 0.4	1.4 \pm 0.8	5.6 \pm 3.5	4.7 \pm 0.6	1.8 \pm 0.6
15	3.4 \pm 0.2	0.9 \pm 0.8	3.6 \pm 3.5	4.3 \pm 0.4	1.8 \pm 0.4
16	3.3 \pm 0.5	1.4 \pm 0.8	6.2 \pm 4.0	4.5 \pm 0.9	1.7 \pm 0.9
17	3.4 \pm 0.1	1.8 \pm 0.0	8.4 \pm 0.8	4.6 \pm 0.3	1.6 \pm 0.3
18	3.1 \pm 0.0	0.9 \pm 0.8	2.9 \pm 2.3	3.9 \pm 0.1	0.7 \pm 0.1
19	3.2 \pm 0.0	0.9 \pm 0.8	3.3 \pm 2.9	4.3 \pm 0.2	1.9 \pm 0.2
20	3.3 \pm 0.1	1.4 \pm 0.8	5.9 \pm 4.0	4.6 \pm 0.2	1.8 \pm 0.2
21	3.0 \pm 0.1	0.9 \pm 0.8	4.0 \pm 4.1	4.4 \pm 0.2	1.7 \pm 0.3
22	3.4 \pm 0.2	0.9 \pm 0.8	3.7 \pm 3.7	4.6 \pm 0.2	1.9 \pm 0.2
23	3.5 \pm 0.1	1.4 \pm 0.8	6.3 \pm 4.1	4.9 \pm 0.3	1.8 \pm 0.3
24	3.1 \pm 0.1	1.2 \pm 0.8	5.1 \pm 4.4	4.3 \pm 0.2	1.6 \pm 0.2
25	3.2 \pm 0.1	1.4 \pm 0.8	6.2 \pm 4.0	4.3 \pm 0.2	1.5 \pm 0.2
26	3.1 \pm 0.1	0.9 \pm 0.8	3.4 \pm 3.2	4.2 \pm 0.1	1.7 \pm 0.1

Table 5-5: Continued.

Run	MMAD, μm (Copley)	MMAD1, μm	GSD1	MMAD2, μm	GSD2
27	3.2 ± 0.2	1.4 ± 0.8	4.8 ± 2.7	4.3 ± 0.1	1.5 ± 0.1
28	3.1 ± 0.1	0.9 ± 0.8	3.5 ± 3.2	4.1 ± 0.1	1.7 ± 0.1
29	3.2 ± 0.1	1.4 ± 0.8	6.0 ± 3.8	4.4 ± 0.3	1.7 ± 0.3
30	3.2 ± 0.1	1.8 ± 0.0	8.3 ± 0.7	4.2 ± 0.3	1.5 ± 0.3
31	3.1	1.8	1.8	2.8	2.8
32	3.3 ± 0.1	1.2 ± 1.0	6.5 ± 7.0	4.3 ± 0.3	1.7 ± 0.3

*Water was collected in product vessel

** Mostly agglomerated, larger particles

Table 5-6: Optimal factor settings for future aerosol development by maximizing the yield, FPFs, and FPD, minimizing GSD1 and GSD2, and setting a target of MMAD1 and MMAD2 being between 1 and 8 μm .

Factor	Value
pH	3
Solution Concentration, Wt %	0.556
Inlet Temperature, $^{\circ}\text{C}$	155
Atomizer, L/hr	447
Solution Flow Rate, mL/min	5

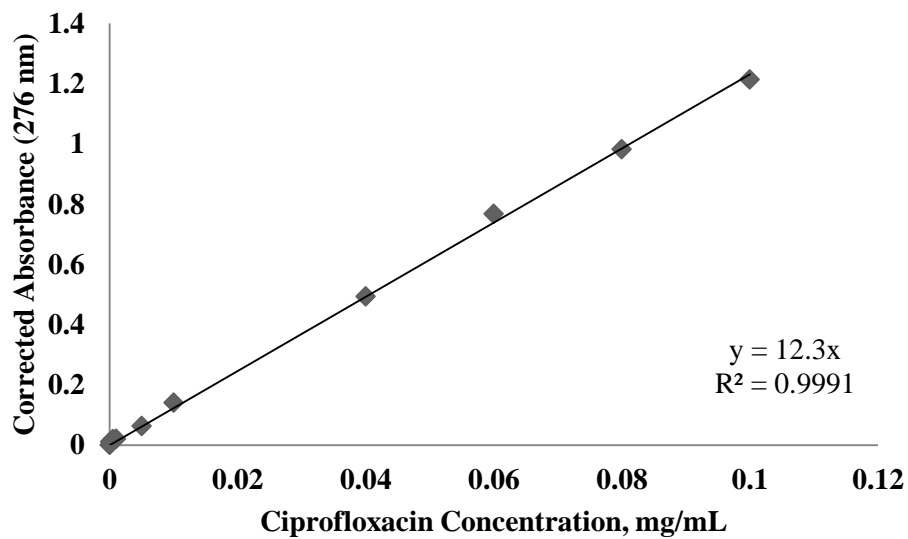


Figure 5-1: Calibration curve of ciprofloxacin concentration versus corrected absorbance readings at 276 nm; the concentration has a linear relationship with absorbance, corrected absorbance is the difference between the absorbance of ciprofloxacin in water minus the absorbance of water alone.

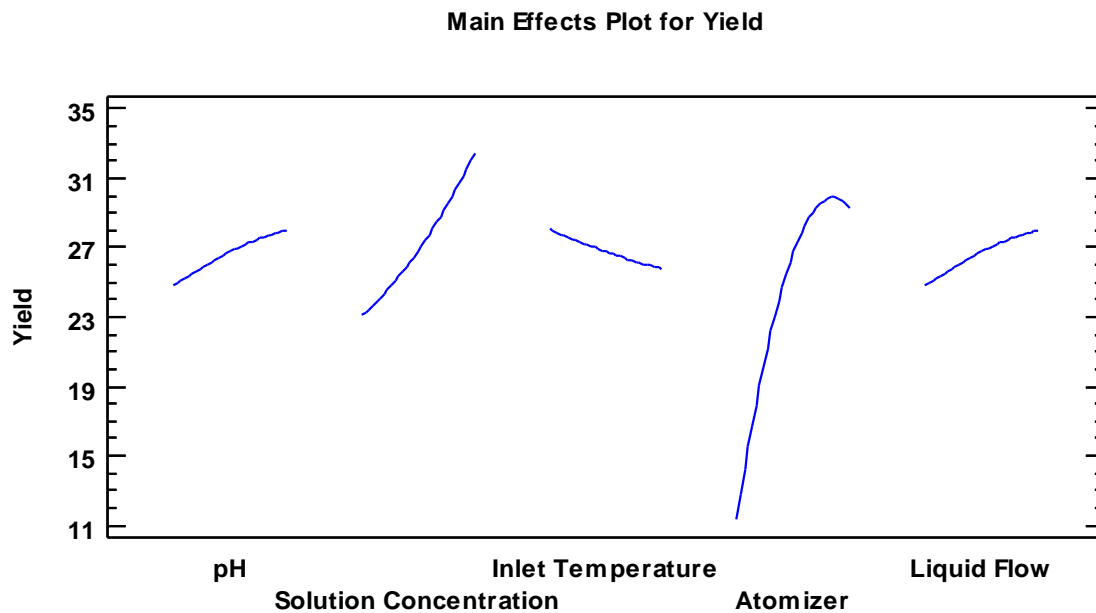


Figure 5-2: The main effects plot of the effect the five factors have on the response variable yield (%); a main effects plot depicts the mean response at each of the five factor levels; pH ranged from 3 to 11, solution concentration ranged from 0.025 wt% to 0.725 wt %, inlet temperature ranged from 155°C to 195°C, atomizer rate ranged from 150 L/hr to 750 L/hr, and liquid flow ranged from 5 mL/min to 13 mL/min.

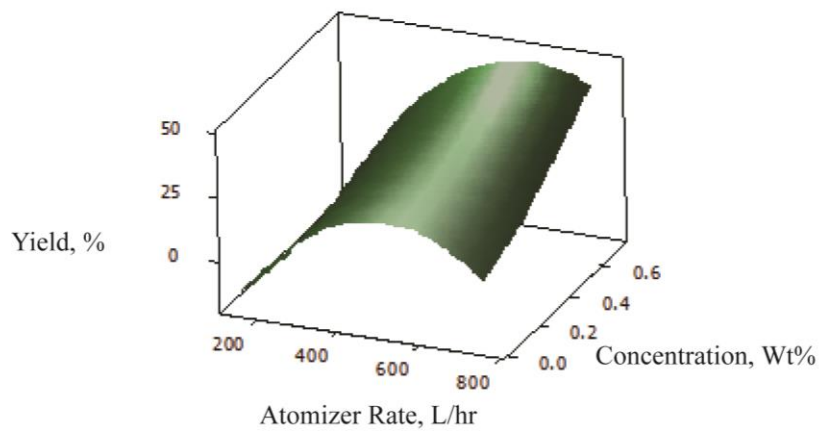


Figure 5-3: Surface plot of atomizer and solution concentration versus percent yield.

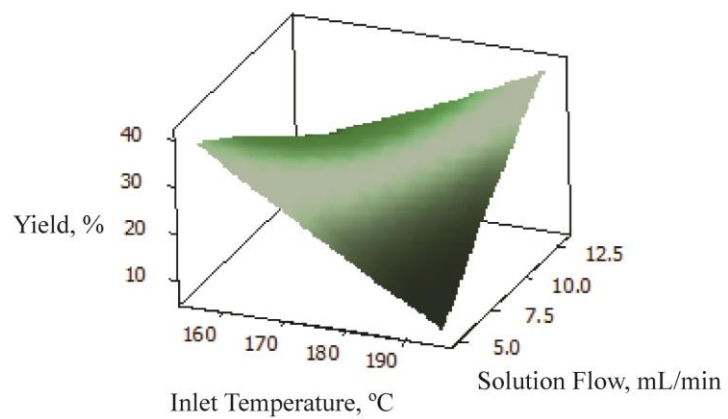


Figure 5-4: Surface plot of inlet temperature and liquid flow versus percent yield; the interaction of inlet temperature with liquid flow significantly affected the percent yield.

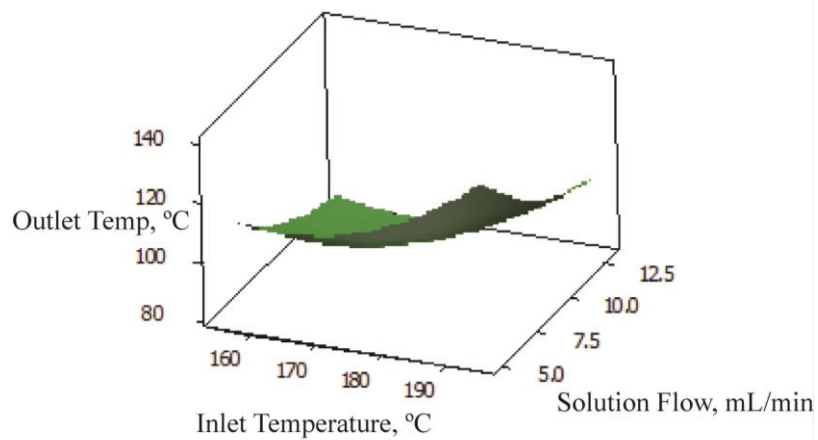


Figure 5-5: Surface plot of inlet temperature and solution liquid flow versus outlet temperature.

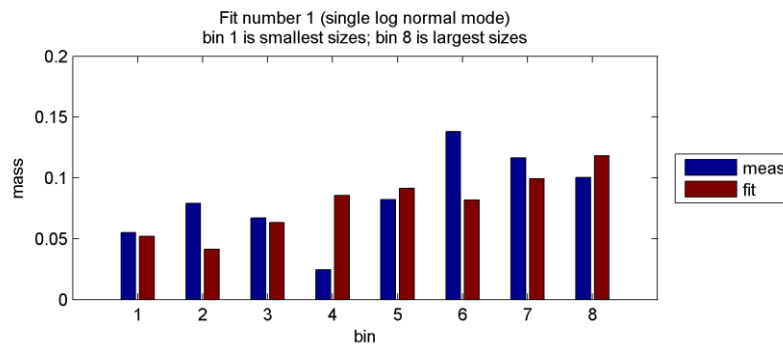


Figure 5-6: Aerosol size distribution by bin versus powder mass (blue = experimentally measured, red = single log normal fit); the powder experimentally measured per bin (blue) was not well fit by a single log normal mode (red); the size distribution of the aerosol impaction studies were run through Dr. Stanier's program (Dr. Charles Stanier, University of Iowa, Department of Chemical and Biochemical Engineering);¹⁷⁴ Sample 2 was passed through the Next Generation Impactor and mass of ciprofloxacin hydrochloride per stage was assessed with absorbance spectroscopy at 276 nm; bins 1 through 8 represent stages 8 through 1 on the impactor respectively to have increasing particle size with increasing bin number.

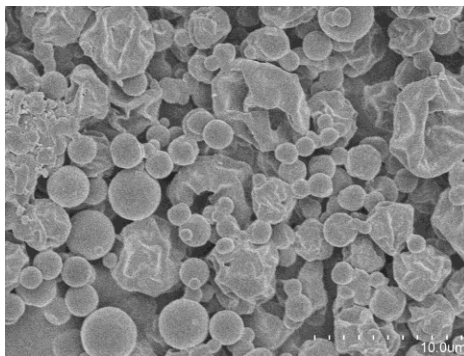


Figure 5-7: Scanning electron microscopy image of Run 24; two populations of particles were found: small, spherical particles and large, collapsed particles, scale 10 μm .

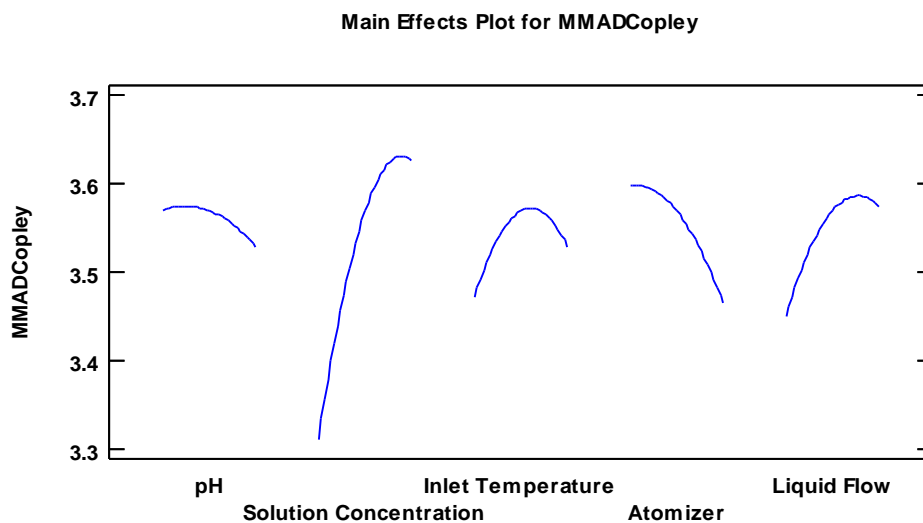


Figure 5-8: The main effects plot of the effect the five factors have on the response variable MMAD from the Copley Citdas software (Copley, Scientific, Nottingham, UK); a main effects plot depicts the mean response at each of the five factor levels, pH ranged from 3 to 11, solution concentration ranged from 0.025 wt% to 0.725 wt %, inlet temperature ranged from 155°C to 195°C, atomizer rate ranged from 150 L/hr to 750 L/hr, and liquid flow ranged from 5 mL/min to 13 mL/min.

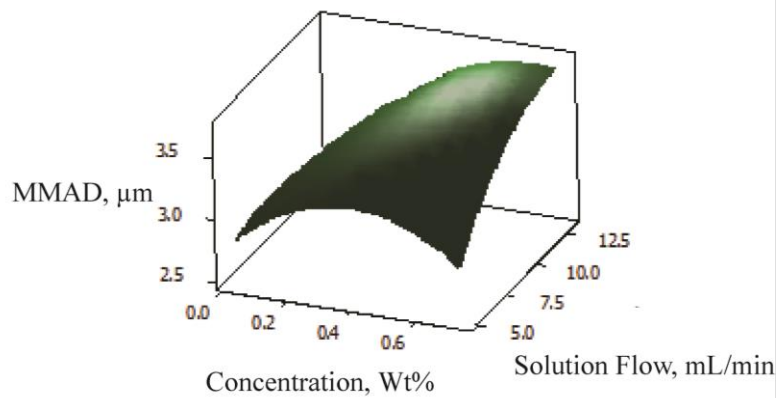


Figure 5-9: Surface plot of solution concentration and solution liquid flow versus MMAD from the Copley Citdas software.

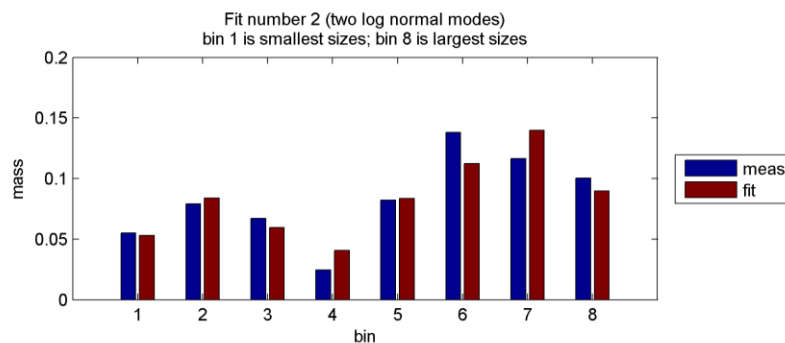


Figure 5-10: Aerosol size distribution by bin versus powder mass (blue = experimentally measured, red = two log normal fit); the aerosols showed a bimodal distribution for aerosol impaction studies and thus were run through Dr. Stanier's program (Dr. Charles Stanier, University of Iowa, Department of Chemical and Biochemical Engineering) for fitting bimodal distributions;¹⁷⁴ Sample 2 was passed through the Next Generation Impactor and mass of ciprofloxacin hydrochloride per stage was assessed with absorbance spectroscopy at 276 nm; bins 1 through 8 represent stages 8 through 1 on the Impactor respectively to have increasing particle size with increasing bin number.

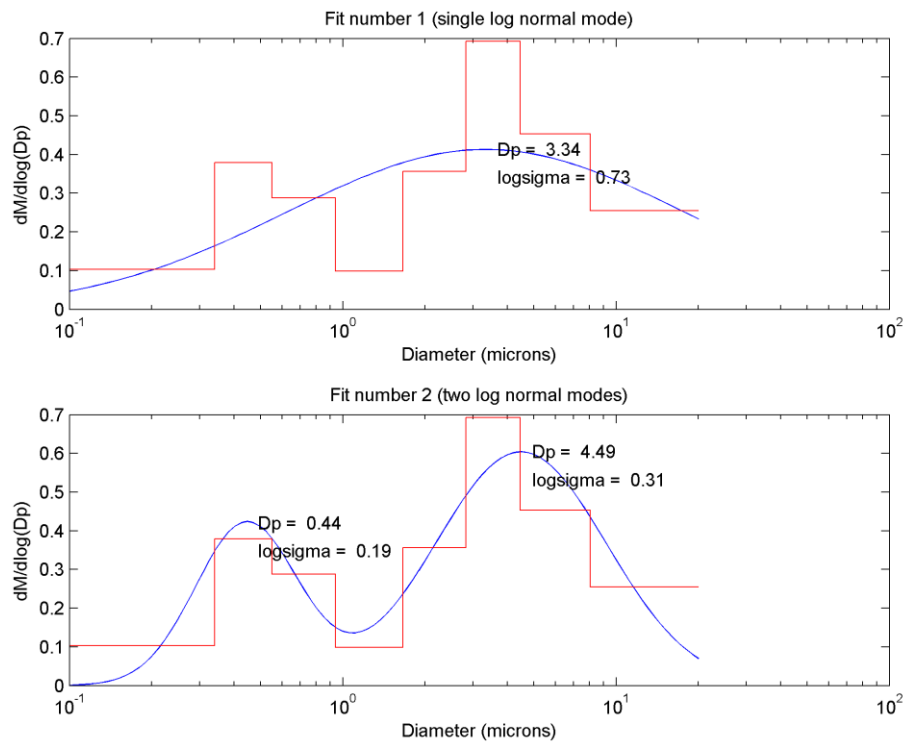


Figure 5-11: Frequency particle size distribution curve; top: single log normal mode fit to the size distribution; bottom: two log normal modes fit to the size distribution; the single mode fit of MMAD (D_p) 3.34 matches the Next Generation Impactor software Copley Citdas for MMAD; however, this software cannot calculate bimodal distributions; the two log normal fit provided MMAD (D_p) and GSD ($10^{\log\sigma}$) values for each mode.¹⁷⁴

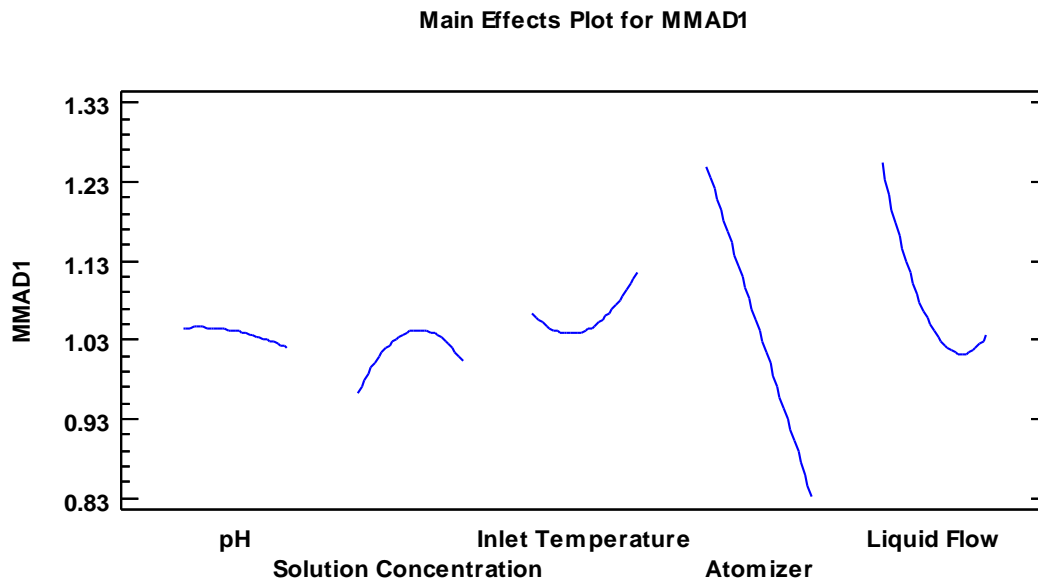


Figure 5-12: The main effects plot of the effect the five factors have on the response variable MMAD1; a main effects plot depicts the mean response at each of the five factor levels, pH ranged from 3 to 11, solution concentration ranged from 0.025 wt% to 0.725 wt %, inlet temperature ranged from 155°C to 195°C, atomizer rate ranged from 150 L/hr to 750 L/hr, and liquid flow ranged from 5 mL/min to 13 mL/min.

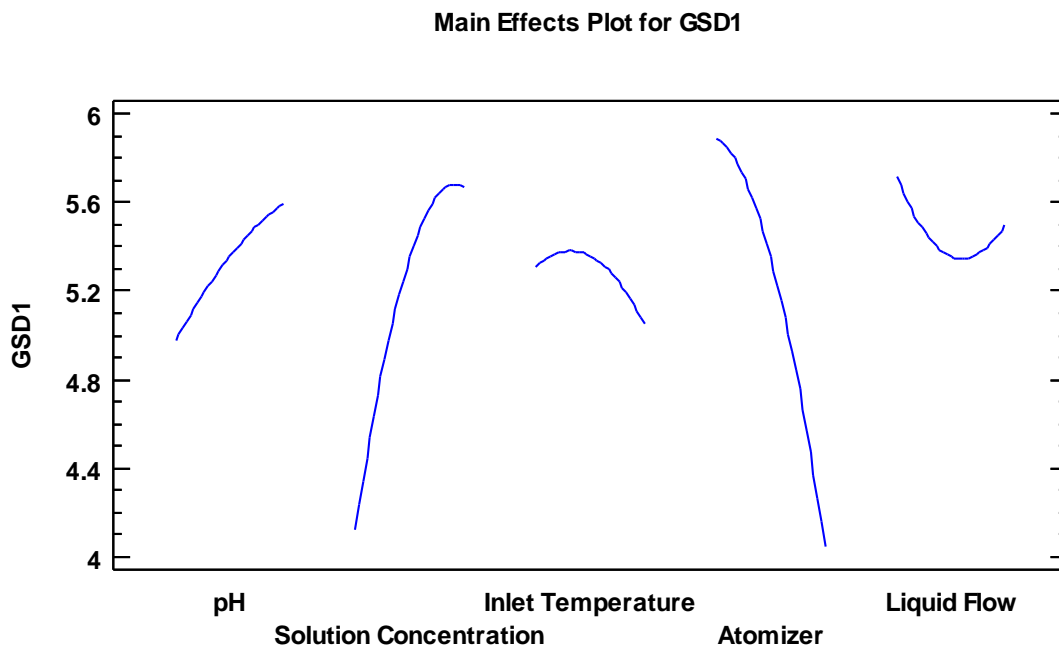


Figure 5-13: The main effects plot of the effect the five factors have on the response variable GSD1; a main effects plot depicts the mean response at each of the five factor levels, pH ranged from 3 to 11, solution concentration ranged from 0.025 wt% to 0.725 wt %, inlet temperature ranged from 155°C to 195°C, atomizer rate ranged from 150 L/hr to 750 L/hr, and liquid flow ranged from 5 mL/min to 13 mL/min.

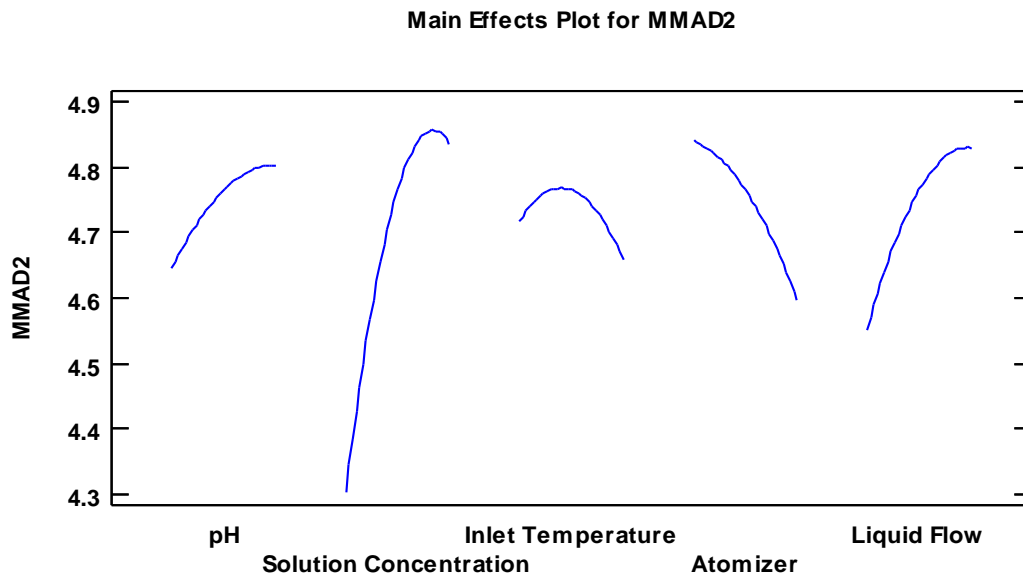


Figure 5-14: The main effects plot of the effect the five factors have on the response variable MMAD2; a main effects plot depicts the mean response at each of the five factor levels, pH ranged from 3 to 11, solution concentration ranged from 0.025 wt% to 0.725 wt %, inlet temperature ranged from 155°C to 195°C, atomizer rate ranged from 150 L/hr to 750 L/hr, and liquid flow ranged from 5 mL/min to 13 mL/min.

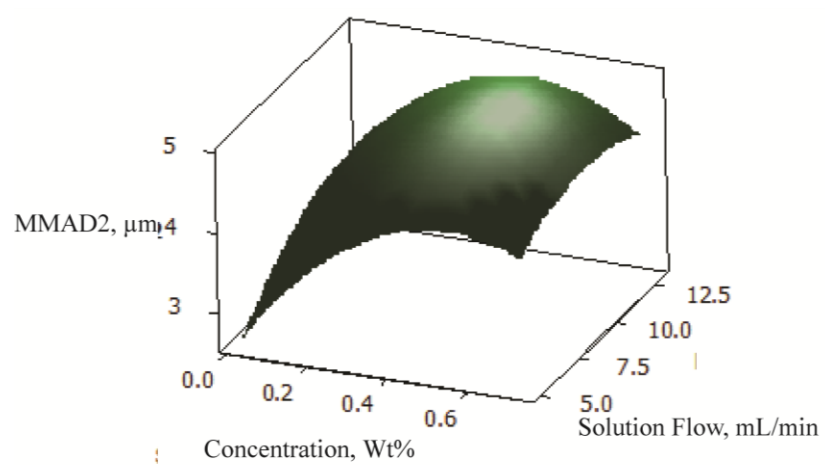


Figure 5-15: Surface plot of the significant parameters solution concentration and solution liquid flow versus MMAD2.

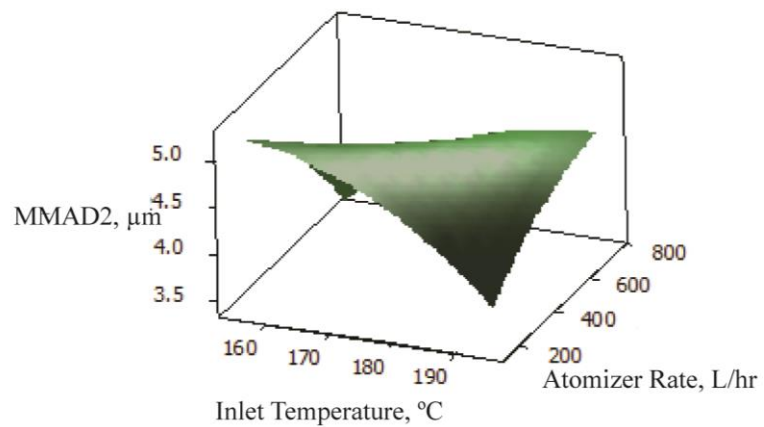


Figure 5-16: Surface plot of inlet temperature and atomizer rate versus MMAD2; the interaction of inlet temperature and atomizer significantly affected MMAD2.

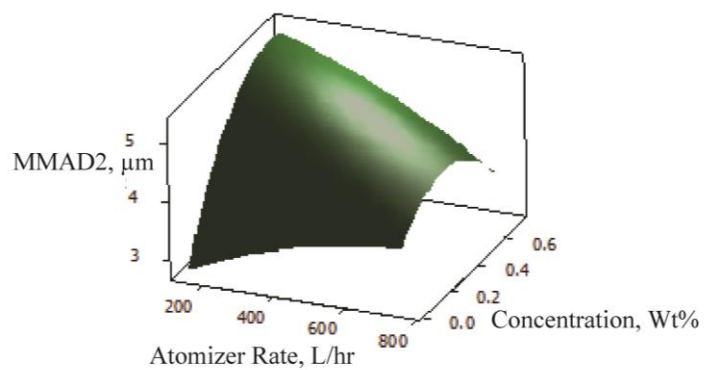


Figure 5-17: Surface plot of atomizer rate and solution concentration versus MMAD₂; the interaction of solution concentration and atomizer rate significantly affected MMAD₂.

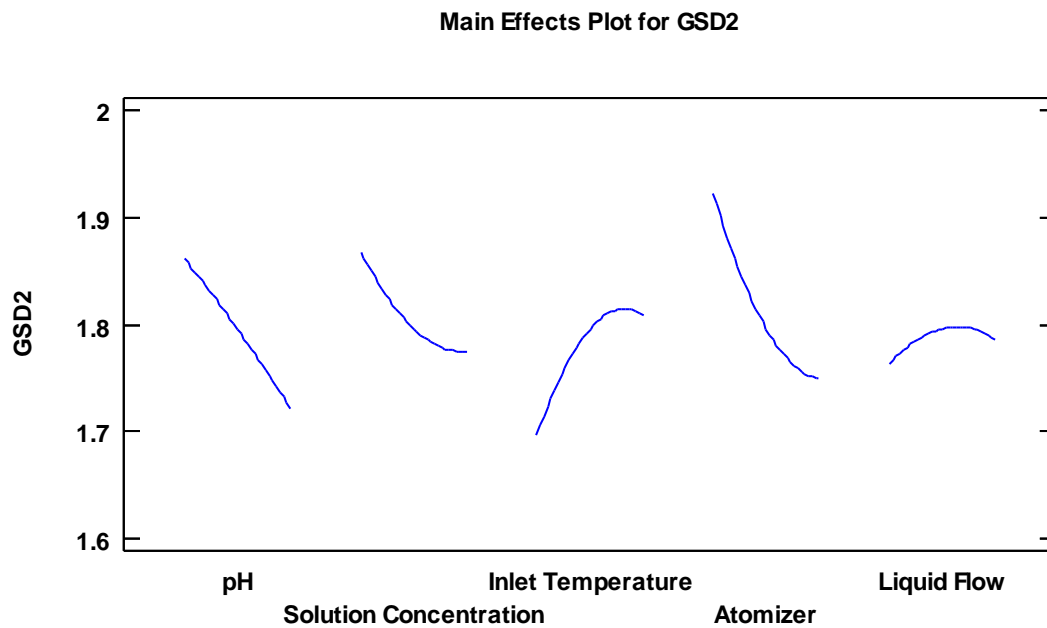


Figure 5-18: The main effects plot of the effect the five factors have on the response variable GSD2; a main effects plot depicts the mean response at each of the five factor levels, pH ranged from 3 to 11, solution concentration ranged from 0.025 wt% to 0.725 wt %, inlet temperature ranged from 155°C to 195°C, atomizer rate ranged from 150 L/hr to 750 L/hr, and liquid flow ranged from 5 mL/min to 13 mL/min.

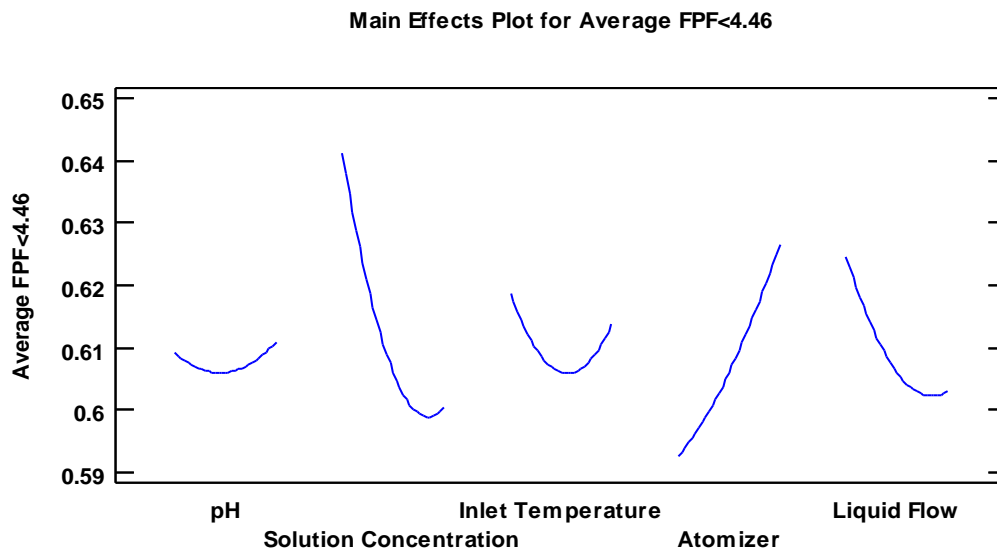


Figure 5-19: The main effects plot of the effect the five factors have on the response variable FPF < 4.46 μm ; a main effects plot depicts the mean response at each of the five factor levels, pH ranged from 3 to 11, solution concentration ranged from 0.025 wt% to 0.725 wt %, inlet temperature ranged from 155°C to 195°C, atomizer rate ranged from 150 L/hr to 750 L/hr, and liquid flow ranged from 5 mL/min to 13 mL/min.

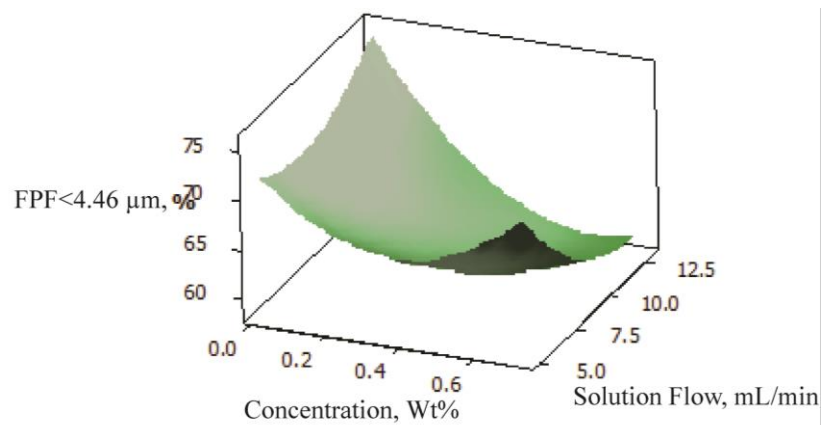


Figure 5-20: Surface plot of solution concentration and the parameter solution liquid flow versus FPF<4.46 μm.

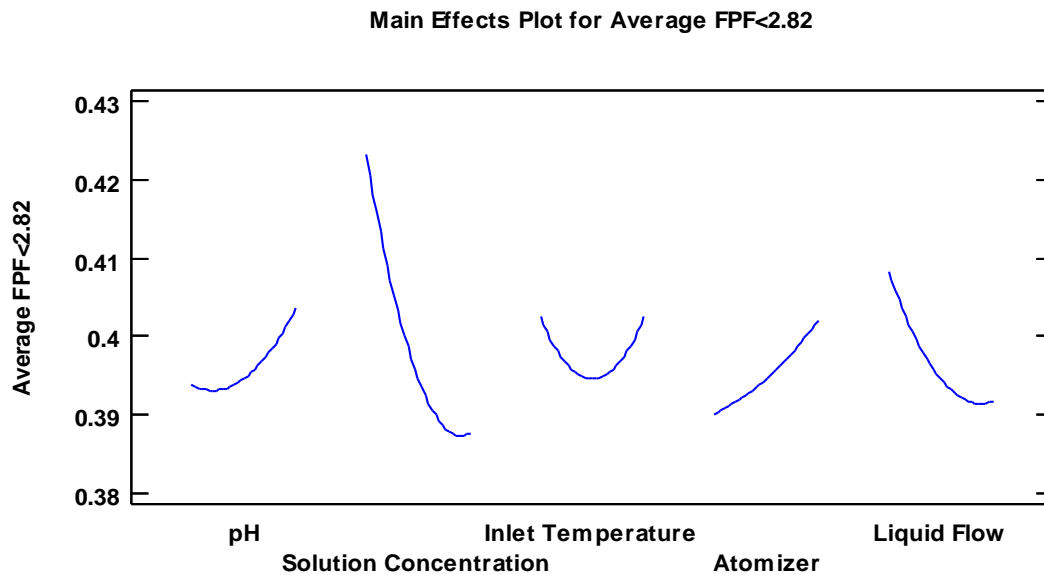


Figure 5-21: The main effects plot of the effect the five factors have on the response variable FPF < 2.82 μm ; a main effects plot depicts the mean response at each of the five factor levels, pH ranged from 3 to 11, solution concentration ranged from 0.025 wt% to 0.725 wt %, inlet temperature ranged from 155°C to 195°C, atomizer rate ranged from 150 L/hr to 750 L/hr, and solution flow rate ranged from 5 mL/min to 13 mL/min.

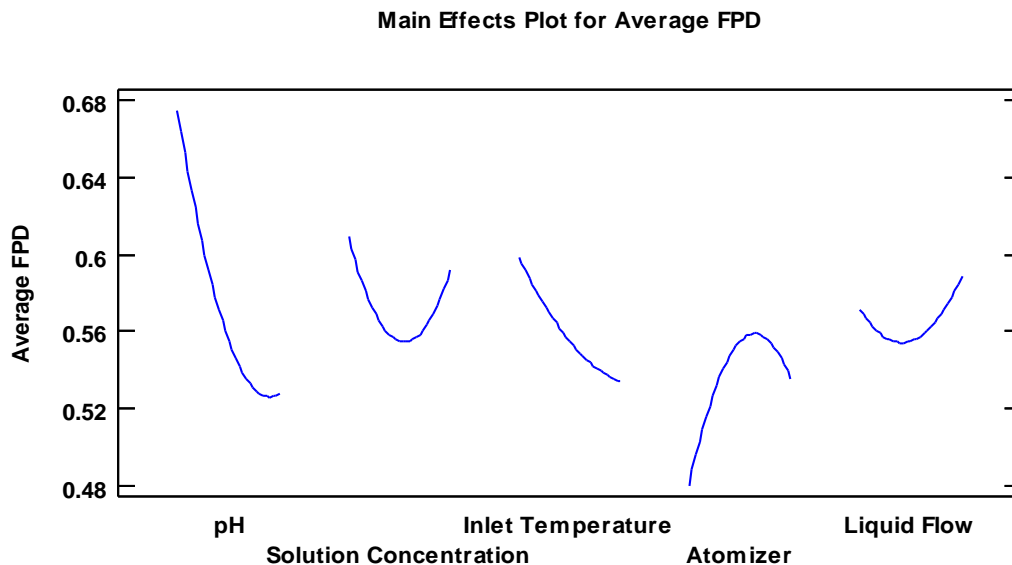


Figure 5-22: The main effects plot of the effect the five factors have on the response variable fine particle fraction (FPD); a main effects plot depicts the mean response at each of the five factor levels, pH ranged from 3 to 11, solution concentration ranged from 0.025 wt% to 0.725 wt %, inlet temperature ranged from 155°C to 195°C, atomizer rate ranged from 150 L/hr to 750 L/hr, and liquid flow ranged from 5 mL/min to 13 mL/min.

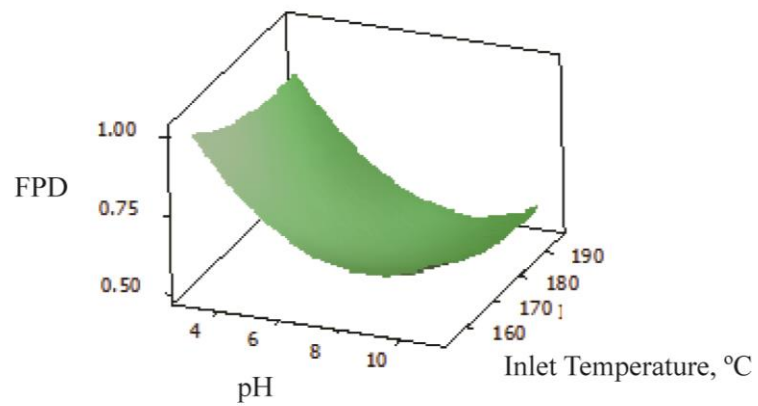


Figure 5-23: Surface plot of pH and the parameter inlet temperature versus FPD.

CHAPTER 6

CONCLUSIONS AND FUTURE PERSPECTIVES

6.1 Conclusions

This research demonstrated that combination treatments of nutrient dispersion compounds and antibiotics can synergistically reduce *Pseudomonas aeruginosa* biofilms. Young, 1-day-old biofilms, in a high-throughput assay, were more susceptible to co-treatments than more mature 4-day-old biofilms based on a confocal microscopy analysis. A computer software program, STAINIFICATION, was developed to make quantification of confocal images of biofilms more time efficient and to introduce novel analysis options. This allows for separate evaluation of bacteria within the biofilm and dispersed bacteria for susceptibility to antibiotics. It also enables for the first time quantification of biofilms grown on an uneven surface, such as tissue. A proof-of-concept study demonstrated polydispersed dry powder aerosols of antibiotic and nutrient dispersion compound could be developed with properties adequate for deposition in the lungs.

In Chapter 2, dispersion compounds were shown to enhance biofilm killing with aminoglycosides, amikacin disulfate and tobramycin sulfate, and cyclic polypeptides, polymyxin B sulfate and colistin methanesulfonate. Co-treatment of 100 µg/mL colistin methanesulfonate with 10 mM sodium citrate or 75 mM significantly reduced the live biofilm bacteria present beyond the antibiotic control, indicating both enhanced antibiotic action and a preference for bacteria to disperse and remain out of the biofilm after 24 hours of treatment. In addition, we observed that xylitol acts as a dispersion compound. It was found that xylitol, sodium citrate, and succinic acid caused bacterial dispersion after 12 hours of treatment in the minimum biofilm eradication concentration assay.

In Chapter 3, the most promising combination treatments against mature biofilms included amikacin disulfate, colistin methanesulfonate, and erythromycin with sodium

citrate. Succinic acid and xylitol had been effective dispersion compounds to be used with antibiotics against young biofilms in chapter 2, but were not effective at the same concentrations against mature biofilms. Thus biofilm age plays an important role on dispersion compounds and antibiotics synergistically killing *P. aeruginosa* biofilms. The concentrations may need to be increased to be effective against more mature biofilms. Glutamic acid was tested at a lower concentration and may require a higher concentration to be effective with antibiotics against the mature biofilms as well.

In Chapter 4, STAINIFICATION is available for researchers to more time efficiently analyze connected-bacteria, unconnected bacteria, matrix, and surface components in confocal microscopy images. STAINIFICATION has a user friendly interface to make image analysis straight forward. STAINIFICATION has novel thresholding and quantification abilities. A local Otsu threshold is a new option in biofilm-specific quantification programs. A colocalization adjustment option is available to prevent double counting of colocalized pixels when assessing bacteria viability with membrane integrity nucleic acid stains. The utility of the thresholding options and the viability assessments were demonstrated with confocal images of *Pseudomonas aeruginosa* biofilms. The modified connected volume filtration algorithm allows connected-biofilm bacteria to be quantified on an uneven surface. Furthermore, the parameters of modified substratum coverage and percent or volume bacteria associated with surface have been introduced. The utility of the uneven surface algorithms were demonstrated with confocal images of *Staphylococcus aureus* biofilms grown on cultured human airway epithelial cells and *Neisseria gonorrhoeae* biofilms grown on transformed cervical epithelial cells.

In Chapter 5, polydispersed dry powder aerosols were developed with mass median aerodynamic diameters in the range of 1 μm to 8 μm and with high fine particle fractions and fine particle dose values for adequate deposition. This work demonstrated that dry powder aerosols with good flowability and deposition properties could be

developed with 10% leucine and 90% drug formulations of antibiotic and dispersion compound. The significant parameters from this study were solution concentration, atomizer rate, solution flow rate, pH, interaction of inlet temperature and solution flow rate, interaction of inlet temperature and atomizer rate, and interaction of solution concentration and atomizer rate. These parameters should be considered in further aerosol development. Solution concentration was the most important parameter, significantly affecting yield, mass median aerodynamic diameter 2, and the fine particle fraction for particles less than 4.46 μm . For future formulations, it may be advantageous to investigate the pH parameter below pH 3 to examine below the lowest pKa of formulation compounds and to investigate a wider range of solution concentration since this was the most important parameter.

6.2 Future Perspectives

To better elucidate the mechanisms of action for xylitol, it is recommended to use a polymerase chain reaction. Bacterial RNA can be extracted and purified by using the RNeasy Protect Bacteria Mini Kit with on-column DNase I digestion (Qiagen, Valencia, CA). Specific genes to investigate will need to be chosen. It is recommended to focus on genes responsible for expression of pili (attachment appendages) and flagella (motility appendage).

Xylitol treatment was synergistic at reducing biofilm growth with four antibiotics against young *Pseudomonas aeruginosa* biofilms; however it was not synergistic at the same concentration for reducing mature biofilm viability. Therefore, it should be investigated further in the mature biofilm model at higher concentrations.

The biofilm matrix should be investigated in the future to prove that during dispersion the matrix is weakened, which could be shown as a decrease in quantity of matrix component and an increase in enzymatic activity. The amount of matrix material

can be quantified via confocal microscopy or by isolating and taking dry weights of the matrix components.³⁴⁻³⁵ Atomic force microscopy can also be used to investigate the surface of the matrix.³⁴ The enzymatic activity of alginate lyase can be quantified via an assay.¹⁸¹

Combination treatments of antibiotics and dispersion compounds have been shown to be effective at reducing live mucoid laboratory strain *Pseudomonas aeruginosa*. The high-throughput screening MBEC assay should be used with clinically relevant *Pseudomonas aeruginosa* strains from The University of Iowa Hospitals and Clinics to verify that combination treatments are effective against infections that better reflect chronic infections.

Promising combination treatments should be evaluated in a murine model with the aid of the Cystic Fibrosis Research Center at The University of Iowa. A chronic *Pseudomonas aeruginosa* infection can be established in mice by infecting one side of the lungs with a clinical bacterial strain immobilized in agar beads.¹⁸² After nebulized treatments with antibiotics alone or in combination with dispersion compounds, histopathology and bacterial counts (log(CFU/mL)) should be investigated to evaluate a reduction in infection.

In our aerosol study, solution concentration was the most important parameter for developing aerosols with high yield and adequate deposition. Future dry powder aerosol work should investigate higher concentrations of solution concentration and should investigate the effect of pH spanning across the pK_as of compounds in the formulation. Proof-of-concept work has shown an aerosol containing an antibiotic and dispersion compound could be formulated with good aerodynamic properties. The next step will be to generate dry powder aerosols of promising compounds and to evaluate their effectiveness against biofilms *in vitro* and *in vivo*. Also it will be important to assess the deposition locations *in vivo* for the aerosols.

APPENDIX
SUPPLEMENTAL CODE

A.1 Colocalization Adjustment

```

for i=1:Lastimageslice;
    for Rowpixel=1:Numberpixelsinrow;
        for Colpixel=1:Numberpixelsincolumn;
            if
double (ChannelRedThresholdLogic (Rowpixel,Colpixel,i))==1 &&
double (ChannelGreenThresholdLogic (Rowpixel,Colpixel,i))==1 ||
double (ChannelRedThresholdLogic (Rowpixel,Colpixel,i))==1;
                AllRedPixels (Rowpixel, Colpixel,i)=1;
                AllGreenPixels (Rowpixel,Colpixel, i)=0;

            elseif
double (ChannelGreenThresholdLogic (Rowpixel,Colpixel,i))==1 &&
double (ChannelRedThresholdLogic (Rowpixel,Colpixel,i))==0;
                AllRedPixels (Rowpixel,Colpixel,i)=0;
                AllGreenPixels (Rowpixel,Colpixel, i)=1;

            elseif
double (ChannelRedThresholdLogic (Rowpixel,Colpixel,i))==0 ||
double (ChannelGreenThresholdLogic (Rowpixel,Colpixel,i))==0;
                AllRedPixels (Rowpixel,Colpixel,i)=0;
                AllGreenPixels (Rowpixel,Colpixel, i)=0;
            end;
        end;
    end;
end;

```

A.2 Connected Volume Filtration (CVF) on Multiple Channels

```

% Connected volume filtration code was provided open source by
Dr. Arne Heydorn in his
% software program COMSTAT. Permission was obtained on March 7,
2012, by Dr. Heydorn to
% use his CVF algorithm. Source code can be obtained by Dr.
Heydorn at www.imageanalysis.dk.
%
% License for CVF
% Redistribution and use in source and binary forms, with or
without
% modification, are permitted provided that the following
conditions are met:
%
% 1. If the program is modified, redistributions must include a
notice
% indicating that the redistributed program is not identical to
the software
% distributed by the Department of Microbiology, Technical
University of Denmark.
% Redistributions must also include a notice indicating that the
redistributed
% program includes software developed by the Department of
Microbiology,
% Technical University of Denmark.
%
% 2. All advertising materials mentioning features or use of this
software must
% display the following acknowledgment: This product includes
software developed
% by the Department of Microbiology, Technical University of
Denmark.
%
% We also request that use of this software be cited in
publications as
%
% Heydorn, A., Nielsen, A.T., Hentzer, M., Sternberg, C.,
Givskov, M., Ersbøll,
% B.K., Molin, S. (2000) Quantification of biofilm structures by
the novel computer
% program COMSTAT. Microbiology 146 (10) 2395-2407
%
% The software is provided "AS-IS" and without warranty of any
kind, express,
% implied or otherwise, including without limitation, any
warranty of merchantability
% or fitness for a particular purpose. In no event shall the
Technical University

```

```

    % of Denmark or the authors be liable for any special,
    incidental, indirect or
    % consequential damages of any kind, or any damages whatsoever
    resulting from loss
    % of use, data or profits, whether or not advised of the
    possibility of damage, and
    % on any theory of liability, arising out of or in connection
    with the use or
    % performance of this software. This code was written using
    MATLAB 3.1 (MathWorks,
    % www.mathworks.com) and may be subject to certain additional
    restrictions
    % as a result.

    %Connect all R and G bacteria pixels for connected volume
    filtration
    Connect=zeros(pixelRow, pixelCol, max(max(yy)));
    for i=1:yy;
    for Rowpixel=1:pixelRow;
        for Colpixel=1:pixelCol;
            if
double(ChannelRedThresholdLogic(Rowpixel,Colpixel,i)) &&
double(ChannelGreenThresholdLogic(Rowpixel,Colpixel,i)) == 1 ||
double(ChannelRedThresholdLogic(Rowpixel,Colpixel,i)) ==1 ||
double(ChannelGreenThresholdLogic(Rowpixel,Colpixel,i)) ==1,
                Connect(Rowpixel,Colpixel,i)=1;
            else
                Connect(Rowpixel,Colpixel,i)=0;
            end;
        end;
    end;
end;

%Connected Volume Filtration
filt_images=zeros(pixelRow, pixelCol, max(max(yy)));
filt_images(:, :, 1)=double(Connect(:, :, 1)>0);
areainthislayer(:, :, 1)=double(Connect(:, :, 1)>0);
    for i=2:yy;
        %pixel-by-pixel comparision between slices
        commonarea=uint8(areainthislayer(:, :, i-
1).*double((Connect(:, :, i)>0))); % what pixels are common between the
two layers
        [vectorx,vector y]=find(commonarea); % vectors containing the
nonzero elements of commonarea
        %8 neighborhood connection for above slice
        %allows for horizontal growth of biofilm
        areainthislayer(:, :, i)=double(bwselect(Connect(:, :, i),vector y,vec
torx,8));
        filt_images(:, :, i)=areainthislayer(:, :, i); % expand the area
inherited from the layer below
    end;

```

A.3 Maintaining Connected-Biofilm and Unconnected Bacteria Separately

```

for i=1:Lastimageslice;
    for Rowpixel=1:Numberpixelsinrow;
        for Colpixel=1:Numberpixelsincolumn;

            if AllRedPixels (Rowpixel,Colpixel,i) ==1 &&
filt_images (Rowpixel,Colpixel,i) ==1;
                ConnectedBiofilmRedPixel (Rowpixel,Colpixel,i)=1;
                UnconnectedBacteriaRedPixel (Rowpixel,Colpixel,i)=0;
            elseif AllRedPixels (Rowpixel,Colpixel,i) ==1 &&
filt_images (Rowpixel,Colpixel,i) ==0;
                ConnectedBiofilmRedPixel (Rowpixel,Colpixel,i)=0;
                UnconnectedBacteriaRedPixel (Rowpixel,Colpixel,i)=1;
            elseif AllRedPixels (Rowpixel,Colpixel,i) ==0 &&
filt_images (Rowpixel,Colpixel,i) ==1 ||
AllRedPixels (Rowpixel,Colpixel,i) ==0 &&
filt_images (Rowpixel,Colpixel,i) ==0;
                ConnectedBiofilmRedPixel (Rowpixel,Colpixel,i)=0;
                UnconnectedBacteriaRedPixel (Rowpixel,Colpixel,i)=0;
            end;

            if AllGreenPixels (Rowpixel,Colpixel,i)==1 &&
filt_images (Rowpixel,Colpixel,i) ==1;
                ConnectedBiofilmGreenPixel (Rowpixel,Colpixel,i)=1;
                UnconnectedBacteriaGreenPixel (Rowpixel,Colpixel,i)=0;
            elseif AllGreenPixels (Rowpixel,Colpixel,i)==1 &&
filt_images (Rowpixel,Colpixel,i) ==0;
                ConnectedBiofilmGreenPixel (Rowpixel,Colpixel,i)=0;
                UnconnectedBacteriaGreenPixel (Rowpixel,Colpixel,i)=1;
            elseif AllGreenPixels (Rowpixel,Colpixel,i)==0 &&
filt_images (Rowpixel,Colpixel,i) ==0 ||
AllGreenPixels (Rowpixel,Colpixel,i)==0 &&
filt_images (Rowpixel,Colpixel,i) ==1;
                ConnectedBiofilmGreenPixel (Rowpixel,Colpixel,i)=0;
                UnconnectedBacteriaGreenPixel (Rowpixel,Colpixel,i)=0;

            end;

        end;
    end;
end;

```

A.4 Viability Quantification Parameters

```

PercentOverallConnectedBiofilmRed=sum(sum(sum(ConnectedBiofilmRed
Pixel(:, :, :)))./(sum(sum(sum(ConnectedBiofilmRedPixel(:, :, :)))
+sum(sum(sum(ConnectedBiofilmGreenPixel(:, :, :)))))*100;
PercentOverallConnectedBiofilmGreen=sum(sum(sum(ConnectedBiofilmG
reenPixel(:, :, :)))./(sum(sum(sum(ConnectedBiofilmRedPixel(:, :, :)))
+sum(sum(sum(ConnectedBiofilmGreenPixel(:, :, :)))))*100;
PercentOverallUnconnectedBacteriaRed=sum(sum(sum(UnconnectedBacte
riaRedPixel(:, :, :)))./(sum(sum(sum(UnconnectedBacteriaRedPixel(:, :, :))
)+sum(sum(sum(UnconnectedBacteriaGreenPixel(:, :, :)))))*100;
PercentOverallUnconnectedBacteriaGreen=sum(sum(sum(UnconnectedBac
teriaGreenPixel(:, :, :)))./(sum(sum(sum(UnconnectedBacteriaRedPixel(:, :
, :)))
+sum(sum(sum(UnconnectedBacteriaGreenPixel(:, :, :)))))*100;

for i=1:Lastimageslice;
PercentRedConnectedBiofilmBySlice(i)=sum(sum(ConnectedBiofilmRedPixel(
:, :, i))./(sum(sum(ConnectedBiofilmRedPixel(:, :, i))+sum(sum(Connecte
dBiofilmGreenPixel(:, :, i)))))*100;
PercentGreenConnectedBiofilmBySlice(i)=sum(sum(ConnectedBiofilmGreenPix
el(:, :, i))./(sum(sum(ConnectedBiofilmRedPixel(:, :, i))+sum(sum(Connect
edBiofilmGreenPixel(:, :, i)))))*100;
PercentRedUnconnectedBacteriaBySlice(i)=sum(sum(UnconnectedBacteriaRedP
ixel(:, :, i))./(sum(sum(UnconnectedBacteriaRedPixel(:, :, i))+sum(sum(Un
connectedBacteriaGreenPixel(:, :, i)))))*100;
PercentGreenUnconnectedBacteriaBySlice(i)=sum(sum(UnconnectedBacteriaGr
eenPixel(:, :, i))./(sum(sum(UnconnectedBacteriaRedPixel(:, :, i))+sum(su
m(UnconnectedBacteriaGreenPixel(:, :, i)))))*100;
end;

```

A.5 Saving “.tif” Processed Images

```

    folder='Sample Name';
    parentfolderConnectedBiofilm=strcat(folder, '\ConnectedBiofilmBact
eria\');
    parentfolderUnconnectedBacteria=strcat(
folder, '\UnconnectedBacteria\');
    mkdir(parentfolderConnectedBiofilm);
    mkdir(parentfolderUnconnectedBacteria);

    for i=1:Lastimageslice;
FinalConnectedBiofilmBacteriaRed(:,:,i)=ConnectedBiofilmRedPixel(:,:,i)
.*double(OriginalBacteria(:,:,i));
        name = ['ConnectedBiofilmBacteriaRed',int2str(i),'.tif'];
        filename= strcat(parentfolderConnectedBiofilm, name);
imwrite(uint8(FinalConnectedBiofilmBacteriaRed(:,:,i)),filename,'tiff')
;
FinalConnectedBiofilmBacteriaGreen(:,:,i)=ConnectedBiofilmGreenPixel(:,
:,i).*double(OriginalBacteria(:,:,i));
        name = ['ConnectedBiofilmBacteriaGreen',int2str(i),'.tif'];
        filename= strcat(parentfolderConnectedBiofilm, name);
imwrite(uint8(FinalConnectedBiofilmBacteriaGreen(:,:,i)),filename,'tiff
');
FinalUnconnectedBacteriaRed(:,:,i)=UnconnectedBacteriaRedPixel(:,:,i).*
double(OriginalBacteria(:,:,i));
        name = ['UnconnectedBacteriaRed',int2str(i),'.tif'];
        filename= strcat(parentfolderUnconnectedBacteria, name);
imwrite(uint8(FinalUnconnectedBacteriaRed(:,:,i)),filename,'tiff');
FinalUnconnectedBacteriaGreen(:,:,i)=UnconnectedBacteriaGreenPixel(:,
i).*double(OriginalBacteria(:,:,i));
        name = ['UnconnectedBacteriaGreen',int2str(i),'.tif'];
        filename= strcat(parentfolderUnconnectedBacteria, name);
imwrite(uint8(FinalUnconnectedBacteriaGreen(:,:,i)),filename,'tiff');
    end;

```

A.6 Uneven Surface Scripts

```

%Test Image 1
%Images After Thresholding
Surface(:,:,1)=[0,0,0,1,1,1,1,1,1,1;
                0,0,0,0,1,1,1,1,1,1;
                0,0,0,0,1,1,1,1,1,1;
                0,0,0,0,0,1,1,1,1,1];

Surface(:,:,2)=[0,1,0,0,0,0,0,0,0,0;
                0,1,1,1,0,0,0,0,0,0;
                0,1,1,1,0,1,1,1,0,0;
                0,1,1,1,0,1,1,1,1,1];

Surface(:,:,3)=[0,0,0,0,0,0,0,0,0,0;
                0,0,0,0,0,0,0,0,0,0;
                0,1,0,0,0,0,0,0,0,0;
                0,1,0,0,0,0,0,0,0,0];

Surface(:,:,4)=[0,0,0,0,0,0,0,0,0,0;
                0,0,0,0,0,0,0,0,0,0;
                0,0,0,0,0,0,0,0,0,0;
                0,0,0,0,0,0,0,0,0,0];

Bacteria(:,:,1)=[0,0,0,0,0,0,0,0,0,0;
                 0,0,0,0,0,0,0,0,0,0;
                 0,0,0,0,0,0,0,0,0,0;
                 0,0,0,0,0,0,0,0,0,0];

Bacteria(:,:,2)=[0,0,0,1,0,0,0,1,0,0;
                 0,0,0,0,1,1,1,0,0,0;
                 0,0,0,0,1,0,0,0,1,1;
                 0,0,0,0,0,0,0,0,0,0];

Bacteria(:,:,3)=[0,0,0,1,1,0,0,0,0,0;
                 1,1,0,1,0,0,0,0,0,0;
                 0,0,0,0,1,1,1,1,1,0;
                 0,0,0,0,1,0,0,1,0,0];

Bacteria(:,:,4)=[0,0,0,1,1,0,0,0,0,0;
                 0,0,0,1,1,0,1,0,0,0;
                 0,0,0,1,1,0,1,1,0,0;
                 0,0,0,0,1,1,1,1,0,0];

pixelCol=10;
pixelRow=4;
totalpixel=pixelCol.*pixelRow;
%calibration to microns
micronx=0.5;
microny=0.5;
micronz=1;

```

```
%Number of image slices
yy=4;
lsm.yy=yy;

%Connected Volume Filtration (CVF) of the Bacteria and Surface
% Connected volume filtration code was provided open source by
Dr. Arne Heydorn in his
% software program COMSTAT. Permission was obtained on March 7,
2012, by Dr. Heydorn to
% use his CVF algorithm. Source code can be obtained by Dr.
Heydorn at www.imageanalysis.dk.88
%
% License for CVF
% Redistribution and use in source and binary forms, with or
without
% modification, are permitted provided that the following
conditions are met:
%
% 1. If the program is modified, redistributions must include a
notice
% indicating that the redistributed program is not identical to
the software
% distributed by the Department of Microbiology, Technical
University of Denmark.
% Redistributions must also include a notice indicating that the
redistributed
% program includes software developed by the Department of
Microbiology,
% Technical University of Denmark.
%
% 2. All advertising materials mentioning features or use of this
software must
% display the following acknowledgment: This product includes
software developed
% by the Department of Microbiology, Technical University of
Denmark.
%
% We also request that use of this software be cited in
publications as
%
% Heydorn, A., Nielsen, A.T., Hentzer, M., Sternberg, C.,
Givskov, M., Ersbøll,
% B.K., Molin, S. (2000) Quantification of biofilm structures by
the novel computer
% program COMSTAT. Microbiology 146 (10) 2395-2407
%
% The software is provided "AS-IS" and without warranty of any
kind, express,
% implied or otherwise, including without limitation, any
warranty of merchantability
% or fitness for a particular purpose. In no event shall the
Technical University
% of Denmark or the authors be liable for any special,
incidental, indirect or
```



```

    % consequential damages of any kind, or any damages whatsoever
    resulting from loss
    % of use, data or profits, whether or not advised of the
    possibility of damage, and
    % on any theory of liability, arising out of or in connection
    with the use or
    % performance of this software. This code was written using
    MATLAB 3.1 (MathWorks,
    % www.mathworks.com) and may be subject to certain additional
    restrictions
    % as a result.

%Modification of the CVF code

%April 2012: Stacy Sommerfeld Ross modified the CVF from Dr.
Heydorn to fit her application
%and variables (see below). This modified CVF (MCVF) is used to
complete connected
%volume filtration on bacteria grown on uneven surfaces, in this
case Surface.
%This code is provided "as is" without warranty.

%Connected Volume Filtration for Bacteria and Surface
BiofilmConnectedtoSurface=zeros(pixelRow, pixelCol, yy);

%Classifying Starting Point for Connected Volume Filtration
BiofilmConnectedtoSurface(:,:,1)=Bacteria(:,:,1); %This allows
for any biofilm growing directly on the substratum
HorizontalGrowthForBacteriaAttachedtoBStart(:,:,1)=Bacteria(:,:,1
);

    for i = 2:yy;
        commonarea(:,:,i-1)=uint8(Surface(:,:,i-
1).*double((Bacteria(:,:,i)>0))); % what pixels are common between the
two layers
        [vectorx, vectory]=find(commonarea(:,:,i-1)); % vectors
containing the nonzero elements of commonarea
        BiofilmConnectedtoSurface(:,:,i)=commonarea(:,:,i-1); % expand
the area enherited from the layer below

HorizontalGrowthForBacteriaAttachedtoBStart(:,:,i)=double(bwselect(Bact
eria(:,:,i), vectory, vectorx, 8));
        clear vectorx
        clear vectory
    end;

BiofilmConnectedtoSurfaceforSubstratum=BiofilmConnectedtoSurface;
for i=1:yy
    for Rowpixel=1:pixelRow;
        for Colpixel=1:pixelCol;

```

```

        if
double (BiofilmConnectedtoSurface (Rowpixel, Colpixel, i)) ==1  &&
double (Surface (Rowpixel, Colpixel, i)) ==1

BiofilmConnectedtoSurfaceforSubstratum (Rowpixel, Colpixel, i) =0;
        elseif
double (BiofilmConnectedtoSurface (Rowpixel, Colpixel, i)) ==1  &&
double (Surface (Rowpixel, Colpixel, i)) ==0

BiofilmConnectedtoSurfaceforSubstratum (Rowpixel, Colpixel, i) =1;
        elseif
double (BiofilmConnectedtoSurface (Rowpixel, Colpixel, i)) ==0  &&
double (Surface (Rowpixel, Colpixel, i)) ==0

BiofilmConnectedtoSurfaceforSubstratum (Rowpixel, Colpixel, i) =0;
        elseif
double (BiofilmConnectedtoSurface (Rowpixel, Colpixel, i)) ==0  &&
double (Surface (Rowpixel, Colpixel, i)) ==1

BiofilmConnectedtoSurfaceforSubstratum (Rowpixel, Colpixel, i) =0;
        end;
        end;
        end;

        %Modified Substratum Coverage
        Substratum_Modified = sum (sum (sum (BiofilmConnectedtoSurfaceforSubst
ratum (:, :, :))) / (pixelCol * pixelRow) * 100;

        for i = 1:yy
            for Rowpixel = 1:pixelRow;
                for Colpixel = 1:pixelCol;
                    if double (Bacteria (Rowpixel, Colpixel, i)) ==1  &&
double (Surface (Rowpixel, Colpixel, i)) ==1
                        BacteriaColocalized (Rowpixel, Colpixel, i) =1;
                    elseif double (Bacteria (Rowpixel, Colpixel, i)) ==1
&& double (Surface (Rowpixel, Colpixel, i)) ==0
                        BacteriaColocalized (Rowpixel, Colpixel, i) =0;
                    elseif double (Bacteria (Rowpixel, Colpixel, i)) ==0
&& double (Surface (Rowpixel, Colpixel, i)) ==0
                        BacteriaColocalized (Rowpixel, Colpixel, i) =0;
                    elseif double (Bacteria (Rowpixel, Colpixel, i)) ==0
&& double (Surface (Rowpixel, Colpixel, i)) ==1
                        BacteriaColocalized (Rowpixel, Colpixel, i) =0;
                    end;
                end;
            end;
        end;

        %Bacteria Associated with Surface
        for i = 1:yy
PercentBacteriaAssociatedwithSurface (i) = sum (sum (BacteriaColocalized (:, :
, i))) / sum (sum (Bacteria (:, :, i))) * 100;
NumberofBacteriaandSurfaceSamePixel (i) = sum (sum (BacteriaColocalized (:, :,

```

```

i));
VolumeofBacteriaandSurfaceSamePixel(i)=NumberofBacteriaandSurfaceSamePixel(i)*(micronx*microny*micronz);
    end;
    PercentBacteriaAssociatedwithSurface=PercentBacteriaAssociatedwithSurface';
    NumberofBacteriaandSurfaceSamePixel=NumberofBacteriaandSurfaceSamePixel';
    VolumeofBacteriaandSurfaceSamePixel=VolumeofBacteriaandSurfaceSamePixel';
    TotalBacteriaAssociatedwithSurface=sum(sum(sum(BacteriaColocalized)))/sum(sum(sum(Bacteria)))*100;
    TotalNumberofBacteriaandSurfaceSamePixel=sum(sum(sum(BacteriaColocalized)));
    TotalVolumeofBacteriaandSurfaceSamePixel=TotalNumberofBacteriaandSurfaceSamePixel*(micronx*microny*micronz);
    %Any "NAN - Not a real number" will be made 0.
    PercentBacteriaAssociatedwithSurface(isnan(PercentBacteriaAssociatedwithSurface))=0;

    for i=1:yy;
        for Rowpixel=1:pixelRow;
            for Colpixel=1:pixelCol;
                if
double(BiofilmConnectedtoSurface(Rowpixel,Colpixel,i))==1 ||
double(HorizontalGrowthForBacteriaAttachedtoBStart(Rowpixel,Colpixel,i))=1
                    BasisforSubstratum(Rowpixel,Colpixel,i)=1;

                    else
                        BasisforSubstratum(Rowpixel,Colpixel,i)=0;
                    end;
                end;
            end;
        end;
    end;

    %Determine the start points where the Biofilm Attaches to the Surface or
    %Substratum
    k=1;
    for i = 1:yy;
        if sum(sum(BiofilmConnectedtoSurface(:, :, i)))>=1
            StartIndex(k)=i;
            k=k+1;
        end;
    end;

    %Connect biofilm upward from each starting slice
    Storage=zeros(pixelRow, pixelCol, yy);
    NN=size(StartIndex);
    for q=1:NN(2);
        SliceIndex=StartIndex(q);
        areainthislayer(:, :, 1)=BasisforSubstratum(:, :, SliceIndex);

```

```

    for k = SliceIndex:yy-1;
        commonarea3=uint8(areainthislayer(:, :, k-
SliceIndex+1).*double((Bacteria(:, :, k+1)>0))); % what pixels are common
between the two layers
        [vectorx,vector]=find(commonarea3); % vectors containing
the nonzero elements of commonarea
        %8 neighborhood connection for above slice
        %allows for horizontal growth of biofilm
        areainthislayer(:, :, k-
SliceIndex+2)=double(bwselect(Bacteria(:, :, k+1),vector,vectorx,8));
        BiofilmAttachedtoBiofilm(:, :, k-
SliceIndex+1)=areainthislayer(:, :, k-SliceIndex+2);

        %Keep track of where biofilm pixels grew
        for Rowpixel=1:pixelRow;
            for Colpixel=1:pixelCol;
                if BiofilmAttachedtoBiofilm(Rowpixel,Colpixel,k-
SliceIndex+1)==1
                    Storage(Rowpixel, Colpixel, k+1)=1;
                end;
            end;
        end;

    end;

end;

%Put together the starting point BiofilmConnectedtoSurface and
the BiofilmAttachedtoBiofilm in Storage
filt_images=zeros(pixelRow,pixelCol,yy);
for i = 1:yy;
    for Rowpixel=1:pixelRow;
        for Colpixel=1:pixelCol;

            if
double(BiofilmConnectedtoSurface(Rowpixel,Colpixel,i)) ||
double(BasisforSubstratum(Rowpixel,Colpixel,i)) ==1 ||
double(Storage(Rowpixel,Colpixel,i)) ==1
                filt_images(Rowpixel,Colpixel,i)=1;
            end;
        end;
    end;
end;

%Quantification
UnconnectedBacteriaPixel=zeros(max(max(pixelRow)),
max(max(pixelCol)), max(max(yy)));
ConnectedBiofilmBacteriaPixel=zeros(max(max(pixelRow)),
max(max(pixelCol)), max(max(yy)));
AllSurfacePixels=double(Surface);

```

```

AllBacteriaPixels=double(Bacteria);

    for i=1:yy;
        for Rowpixel=1:pixelRow;
            for Colpixel=1:pixelCol;

                if AllBacteriaPixels(Rowpixel, Colpixel,i)==1
&& filt_images(Rowpixel, Colpixel,i) ==1;
                    ConnectedBiofilmBacteriaPixel(Rowpixel,
Colpixel,i)=1;
                    UnconnectedBacteriaPixel(Rowpixel,
Colpixel,i)=0;
                elseif AllBacteriaPixels(Rowpixel,
Colpixel,i)==1 && filt_images(Rowpixel, Colpixel,i) ==0;
                    ConnectedBiofilmBacteriaPixel(Rowpixel,
Colpixel,i)=0;
                    UnconnectedBacteriaPixel(Rowpixel,
Colpixel,i)=1;
                elseif AllBacteriaPixels(Rowpixel,
Colpixel,i)==0 && filt_images(Rowpixel, Colpixel,i) ==0 ||
AllBacteriaPixels(Rowpixel, Colpixel,i)==0 && filt_images(Rowpixel,
Colpixel,i) ==1;
                    ConnectedBiofilmBacteriaPixel(Rowpixel,
Colpixel,i)=0;
                    UnconnectedBacteriaPixel(Rowpixel,
Colpixel,i)=0;

                end;

            end;
        end;
    end;

%Preallocate space
AreaConnectedBiofilmBacteriaBySlice=zeros(max(max(yy)), 1);
AreaUnconnectedBacteriaBySlice=zeros(max(max(yy)), 1);
AreaSurfacebySlice=zeros(max(max(yy)), 1);
AreaPSurfacebySlice=zeros(max(max(yy)), 1);
TotSurfaceBySlice=zeros(max(max(yy)), 1);
TotConnectedBiofilmBacteriaBySlice=zeros(max(max(yy)), 1);
TotUnconnectedBacteriaBySlice=zeros(max(max(yy)), 1);
AreaPercentConnectedBiofilmBacteriaBySlice=zeros(max(max(yy)),
1);
AreaPercentUnconnectedBacteriBySlice=zeros(max(max(yy)), 1);
TotalinMicrons=micronx*microny*pixelCol*pixelRow;

%Surface
AreaSurfaceOverall=sum(sum(sum(Surface(:, :, :))))*micronx*microny;
AreaPSurfaceOverall=AreaSurfaceOverall/(TotalinMicrons*yy)*100;
TotSurface=sum(sum(sum(Surface(:, :, :))));

%Bacteria
AreaConnectedBiofilmBacteria=sum(sum(sum(ConnectedBiofilmBacteriaPixel(
(:, :, :))))*micronx*microny;

```

```

AreaUnconnectedBacteria=sum(sum(sum(UnconnectedBacteriaPixel(:,:,:))))*
micronx*microny;
AreaPercentConnectedBiofilmBacteria=AreaConnectedBiofilmBacteria/(Total
inMicrons*yy)*100;
AreaPercentUnconnectedBacteria=AreaUnconnectedBacteria/(TotalinMicrons*
yy)*100;
TotConnectedBiofilmBacteria=sum(sum(sum(ConnectedBiofilmBacteriaPixel(
(:,:,:)))));
TotUnconnectedBacteria=sum(sum(sum(UnconnectedBacteriaPixel(:,:,:)))));

    for i=1:yy;
        %Surface
        AreaSurfacebySlice(i)=sum(sum(Surface(:,:,i)))*micronx*microny;
        AreaPSurfacebySlice(i)=AreaSurfacebySlice(i)/TotalinMicrons*100;
        TotSurfaceBySlice(i)=sum(sum(sum(Surface(:,:,i))));

        %Bacteria
        AreaConnectedBiofilmBacteriaBySlice(i)=sum(sum(ConnectedBiofilmBacteria
Pixel(:,:,i)))*micronx*microny;
        AreaUnconnectedBacteriaBySlice(i)=sum(sum(UnconnectedBacteriaPixel(:,:,
i)))*micronx*microny;
        AreaPercentConnectedBiofilmBacteriaBySlice(i)=AreaConnectedBiofilmBacte
riaBySlice(i)/TotalinMicrons*100;
        AreaPercentUnconnectedBacteriBySlice(i)=AreaUnconnectedBacteriaBySlice(
i)/TotalinMicrons*100;
        TotConnectedBiofilmBacteriaBySlice(i)=sum(sum(sum(ConnectedBiofilmBacte
riaPixel(:,:,i))));
        TotUnconnectedBacteriaBySlice(i)=sum(sum(sum(UnconnectedBacteriaPixel(
(:,:,i))));
        end;

        %Saving the Data
        StackIndex=1;
        lsm.slice=yy;
        header={'Publication'};
        filename=horzcat(num2str(StackIndex), '.xlsx');
        colnames={'','Number of Connected Biofilm Pixels', 'Area
Connected Biofilm, um^2', 'Area Connected Biofilm, %', 'Number of
Unconnected Bacteria Pixels', 'Area Unconnected Bacteria, um^2', 'Area
Unconnected Bacteria, %', 'Number of Surface Pixels', 'Area Surface,
um^2', 'Area Surface, %', 'Number Bacteria and Surface Pixels the
Same', 'Volume Bacteria and Surface Pixels the Same', 'Pecent Bacteria
Associated with Surface, %', 'Modified Substratum Coverage, %'};

        %Biofilm Associated Bacteria
        GA=vertcat(AreaConnectedBiofilmBacteria,
AreaConnectedBiofilmBacteriaBySlice(:));
        SubstratumSave=vertcat(Substratum_Modified,0);
        TotalConnectedBiofilmBacteria=vertcat(TotConnectedBiofilmBacteria
,TotConnectedBiofilmBacteriaBySlice(:));
        AreaPercentBio=vertcat(AreaPercentConnectedBiofilmBacteria,
AreaPercentConnectedBiofilmBacteriaBySlice(:));
        AssociatedBacteria=vertcat(TotalBacteriaAssociatedwithSurface,
PercentBacteriaAssociatedwithSurface(:));

```

```

    NumberAssociated=vertcat (TotalNumberOfBacteriaandSurfaceSamePixel
,NumberOfBacteriaandSurfaceSamePixel ());
    VolumeAssociated=vertcat (TotalVolumeofBacteriaandSurfaceSamePixel
,VolumeofBacteriaandSurfaceSamePixel ());

    %Non-Biofilm Associated Bacteria
    FGA=vertcat (AreaUnconnectedBacteria,AreaUnconnectedBacteriaBySlic
e ());
    TotalUnconnectedBacteria=vertcat (TotUnconnectedBacteria,
TotUnconnectedBacteriaBySlice ());
    AreaPercentUnconnectedBacteriaCombined=vertcat (AreaPercentUnconne
ctedBacteria, AreaPercentUnconnectedBacteriBySlice ());

    %Surface
    TA=vertcat (AreaSurfaceOverall, AreaSurfacebySlice ());
    TotalSurface=vertcat (TotSurface, TotSurfaceBySlice ());
    SurfacePercent=vertcat ( AreaPSurfaceOverall,
AreaPSurfacebySlice ());

    %Thank you to Scott Hirsch for providing permission to use his
xlswrite
    %code in this application.
    (http://www.mathworks.com/matlabcentral/fileexchange/2855-xlswrite)
    %See xlswrite_BMT_Example.m for license information.
    xlswrite_Image (StackIndex,TotalConnectedBiofilmBacteria, GA,
AreaPercentBio,TotalUnconnectedBacteria, FGA,
AreaPercentUnconnectedBacteriaCombined, TotalSurface, TA,
SurfacePercent, NumberAssociated, VolumeAssociated, AssociatedBacteria,
SubstratumSave, header, colnames, filename);

    %Generating ".tif" Sequences of Components
    FinalConnectedBiofilmBacteria=zeros (max (max (pixelRow)),
max (max (pixelCol)), max (max (yy)));
    FinalUnconnectedBacteria=zeros (max (max (pixelRow)),
max (max (pixelCol)), max (max (yy)));

    folder=['Sample', int2str (StackIndex)];
    parentfolderConnectedBiofilm=strcat (folder, '\ConnectedBiofilmBact
eriaImages\');
    parentfolderUnconnectedBacteria=strcat (
folder, '\UnconnectedBacteriaImages\');
    parentfolderOverall=strcat ( folder, '\OverallBacteriaImages\');
    parentfolderSurface=strcat ( folder, '\SurfaceImages\');
    parentfolderBacteriaSurface=strcat (
folder, '\BacteriaAssociatedWithSurfaceImages\');
    parentfolderBacteriaStars=strcat (
folder, '\ModifiedSubstratumCoverageBacteria\');
    mkdir (parentfolderConnectedBiofilm);
    mkdir (parentfolderUnconnectedBacteria);
    mkdir (parentfolderOverall);
    mkdir (parentfolderSurface);
    mkdir (parentfolderBacteriaSurface);
    mkdir (parentfolderBacteriaStars);

```

```

        for i=1:yy;

FinalConnectedBiofilmBacteria(:, :, i)=ConnectedBiofilmBacteriaPixel(:, :,
i).*double(OriginalBacteria(:, :, i));
        name =
['ConnectedBiofilmBacteria',int2str(i),'.tif'];
        filename= strcat(parentfolderConnectedBiofilm, name);
imwrite(uint8(FinalConnectedBiofilmBacteria(:, :, i)),filename,'tiff');
FinalUnconnectedBacteria(:, :, i)=UnconnectedBacteriaPixel(:, :, i).*double
(OriginalBacteria(:, :, i));
        name = ['UnconnectedBacteria',int2str(i),'.tif'];
        filename= strcat(parentfolderUnconnectedBacteria,
name);
imwrite(uint8(FinalUnconnectedBacteria(:, :, i)),filename,'tiff');
        end;

        FinalOverallBacteria=zeros(max(max(pixelRow)),
max(max(pixelCol)), max(max(yy)));
        FinalSurface=zeros(max(max(pixelRow)), max(max(pixelCol)),
max(max(yy)));
        FinalBacteriaAssociatedWithSurface=zeros(max(max(pixelRow)),
max(max(pixelCol)), max(max(yy)));

        for i=1:yy;

FinalOverallBacteria(:, :, i)=AllBacteriaPixels(:, :, i).*double(OriginalBa
cteria(:, :, i));
        name = ['OverallBacteria',int2str(i),'.tif'];
        filename= strcat(parentfolderOverall, name);
imwrite(uint8(FinalOverallBacteria(:, :, i)),filename,'tiff');
FinalSurface(:, :, i)=double(Surface(:, :, i)).*double(OriginalSurface(:, :,
i));
        name = ['Surface',int2str(i),'.tif'];
        filename= strcat(parentfolderSurface, name);

imwrite(uint8(FinalSurface(:, :, i)),filename,'tiff');
FinalBacteriaAssociatedWithSurface(:, :, i)=double(BacteriaColocalized(:,
:, i)).*double(OriginalBacteria(:, :, i));
        name =
['BacteriaAssociatedWithSurface',int2str(i),'.tif'];
        filename= strcat(parentfolderBacteriaSurface, name);
imwrite(uint8(FinalBacteriaAssociatedWithSurface(:, :, i)),filename,'tiff
');
FinalBacteriaStars(:, :, i)=double(BiofilmConnectedtoSurface(:, :, i)).*dou
ble(OriginalBacteria(:, :, i));
        name =
['ModifiedSubstratumCoverageBacteria',int2str(i),'.tif'];
        filename= strcat(parentfolderBacteriaStars, name);
imwrite(uint8(FinalBacteriaStars(:, :, i)),filename,'tiff');
        end;

```


REFERENCES

1. Cystic Fibrosis Foundation. Cystic Fibrosis Foundation Patient Registry. 2011 Annual Data Report. www.cff.org (accessed March 21, 2013).
2. Cystic Fibrosis Foundation. About Cystic Fibrosis. www.cff.org/AboutCF (accessed March 21, 2013).
3. Emerson, J.; Rosenfeld, M.; McNamara, S.; Ramsey, B.; Gibson, R. L., *Pseudomonas aeruginosa* and other predictors of mortality and morbidity in young children with cystic fibrosis. *Pediatric Pulmonology* **2002**, *34* (2), 91-100.
4. Zlosnik, J. E.; Hird, T. J.; Fraenkel, M. C.; Moreira, L. M.; Henry, D. A.; Speert, D. P., Differential mucoid exopolysaccharide production by members of the *Burkholderia cepacia* complex. *Journal of Clinical Microbiology* **2008**, *46* (4), 1470-3.
5. Boucher, R. C., An overview of the pathogenesis of cystic fibrosis lung disease. *Advanced Drug Delivery Reviews* **2002**, *54* (11), 1359-71.
6. Matsui, H.; Grubb, B. R.; Tarran, R.; Randell, S. H.; Gatzky, J. T.; Davis, C. W.; Boucher, R. C., Evidence for periciliary liquid layer depletion, not abnormal ion composition, in the pathogenesis of cystic fibrosis airways disease. *Cell* **1998**, *95* (7), 1005-15.
7. Mathee, K.; Ciofu, O.; Sternberg, C.; Lindum, P. W.; Campbell, J. I.; Jensen, P.; Johnsen, A. H.; Givskov, M.; Ohman, D. E.; Molin, S.; Hoiby, N.; Kharazmi, A., Mucoid conversion of *Pseudomonas aeruginosa* by hydrogen peroxide: a mechanism for virulence activation in the cystic fibrosis lung. *Microbiology* **1999**, *145* (Pt 6), 1349-57.
8. Grasemann, H.; Ioannidis, I.; Tomkiewicz, R. P.; de Groot, H.; Rubin, B. K.; Ratjen, F., Nitric oxide metabolites in cystic fibrosis lung disease. *Archives of Disease in Childhood* **1998**, *78* (1), 49-53.
9. Mulcahy, H.; Charron-Mazenod, L.; Lewenza, S., Extracellular DNA chelates cations and induces antibiotic resistance in *Pseudomonas aeruginosa* biofilms. *PLoS Pathogens* **2008**, *4* (11), e1000213.
10. Mulcahy, H.; Lewenza, S., Magnesium limitation is an environmental trigger of the *Pseudomonas aeruginosa* biofilm lifestyle. *PLoS One* **2011**, *6* (8), e23307.
11. Cystic Fibrosis Foundation. Drug Development Pipeline. www.cff.org/treatments/Pipeline/ (accessed March 21, 2013).

12. Kirkby, S.; Novak, K.; McCoy, K., Update on antibiotics for infection control in cystic fibrosis. *Expert Review of Anti-infective Therapy* **2009**, 7 (8), 967-80.
13. Flume, P. A.; O'Sullivan, B. P.; Robinson, K. A.; Goss, C. H.; Mogayzel, P. J., Jr.; Willey-Courand, D. B.; Bujan, J.; Finder, J.; Lester, M.; Quittell, L.; Rosenblatt, R.; Vender, R. L.; Hazle, L.; Sبادosa, K.; Marshall, B.; Cystic Fibrosis Foundation, P. T. C., Cystic fibrosis pulmonary guidelines: chronic medications for maintenance of lung health. *American Journal of Respiratory and Critical Care Medicine* **2007**, 176 (10), 957-69.
14. Hubert, D.; Leroy, S.; Nove-Josserand, R.; Murriss-Espin, M.; Mely, L.; Dominique, S.; Delaisi, B.; Kho, P.; Kovarik, J. M., Pharmacokinetics and safety of tobramycin administered by the PARI eFlow rapid nebulizer in cystic fibrosis. *Journal of Cystic Fibrosis : Official Journal of the European Cystic Fibrosis Society* **2009**, 8 (5), 332-7.
15. Novartis. Tobramycin Inhalation Solution.
www.pharma.us.novartis.com/product/pi/pdf/tobi.pdf (accessed December 7, 2012).
16. Bayer Healthcare. Bayer Healthcare Pipeline Overview.
www.bayerpharma.com/en/research-and-development/development-pipeline/pop_up_development_pipeline.php (access December 7, 2012).
17. Bjarnsholt, T.; Jensen, P. Ø.; Fiandaca, M. J.; Pedersen, J.; Hansen, C. R.; Andersen, C. B.; Pressler, T.; Givskov, M.; Høiby, N., *Pseudomonas aeruginosa* biofilms in the respiratory tract of cystic fibrosis patients. *Pediatric Pulmonology* **2009**, 44 (6), 547-558.
18. Aaron, S. D.; Ferris, W.; Ramotar, K.; Vandemheen, K.; Chan, F.; Saginur, R., Single and combination antibiotic susceptibilities of planktonic, adherent, and biofilm-grown *Pseudomonas aeruginosa* isolates cultured from sputa of adults with cystic fibrosis. *Journal of Clinical Microbiology* **2002**, 40 (11), 4172-9.
19. Tre-Hardy, M.; Vanderbist, F.; Traore, H.; Devleeschouwer, M. J., In vitro activity of antibiotic combinations against *Pseudomonas aeruginosa* biofilm and planktonic cultures. *International Journal of Antimicrobial Agents* **2008**, 31 (4), 329-36.
20. Fauvart, M.; De Groote, V. N.; Michiels, J., Role of persister cells in chronic infections: clinical relevance and perspectives on anti-persister therapies. *Journal of Medical Microbiology* **2011**, 60 (Pt 6), 699-709.
21. Shih, P. C.; Huang, C. T., Effects of quorum-sensing deficiency on *Pseudomonas aeruginosa* biofilm formation and antibiotic resistance. *The Journal of Antimicrobial Chemotherapy* **2002**, 49 (2), 309-14.

22. Tenover, F. C., Mechanisms of antimicrobial resistance in bacteria. *The American Journal of Medicine* **2006**, *119* (6), S3-S10.
23. Lawrence, J. R.; Korber, D. R.; Hoyle, B. D.; Costerton, J. W.; Caldwell, D. E., Optical sectioning of microbial biofilms. *Journal of Bacteriology* **1991**, *173* (20), 6558-67.
24. Dirckx, P.; Stewart, P., Biofilm Formation in Three Steps. <http://www.biofilm.montana.edu/resources/images/multicellularextracellular/biofilm-formation-3-steps.html> (accessed March 21, 2013).
25. Harmsen, M.; Yang, L.; Pamp, S. J.; Tolker-Nielsen, T., An update on *Pseudomonas aeruginosa* biofilm formation, tolerance, and dispersal. *FEMS Immunology and Medical Microbiology* **2010**, *59* (3), 253-68.
26. Tielker, D.; Hacker, S.; Loris, R.; Strathmann, M.; Wingender, J.; Wilhelm, S.; Rosenau, F.; Jaeger, K.-E., *Pseudomonas aeruginosa* lectin LecB is located in the outer membrane and is involved in biofilm formation. *Microbiology* **2005**, *151* (5), 1313-1323.
27. Flemming, H. C.; Wingender, J., The biofilm matrix. *Nature Reviews. Microbiology* **2010**, *8* (9), 623-33.
28. Sutherland, I. W., The biofilm matrix—an immobilized but dynamic microbial environment. *Trends in Microbiology* **2001**, *9* (5), 222-227.
29. Wingender, J.; Neu, T. R.; Flemming, H.-C., *Microbial Extracellular Polymeric Substances: Characterization, Structure, and Function*. Springer Verlag: Berlin, 1999.
30. Hentzer, M.; Teitzel, G. M.; Balzer, G. J.; Heydorn, A.; Molin, S.; Givskov, M.; Parsek, M. R., Alginate overproduction affects *Pseudomonas aeruginosa* biofilm structure and function. *Journal of Bacteriology* **2001**, *183* (18), 5395-401.
31. Purevdorj, B.; Costerton, J. W.; Stoodley, P., Influence of hydrodynamics and cell signaling on the structure and behavior of *Pseudomonas aeruginosa* biofilms. *Applied and Environmental Microbiology* **2002**, *68* (9), 4457-64.
32. Kaplan, J. B., Biofilm dispersal: mechanisms, clinical implications, and potential therapeutic uses. *Journal of Dental Research* **2010**, *89* (3), 205-18.
33. Ryder, C.; Byrd, M.; Wozniak, D. J., Role of polysaccharides in *Pseudomonas aeruginosa* biofilm development. *Current Opinion in Microbiology* **2007**, *10* (6), 644-8.

34. Vu, B.; Chen, M.; Crawford, R. J.; Ivanova, E. P., Bacterial extracellular polysaccharides involved in biofilm formation. *Molecules* **2009**, *14* (7), 2535-54.
35. Mayer, C.; Moritz, R.; Kirschner, C.; Borchard, W.; Maibaum, R.; Wingender, J.; Flemming, H. C., The role of intermolecular interactions: studies on model systems for bacterial biofilms. *International Journal of Biological Macromolecules* **1999**, *26* (1), 3-16.
36. Abdi-Ali, A.; Mohammadi-Mehr, M.; Agha Alaei, Y., Bactericidal activity of various antibiotics against biofilm-producing *Pseudomonas aeruginosa*. *International Journal of Antimicrobial Agents* **2006**, *27* (3), 196-200.
37. Kumon, H.; Tomochika, K.; Matunaga, T.; Ogawa, M.; Ohmori, H., A sandwich cup method for the penetration assay of antimicrobial agents through *Pseudomonas* exopolysaccharides. *Microbiology and Immunology* **1994**, *38* (8), 615-9.
38. Walters III, M. C.; Roe, F.; Bugnicourt, A.; Franklin, M. J.; Stewart, P. S., Contributions of antibiotic penetration, oxygen limitation, and low metabolic activity to tolerance of *Pseudomonas aeruginosa* biofilms to ciprofloxacin and tobramycin. *Antimicrobial Agents and Chemotherapy* **2003**, *47* (1), 317-323.
39. King, P.; Citron, D. M.; Griffith, D. C.; Lomovskaya, O.; Dudley, M. N., Effect of oxygen limitation on the in vitro activity of levofloxacin and other antibiotics administered by the aerosol route against *Pseudomonas aeruginosa* from cystic fibrosis patients. *Diagnostic Microbiology and Infectious Disease* **2010**, *66* (2), 181-6.
40. Van Bambeke, F.; Glupczynski, Y.; Tulkens, P. M., Mechanisms of action. In *Infectious Diseases; Elsevier Science: New York*, 2010, p. 1288-1307.
41. Costerton, J. W.; Stewart, P. S.; Greenberg, E. P., Bacterial biofilms: a common cause of persistent infections. *Science* **1999**, *284* (5418), 1318-22.
42. Doring, G.; Pier, G. B., Vaccines and immunotherapy against *Pseudomonas aeruginosa*. *Vaccine* **2008**, *26* (8), 1011-24.
43. Pennington, J. E.; Reynolds, H. Y.; Wood, R. E.; Robinson, R. A.; Levine, A. S., Use of a *Pseudomonas aeruginosa* vaccine in patients with acute leukemia and cystic fibrosis. *The American Journal of Medicine* **1975**, *58* (5), 629-636.
44. Döring, G.; Meisner, C.; Stern, M., A double-blind randomized placebo-controlled phase III study of a *Pseudomonas aeruginosa* flagella vaccine in cystic fibrosis patients. *Proceedings of the National Academy of Sciences* **2007**, *104* (26), 11020-11025.

45. Astrazeneca, Development Pipeline.
www.astrazeneca.com/cs/Satellite?blobcol=urldata&blobheader=application%2Fpdf&blobheadername1=Content-Disposition&blobheadername2=MDT-Type&blobheadervalue1=inline%3B+filename%3DDownload-R%26amp%3BD-Pipeline-Summary.pdf&blobheadervalue2=abinary%3B+charset%3DUTF-8&blobkey=id&blobtable=MungoBlobs&blobwhere=1285641506662&ssbinary=true (accessed December 21, 2012).
46. Hauber, H. P.; Schulz, M.; Pforte, A.; Mack, D.; Zabel, P.; Schumacher, U., Inhalation with fucose and galactose for treatment of *Pseudomonas aeruginosa* in cystic fibrosis patients. *International Journal of Medical Sciences* **2008**, *5* (6), 371-6.47.
47. Coban, A. Y.; Ekinçi, B.; Durupinar, B., A multidrug efflux pump inhibitor reduces fluoroquinolone resistance in *Pseudomonas aeruginosa* isolates. *Chemotherapy* **2004**, *50* (1), 22-6.
48. Nelson, D.; Loomis, L.; Fischetti, V. A., Prevention and elimination of upper respiratory colonization of mice by group A streptococci by using a bacteriophage lytic enzyme. *Proceedings of the National Academy of Sciences of the United States of America* **2001**, *98* (7), 4107-12.
49. Wu, H.; Song, Z.; Hentzer, M.; Andersen, J. B.; Molin, S.; Givskov, M.; Hoiby, N., Synthetic furanones inhibit quorum-sensing and enhance bacterial clearance in *Pseudomonas aeruginosa* lung infection in mice. *The Journal of Antimicrobial Chemotherapy* **2004**, *53* (6), 1054-61.
50. Goure, J.; Broz, P.; Attree, O.; Cornelis, G. R.; Attree, I., Protective anti-V antibodies inhibit *Pseudomonas* and *Yersinia* translocon assembly within host membranes. *The Journal of Infectious Diseases* **2005**, *192* (2), 218-25.
51. Halwani, M.; Yebio, B.; Suntres, Z. E.; Alipour, M.; Azghani, A. O.; Omri, A., Co-encapsulation of gallium with gentamicin in liposomes enhances antimicrobial activity of gentamicin against *Pseudomonas aeruginosa*. *The Journal of Antimicrobial Chemotherapy* **2008**, *62* (6), 1291-7.
52. Alkawash, M. A.; Soothill, J. S.; Schiller, N. L., Alginate lyase enhances antibiotic killing of mucoid *Pseudomonas aeruginosa* in biofilms. *APMIS : Acta Pathologica, Microbiologica, et Immunologica Scandinavica* **2006**, *114* (2), 131-8.
53. Barraud, N.; Hassett, D. J.; Hwang, S. H.; Rice, S. A.; Kjelleberg, S.; Webb, J. S., Involvement of nitric oxide in biofilm dispersal of *Pseudomonas aeruginosa*. *Journal of Bacteriology* **2006**, *188* (21), 7344-53.

54. Gjermansen, M.; Ragas, P.; Sternberg, C.; Molin, S.; Tolker-Nielsen, T., Characterization of starvation-induced dispersion in *Pseudomonas putida* biofilms. *Environmental Microbiology* **2005**, *7* (6), 894-906.
55. Sauer, K.; Cullen, M. C.; Rickard, A. H.; Zeef, L. A.; Davies, D. G.; Gilbert, P., Characterization of nutrient-induced dispersion in *Pseudomonas aeruginosa* PAO1 biofilm. *Journal of Bacteriology* **2004**, *186* (21), 7312-26.
56. Thormann, K. M.; Saville, R. M.; Shukla, S.; Spormann, A. M., Induction of rapid detachment in *Shewanella oneidensis* MR-1 biofilms. *Journal of Bacteriology* **2005**, *187* (3), 1014-21.
57. Bartell, P. F.; Orr, T. E.; Lam, G. K., Polysaccharide depolymerase associated with bacteriophage infection. *Journal of Bacteriology* **1966**, *92* (1), 56-62.
58. Harper, D. R.; Enright, M. C., Bacteriophages for the treatment of *Pseudomonas aeruginosa* infections. *Journal of Applied Microbiology* **2011**, *111* (1), 1-7.
59. Davies, D. G., Biofilm Dispersion. In *Biofilm Highlights*; Springer: Berlin, 2011, p 1-28.
60. Boyd, A.; Chakrabarty, A. M., Role of alginate lyase in cell detachment of *Pseudomonas aeruginosa*. *Applied and Environmental Microbiology* **1994**, *60* (7), 2355-9.
61. Chen, X.; Stewart, P. S., Biofilm removal caused by chemical treatments. *Water Research* **2000**, *34* (17), 4229-4233.
62. Banin, E.; Brady, K. M.; Greenberg, E. P., Chelator-induced dispersal and killing of *Pseudomonas aeruginosa* cells in a biofilm. *Applied and Environmental Microbiology* **2006**, *72* (3), 2064-9.
63. Boles, B. R.; Thoendel, M.; Singh, P. K., Rhamnolipids mediate detachment of *Pseudomonas aeruginosa* from biofilms. *Molecular Microbiology* **2005**, *57* (5), 1210-23.
64. Rogers, S. A.; Huigens III, R. W.; Cavanagh, J.; Melander, C., Synergistic effects between conventional antibiotics and 2-aminoimidazole-derived antibiofilm agents. *Antimicrobial Agents and Chemotherapy* **2010**, *54* (5), 2112-2118.
65. Lu, T. K.; Collins, J. J., Dispersing biofilms with engineered enzymatic bacteriophage. *Proceedings of the National Academy of Sciences of the United States of America* **2007**, *104* (27), 11197-202.

66. Lamppa, J. W.; Griswold, K. E., Alginate lyase exhibits catalysis-independent biofilm dispersion and antibiotic synergy. *Antimicrobial Agents and Chemotherapy* **2013**, *57* (1), 137-45.
67. Morgan, R.; Kohn, S.; Hwang, S. H.; Hassett, D. J.; Sauer, K., BdlA, a chemotaxis regulator essential for biofilm dispersion in *Pseudomonas aeruginosa*. *Journal of Bacteriology* **2006**, *188* (21), 7335-43.
68. Davies, D. G.; Marques, C. N., A fatty acid messenger is responsible for inducing dispersion in microbial biofilms. *Journal of Bacteriology* **2009**, *191* (5), 1393-1403.
69. Boles, B. R.; Horswill, A. R., Agr-mediated dispersal of *Staphylococcus aureus* biofilms. *PLoS Pathogens* **2008**, *4* (4), e1000052.
70. Mesibov, R.; Adler, J., Chemotaxis toward amino acids in *Escherichia coli*. *Journal of Bacteriology* **1972**, *112* (1), 315-26.
71. Moulton, R. C.; Montie, T. C., Chemotaxis by *Pseudomonas aeruginosa*. *Journal of Bacteriology* **1979**, *137* (1), 274-80.
72. Darzins, A., Characterization of a *Pseudomonas aeruginosa* gene cluster involved in pilus biosynthesis and twitching motility: sequence similarity to the chemotaxis proteins of enterics and the gliding bacterium *Myxococcus xanthus*. *Molecular Microbiology* **2006**, *11* (1), 137-153.
73. Yarwood, J. M.; Bartels, D. J.; Volper, E. M.; Greenberg, E. P., Quorum sensing in *Staphylococcus aureus* biofilms. *Journal of Bacteriology* **2004**, *186* (6), 1838-50.
74. Biosurface Technologies Corporation. Rotating Disk Reactor. www.biofilms.biz/wp-content/uploads/2012/03/RDR-Pricing-2012.pdf (accessed December 21, 2012).
75. Biosurface Technologies Corporation. CDC Reactor. www.biofilms.biz/wp-content/uploads/2012/06/CDC-Pricing-20121.pdf (accessed December 21, 2012).
76. Ammons, M. C.; Ward, L. S.; Fisher, S. T.; Wolcott, R. D.; James, G. A., In vitro susceptibility of established biofilms composed of a clinical wound isolate of *Pseudomonas aeruginosa* treated with lactoferrin and xylitol. *International Journal of Antimicrobial Agents* **2009**, *33* (3), 230-6.
77. Buckingham-Meyer, K.; Goeres, D. M.; Hamilton, M. A., Comparative evaluation of biofilm disinfectant efficacy tests. *Journal of Microbiological Methods* **2007**, *70* (2), 236-44.

78. Goeres, D. M.; Hamilton, M. A.; Beck, N. A.; Buckingham-Meyer, K.; Hilyard, J. D.; Loetterle, L. R.; Lorenz, L. A.; Walker, D. K.; Stewart, P. S., A method for growing a biofilm under low shear at the air-liquid interface using the drip flow biofilm reactor. *Nature Protocols* **2009**, *4* (5), 783-788.
79. Borriello, G.; Richards, L.; Ehrlich, G. D.; Stewart, P. S., Arginine or nitrate enhances antibiotic susceptibility of *Pseudomonas aeruginosa* in biofilms. *Antimicrobial Agents and Chemotherapy* **2006**, *50* (1), 382-4.
80. Pitts, B.; Hamilton, M. A.; Zelter, N.; Stewart, P. S., A microtiter-plate screening method for biofilm disinfection and removal. *Journal of Microbiological Methods* **2003**, *54* (2), 269-76.
81. de Beer, D.; Stoodley, P.; Lewandowski, Z., Liquid flow in heterogeneous biofilms. *Biotechnology and Bioengineering* **1994**, *44* (5), 636-641.
82. Innovotech, Minimum Biofilm Eradication Concentration Assay Manual.
83. Ceri, H.; Olson, M. E.; Stremick, C.; Read, R. R.; Morck, D.; Buret, A., The Calgary Biofilm Device: new technology for rapid determination of antibiotic susceptibilities of bacterial biofilms. *Journal of Clinical Microbiology* **1999**, *37* (6), 1771-6.
84. Harrison, J. J.; Ceri, H.; Stremick, C. A.; Turner, R. J., Biofilm susceptibility to metal toxicity. *Environmental Microbiology* **2004**, *6* (12), 1220-7.
85. Fuxman Bass, J. I.; Russo, D. M.; Gabelloni, M. L.; Geffner, J. R.; Giordano, M.; Catalano, M.; Zorreguieta, A.; Trevani, A. S., Extracellular DNA: a major proinflammatory component of *Pseudomonas aeruginosa* biofilms. *Journal of Immunology* **2010**, *184* (11), 6386-95.
86. Percival, S. L.; Bowler, P.; Woods, E. J., Assessing the effect of an antimicrobial wound dressing on biofilms. *Wound Repair and Regeneration : Official Publication of the Wound Healing Society [and] the European Tissue Repair Society* **2008**, *16* (1), 52-7.
87. Sommerfeld Ross, S.; Fiegel, J., Nutrient dispersion enhances conventional antibiotic activity against *Pseudomonas aeruginosa* biofilms. *International Journal of Antimicrobial Agents* **2012**, *40* (2), 177-81.
88. Clontz, L., The USP Microbial Limit Tests. In *Microbial Limit and Bioburden Tests: Validation Approaches and Global Requirements*. CRC: Boca Rotan, 2008.
89. Monod, J., The growth of bacterial cultures. *Annual Reviews in Microbiology* **1949**, *3* (1), 371-394.

90. Rogers, S. A.; Krayner, M.; Lindsey, J. S.; Melander, C., Tandem dispersion and killing of bacteria from a biofilm. *Organic & Biomolecular Chemistry* **2009**, *7* (3), 603-6.
91. Hoben, H. J.; Somasegaran, P., Comparison of the Pour, Spread, and Drop Plate Methods for Enumeration of *Rhizobium* spp. in Inoculants Made from Presterilized Peat. *Applied and Environmental Microbiology* **1982**, *44* (5), 1246-7.
92. Herigstad, B.; Hamilton, M.; Heersink, J., How to optimize the drop plate method for enumerating bacteria. *Journal of Microbiological Methods* **2001**, *44* (2), 121-129.
93. Hibbs, A. R., *Confocal Microscopy for Biologists*. Kluwer Academic/Plenum Publishers: New York, 2004, p. 1-30.
94. Gillis, R. J.; Iglewski, B. H., Azithromycin retards *Pseudomonas aeruginosa* biofilm formation. *Journal of Clinical Microbiology* **2004**, *42* (12), 5842-5.
95. National Institute of Health. ImageJ. <http://rsb.info.nih.gov/ij/index.html> (accessed December 21, 2012).
96. Heydorn, A.; Nielsen, A. T.; Hentzer, M.; Sternberg, C.; Givskov, M.; Ersboll, B. K.; Molin, S., Quantification of biofilm structures by the novel computer program COMSTAT. *Microbiology* **2000**, *146* (Pt 10), 2395-407.
97. Fernández, L.; Gooderham, W. J.; Bains, M.; McPhee, J. B.; Wiegand, I.; Hancock, R. E., Adaptive resistance to the “last hope” antibiotics polymyxin B and colistin in *Pseudomonas aeruginosa* is mediated by the novel two-component regulatory system ParR-ParS. *Antimicrobial Agents and Chemotherapy* **2010**, *54* (8), 3372-3382.
98. Pubchem. <http://pubchem.ncbi.nlm.nih.gov/> (accessed April 24, 2013).
99. Richards, J. J.; Ballard, T. E.; Melander, C., Inhibition and dispersion of *Pseudomonas aeruginosa* biofilms with reverse amide 2-aminoimidazole oroidin analogues. *Organic & Biomolecular Chemistry* **2008**, *6* (8), 1356-63.
100. Harrison, J. J.; Stremick, C. A.; Turner, R. J.; Allan, N. D.; Olson, M. E.; Ceri, H., Microtiter susceptibility testing of microbes growing on peg lids: a miniaturized biofilm model for high-throughput screening. *Nature Protocols* **2010**, *5* (7), 1236-54.

101. Chattoraj, S. S.; Ganesan, S.; Jones, A. M.; Helm, J. M.; Comstock, A. T.; Bright-Thomas, R.; LiPuma, J. J.; Hershenson, M. B.; Sajjan, U. S., Rhinovirus infection liberates planktonic bacteria from biofilm and increases chemokine responses in cystic fibrosis airway epithelial cells. *Thorax* **2011**, *66* (4), 333-9.
102. De Kievit, T. R.; Parkins, M. D.; Gillis, R. J.; Srikumar, R.; Ceri, H.; Poole, K.; Iglewski, B. H.; Storey, D. G., Multidrug efflux pumps: expression patterns and contribution to antibiotic resistance in *Pseudomonas aeruginosa* biofilms. *Antimicrobial Agents and Chemotherapy* **2001**, *45* (6), 1761-70.
103. Harrison, J. J.; Turner, R. J.; Ceri, H., Persister cells, the biofilm matrix and tolerance to metal cations in biofilm and planktonic *Pseudomonas aeruginosa*. *Environmental Microbiology* **2005**, *7* (7), 981-94.
104. Hengzhuang, W.; Wu, H.; Ciofu, O.; Song, Z.; Høiby, N., Pharmacokinetics/pharmacodynamics of colistin and imipenem on mucoid and nonmucoid *Pseudomonas aeruginosa* biofilms. *Antimicrobial Agents and Chemotherapy* **2011**, *55* (9), 4469-4474.
105. Vazquez, J. L.; Berlanga, M.; Merino, S.; Domenech, O.; Vinas, M.; Montero, M. T.; Hernandez-Borrell, J., Determination by fluorimetric titration of the ionization constants of ciprofloxacin in solution and in the presence of liposomes. *Photochemistry and Photobiology* **2001**, *73* (1), 14-9.
106. Kane, R. S.; Glink, P. T.; Chapman, R. G.; McDonald, J. C.; Jensen, P. K.; Gao, H.; Pasa-Tolic, L.; Smith, R. D.; Whitesides, G. M., Basicity of the amino groups of the aminoglycoside amikacin using capillary electrophoresis and coupled CE-MS-MS techniques. *Analytical Chemistry* **2001**, *73* (16), 4028-36.
107. Pagano, T. G.; Gong, Y.; Kong, F.; Tsao, R.; Fawzi, M.; Zhu, T., Structural characterization of the tobramycin-piperacillin reaction product formed at pH 6.0. *The Journal of Antibiotics* **2011**, *64* (10), 673-677.
108. Kwa, A. L.; Tam, V. H.; Falagas, M. E., Polymyxins: a review of the current status including recent developments. *Annals of the Academy of Medicine, Singapore* **2008**, *37* (10), 870-83.
109. Butler, J. N.; Cogley, D. R., *Ionic equilibrium: solubility and pH calculations*. John Wiley & Sons: New York, 1998, p. 155-165.
110. Ammons, M. C.; Ward, L. S.; Dowd, S.; James, G. A., Combined treatment of *Pseudomonas aeruginosa* biofilm with lactoferrin and xylitol inhibits the ability of bacteria to respond to damage resulting from lactoferrin iron chelation. *International Journal of Antimicrobial Agents* **2011**, *37* (4), 316-23.

111. Trahan, L.; Mouton, C., Selection for *Streptococcus mutans* with an altered xylitol transport capacity in chronic xylitol consumers. *Journal of Dental Research* **1987**, *66* (5), 982-988.
112. Zabner, J.; Seiler, M. P.; Launspach, J. L.; Karp, P. H.; Kearney, W. R.; Look, D. C.; Smith, J. J.; Welsh, M. J., The osmolyte xylitol reduces the salt concentration of airway surface liquid and may enhance bacterial killing. *Proceedings of the National Academy of Sciences of the United States of America* **2000**, *97* (21), 11614-9.
113. American Type Culture Collection. Reviving freeze-dried cultures. www.atcc.org/CulturesandProducts/TechnicalSupport/HowtoReviveCultures/tabid/695/Default.aspx (accessed December 21, 2012).
114. American Type Culture Collection. Reference strains: how many passages are too many? www.atcc.org/Portals/1/Pdf/tb06.pdf (accessed December 21, 2012).
115. Addgene. Streaking and isolating bacteria on an LB agar plate. www.addgene.org/plasmid_protocols/streak_plate (accessed December 21, 2012).
116. Omar, A., Innovotech Inc. Personal Communication. **2013**.
117. Durairaj, L.; Launspach, J.; Watt, J. L.; Businga, T. R.; Kline, J. N.; Thorne, P. S.; Zabner, J., Safety assessment of inhaled xylitol in mice and healthy volunteers. *Respiratory Research* **2004**, *5*, 13.
118. Winslow, C. E.; Dolloff, A. F., Relative Importance of Additive and Antagonistic Effects of Cations Upon Bacterial Viability. *Journal of Bacteriology* **1928**, *15* (2), 67-92.
119. Miller, G.; Sabatelli, F.; Naples, L.; Hare, R.; Shaw, K., Resistance to aminoglycosides in *Pseudomonas*. Aminoglycoside Resistance Study Groups. *Trends in Microbiology* **1994**, *2*, 347-353.
120. Haagensen, J. A.; Klausen, M.; Ernst, R. K.; Miller, S. I.; Folkesson, A.; Tolker-Nielsen, T.; Molin, S., Differentiation and distribution of colistin- and sodium dodecyl sulfate-tolerant cells in *Pseudomonas aeruginosa* biofilms. *Journal of Bacteriology* **2007**, *189* (1), 28-37.
121. Li, J.; Turnidge, J.; Milne, R.; Nation, R. L.; Coulthard, K., In Vitro Pharmacodynamic Properties of Colistin and Colistin Methanesulfonate against *Pseudomonas aeruginosa* Isolates from Patients with Cystic Fibrosis. *Antimicrobial Agents and Chemotherapy* **2001**, *45* (3), 781-785.

122. Bergen, P. J.; Li, J.; Rayner, C. R.; Nation, R. L., Colistin methanesulfonate is an inactive prodrug of colistin against *Pseudomonas aeruginosa*. *Antimicrobial Agents and Chemotherapy* **2006**, *50* (6), 1953-1958.
123. Hancock, R.; Wong, P., Compounds which increase the permeability of the *Pseudomonas aeruginosa* outer membrane. *Antimicrobial Agents and Chemotherapy* **1984**, *26* (1), 48-52.
124. Tre-Hardy, M.; Mace, C.; El Manssouri, N.; Vanderbist, F.; Traore, H.; Devleeschouwer, M. J., Effect of antibiotic co-administration on young and mature biofilms of cystic fibrosis clinical isolates: the importance of the biofilm model. *International Journal of Antimicrobial Agents* **2009**, *33* (1), 40-5.
125. Olson, M. E.; Ceri, H.; Morck, D. W.; Buret, A. G.; Read, R. R., Biofilm bacteria: formation and comparative susceptibility to antibiotics. *Canadian Journal of Veterinary Research* **2002**, *66* (2), 86-92.
126. Teitzel, G. M.; Parsek, M. R., Heavy metal resistance of biofilm and planktonic *Pseudomonas aeruginosa*. *Applied and Environmental Microbiology* **2003**, *69* (4), 2313-20.
127. Stites, S. W.; Walters, B.; O'Brien-Ladner, A. R.; Bailey, K.; Wesselius, L. J., Increased iron and ferritin content of sputum from patients with cystic fibrosis or chronic bronchitis. *Chest* **1998**, *114* (3), 814-9.
128. Geller, D. E.; Pitlick, W. H.; Nardella, P. A.; Tracewell, W. G.; Ramsey, B. W., Pharmacokinetics and bioavailability of aerosolized tobramycin in cystic fibrosis. *Chest* **2002**, *122* (1), 219-26.
129. Bhaskar, K. R.; Reid, L., Application of density gradient methods for the study of mucus glycoprotein and other macromolecular components of the sol and gel phases of asthmatic sputa. *The Journal of Biological Chemistry* **1981**, *256* (14), 7583-9.
130. Vanbever, R.; Mintzes, J. D.; Wang, J.; Nice, J.; Chen, D.; Batycky, R.; Langer, R.; Edwards, D. A., Formulation and physical characterization of large porous particles for inhalation. *Pharmaceutical Research* **1999**, *16* (11), 1735-42.
131. Pamp, S. J.; Gjermansen, M.; Johansen, H. K.; Tolker-Nielsen, T., Tolerance to the antimicrobial peptide colistin in *Pseudomonas aeruginosa* biofilms is linked to metabolically active cells, and depends on the pmr and mexAB-oprM genes. *Molecular Microbiology* **2008**, *68* (1), 223-40.
132. Xu, H.; Teo, K.; Neo, H.; Liu, Y., Chemically inhibited ATP synthesis promoted detachment of different-age biofilms from membrane surface. *Applied Microbiology and Biotechnology* **2012**, *95* (4), 1073-82.

133. O'Hara, K.; Kawabe, T.; Taniguchi, K.; Ohnuma, M.; Nakagawa, M.; Naitou, Y.; Sawai, T., A new simple assay for determining aminoglycoside inactivation in intact cells of *Pseudomonas aeruginosa*. *Microbios* **1997**, *90* (364-365), 177-86.
134. Daims, H.; Wagner, M., Quantification of uncultured microorganisms by fluorescence microscopy and digital image analysis. *Applied Microbiology and Biotechnology* **2007**, *75* (2), 237-48.
135. Wilkinson, M. H., Automated and manual segmentation techniques in image analysis of microbes. *Digital Image Analysis of Microbes, 1st Ed.*: John Wiley & Sons Inc: New York 1998, p. 135-171.
136. Otsu, N., A threshold selection method from gray-level histograms. *Automatica* **1975**, *11* (285-296), 23-27.
137. Sonka, M.; Hlavac, V.; Boyle, R., *Image processing, analysis, and machine vision*, 3rd ed.; Thomson Learning: Toronto, 1999, p. 123-131.
138. Mueller, L. N.; de Brouwer, J. F.; Almeida, J. S.; Stal, L. J.; Xavier, J. B., Analysis of a marine phototrophic biofilm by confocal laser scanning microscopy using the new image quantification software PHILIP. *BMC Ecology* **2006**, *6*, 1.
139. Vorregaard, M.; Ersboll, B. K.; Haagenen, J. A.; Molin, S.; Sternberg, C., Technical Universtiy of Denmark. Personal Communication. 2011.
140. Sommerfeld Ross, S.; Reinhardt, J. M.; Fiegel, J., Enhanced analysis of bacteria susceptibility in connected biofilms. *Journal of Microbiological Methods* **2012**, *90* (1), 9-14.
141. Sternberg, C., COMSTAT. www.comstat.dk (accessed September 16, 2010).
142. Li, P. LSM File Toolbox
<http://www.mathworks.com/matlabcentral/fileexchange/8412-lsm-file-toolbox>
(accessed May 15, 2009).
143. Hirsch, S. Xlswrite
<http://www.mathworks.com/matlabcentral/fileexchange/2855-xlswrite> (accessed May 15, 2009).
144. Karp, P. H.; Moninger, T. O.; Weber, S. P.; Nesselhauf, T. S.; Launspach, J. L.; Zabner, J.; Welsh, M. J., An in vitro model of differentiated human airway epithelia. Methods for establishing primary cultures. *Methods in Molecular Biology* **2002**, *188*, 115-37.

145. Starner, T. D.; Zhang, N.; Kim, G.; Apicella, M. A.; McCray, P. B., Jr., *Haemophilus influenzae* forms biofilms on airway epithelia: implications in cystic fibrosis. *American Journal of Respiratory and Critical Care Medicine* **2006**, *174* (2), 213-20.
146. Falsetta, M. L.; Bair, T. B.; Ku, S. C.; Vanden Hoven, R. N.; Steichen, C. T.; McEwan, A. G.; Jennings, M. P.; Apicella, M. A., Transcriptional profiling identifies the metabolic phenotype of gonococcal biofilms. *Infection and Immunity* **2009**, *77* (9), 3522-32.
147. Klingelutz, A. J.; Barber, S. A.; Smith, P. P.; Dyer, K.; McDougall, J. K., Restoration of telomeres in human papillomavirus-immortalized human anogenital epithelial cells. *Molecular and Cellular Biology* **1994**, *14* (2), 961-9.
148. Stewart, P. S.; Franklin, M. J., Physiological heterogeneity in biofilms. *Nature Reviews. Microbiology* **2008**, *6* (3), 199-210.
149. Keehoon, L.; Costerton, J. W.; Ravel, J.; Auerbach, R. K.; Wagner, D. M.; Keim, P.; Leid, J. G., Phenotypic and functional characterization of *Bacillus anthracis* biofilms. *Microbiology* **2007**, *153* (Pt 6), 1693-701.
150. Lim, K. H.; Jones, C. E.; vanden Hoven, R. N.; Edwards, J. L.; Falsetta, M. L.; Apicella, M. A.; Jennings, M. P.; McEwan, A. G., Metal binding specificity of the MntABC permease of *Neisseria gonorrhoeae* and its influence on bacterial growth and interaction with cervical epithelial cells. *Infection and Immunity* **2008**, *76* (8), 3569-76.
151. Savidge, T.; Walker-Smith, J.; Phillips, A., Novel insights into human intestinal epithelial cell proliferation in health and disease using confocal microscopy. *Gut* **1995**, *36* (3), 369-374.
152. Unger, R. E.; Huang, Q.; Peters, K.; Protzer, D.; Paul, D.; Kirkpatrick, C. J., Growth of human cells on polyethersulfone (PES) hollow fiber membranes. *Biomaterials* **2005**, *26* (14), 1877-84.
153. Ren, D.; Zuo, R.; Gonzalez Barrios, A. F.; Bedzyk, L. A.; Eldridge, G. R.; Pasmore, M. E.; Wood, T. K., Differential gene expression for investigation of *Escherichia coli* biofilm inhibition by plant extract ursolic acid. *Applied and Environmental Microbiology* **2005**, *71* (7), 4022-34.
154. Saiman, L.; Siegel, J., Infection control in cystic fibrosis. *Clinical Microbiology Reviews* **2004**, *17* (1), 57-71.

155. PR Newswire. FDA Advisory Committee supports use of tobramycin inhalation powder from Novartis for patients with cystic fibrosis. www.prnewswire.com/news-releases/fda-advisory-committee-supports-use-of-tobramycin-inhalation-powder-from-novartis-for-patients-with-cystic-fibrosis-168690736.html (accessed December 7, 2012).
156. Geller, D. E.; Konstan, M. W.; Smith, J.; Noonberg, S. B.; Conrad, C., Novel tobramycin inhalation powder in cystic fibrosis subjects: pharmacokinetics and safety. *Pediatric Pulmonology* **2007**, *42* (4), 307-313.
157. Masters, K. *Spray drying handbook*, 3rd Ed.; John Wiley & Sons Inc: New York 1976, p. 80-110.
158. Fiegel, J.; Garcia-Contreras, L.; Thomas, M.; VerBerkmoes, J.; Elbert, K.; Hickey, A.; Edwards, D., Preparation and in vivo evaluation of a dry powder for inhalation of capreomycin. *Pharmaceutical Research* **2008**, *25* (4), 805-811.
159. Prota, L.; Santoro, A.; Bifulco, M.; Aquino, R. P.; Mencherini, T.; Russo, P., Leucine enhances aerosol performance of naringin dry powder and its activity on cystic fibrosis airway epithelial cells. *International Journal of Pharmaceutics* **2011**, *412* (1-2), 8-19.
160. Sou, T.; Kaminskas, L. M.; Nguyen, T. H.; Carlberg, R.; McIntosh, M. P.; Morton, D. A., The effect of amino acid excipients on morphology and solid-state properties of multi-component spray-dried formulations for pulmonary delivery of biomacromolecules. *European Journal of Pharmaceutics and Biopharmaceutics*, **2012**. *83* (2), 234-243.
161. Ståhl, K.; Claesson, M.; Lilliehorn, P.; Lindén, H.; Bäckström, K., The effect of process variables on the degradation and physical properties of spray dried insulin intended for inhalation. *International Journal of Pharmaceutics* **2002**, *233* (1), 227-237.
162. Tewa-Tagne, P.; Degobert, G.; Briancon, S.; Bordes, C.; Gauvrit, J. Y.; Lanteri, P.; Fessi, H., Spray-drying nanocapsules in presence of colloidal silica as drying auxiliary agent: formulation and process variables optimization using experimental designs. *Pharmaceutical Research* **2007**, *24* (4), 650-61.
163. Hinds, W. C., *Aerosol Technology: Properties, Behavior, and Measurement of airborne Particles*, 2nd Ed.; John Wiley & Sons: New York, 1999.

164. Najafabadi, A. R.; Gilani, K.; Barghi, M.; Rafiee-Tehrani, M., The effect of vehicle on physical properties and aerosolisation behaviour of disodium cromoglycate microparticles spray dried alone or with L-leucine. *International Journal of Pharmaceutics* **2004**, 285 (1-2), 97-108.
165. Raula, J.; Lahde, A.; Kauppinen, E. I., Aerosolization behavior of carrier-free L-leucine coated salbutamol sulphate powders. *International Journal of Pharmaceutics* **2009**, 365 (1-2), 18-25.
166. Thomas, E. K., Development of a dry powder aerosol for the dispersion and eradication of respiratory biofilms. Masters Dissertation, University of Iowa, Iowa City, IA, 2009.
167. Ross, S. S.; Thomas, E. K.; Stohs, B.; Fiegel, J. L., Treating Lung Biofilm Infections: Dispersion and Eradication Via Dry Powder Aerosols. *Respiratory Drug Delivery* **2010**, 3, 813-817.
168. Yu, L.; Ng, K., Glycine crystallization during spray drying: the pH effect on salt and polymorphic forms. *Journal of Pharmaceutical Sciences* **2002**, 91 (11), 2367-75.
169. Neil, M.; Smith, A.; Heckleman, P., The Merck Index. *Encyclopedia of Chemicals, Drugs and Biologicals*, 14th edition, Merck Research Laboratories, USA 2006, 140.
170. Billon, A.; Bataille, B.; Cassanas, G.; Jacob, M., Development of spray-dried acetaminophen microparticles using experimental designs. *International Journal of Pharmaceutics* **2000**, 203 (1), 159-168.
171. Buchi, Spray Drying Training Papers.
www.google.com/url?sa=t&rct=j&q=&esrc=s&source=web&cd=1&ved=0CDIQFjAA&url=http%3A%2F%2Fwww.buchi.com%2FNano-Spray-Dryer-B-90.12378.0.html%3F%26no_cache%3D1%26file%3D308%26uid%3D64652&ei=CeBIUfqXF4GF2gXO3YCQBg&usg=AFQjCNFmbWVK0zIEDSfHhp4up18NESP0Kg&sig2=9yP_Xoi_BBW-JFjXgu7Mzg&bvm=bv.43828540,d.b2I
(accessed March 21, 2013).
172. Tiddens, H. A.; Geller, D. E.; Challoner, P.; Speirs, R. J.; Kesser, K. C.; Overbeek, S. E.; Humble, D.; Shrewsbury, S. B.; Standaert, T. A., Effect of dry powder inhaler resistance on the inspiratory flow rates and volumes of cystic fibrosis patients of six years and older. *Journal of Aerosol Medicine : the official Journal of the International Society for Aerosols in Medicine* **2006**, 19 (4), 456-65.
173. Copley Scientific. Copley Inhaler Testing Data Analysis Software Manual. 2002.

174. Stanier, C., University of Iowa, Department of Chemical and Biochemical Engineering, Personal Communication. **2012**.
175. Seville, P. C.; Learoyd, T. P.; Li, H.-Y.; Williamson, I.; Birchall, J. C., Amino acid-modified spray-dried powders with enhanced aerosolisation properties for pulmonary drug delivery. *Powder Technology* **2007**, *178* (1), 40-50.
176. Maltesen, M. J.; Bjerregaard, S.; Hovgaard, L.; Havelund, S.; van de Weert, M., Quality by design - Spray drying of insulin intended for inhalation. *European Journal of Pharmaceutics and Biopharmaceutics* **2008**, *70* (3), 828-38.
177. Wan, L. S.; Heng, P. W.; Chia, C. G., Preparation of coated particles using a spray drying process with an aqueous system. *International Journal of Pharmaceutics* **1991**, *77* (2), 183-191.
178. Sou, T.; Orlando, L.; McIntosh, M. P.; Kaminskas, L. M.; Morton, D. A., Investigating the interactions of amino acid components on a mannitol-based spray-dried powder formulation for pulmonary delivery: A design of experiment approach. *International Journal of Pharmaceutics* **2011**, *421* (2), 220-9.
179. Andya, J. D.; Maa, Y. F.; Costantino, H. R.; Nguyen, P. A.; Dasovich, N.; Sweeney, T. D.; Hsu, C. C.; Shire, S. J., The effect of formulation excipients on protein stability and aerosol performance of spray-dried powders of a recombinant humanized anti-IgE monoclonal antibody. *Pharmaceutical Research* **1999**, *16* (3), 350-8.
180. Learoyd, T. P.; Burrows, J. L.; French, E.; Seville, P. C., Sustained delivery by leucine-modified chitosan spray-dried respirable powders. *International Journal of Pharmaceutics* **2009**, *372* (1-2), 97-104.
181. Preston, L. A.; Wong, T. Y.; Bender, C. L.; Schiller, N. L., Characterization of alginate lyase from *Pseudomonas syringae* pv. *syringae*. *Journal of Bacteriology* **2000**, *182* (21), 6268-71.
182. Starke, J. R.; Edwards, M. S.; Langston, C.; Baker, C. J., A mouse model of chronic pulmonary infection with *Pseudomonas aeruginosa* and *Pseudomonas cepacia*. *Pediatric Research* **1987**, *22* (6), 698-702.